Assessment of new real-time in-situ optical coherence tomography instrumentation and techniques for diagnosing and monitoring oral and cutaneous lesions

By

Dara Burhan Muhammad Rashed

BDS, MSc (OMFS)

A thesis submitted in partial fulfilment of the requirements of the University College London for the degree of Ph.D.

Department of Oral and Maxillofacial Surgery

Eastman Dental Institute

University College London

256 Gray's Inn Road

London WC1X 8LD

May 2015

Declaration

I, Dara B. Muhammad Rashed, confirm that the work presented in this thesis is my own. Where information has been derived from other sources, I confirm that this has been acknowledged in the thesis.

Dara B Muhammad Rashed Signature……..

Date / /

Abstract

Head and neck cancer is the sixth most common cancer worldwide, with 686,328 new cases per year. Most head and neck cancers are squamous cell carcinomas of the oral cavity and oropharynx, and are burdened by high mortality (50% at 5 years from diagnosis), notwithstanding recent progress in treatment methods. The vast majority of oro-pharyngeal cancers are late diagnosed, with significant adverse effects on cure, morbidity and prognosis. There is general consensus that earlier diagnosis contributes to better outcome measures. Current diagnostic standards consist of clinical examination and surgical biopsy, which are associated with delayed presentation, diagnosis and greater mortality. There is an unmet need for effective diagnostic techniques to aid early identification of cancers.

Optical coherence tomography (OCT) is one of a number of non-invasive real-time imaging systems, introduced during the last two decades aiming to provide tissue information similar to conventional histopathological examination. The technique is similar to a B-mode ultrasound section, but employs a scanning near infrared light source rather than ultrasound waves, generating cross-sectional images of the sample tissue in an X-Z orientation.

In this study, I investigated a modified OCT oral instrument (VivoSight® Michelson Diagnostics Ltd, Orpington, Kent, UK) with adapted probe for intraoral use. The new oral instrument was not CE marked, was uncalibrated and consequently a non-standard instrument. Therefore, prior to clinical application, the new instrument required calibration and comparison with the conventional instrument to assess and confirm performance in image quality and resolution in X, Y, and Z-planes.

A series of laboratory engineering standards were created and compared by scanning with both instruments in X, Y & Z planes.

A second series of experiments were conducted using porcine tissue as models for human tissue, confirming the similarities of fact and artefact observable when the two instruments were applied to challenging imaging scenarios, in particular, the effects of dissimilar target tissue refractive indices on the OCT image. The effects (tissue dimensional changes) of fixing samples in formalin-containing media and tissue processing were also then investigated using this non-invasive measuring technique.

With ethical approvals obtained, the human research moved on to measure the thickness of the epidermis and epithelium layers of skin and oral cavity in healthy subjects in vivo. With this normal data established, we interrogated suspicious lesions in the head and neck region including the oral cavity, scanning the lesions/biopsies in vivo and ex vivo, respectively, studying the oral instrument's capabilities in detecting and diagnosing lesions, yielding sensitivity, specificity and accuracy data for the OCT technique, compared with the gold standard histopathology.

Overall, we concluded that the OCT oral instrument is behaving similarly to the commercially available skin instrument in X, Y and Z planes, despite reconfiguration of the optical path lengths in sample and reference arms, suggesting the modified instrument is a direct surrogate for the CE certified OCT skin instrument in measurement of cutaneous and oral tumour thickness and depth.

Our findings suggest that OCT has good sensitivity and specificity, easily discriminating healthy tissues, premalignant and malignant lesions in both cutaneous and oral arenas. Imaging depth limitations still preclude OCT from replacing histopathology but we envisage that further refinement of OCT in terms of improving its resolution and imaging depth as well as reducing probe diametre and increasing its flexibility could assists in gradual reduction of the need for biopsy, surgical margin delineation and offer evaluation/monitoring of the efficacy of malignancy treatments through regular follow-up visits.

Acknowledgements

I would firstly like to thank Colin Hopper, Conal Perrett, Stefano Fedele and Richard Cook, my supervisors, for taking me on as a PhD student in the first place. I am particularly indebted to Colin Hopper and Conal Perrett who took me, a scientific novice, into their clinics and theatres and introduced me to scientific research. Their patience, advice and guidance have been invaluable. Richard Cook and Stefano Fedele have been great sources of inspiration to me and have shown uncompromising support and encouragement since I first met them.

My sincere wishes and thanks to all the staff of Biomaterials and Tissue Engineering Department at UCL/ Eastman Dental Institute and all the staff of Biomaterials, Biomimetic, and Biophotonic Research Group at King's College London Dental Institute for their help and cooperation. Special thanks go to Dr Aviva Petrie, Head of Biostatistics Unit, for her help in the statistical analyses of the data in this thesis.

I would also like to thank my study friends, Ahmad and Zaid for their support and help. I am indebted to my brother, Amanj, for his invaluable advice and support throughout the period of my clinical study. I am obliged to Ministry of Higher Education and Scientific Research (MOHESR) in Baghdad/Iraq for their substantial financial support and travel grants, enabling my studies to be completed.

I am also grateful to all the staff at Head and Neck/ Maxillofacial Surgery Department and Dermatology Department/ UCLH, for their help throughout the period of clinical studies. Many thanks go to Mr Nicholas Kalavrezos, Mr Colin Liew and Mr Michael Ho for offering me their biopsies and surgical specimens. I would like to acknowledge Dr Amrita Jay and Dr Alex Freeman for their participation in interpreting the histopathology slides.

Finally, thank you to my family and especially to Sundus and Maryam, to whom this thesis is dedicated.

Index of Contents

Chapter 1

Review of Literature

Chapter 2

Chapter 3

Chapter 4

Validation of the modified OCT oral instrument compared to the commercial standard OCT dermatology instrument…..……..107

Table of Tables

Table of Figures

List of Abbreviations

OCT	Optical Coherence Tomography
NIR	Near Infrared
BCC	Basal Cell Carcinoma
MMS	Mohs Micrographic Surgery
RI	Refractive Index
CIS	Carcinoma In Situ
SCC	Squamous Cell Carcinoma
PML	Potentially Malignant Lesion
PMD	Potentially Malignant Disorder
HNSCC	Head & Neck Squamous Cell Carcinoma
OSCC	Oral Squamous Cell Carcinoma
PDT	Photodynamic Therapy
PVL	Proliferative Verrucous Leukoplakia
AK	Actinic Keratosis
BCC	Basal Cell Carcinoma
NMSC	Non-Melanoma Skin Cancer
BMN	Benign Melanocytic Naevus
MM	Malignant Melanoma
OLP	Oral Lichen Planus
OSF	Oral Submucous Fibrosis
ICD	International Classification of Diseases
IARC	International Agency for Research on Cancer
SEER	Surveillance Epidemiology and End Results
CRC	Cnacer Research Campaign
TNM	Tumour Node Metastasis
UICC	Union for International Cancer Control

AJCC	American Joint Committee on Cancer
RND	Radical Neck Dissection
SND	Selective Neck Dissection
EBRT	External Beam Radiation Therapy
IMRT	Intensity Modulated Radiation Therapy
Gy	Gray
EGFR	Epidermal Growth Factor Receptor
TB	Toluidine Blue
LOH	Loss Of Heterozygosity
NADH	Nicotine Adenine Dinucleotide Hydrogenase
FAD	Flavin Adenine Dinucleotide
VELScope	Visually Enhanced Lesion Scope
ACS	American Cancer Society
RPE	Retinal Pigment Epithelium
SD	Standard Deviation
HPV	Human Papilloma Virus
SHS	Second-hand Smoke
SLD	Superluminescent Diode
VP	Vulnerable Plaque
CI	Confidence Interval

Chapter 1

Review of literature concerning oral cancer

Chapter one

Oral Cancer

1.1 Definition

The term oral cancer generally includes squamous cell carcinoma (SCC) of the lip, gingiva, tongue, floor of the mouth, oropharynx and other ill-defined sites and unspecified parts of the mouth that are registered in ICD-10 (International Classification of Diseases) as C00, C01, C02, C03, C04, C06, C10, and C14 (Table 1.1). Oral cancer accounts for more than 90% of all malignant diseases in the mouth (Chen et al, 1990). Other examples of malignancy that are found in the mouth include salivary gland tumours, sarcomas, liposarcomas (Nunes et al, 2002) and lymphomas (Flaitz et al, 2002); these are relatively infrequent and tend to have dissimilar aetiological factors to SCC (Pindborg, 1977).

Table (1.1) List of relevant malignant diseases and their ICD-10 identification numbers.

ICD-10	**Disease**
C00	Malignant neoplasm of the lip
C01/02	Malignant neoplasm of the tongue
C03	Malignant neoplasm of the gum
C04	Malignant neoplasm of the floor of the mouth
C05	Malignant neoplasm of the palate
C06	Malignant neoplasm of other and unspecified parts of the mouth
C10	Malignant neoplasm of the oropharynx
C14	Malignant neoplasm of other and ill-defined sites in the lip, oral cavity and pharynx

1.2 Epidemiology

1.2.1 Global incidence

Oral and pharyngeal cancer is the sixth most common cancer worldwide when grouped together, although in high incidence areas it is ranked in the top three of cancer list (Warnakulasuriya, 2010). The yearly estimated incidence is approximately 275,000 for oral and 130,300 for pharyngeal cancers discounting nasopharynx, with occurrence of around two-thirds of these cases in the developing countries (Ferlay et al, 2004). There is a broad (nearly 20-fold) geographical variation in the incidence of oral cancer, which is in turn related to risk factors exposure. The highest incidence rates for OSCC (excluding lip) are found in the South and Southeast Asia (e.g. Sri Lanka, India, Pakistan and Taiwan), parts of Eastern (e.g. Hungary, Slovakia and Slovenia) and Western Europe (e.g. France), Pacific regions (e.g. Papua New Guinea and Melanesia) and parts of the Caribbean and Latin America (e.g. Puerto Rico, Brazil, and Uruguay)(Warnakulasuriya, 2009).

In India, Pakistan, Sri Lanka, and Bangladesh oral cancer is the commonest malignancy in males and might contribute nearly to 25% of all new cases of cancer. In countries with low incidence rates, as in the UK OSCC accounts for 3% of all cancers (Warnakulasuriya, 2009 & 2010**)**.

In 2008 worldwide, an estimated 263,900 new cases and 128,000 deaths from oral SCC, including cancer of the lip vermilion occurred. In general, the highest rates of cancer of the oral cavity are found in South-Central Asia, Melanesia, and Central and Eastern Europe and the lowest in Eastern Asia, Africa, and Central America for either sex (Jemal et al, 2011). Major risk factors include tobacco smoking, alcohol consumption, smokeless tobacco, and HPV infections, with the traditional two risk factors (smoking and alcohol) having synergistic effects (Blot et al, 1988; Hashibe et al, 2009). The impact of each of these risk factors to the global burden of oral malignancy differs from region to region (Blot et al, 1988; International Agency for Research on Cancer (IARC), 2004, 2007; D'Souza et al, 2009; US Department of Health and Human Services, 2004). Globally, smoking accounts for 42% of deaths from oral cancer, including the pharynx, and heavy alcohol drinking for 16% of the deaths; the corresponding percentages are around 70% and 30%, respectively in high-income countries (Danaei et al, 2005). The major risk factors for OSCC in India, Taiwan and other neighbouring countries are betel quid/pan chewing with or without tobacco as well as smokeless

tobacco products (IARC, 2004; Jayalekshmi et al, 2009; Wen et al, 2010). Indeed, the recent increase in OSCC incidence rate observed in Taiwan could have been partly because of the increased consumption of alcohol and areca nut/betel quid chewing (Ho et al, 2002).

Oral squamous cell carcinoma (OSCC) mortality rates amongst men fell considerably over the past decades in most countries, including those of Asia and Europe (Garavello et al, 2010; Mayne et al, 2006), however the rates in several Eastern European countries continued to increase, including Slovakia and Hungary. In most European countries, the increasing number of affected women mostly reveals the ongoing tobacco epidemic (Garavello et al, 2010). These figures contrast with the decreasing trends in the UK and the US in both sexes and at all ages (Jemal et al, 2006; Garavello et al, 2010; DeLancey et al, 2008) where the tobacco epidemic started and dropped earlier. Yet, incidence rates are increasing in young adults for OSCC sites that is related to HPV infections, for example base of the tongue, oropharynx and tonsil, in some European countries and in the United States (Chaturvedi et al, 2008; Shiboski et al, 2005), which is postulated to be related to changes in sexual behaviour (D'Souza et al, 2009; Marur et al, 2010).

In the European Union (EU) countries, there were 67,000 new cases and cancer of the oral and pharyngeal areas was the 7th most common malignancy (Boyle and Ferlay, 2005). Cyprus and Greece have the lowest male incidence rates, while the highest rates are found in Hungary and France within the EU countries. Black and associates (1997), in one report point that in France the oral cancer rate in males was almost seven times higher than that for males in Greece. In Northern or Southern Europe, the incidence rates are lower if compared with Western Europe, though highest mortality rates are reported from Eastern Europe.

France has the highest incidence rates within the EU and around 15,500 cancers of lip, oral cavity and pharynx are reported yearly. The reported male incidence rates in France were 32.2 and 4.7 for females per 100,000 standardised to European populations. The male incidence rate of both oral and oropharyngeal malignancy in northern France is very high with a rate of nearly 42.3 per 100,000 amongst males in the Somme and Bas Rhine regions. Almost 5000 deaths are reported annually (Remontet et al, 2002). Northern regions of Italy, Germany, Spain, Switzerland, and Portugal have reported intermediate rates in compare with other countries of EU.

Within EU, Sweden, Finland, and Greece have the lowest incidence rates. Numerous Eastern and Central European countries, for example Slovakia, Slovenia, and Hungary have reported high rates for OSCC in the recent decades. This is especially true for Hungary where rates of incidence and mortality have doubled (Banoczy & Squier, 2004).

In the US around 34,360 of oral and pharynx cancer cases are reported. Age-adjusted incidence rates for males were 15.6 per 100,000 and 6.1 for females (10.5 for either sex). Higher incidence rates were observed amid the black men in the US mainly for oropharynx (Surveillance Epidemiology and End Results (SEER), Cancer statistics review1975–2004).

Cancers of oral cavity and pharynx rank fifth in males and sixth in females in the Caribbean and South America. The highest incidence levels are found in the region comprising of Uruguay, Argentina, Southern Brazil, though highest rates are observed in Brazil. After those in India and France, the population of male in Brazil has the highest risk for OSCC in the globe and occupies the 7^{th} in the rank of the most common malignancy in the Brazilian population (Wunsch-Fiho & de Camargo, 2001). In Brazil 14,160 new cases of cancer of the mouth and pharynx (C00-10) are expected to occur in 2008, where 10,380 (11 per 100,000) and 3780 (3.9 per 100,000) in males and females respectively [National Cancer Institute (Brazil); 2007]. The distribution of new OSCC cases throughout the states and capital cities of the country is quite varied, and around 30% of all OSCC cases occur in capital cities. Overall, northern and north-eastern regions have lower rates, whereas higher rates are in southern and south-eastern regions of the country. In Brazil, several cancer registries indicate that Puerto Alegre and Sao Paulo have registered highest incidence rates for cancer of the oral cavity and tongue (National Cancer Institute (Brazil); 2007).

Quito, Equador was the city where the lowest male incidence rates has been observed with 2.4 cases per 100,000, while Bangalore, India where the highest females incidence rates was observed with an average 11.2 cases per 100,000 (Parkin et al, 2002).

The highest reported incidence rates of OSCC in the Caribbean was observed in Puerto Rico with an average of more than 15 per 100,000 (Wunsch-Fiho& de Camargo, 2001). Cuba has intermediate incidence rates of OSCC. In 1986 in men with history of heavy cigar smoking, the incidence rate was around 7.2 per 100,000 and remained constant for more than a decade (Garrote et al, 2001).

There is difficulty in extrapolating the true incidence rates in African countries due to data are limited to few cancer registries; nevertheless reported incidence rates do not display evidence that OSCC in the African continent is a serious problem. Some researchers in a descriptive studies from Sudan suggest that rates of OSCC in men are high, relating the high incidence rate to toombak, type of oral snuff admixed with sodium bicarbonate (Idris et al, 1995).

Several countries with the highest OSCC incidence rates globally are situated in South and Southeast Asia region. Worldwide, India is the country that is always cited to have the highest incidence rate, yet in some recent reports Pakistan and Sri Lanka are at the top of ranking list. In South Asia, Sri Lanka has the highest rates of OSCC incidence according to Globocan data (Ferlay et al, 2004). In men is the most common cancer with 15.5% of all malignancies reported in the oral cavity. The age standardised incidence for lip and anterior parts of mouth in 2000 was about 10.2 and for posterior oral cavity and oropharynx was around 3.6 per 100,000, reaching to approximately 13.8 per 100,000 together for lip, oral mouth and oropharynx (Sri Lanka National Cancer Control Programme, 2005). In Japan cancer of the oral cavity is uncommon. In 2001, the incidence rate (C00-14) in Japan based on 10 population-based cancer registries data was about 5.3 per 100,000, which is adjusted to world population. The total cases of cancers in these sites were around 9612, the distribution of cases were 6,984 in males and 2,628 in females (Marugame et al, 2007).

The highest reported incidence rates for lip cancers are in white populations in Australia and Canada. For instance, in Australians more than 50% of OSCC are found on the lip. It is rare in black populations (Sugerman & Savage, 2002).

1.2.2 UK incidence

In the UK, the 12th most common cancer amongst males is cancer of the oral cavity, accounting for more than 2% of all new cancer cases in men. OSCC is the 16th most common cancer among females accounting for over 1% of all new cancer cases in women. In 2009 in the UK, there were 6,236 new OSCC cases (Table 1.2); distribution of cases was around 4,097 (66%) in males and 2,139 (34%) in females, giving a male: female ratio of 1.9:1.0 (Office for National Statistics, 2011; ISD Scotland, 2011; Welsh Cancer Intelligence and Surveillance, 2011; Northern Ireland Cancer Registry, 2011).

Table (1.2) Oral cancer (C00-C06, C09, C10 and C12-C14), number of new cases, European Age-Standardised (AS) incidence rates per 100,000 populations, UK, 2009.

		England	**Wales**	**Scotland**	**Northern Ireland**	**UK**
Male	Cases	3,246	236	501	114	4,097
	AS Rate	11.4	13.4	17.1	12.7	12.0
Female	Cases	1,689	121	270	59	2,139
	AS Rate	5.0	5.7	7.1	5.7	5.3
Persons	Cases	4,935	357	771	173	6,236
	AS Rate	8.1	9.4	11.9	9.0	8.5

In Scotland, the European age-standardised incidence rates (AS rates) are considerably higher if compared with Northern Ireland, Wales and England for men, while for women if compared with England only. The rates do not differ significantly for both genders between Northern Ireland, England and Wales. The geographical variation across the UK in oral cancer incidence rates mainly reveals the prevalence of the two traditional risk factors for the major OSCC types (smoking and alcohol consumption). The difference between south and north across the UK in oral cancer incidence largely for men has existed since at least the 1990s (Quinn et al, 2005). More recent data demonstrates that the highest oral cancer incidence rates for men (ICD-10 C02-C04, C06) are still in Scotland, Northern Ireland and the north of England (Oxford Cancer Intelligence Unit, 2012). For women across the UK clear divide is much less pronounced, although the highest incidence rates for OSCC are also in Northern Ireland and Scotland.

Some studies that reflect the influence of life style describe patterns of incidence of OSCC amongst migrant groups. In Britain, some studies on minority ethnic and migrants populations have reported considerably higher cancer incidence rates in South Asian populations living in Birmingham, Yorkshire and Greater London (Bedi, 1996; Warnakulasuriya et al, 1999a). Risk of cancer mortality in the native population from 1973 to 1985, compared with cancer mortality in people born in the Indian subcontinent who migrated to Wales and England, revealed highly significant raised risks for cancers of the oral cavity and pharynx in Indian ethnic migrants (Swerdlow et al, 1995).

OSCC is increasing in young adults and most cancer registries in the UK record 6% of all oral cancers in people below the age of 45 years. In Scotland**,** incidence rates are higher than the rest of the UK for both genders. The lifetime risk of developing mouth cancer in Scotland is greatly higher (1.84% in men and 0.74% in women) than the other regions of the UK (1.06% in males and for females is about 0.48% for UK as a whole)(Conway et al, 2006).

1.3 Age and gender

Cancer of the oral cavity is more common in males than in females in most countries. The reported gender differences are mainly due to male heavier indulgence in risk habits and sunlight exposure (particularly for cancer of the lower lip vermilion) as a part of outdoor occupations. The ratio of males to females that has been diagnosed with OSCC, though has dropped over the last few decades and is currently nearly 1.5:1.0 for cancer of the oral cavity and around 2.8:1.0 for oropharyngeal cancer (Warnakulasuriya, 2009).

The risk of developing OSCC increases with age and most of cancer cases occur in those people aged 50 or over (Warnakulasuriya, 2009). From 2005 to 2009 in the US, the median age at diagnosis for cancer of the mouth and pharynx was 62 years of age, whereas 61 years of age was the median age at diagnosis for tongue cancer (SEER, 2009).

Approximately 6% of cancers of the oral cavity occur in young people below 45 years of age (Llewellyn et al, 2001). In countries with high incidence rates, many oral cancer cases are reported before 40 years of age. A rise in oral and oropharyngeal cancer incidence and mortality rates is reported from many EU countries and parts of the US in young adults (Moller, 1989; Macfarlene et

al, 1994a, 1994b; Shiboski et al, 2005). In Scotland, between 1990-1999 the oral cancer men incidence rates under the age of 45 has more than doubled from around 0.6 to 1.3 per 100,000 (Conway et al, 2006). The disease in young adults is fortunately not more aggressive than that occurring in older people either in South of England or in the US (Shiboski et al, 2005; Warnakulasuriya et al, 2007a).

1.4 Anatomic sites

The most common site amongst the US and a European population for cancer of the oral cavity is the tongue, amounting to 40–50% of OSCC. In 2009 in the UK, cancer of the mouth and tongue collectively was about 60% of cases (Office for National Statistics, 2011; ISD Scotland, 2011; Welsh Cancer Intelligence and Surveillance, 2011; Northern Ireland Cancer Registry, 2011). Cancer of the buccal mucosa is very common in the Asian populations because of betel quid/tobacco chewing habits (Warnakulasuriya, 2009). Around 40% of OSCC in Sri Lanka are located on buccal mucosa (National Cancer Control Programme, Sri Lanka, 2005). Lip cancer is accounting for more than 5% of cases. Some evidence are existed that cancer of the lip is associated with exposure to ultraviolet radiation from sunshine or sunbeds (tanning beds) (Lucas et al, 2006). Floor of mouth, gingivae and palate are other intraoral sites for cancer of the oral cavity.

1.5 Socio-economic deprivation

Cancer of the oral cavity is related to deprivation and socio-economic status, with the highest incidence of oral cancer rates occurring in the most deprived sections of the population (Thames Cancer Registry, 2007). The association is especially strong for males, where the risk of developing a malignancy was above 4 times higher in the disadvantaged categories in compare to the least disadvantaged categories [Cancer Research Cmpaign (CRC), 2000]. Pukkala and co-workers (1994) in a study found in the lowest social class that cancer of the lip is 5 times more common when compared to the highest class.

Given the most well established risk factors for OSCC are smoking and alcohol misuse, it is not surprising that the rates of the cancer of the mouth incidence is strongly linked with deprivation. Data for 2000-2004 demonstrates European AS incidence rates for cancer of the head and neck

(ICD-10 C00-C14, C30-C32) are approximately 130% higher, which is more than double for males living in more disadvantaged areas compared with the least disadvantaged, while for females is up to 74% higher (National Cancer Intelligence Network (NCIN), 2008a). Likewise, for Wales and Northern Ireland akin results have also been published (Donnelly et al, 2009; Cancer in Wales, 2012). For 2005-2009 in Scotland, a study reveals that deprivation gap is somewhat larger, with European AS incidence OSCC rates being 3 times higher in the most underprivileged population (ISD Scotland, 2012).

1.6 Epidemiologic trends over time

In the USA and in some countries in the Europe, there have been reported an increase in the trends of OSCC in younger males and middle-aged especially for tongue cancer (Annertz et al, 2002; Shantz and Yu, 2002; Llwellyn et al, 2001).

In Western Europe, the age-standardised incidence of OSCC in the last twenty years has gradually increased. In the UK for instance since 1989, an average rise of 2.7% annually has been reported. Since post Second World War in the UK, the rising trends of OSCC has been linked with increased alcohol consumption (Hindle et al, 1996). Since the mid 1970s in Britain, there has been an overall increase in OSCC incidence rates with majority of the increase happening since the late 1980s for both genders. European age standardised (AS) incidence rates for oral cancer have increased by 25% for males and 28% for females in the last 15 years period, between 1998-2000 and 2007-2009 (Office for National Statistics, 2011; ISD Scotland, 2011; Welsh Cancer Intelligence and Surveillance, 2011).

From 1974-1990 in the USA, rising trends for incidence of oral cancer in black males were noted. However, from 1995 to 2004, trends for oral and pharyngeal cancer have considerably plummeted, with around -1.5% annual percentage change (APC) for all races (-1.6% and -1.8% for males for females respectively). Data from France from 1980 to 2000 also indicates a decline for males. The incidence in males over 20 years dropped from 40.2 to 32.2 per 100,000, with the APC being -1.0% from 1978 to 2000. Nevertheless, women incidence rates rose in 1980 from 3.3 per 100,000 to 4.7 per 100,000 in 2000; with the APC was +1.73% (Warnakulasuriya, 2009). The incidence rates in Japan in 1975 has doubled from 2.7 per 100,000 to 5.4 in 1995, and has remained steady up to 2001 (Marugame et al, 2007).

Changing patterns has been observed in both cancer of the lip and oral cavity. There has been a fall in men incidence rates of carcinoma of the lip vermilion over around three decades period, nonetheless, other studies show a rise in carcinoma of the tongue, mostly in younger patients, presently owing to binge drinking and smoking amongst younger people (Scully and Moles, 2008). Since the 1980s in Central and East Europe, there has been a rise in mortality rates in men alongside an increase in tobacco cosumption (Bray et al, 2002; La Vecchia et al, 2004). There has also been an increase in men from Western Europe, but in some countries where cancer of the lung has declined, which hints that it is not in those populations linked so much to tobacco use as to alcohol. While in women, there has been a small rise connected with more tobacco and alcohol use (Scully &Bagan, 2009).

1.7 Survival rates

Those patients who are effectively treated for cancer of the oral cavity often have to live with the devastating results of their treatment (British Dental Association, 2000). These may influence the function and appearance of the patient, for instance eating, drinking, swallowing and speaking might become challenging, and these defects may create other problems such as nutritional deficiency and depression. Consequently, quality of life issues are particularly essential for these patients' categories (Warnakulasuriya, 2009).

Five-year survival rates for oral, tongue and oropharyngeal cancers are approximately 50% for most countries. Lip cancers possess the best outcome with more than 90% of patients have five-year survival rate. Hypopharyngeal carcinomas have the lowest survival rate. Generally, as the disease advance (Stage IV) and the inaccessibility of the tumour increase, for example cancer of the hypopharynx, the prognosis will considerably decrease. Females had higher survival rates for oral and tongue cancers than males (Warnakulasuriya, 2009). Five-year survival rate is considerably influenced by TNM staging system at presentation. For mobile tongue at stage 1 disease, the five-year survival rate is 80%, whereas for stage 1V disease the survival plummets to 15% (Rubin, 1993). The survival rates for oral cancer in the UK have not shown any improvement over the last thirty years period (Warnakulasuriya, 2009). As for most OSCC, survival for affluent groups is better compared with the deprived groups (Edwards & Jones, 1999) and for younger compared to older patients (Shiboski et al, 2005; Warnakulsuriya et al, 2007a).

1.8 Trends

Age-adjusted death rates from OSCC for most countries have been estimated at 3–4 per 100,000 and 1.5–2.0 per 100,000 for males and females respectively. In most countries of the Europe, mortality rates between 1950s and 1980s from cancer of the oral cavity had been rising significantly (La Vecchia et al, 2004). Amongst the Germans for example around four-fold rise was observed during this period. In the UK, Scottish males have the highest mortality rates that reflect their high incidence rates (Conway et al, 2006). An OSCC mortality rate has risen in the last two decades amongst French females. Mortality rates in 2000 stood at an average 4.7 per 100,000 and APC of nearly +1.73% was observed between the years 1980 and 2000 (Remontet et al, 2002). The most substantial rises were observed in men in several countries of East Europe (Hungary, Slovakia, Bulgaria, Czech Republic, Poland, and Romania) (La Vecchia et al, 2004). In mid1990s, remarkable high mortality rates of about 20.2 per 100,000 were noted in Hungary.

In the US from 2005-2009, the median age at death was 67 years of age for mouth and pharynx cancer, while for cancer of the tongue the median age was 66 years of age. Mortality rates of about 2.5 per 100,000 for males and females annually for cancer of the oral cavity and pharynx have been reported in the US based on patients who died in 2005 to 2009, while for tongue cancer, the age-adjusted death rate was 0.6 per 100,000 yearly for both genders. Black male mortality rates (6.8 per 100,000) are greater when compared with rates of white or Hispanic (SEER, 2009). Amongst young people in most Western countries there has been a slight but steady rise in rates of mortality (Llwellyn et al, 2001). This is particularly noted in the US for cancer of the oropharynx populations (SEER, 2009).

1.9 Risk factors

The most important aetiological factors are tobacco, excess consumption of alcohol (La Vecchia et al, 1997) and betel quid chewing (IARC, 2004), these factors act separately or synergistically (Blot et al, 1988). Other factors such as HPV infection might also be involved (Herrero et al, 2003), especially for cancer of the tonsil and oropharynx in younger people (D'Souza et al, 2007).

1.9.1 Tobacco

Tobacco whether smoked, for example cigarette, cigar and pipe smoking (Lee et al, 2009; Macfarlene et al, 1995) or smokeless tobacco (chewed or taken as snuff) (US Department of Health & Human Services, 1986; Llwellyn et al, 2001; Wanakulasuriya & Ralhan, 2007; Boffetta et al, 2008) are undoubtedly a major carcinogen causing both initiation and promotion of OSCC. Cigarette smoking was first identified in 1957 as a potential risk factor for cancer of the mouth and oropharynx (Wynder & Bross, 1957) and later by other researchers in the past twenty years (Gupta et al, 1996).

A number of risk factors of OSCC have been identified in western countries by epidemiological studies with tobacco and alcohol consumption being the most two important risk factors (IARC, 1986; Macfarlene et al, 1995; Llwellyn et al, 2001; Scully & Moles, 2008). The synergistic effect of tobacco and alcohol use is multiplicative in the oral cavity (Johnson, 2001). Also, the relative risk of developing OSCC might increase by threefold when tobacco added to betel quid (Johnson et al, 1996). The strong relationship between tobacco use with oral and pharyngeal carcinoma is well established (Neville & Day, 2002).

Epidemiological studies demonstrate that the relative risk of developing cancer of the oral cavity is 5-9 times higher for smokers than for non-smokers, while in extremely heavy smoker (who smoke 80 or more cigarettes/day) the risk might rise to approximately 17 times greater (Mashberg et al, 1993; Jovanovic et al, 1993; Andre et al, 1995; Blot et al, 1988; Lewin et al, 1998; Neville et al, 2002). Furthermore, patients who received treatment for cancer of the oral cavity and continue smoking have a 2-6 times higher risk of developing a second malignancy of the upper aerodigestive tract when compared to those who stop smoking (Silverman & Griffith, 1972; Silverman & Shillitoe, 1998).

Pipe smoking in the earlier parts of the last century was linked with lip malignancy (majority of lip cancers occur on the lower lip) and the reduction in popularity of pipe smoking could be related with some of the decline in cancer of the lip. In Spain, a case control study revealed that the risk of lip cancer increased when smokers leave the cigarette on the lip (Perea-Milla Lopez et al, 2003). The risk of developing OSCC is dependent upon the duration of smoking and the number of smoked cigarettes/day while smoking cessation results in a drop in the risk (Rodriguez et al, 2004; Castellsague et al, 2004; Blot et al, 1988). Yet, Bosetti and associates (2008) in a recent study reported that it takes two decades or longer for the reduction of the risk to that of never smokers.

The rise in risk for cancer of the oral cavity have also linked with snuff and chewing tobacco (Brown et al, 1965). In the southern US, one study of chronic female snuff users were estimated to have 4 times higher risk of developing OSCC (Winn et al, 1981). Furthermore, a considerable number of OSCC in the users of smokeless tobacco develop at the site where the tobacco is placed. Though, smokeless tobacco use seems to be related with a much lower risk of developing oral cancer than the risk associated with smoked tobacco. Bouquot & Meckstroth (1998) reported that oral cancer incidence in West Virginia is below the national average, albeit this state in the USA has the highest level of tobacco chewing consumption. Several authors in other studies from Scandinavia have suggested that the Swedish snuff consumption, which has lower nitrosamine levels and is non-fermented, is not related with an increased risk for cancer of the oral cavity (Lewin et al, 1998; Johnson, 2001).

Smokeless tobacco is also used in many Asian countries including India, Pakistan, Iran and Afghanistan. Sudan is also within the countries that use tobacco products without combustion. Tobacco is usually mixed with other ingredients such as cardamom oil, sesame oil, lime, areca, ash, menthol, and betel leaf and the mixture is placed in contact with the oral mucous membrane. Paan, betel quid, khaini, mishri, gutka, niswaar, and toombak are some examples of smokeless tobacco products and are used by circa 20% of world's population (Cogliano et al, 2004).

A recent study in the UK in 2010 estimated that approximately 70% of cancer of the mouth and pharynx in males and about 55% in females were caused by tobacco smoking (Parkin, 2011a).

Around 2% of British males in 2009 smoked at least 1 cigar/month, while below half of 1% of men said they smoked a pipe (Office for National Statistics, 2010). Very few females smoke cigars or pipes in the UK. In a case control study carried out in Cuba of OSCC, the odds ratio associated with smoking four or more cigars/day was comparable with that for smoking thirty or more cigarettes/day. Indian females (certain women in the Indian state of Andhra Pradesh) who practice reverse chutta smoking, with the cigar lighted end inside the mouth, have especially high risk rates of cancer of the palatal mucosa (Gupta et al, 1984). Smoking bidi(s), which are made of hand-rolled tobacco wrapped in tendu leaf, also rises the risk of oral malignancy (Rahman et al, 2003).

Smoke inhaled by individuals other than the intended 'active' smoker is called passive smoking, which is also called environmental tobacco smoke (ETS) or second-hand smoke (SHS). SHS occurs when tobacco smoke permeates any environment and the smoke inhaled by persons within that environment. Evidence is existed that involuntary smoking or exposure to SHS might increase developing cancer of the oral cavity, with nearly 63% risk increase shown for non-smokers exposed at home or at workplaces and indoor public places to SHS. There was about 84% risk increase of developing oral cancer amongst non-smokers who exposed for more than 15 years to involuntary smoking at home and at work (IARC, 2004; Lee et al, 2009).

1.9.2 Alcohol

Alcohol is considered as a major risk factor for OSCC and a recent study carried out in the UK on alcohol consumption effect on oral cancer estimated that about 37% of cancer of the mouth and pharynx in males and around 17% in females in 2010 were linked to alcohol consumption (Parkin, 2011b). Bagnardi and colleagues (2001) in a meta-analysis reported risk ratios for alcohol intake of 25 grams/day of 1.8 risk ratio, and for 50 grams/day of 2.9, while for 100 grams/day the risk ratio was about 6.1 after adjustment for smoking. Doubling in increased risk for developing OSCC has been shown in a study by Castellsague and associates (2004) for people drinking 14 grams of alcohol daily. Those people who smoke and drink have a much higher risk of developing cancer of the oral cavity than those who only drink alcohol or use tobacco (Blot, 1992). About more than 80% increase risk of OSCC is estimated to be due to both tobacco and alcohol use. In addition, heavy smokers and drinkers have 38 times the risk of abstainers from smoking and drinking (Blot et al, 1988).

Andre and co-workers (1995) in a case-control study in France reported that extremely heavy drinkers who consume 100 grams of alcohol daily had a 30 times higher risk of developing cancer of the oral cavity and oropharynx. Other researchers showed (in relation to synergistic effect of alcohol and smoking) that patients who are both heavy drinkers and heavy smokers can have above 100 times higher risk for developing oral malignancy (Andre et al, 1995; Blot et al, 1988). Several recent studies have also reported that both tobacco use and alcohol consumption increase the risk of developing oral cancer in synergistic rather than additive manner (Blot et al, 1998; Lewin et al, 1998; Talamini et al, 2002; Castellsague et al, 2004).

Globally, an author notes that 25% OSCC are owing to tobacco usage (smoked and/or chewed), 7-19% to alcohol consumption, 10–15% to deficiency in micronutrient, and in excess of 50% to areca nut/betel quid chewing in regions where chewing prevalence are high (Petti, 2009). The risk of increased oral cancer development that has been observed in southern part of Europe is likely to be associated with binge drinking (heavy alcohol abuse) (Macfarlene et al, 1996; Le Vecchia et al, 1999). In a study, Pelucchi et al (2003) reported that heavy alcohol drinker have 5 times greater risk of developing oral malignancy than those people whom never drinked alcohol.

OSCC related with heavy alcohol consumption and heavy smoking displays a peak age of onset at the age of 40 years and over (Parkin et al, 1999), however the peak age of onset is generally lower by nearly 10 years in persons who have the habit of areca nut/paan chewing (Reichart & Nguyen, 2008).

There has been a suggestion that it is the total quantity of ingested ethanol is more important rather than the brand (e.g. wine, beer, spirits etc.) of alcohol product (Altieri et al, 2004). In Europe, the rising trends in OSCC mortality rates have been linked to rising levels of alcohol use. The alarming rise in oral malignancies for instance, in Denmark has been ascribed primarily to higher consumption of alcohol (Moller, 1989). An exception to this increase in consumption of alcohol is seen in France, where a fall in consumption of alcohol has been related to the decrease in rates of OSCC mortality in the 1980s (Blot, 1994).

In 2009, the highest consumption of alcohol in Britain was in the age group 45-64 for males, with an average of 19 units a week, and 16-24 years for females with an average of 10 units a week. Since 2000 decrease in binge drinking have also observed particularly in those aged 16-24 (Office for National Statistics, 2010).

1.9.3 Areca nut/pan chewing

Areca nut is used by 600 million people in the world and it is the fourth commonest addictive substance after tobacco, alcohol, and caffeine (Warnakulasuriya, 2002). The chronic betel quid (paan) chewing in India and Southeast Asia has been strongly related with an increased risk of developing cancer of the oral cavity and oropharynx (Pindborg et al, 1984; Murti et al, 1985, 1995). Areca nut alone or in combination with other ingredients such as lime catechu (Indian acacia tree extract) usually with tobacco and sometimes with condiments and sweeteners that are wrapped in betel leaf (Piper betle) is referred to as betel quid or paan. Alkaloid from the areca nut will be released due to added lime, which produces in the user a feeling of well-being and euphoria (Neville & Day, 2002). Areca nut in the component of paan/betel quid or alone is known to be carcinogenic even without addition of tobacco (Van Wyk et al, 1993; Thomas & Kearsley, 1993; Warnakulasuriya, 1995). The risk of developing OSCC is rised hugely if tobacco is smoked or added to the quid. Therefore, Areca nut is considered as an independent risk factor for developing of oral malignancy. Furthermore it is also implicated in the development of oral submucous fibrosis (OSF) and leukoplakia, which are both potentially malignant disorders (PMD) (Warnakulasuriya, 2002). Many researchers reported that the use of betel quid in India is a major contributor of cancer of the oral cavity and oropharynx (Znaor et al, 2003; Jacob et al, 2004; Carpenter et al, 2005; Guha et al, 2007; Reichart & Nguyen, 2008) and accounts for around 50% in males and 90% in females of oral and oropharyngeal malignancy (Balaram et al, 2002). The importance of Areca nut as a risk factor is also increasing in the UK because of the migration of people from Indian subcontinent, China and Southeast Asia (Swerdlow et al, 1995; Bedi, 1996).

1.9.4 Marijuana use

There have been case reports of OSCC in marijuana users (Donald, 1986; Almadori et al, 1990). Other authors in more recent studies found evidence that marijuana smoking (cannabis or hashish) is linked with the rising risk of developing cancer of the oral cavity (Mao & Oh, 1998; Hashibe et al, 2005). Other researchers considered marijuana to be a potential risk factor and could be in part accounted for the increase in OSCC that is seen amongst young adults (Zhang et al, 1999; Silverman, 2001; Schantz & Yu, 2002). Still, Neville & Day (2002) suggested that additional studies are required to confirm the purported relationship of marijuana and cancer of the oral cavity among younger patients.

1.9.5 Mouthwash use

There is controversy by many authors in regard to the likelihood that the regular use of mouthwashes, especially those containing high levels (25% or higher) of alcohol could be dangerous (Boyle et al, 1992). It seems that there is small risk and only possible to be expressed in smokers (Johnson et al, 1996). Nevertheless, most of the researches demonstrate no rise in risk for developing oral cancer with use of alcoholic mouthwash (Guha et al, 2007; Winn et al, 1991 & 2001; Garrote et al, 2001; Talamini et al, 2000; D'Souza et al, 2007).

1.9.6 Diet and nutrition

Pavia and associates (2006) in a meta-analysis of observational studies reported a substantial risk decrease of nearly 50% for each additional serving of vegetables or fruit daily. In another large cohort prospective study, Freedman and colleagues (2008) showed a smaller considerable risk drop for cancer of oral cavity of about 26% for each additional serving of vegetables, however no connection found for fruit consumption. Results might differ by smoking status, with a case-control study carried out by Kreimer and co-workers (2006) reporting that the highest consumption of vegetables and fruit will reduce risk of OSCC among alcohol users and smokers but not amongst individuals who had never drunk alcohol or smoked. Other researchers in another study in 2010 estimated that approximately 57% of cancer of the mouth and pharynx in males and about 54% in females in the UK were connected to individuals eating less than five portions of fruit and vegetables/day (400g/day) (Parkin and Boyd, 2011). Still, there is significantly more uncertainty

concerning the associations between cancer of the oral cavity and pharynx and diet than for other risk factors, for example alcohol and smoking (Parkin et al, 2011; Parkin and Boyd, 2011). The intake of enough portions (five/day) of vegetables and fruit is established to be associated with a reduction of OSCC risk, and each portion of vegetable or fruit lowers the risk by as a minimum a quarter (Warnakulasuriya, 2009). This suggests that a diet containing insufficient amount of antioxidants is another factor that predisposes for cancer of the oral cavity development (O'Shaughnessy et al, 2002) and for precancerous lesions (Nagao et al, 2000). Warnakulasuriya (2010) suggested that randomised clinical trials (RCT) are required on dietary supplementation efficacy to lower the risk of OSCC by chemoprevention and to reverse PMDs (leukoplakia and erythroplasia) in the high risk groups as well.

Petti (2009) reported that detrimental life style is intake of high sugar and/or fat, resulting in a low vegetable and/or fruit consumption might also be associated with an increased risk of oral cancer (Winn et al, 1984; Winn, 1995; Pavia et al, 2006; Garavello et al, 2008). A diet that is rich in fruit (Winn, 1995) and vegetables (Lucenteforte et al, 2008), especially orange and yellow vegetables (Sapkota et al, 2008**)** has been revealed to be protective against majority of epithelial malignancies including OSCC and gastro-intestinal system and breast cancers possibly because of high levels of antioxidant (Suzuki et al, 2006) and folate (Pelucchi et al, 2003). Mayor (2002) in a research reported declines of about 60% of stomach cancers, 21% of breast cancers and around 43% of colorectal malignancies. Iron deficiency and low levels of antioxidant such as glutathione (GSH) is quite the reverse appear to increase the risk of cancer of the oral cavity (Richie et al, 2008). Many authors in several studies have reported that high consumption of vegetables and fruit, even in the presence of alcohol abuse and heavy smoking, could prevent nearly a quarter of head and neck cancer cases (Boccia et al, 2008) and around half of the oral cancer cases (Levi et al, 1998; Franceschi et al, 1991, 1999; Pavia et al, 2006).

1.9.7 Ultraviolet radiation

Ultraviolet radiation is a carcinogen for the different forms of skin cancer, including squamous cell carcinoma (SCC), basal cell carcinoma (BCC) and malignant melanoma. This is particularly the case in persons with fair-skinned who lives in countries, for instance Australia where there is a lot of sunshine (Johnson, 1991). In contrast to cancer of the oral cavity and oropharynx, the lip vermilion carcinoma are more similar epidemiologically to skin SCC and occur largely in white

males (Neville et al, 2002). Carcinomas of the lip are more strongly linked with chronic exposure to sunlight, though occasionally they have been related to the site where smokers have habitually held pipestems or cigarettes (Silverman &Shillitoe, 1998). These tumours are more common in males, probably because they are more likely to have vocations, for example farming and fishing and/or avocations that consequently result in more cumulative sun exposure. The most common location of oral malignancy at one time was on the lip; nevertheless, the incidence of malignancy has dropped considerably over the past five decades in this site since fewer males hold outdoor occupations (Neville et al, 2002; Silverman, 1998).

The International Agency for Research on Cancer (IARC) reports that there is limited proof for relationship between cancer of the lip vermillion and solar radiation (Cogliano et al, 2011). According to the report of WHO, the evidence is generally indirect, for example the fact that most of the cancer occurring on the lower lip that receives more sun exposure comparing to the upper lip (Lucas et al, 2006).

1.9.8 Human papillomavirus and immunosuppression

There is evidence of increased risk in cancer of the oral cavity and oropharynx when there is infection with high-risk human papillomaviruses (HPV), especially HPV-16 (Miller & White, 1996; Sugerman & Shillitoe, 1997; Lindel et al, 2001; Gillison & Shah, 2001; Gillison, 2004; Mork et al, 2011; Kreimer et al, 2005; Smith et al, 2004; Herrero et al, 2003). Sugerman & Shillitoe (1997) found that HPV-16 has been detected in approximately 22% of OSCC, and in up to 14% of cases HPV-18 has been detected. In case of oropharyngeal cancers the association is stronger (D'Souza et al, 2007). In the UK, it has been estimated that about 8% of oral cancers and up to 14% of oropharyngeal carcinomas are linked to infection with high-risk HPV (Parkin, 2011c).

Studies by many authors have shown an increase in risk of developing OSCC in females with previous HPV-associated anogenital cancer that presents evidence of an association with HPV infection (Frisch & Biggar, 1999; Spitz et al, 1992). Besides, the risk of developing oral malignancy increased in their partners; hence the likelihood of sexual transmission has been raised (Scully, 2002, 2005). Furthermore, a history of multiple or high number sexual partners (Scully & Bagan, 2009) or oral sex partners has been linked with an increasing risk in developing cancer of the oropharynx, and sexual debut in young age (starting intercourse at a young age) or history of oral

sex with rising risk of base of the tongue and tonsil cancer, indicating to the role of sexually-transmitted HPV (Heck et al, 2009).

An increased risk of developing OSCC has been shown by many investigators in individuals who have undergone organ transplants or young persons with HIV/AIDS, which supports a role of immunosuppression (Grulich et al, 2007; de Visscher et al, 1997; van Zuuren et al, 1988; Flaitz et al, 1995; Flaitz & Silverman, 1998). King and Thornhill (1996) have noted a considerably greater risk of developing oral malignancy including cancer of the lip in immunosuppressed patients with renal transplant.

1.9.9 Socio-economic status and deprivation

OSCC is related strongly to social and economic deprivation with the occurrence of greatest rates in the most underprivileged categories of the population. In men the association is strong, where the risk of cancer development in males was more than four times higher in the most disadvantaged than the least disadvantaged sections (CRC, 2000). Some researchers found that cancer of the lip is more common in the lowest social class by five times than in the highest class (Pukkala et al, 1994).

1.9.10 Oral hygiene

There might be an association between oral carcinoma and bad oral hygiene (Zheng et al, 1990) and many studies have support that by finding head and neck, and oesophageal dysplasia/ cancer in individuals who have poor oral hygiene (Dye et al, 2007; Guha et al, 2007; Abnet et al, 2008) and reporting that individuals who had had dental care were 62% less probably to be diagnosed with cancer of the oral cavity (Holmes et al, 2008). Michaud and coworkers (2008) found that there is a link between bad oral hygiene and slight increases in other malignancies, such as kidney, pancreas, lung, and haematological. Furthermore, other researchers in a recent study pointed that periodontal disease/teeth loss has been linked with oral, lung, upper gastrointestinal and pancreatic malignancies (Meyer et al, 2008). There are vagueness in the mechanisms involved, however polymicrobial supragingival plaque could create a mutagenic interaction with saliva (Bloching et al, 2007).

1.10 Clinical features

1.10.1 Primary site

OSCC is usually preceded by the occurrence of clinically evident premalignant changes or potentially malignant disorders (PMDs) in the oral mucosa, in particular erythroplakia (erythroplasia) and some leukoplakias (Zain et al, 1997; Neville & Day, 2002). The other PMDs (Table1.3) may include actinic cheilitis, oral submucous fibrosis and some lichen planus (Scully et al, 2008; Scully & Bagan, 2009).

Table (1.3) Potentially malignant disorders (Scully & Bagan, 2009).

Approximate malignant potential	**Disorder**	**Known aetiological factors**
Very high (85%+)	Erythroplakia	Tobacco/alcohol
High in some instances (30%+)	Actinic cheilitis	Sunlight
	Chronic candidosis (candidal leukoplakia)	Candida albicans
	Dyskeratosis congenita	Genetic
	Leukoplakia (nonhomogeneous)	Tobacco/alcohol
	Proliferative verrucous leukoplakia	Human papillomavirus (HPV)? most often no history of tobacco/alcohol
	Sublingual keratosis	Tobacco/alcohol
	Submucous fibrosis	Areca nut
	Syphilitic leukoplakia	Treponema pallidum
	Xeroderma pigmentosum	Genetic
Low (<5%)	Atypia in immunocompromised patients	HPV
	Diabetes	Idiopathic

	Discoid lupus erythematosus	Autoimmune
	Fanconi syndrome	Genetic; anaemia
	Leukoplakia (homogeneous)	Friction/tobacco/alcohol
	Lichen planus	Idiopathic
	Paterson–Kelly-Brown syndrome (sideropenic dysphagia; Plummer–Vinson syndrome)	Iron deficiency
	Scleroderma	Autoimmune

Early OSCC frequently presents as a white patch (leukoplakia), red patch (erythroplasia), or admixture of white and red lesion (erythro-leukoplakia), usually well demarcated with a slight roughness (Mashberg et al, 1989). There might be some discomfort, but often there is no pain. In addition, on palpation there is change in the soft tissue elasticity to harder sensation (induration) (Bagan et al, 2010). As time elapse, superficial ulceration might develop on the mucosal surface. As the OSCC grows to an advanced stage, it might develop to an exophytic mass with a papillary or fungating surface; other cancers have an inward pattern of growth (endophytic growth), which is usually characterised by an ulcerated depressed surface with a rolled raised border (Neville et al, 2002; Silverman et al, 1998).

A common symptom in patients with oral malignancy is pain that represents around 30-40% of their chief complaints. Although the main symptom is pain, it generally arises when the tumours become significant in size when at that time the patient seeks medical help. Consequently, most of the early OSCC frequently goes unnoticed since they are totally asymptomatic or could only be associated with minor discomfort (Neville & Day, 2002; Scully & Bagan, 2009). On the other hand, the symptom may vary in larger and advanced oral cancers from mild discomfort to severe pain, particularly in case of tongue, lip and buccal mucosa, there is usually intense pain at advanced stages (Barnes et al, 2005). Other symptoms include otalgia (ear pain), bleeding, teeth mobility, dysphagia, problems in breathing, speech difficulty, problems in fitness of dentures/prosthesis,

trismus and paraesthesia (Haya-Fernández et al, 2004). Bagan and associates (2010) reported that symptoms like otalgia, change in voice, dysphagia, and cervical tumours were more common in malignancies located at the base of the tongue.

Cervical lymphadenopathy may sometimes be presents in patients without any other symptoms. In terminal stages of the disease, patients might develop skin fistulas, severe anaemia, bleeding, and cachexia (Milian et al, 1993).

Jainkittivong and colleagues (2009) in a 432 oral cancers patients study reported that the first signs or symptoms were swelling and/or pain. Other researchers in a 1,425 OSCC case series analysis reported that the main symptoms were ulceration and swelling, followed by pain, bleeding, decreased mobility of the tongue, dysphagia and paraesthesia (Al-Rawi & Talabani, 2008). Gorsky and associates (2004) in a case series analysis of tongue cancers reported that the chief symptom was pain on the tongue (66.5%), while approximately 29% had a lump on the tongue.

OSCC might appear in any location, however the most common site for OSCC is the tongue and floor of the mouth (Hirata et al, 1975; Oliver et al, 1996; Mashberg et al, 1989; Jovanovic et al, 1993; Brandizzi et al, 2008), which accounts for approximately 40% of all oral cancer cases (Neville & Day, 2002). In western countries, it arises in more than 50% of OSCC cases (Bagan et al, 2010). These cancers most often arise on the ventral surfaces and posterior lateral border of the tongue. Other sites of involvement are the gingiva, buccal mucosa, labial mucosa, retromolar area and soft palate. Less common regions include back of the tongue and hard palate. In some geographic locations the most involved site is lip (Silverman, 1998; Neville et al, 2002; Haya-Fernández et al, 2004).

The lateral surfaces of tongue and mouth floor with back extension to the lateral soft palate and tonsillar region combine, which lead to the formation of a region in the oral mucosa similar to horse-shoe that is at highest risk for developing OSCC. There are two chief factors that some authors have pointed to them, which might explain why the horse-shoe shaped region is at great risk: first, these sites are constantly bathed by saliva containing carcinogens (saliva mixed carcinogens) that pool into the bottom of the mouth; secondly, non-keratinised thinner mucosa is covering these areas of the mouth that provides less defense against carcinogens (Jovanovic et al, 1993).

During oral examination, clinician should be attentive of this high-risk areas when a tongue blade or similar instrument is simply utilised to lower the tongue for the purpose of examining the rest of the mouth, subsequently this will lead to hiding the two most common regions for cancer of the oral cavity (Neville & Day, 2002). Cotton gauze is advocated to be used for holding the tongue tip, which allow the tongue to be pulled to either side and upward so that adequate visualisation and thorough examination of the lateral tongue and floor of the mouth can be achieved (National Institute of Dental and Craniofacial Research, 2001).

In addition to the oral cavity, SCC also frequently arises on the oropharynx and the lip. There is striking tendency of vermilion carcinomas for the lower lip, and commonly arise in light-skinned persons who have long history of solar damage. Usually the tumour occurs in an actinic cheilosis, which is a precancerous condition that is analogous to actinic keratosis of the skin. Actinic cheilosis is recognised by vermilion border atrophy that might develop scaly, dry changes. As the lesion advances, ulcerated regions might develop that heals incompletely, which starts to reappear at a later date. Then gradually the evolving malignant lesion becomes a crusted, non-tender, indurated mass or ulcer (Neville et al, 2002; Silverman et al, 1998).

Oropharyngeal malignancies have a similar clinical appearance that is similar to OSCC. They usually arise on the tonsillar region and lateral soft palate, but might also arise from the base of the tongue. Usually symptoms at presentation include difficulty in swallowing (dysphagia), pain during swallowing (odynophagia), and referred pain to ear (Silverman, 2001; Neville et al, 2002).

1.10.2 Metastases

Metastases from OSCC most commonly arise in the ipsilateral (same side) cervical lymph nodes. Submental lymph nodes might initially be involved from cancer of the floor of mouth and lower lip. Tumours that arise close to the midline, cancer of tongue base, and advanced cancer are commonly metastasised to bilateral or contralateral lymph nodes. Involved nodes are generally firm, enlarged and painless to palpation. Usually the involved node feel immovable and fixed to the underlying tissue if its capsule perforated (extracapsular spread) by the tumour cells and invaded into the surrounding connective tissue. More than 30% of OSCC at the time of first evaluation have cervical

metastases that might be occult or palpable (Shah et al, 1990). The reason behind the fact that more than 66% of patients with primary lesions on the tongue have cervical lymph node disease at the time of diagnosis is due to the profuse blood supply and lymphatic drainage that tongue possess (Ho et al, 1992). Distant metastases are most usual in the lungs, however other parts of the body, for example, brain, bone and liver might be affected (Neville & Day, 2002).

1.11 Potentially malignant disorders

1.11.1 Leukoplakia

Schwimmer was first used the term leukoplakia in 1877 to describe a white lesion of the tongue that possibly represented a syphilitic glossitis (Schwimmer, 1877). Leukoplakia is defined by the World Health Organization as "a white patch or plaque that cannot be characterised clinically or pathologically as any other disease." (Kramer et al, 1978). Per se, leukoplakia must be used as a clinical term only and must not be used as a microscopic diagnosis (Shafer & Waldron, 1961). If for instance a white patch in the oral cavity can be diagnosed as some other lesion or condition, for example lichen planus, candidiasis, leukoedema etc. then it must not be considered as an example of leukoplakia (Axéll et al, 1996).

Leukoplakia occurs in about 2% of population (Petti, 2003) and is seen most commonly in middle-aged and older males, with a rising incidence with age (Neville et al, 2002; Bouquot & Gorlin, 1986). Less than 1% of males under the age of 30 years have leukoplakia, but the prevalence escalates to an alarming 8% in males over 70 years of age (Bouquot & Gorlin, 1986). In females aged over 70, the prevalence is nearly 2%. The most common sites are the buccal mucosa, alveolar mucosa, and lower lip; however, lesions in the floor of mouth, lateral tongue, and lower lip are most likely to show dysplastic or malignant changes (Waldron & Shafer, 1975).

Thin or early leukoplakia develops as a greyish-white plaque that is slightly elevated, which might be well defined or might slowly merge into the surrounding healthy mucosa (Neville et al, 2002; Bouquot &Whitaker, 1994) (Fig. 1.1). It develops into a more white and thick lesion as it progress and occasionally evolving a leathery appearance with fissures on the surface of the lesion (referred to as thick or homogeneous leukoplakia) (Fig. 1.2). While granular or nodular leukoplakias (Fig. 1.3)

refer to some white patches that tend to develop surface irregularities, and those lesions that develop a papillary surface are usually known as verruciform or verrucous leukoplakia (Fig. 1.4).

Figure (1.1) Early or thin leukoplakia on the lateral soft palate (Neville & Day, 2002).

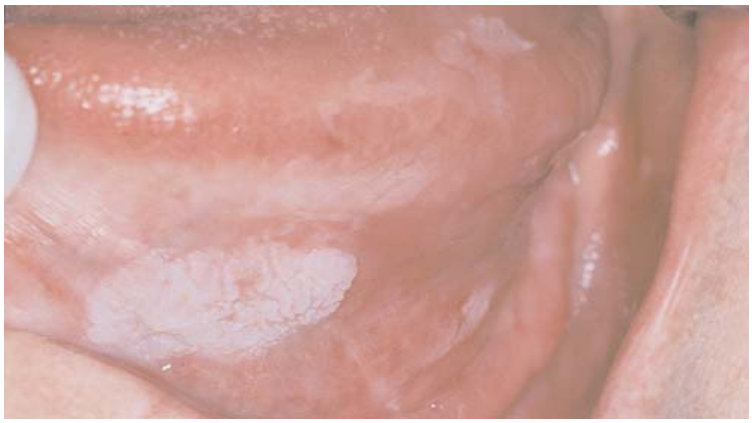

Figure (1.2) Thick leukoplakia on the lateral/ventral tongue. Thinner areas of leukoplakia are visible on the more posterior aspects of the lateral tongue and in the floor of mouth (Neville & Day, 2002).

Figure (1.3) Granular leukoplakia on the posterior lateral border of the tongue. The biopsy showed early invasive SCC. Such a lesion would be easily missed during an oral examination unless the tongue is pulled out and to the side to allow visualisation of this high-risk site (Neville & Day, 2002).

Figure (1.4) Verruciform or verrucous leukoplakia. The papillary component of this lesion on the left side of the picture (patient's right) showed well-differentiated SCC (Neville & Day, 2002).

Proliferative verrucous leukoplakia (PVL) is one of the uncommon variant of leukoplakia characterised by extensive multifocal regions of involvement that usually occurs in individuals without recognised risk factors (Hansen et al, 1985; Kahn et al, 1994; Zakrzewska et al, 1996; Silverman & Gorsky, 1997; Fettig et al, 2000). PVL starts with usual white patches, which are flat initially, but as time elapsed the lesion tend to convert into much thicker and papillary in nature (Fig. 1.5). Another variant of leukoplakias occur blended with adjacent red patches or erythroplasia. This red and white intermingled lesion is called speckled leukoplakia or speckled erythroplasia (Fig.1.6).

Figure (1.5) Proliferative verrucous leukoplakia on the labial gingiva (Neville & Day, 2002).

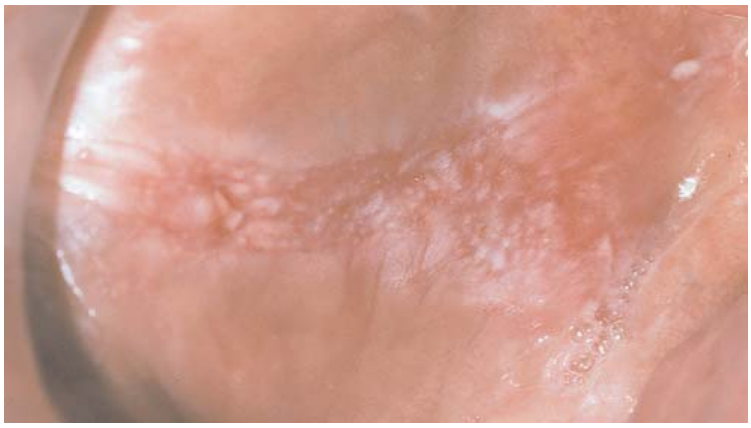

Figure (1.6) Speckled leukoplakia (mixed white and red lesion) of the buccal mucosa (Neville & Day, 2002).

Several studies have reported that the dysplastic or malignant transformation rate in oral leukoplakia could vary from approximately 15.6-39.2% (Shafer & Waldron, 1961; Waldron &Shafer, 1975; Pindborg et al, 1963; Feller et al, 1991).

There is substantial correlation between locations of oral leukoplakia with the rate of finding malignant transformation changes at biopsy. In a clinico-pathologic study of 3256 oral leukoplakia cases, authors reported that the highest risk area was floor of mouth with about 42.9% of leukoplakias presenting some degree of epithelial dysplasia, carcinoma in situ, or unsuspected invasive SCC (Waldron &Shafer, 1975). Other areas that were also identified as high risk regions was lip and tongue, with dysplasia or carcinoma present in approximately 24.0% and about 24.2% of these cases, respectively.

Leukoplakia clinical features might also suggest some association with the possibility that the leukoplakia will demonstrate dysplastic or malignant changes. Generally, the likelihood of finding dysplastic changes will increase when there is thicker leukoplakia. Hence, a verrucous leukoplakia is more possible to display dysplasia compared to a thick homogeneous leukoplakia, which, in turn, is more probable to display dysplasia comparing to a thin leukoplakia. Leukoplakias with an intermixed red component (speckled leukoplakia) are at highest risk for exhibiting dysplasia or carcinoma. Pindborg et al (1963) in a study found that around 51% of speckled leukoplakias showing epithelial dysplasia, while 14% revealed carcinoma.

Several studies have shown that the malignant transformation rates varying from 8.9 to 17.5% (Silverman et al, 1984a; Lind, 1987; Bouquot & Whitaker, 1994). Silverman and coworkers (1984a) reported around 17.5% malignant transformation rate. In this study, only about 6.5% of homogeneous leukoplakias underwent malignant transformation; nevertheless, approximately 36.4% of leukoplakias with evidence of microscopic dysplastic changes and about 23.4% of speckled leukoplakias transformed into malignancy.

PVL is an especially high-risk lesion in contrast with conventional leukoplakia. Silverman & Gorsky (1997) in a follow-up study of 54 cases of PVL reported that around 70.3% of the patients consequently developed SCC.

Though leukoplakia is much common in males than females, many researchers have reported that females with leukoplakic lesions have a greater risk of developing cancer of the oral cavity (Silverman, 1968; Roed-Petersen, 1971; Bánóczy, 1977). In addition, many authors found that the likelihood of leukoplakia to transform into malignancy is higher in individuals who do not smoke than in individuals who do smoke (Einhorn &Wersäll, 1967; Bánóczy, 1977; Roed-Petersen, 1971; Silverman et al, 1984a). This must not be understood as a detraction from tobacco's main role in oral carcinogenesis, however this might indicate that never smokers in whom leukoplakia is originating due to more powerful carcinogenic factors (Neville & Day, 2002).

1.11.2 Erythroplakia

Queyrat was originally used the term erythroplasia to describe a red, premalignant lesion of the penis (Queyrat, 1911). The term erythroplakia is used for a clinically and histopathologically analogous process that appears on the oral mucosa. Erythroplakia, similar to the definition for leukoplakia, is a "clinical term that refers to a red patch that cannot be defined clinically or pathologically as any other condition (Kramer et al, 1978). This definition disregards inflammatory conditions that might cause red clinical appearance.

Oral erythroplakia appears as a red plaque or macule with a soft, velvety texture (Fig. 1.7), which arises more often in older males (Neville et al, 2002) in the fourth to seventh decade of life and has a malignant transformation rates higher than leukoplakia ranging from 14.3-50% (Reichart & Philipsen, 2005). However, several researchers have reported that around 85 to 90% of early asymptomatic cancers of the oral cavity could clinically be described as erythroplakia (Mashberg & Meyers, 1976; Regezi & Sciubba, 1993). The commonest sites of involvement include floor of mouth, lateral tongue, retromolar pad and soft palate. Erythroplakia is frequently well demarcated, although some of them may gradually intermingle into the surrounding oral mucosa. Some lesions might be admixed with white patches, which known as erythroleukoplakia. Usually erythroplakia is asymptomatic, though there might be complains of a sore or burning sensation by some patients.

(Figure 1.7) Erythroplakia on the right lateral border of the tongue (showed carcinoma in situ on biopsy). Adjacent slight leukoplakic changes are also evident (erythro-leukoplakia). (Neville & Day, 2002).

Although erythroplakia is less common than leukoplakia, it is more possible to demonstrate dysplasia or malignancy. In a sister study to their large series of leukoplakia cases, Shafer and Waldron (1975) in a study with 65 cases of erythroplakia of the oral cavity reported that all cases

exhibited some degree of epithelial dysplasia; 51% revealed invasive SCC, 40% were severe epithelial dysplasia or carcinoma in situ (CIS), and the remaining 9% showed mild-to-moderate dysplasia. Thus, leukoplakia is much less worrisome lesion than the true clinical erythroplakia (Meshberg & Samit, 1995). Equally, in a mixed erythroleukoplakia, the white component is much less possibly to show dysplastic changes than is the red component. The clinician must ensure that the red component is included in the specimen when selecting a proper site for biopsy in a mixed lesion (Neville & Day, 2002).

1.11.3 Lichen planus

Lichen planus is relatively common chronic mucocutaneous disease that affects around 0.5-3% of population (Murti et al, 1986; Axell & Rundquist, 1987) which is less common in men than women of 1.5:3 male to female ratio (Mollaoglu, 2000; Mignogna et al, 2001). Other authors reported that lichen planus prevalence is approximately 1% and it mainly affects those age ranges between 30-70 years, remarkably women (Scully & El-Kom, 1985; Kaplan, 1991). Wilson has first described it in 1869, and at the beginning of the 20th century a link with malignant transformation has been suggested (Hallopeau, 1910). The aetiology of lichen planus is idiopathic (Scully et al, 2008; Scully and bagan, 2009). Oral lichen planus (OLP) has a classic appearance of bilateral white lace-like lesions (reticular or papular) on the tongue and buccal mucosa. Other examples of lichen planus include erosive, ulcerative, bullous or atrophic lesions.

Bernard and colleagues (1993) in a retrospective study suggest that there is clinically important malignant potential for lichen planus although it is small. A range of 0.4-5.6 of the annual malignant transformation of OLP has been documented by several studies (Silverman et al, 1985; Murti et al, 1986; Holmstrup et al, 1988; Rajentheran et al, 1999; Eisen, 2002).

1.11.4 Oral submucous fibrosis

Oral submucous fibrosis (OSF) is an irreversible chronic, insidious pre-malignant condition of the oral cavity, oropharynx and upper digestive tract characterised by juxta-epithelial inflammatory reaction and hyalinisation (progressive fibrosis) of the subepithelial stroma (lamina propria and

deeper connective tissues). As the disease advances, the patient experience extreme difficulty in mouth opening, swallowing and speaking (Rajendran, 1994; Cox & Walker, 1996; Aziz, 1997, 2010; Zain et al, 1999). Aetiology of OSF is connected directly to areca nut use, which is very common in the Indian subcontinent, east and Pacific rim countries. Researchers have suggested autoimmune and genetic aetiologies in OSF development, but the consumption of betel nut is considered to be the principal causative factor of OSF (Pindborg and Sirsat, 1966). The rates of morbidity and mortality are related to considerable masticatory dysfunction and oral discomfort, in addition to the rising risk of developing OSCC. OSF malignant transformation rate is ranging from 7-30% (Pindborg and Sirsat, 1966; pindborg et al, 1984; Yusuf & Yong, 2002). In another study in India reported that the rate of malignant transformation is approximately 7.6 %(Murti et al, 1985).

In 1996, global estimates indicated that approximately 2.5 million people have OSF (Cox & Walker, 1996). Nevertheless, in 2002 results from conducted studies (Chiu et al, 2002) indicated that in excess of 5 million people have OSF in India (around 0.5% of the Indian population). Furthermore, it has been estimated by some researchers that about 20% of the world's population use betel nut in some form (Gupta and Warnakulasuriya, 2002). Accordingly, OSF prevalence is probably greater than that noted in the published literature (Aziz, 2010).

1.12 Staging

Staging of oral cancer is essential for establishing appropriate treatment and determining prognosis. TNM system is used to stage tumours, where T represents the size of the primary tumour, N indicates the status of the regional lymph nodes, and M indicates the presence or absence of distant metastases (Table 1.4).

Pierre Denoix has devised the TNM system between 1943 and 1952 for all solid tumour, utilising primary tumour size and extension, its regional lymph node status, and the presence or absence of distant metastases to classify the progression of malignancy (Denoix, 1946).

Union for International Cancer Control (previously named International Union Against Cancer) or UICC (Union Internationale Contre le Cancer) have developed and maintained TNM to accomplish agreement on one internationally recognised standard aimed at classifying the extent of cancer spread. TNM staging system is also used by the American Joint Committee on Cancer (AJCC) and the International Federation of Gynaecology and Obstetrics (FIGO). AJCC and UICC staging systems in 1987 were incorporated into a single staging system.

Primary Tumour (T)

TX Primary tumour cannot be assessed
T0 No evidence of primary tumour
Tis Carcinoma in situ
T1 Tumour 2 cm or less in greatest dimension
T2 Tumour more than 2 cm but not more than 4 cm in greatest dimension
T3 Tumour more than 4 cm in greatest dimension
T4a Moderately advanced local disease★

(Lip) Tumour invades through cortical bone, inferior alveolar nerve, floor of mouth, or skin of face, that is, chin or nose

(Oral cavity) Tumour invades adjacent structures only (e.g. through cortical bone [mandible or maxilla] into deep [extrinsic] muscle of tongue [genioglossus, hyoglossus, palatoglossus, and styloglossus], maxillary sinus, skin of face)

T4b Very advanced local disease

Tumour invades masticator space, pterygoid plates, or skull base and/or encases internal carotid artery

★ *Note*: Superficial erosion alone of bone/ tooth socket by gingival primary is not sufficient to classify a tumour as T4.

Nodal Involvement (N)

NX Regional lymph nodes cannot be assessed
N0 No regional lymph node metastasis
N1 Metastasis in a single ipsilateral lymph node, 3 cm or less in greatest dimension
N2 Metastasis in a single ipsilateral lymph node, more than 3 cm but not more than 6 cm in greatest dimension; or in multiple ipsilateral lymph nodes, none more than 6 cm in greatest dimension; or in bilateral or contralateral lymph nodes, none more than 6 cm in greatest dimension

N2a Metastasis in a single ipsilateral lymph node, more than 3 cm but not more than 6 cm in greatest dimension

N2b Metastasis in multiple ipsilateral lymph nodes, none more than 6 cm in greatest dimension

N2c Metastasis in bilateral or contralateral lymph nodes, none more than 6 cm in greatest dimension

N3 Metastasis in a lymph node more than 6 cm in greatest dimension

---

Distant Metastasis (M)

MX Distant metastasis cannot be assessed

M0 No distant metastasis

M1 Distant metastasis

Stage Grouping

Stage 0	Tis	N0	M0

Stage I	T1	N0	M0
Stage II	T2	N0	M0
Stage III	T3	N0	M0
	T1	N1	M0
	T2	N1	M0
	T3	N1	M0
Stage IV	T4a	N0	M0
	T4a	N1	M0
	T1	N2	M0
	T2	N2	M0
	T3	N2	M0
	T4a	N2	M0
Stage IVB	Any T	N3	M0
	T4B	Any N	M0
Stage IVC	Any T	Any N	M1

Table (1.4) TNM staging of oral cancer (AJCC, 2010).

1.13 Treatment of OSCC

Different treatments methods have been applied for the purpose of treating OSCC including surgery, external beam radiotherapy, photodynamic therapy (PDT), brachytherapy, cytotoxic chemotherapy, cryotherapy, and molecularly targeted pharmacological agents (Shaw et al, 2011).

1.13.1 Surgery

The principal objective of surgical therapy of OSCC is to remove the entire tumour with a healthy tissue (disease free) at the margins, together with any cervical lymph nodes with possibly or proven metastatic involvement (Bogdanov et al, 2008; Shaw et al, 2011). Protection of the airway must be achieved first, with providing sufficient access to the oral cavity, and frequently a temporary tracheostomy is indicated. Usually a neck dissection is achieved next removing the cervical lymph nodes that have a great chance of metastasis or involved. Several purposes can be obtained from neck dissection procedure: the involved nodes are therapeutically removed, appropriate adjuvant therapy will be prescribed by obtaining staging of the neck (staging or diagnostic benefit for

patients), attaining adequate access to the primary tumour, and the use of several neck blood vessels would be permitted in order to achieve microvascular anastamosis and reconstruction of free-flap (Kowalski, 2002; Shaw et al, 2011).

Based on the primary tumour site, the metastatic spread is fairly predictable from head and neck squamous cell carcinoma (HNSCC). There are different groups of lymph nodes found in the neck that are related to OSCC, which are classified into numbered levels; I, II, III, IV and V **(**Fig. 1.8**)**. Following thorough examination of several hundreds of neck dissections for oral cancer, metastases to lymph nodes were found to arise in an inverted cone, where levels I and II have the highest involvement, while levels III, IV and V have increasingly less involvement (Shaw et al, 2011). Primary tumour site affects the metastatic rate to regional lymph nodes. Cancers located on the hard palate or alveolar ridge is less probably to metastasise to lymph nodes in the neck in compare to primary tumours situated in the oral cavity midline structures, for example oral floor or midline oral tongue, where there is increasing risk for bilateral (contralateral) lymph nodes metastases (Ambrosch et al, 1996; Wooglar, 1999).

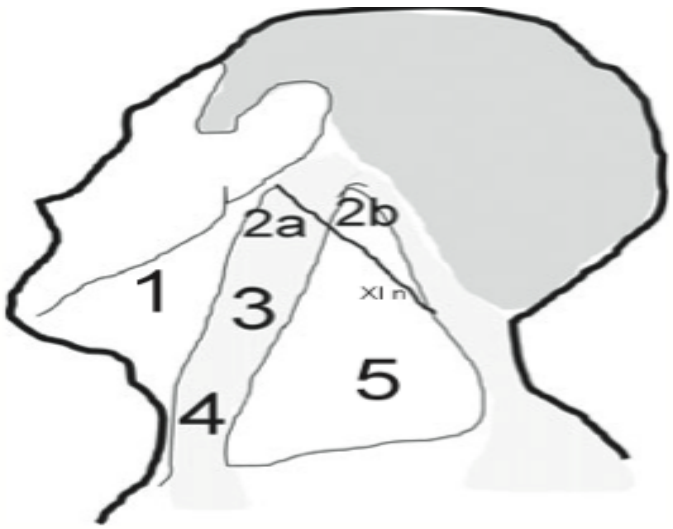

Figure (1.8) Lymph node levels 1-5 (XI n = accessory nerve) (Shaw et al, 2011).

O'Brien and colleagues (2003) reported that a selective neck dissection (SND) in OSCC is performed in most centres with tumour thickness more than 4 mm, addressing the first three levels and sometimes level IV. 'Selective' means that only fascia, lymph nodes and submandibular gland are removed while preserving the accessory nerve, sternocleidomastoid muscle and internal jugular

vein. Elective neck dissection improves loco-regional control rates when performed on patients having an N0 neck tumour (Hughes et al, 1993; Kowalski et al, 2000). Supraomohyoid neck dissection (SOHND) is the most usual neck dissection performed on patients with early cancer of the oral cavity (N0), which removes levels I, II, and III cervical nodes (Spiro et al, 1988). The advancement of selective or functional neck surgery is a rational sequence from the previous forms of radical neck dissection (RND), which was believed that radical excision of levels; I, II, III, IV and V were indispensable. However, Davidson and associates (1993) have realised that level V is seldom linked in OSCC, with around 2.4% in case of clinically positive necks and nearly 0.6% of clinically negative necks, and that shoulder function weakening is unduly related to accessory nerve dissection in level V. Similarly, the lymph nodes that are located posterior to the accessory nerve (level II b**)** are not always removed. In other studies, many researchers advocated the use of sentinel node biopsy, where removal of only the lymph node(s) that directly drain the tumour are performed, and a decision is made in regard to advancement to a more comprehensive neck dissection after analysis of the sentinel lymph nodes (Nieuwenhuis et al, 2003; Ross et al, 2002).

Patients with early stage OSCC have similar survival data that treated with radiotherapy or surgical method, while patients that have advanced oral malignancy are treated best with combined therapy comprising surgical procedure and postoperative radiotherapy. Surgical resection for treating patients with cancer of the oral cavity could be achieved through either the transoral or trans-cervical approach. The approach used is determined by factors including the location and extent of tumour, treatment of suspected or involved nodes in neck area, and planned reconstruction (Day et al, 2003).

In many stage I and stage II oral cavity cancers, surgery can be accomplished without external incisions. In order to confirm complete clearance of the microscopic tumour, a margin of about 1-2 cm of healthy-appearing tissue must be removed. External or trans-cervical approach is required in advanced malignancy, as well as neck dissection, to permit for comprehensive cancer tissue removal, lymphadenectomy (lymph node removal) and reconstruction. Tumour metastases and spread might be assisted by the course of different nerves within the oral cavity that act as routes for tumour invasion. Tumours of the lower alveolar bone might spread to the base of the skull tracking along the inferior alveolar nerve (branch of the mandibular nerve), while tumour of the hard palate

may infiltrate into the pterygo-palatine fossa and base of the skull tracking along the greater and lesser palatine foraminae through the course of the corresponding nerves (Day et al, 2003).

There are similarities in the survival rates amongst these different treatment modalities, which depend upon patient selection, and vary between 83-93% for early tumours (Mazeron et al, 1990; Cole et al, 1994). Majority of tongue cancer patients are treated with surgical resection, plus control of margins and neck dissection. The most challenging structure receiving treatment with radiotherapy is the tongue due to factors such as mobility, diffuse toxicity of radiotherapy through the mucosa, and vicinity to teeth and mandible. Due to the high rates of occult metastatic spread into the cervical nodes, neck irradiation or dissection is crucial in most cases. Many researchers reported that patients with early stages of tongue cancers such as T1 or T2 have local control rate of about 60-80% and a lower survival rate, while the survival rate is below 50% in patients with advanced stage of tongue cancers (Spiro & Strong, 1971; O'Brian et al, 1986). Zelefsky and associates (1990) in another study have reported that the five-year local control rate is around 62% in those patients with stage III and IV cancers of the tongue who were treated with combined surgery and radiation therapy.

1.13.2 Radiotherapy

Opinion regarding treatment of cancer of the oral cavity has generally preferred primary surgery to radiotherapy, although at some other HNSCC sites the role of radiation therapy as a primary method is well established. The high rate of osteoradionecrosis in cancers adjacent to the mandible is the main downside of primary radiotherapy in treating OSCC. Radiation therapy modalities have usually been divided into external beam radiation therapy (EBRT) or localised / interstitial forms known as brachytherapy (also called internal radiotherapy). EBRT application (with or without brachytherapy) has provided an alternative to surgical treatment of patients with cancer of the oral cavity. Patients in early cancer stages, EBRT has similar cure rates, though complications might constraint its use in early stages of tongue cancers and other oral cavity subsites (Wendt et al, 1990). Brachytherapy with implanted sources, for example iridium 192 have been in moderately common use in cases of SCC of mobile tongue; nonetheless, there seem to be lower rates of local control than of primary surgery (Henk, 1992; Podd et al, 1994) and these modalities are more likely appropriate to cancers in early stage, for which surgical method is of optimal advantage as well. There is agreement in general, that primary radiotherapy must not be applied for treating oral cancer

with frank bony invasion because of high complication rates and poor control (Shaw et al, 2011).

The value of radiation therapy post-operatively is well established, though there is still controversy concerning the precise criteria for prescription (Brown et al, 2007). In cases with extracapsular spread in lymph nodes of the neck or frank involvement of the surgical margins, radiotherapy in a post-operative setting is indicated, but it should not be used in cases with uninvolved cervical lymph nodes and clear surgical margins of more than 5 mm (Peters et al, 1993; Shaw et al, 2011). In order to lessen osteoradionecrosis incidence, it is imperative to prudently assess and treat patients' dentition being considered for radiotherapy (Shaw et al, 2011).

In recent years numerous tries have been made to enhance the therapeutic ratio of EBRT in head and neck area. This therapeutic ratio is reflecting control of cancer and survival outcomes set against radiotherapy acute (or early) and late complications. The acute sequelae include lack of energy, mucositis, radiation dermatitis, changes in taste, and xerostomia, while late complications include persistent mucositis, xerostomia, laryngeal oedema (epiglottis and arytenoids), hypothyroidism, skin changes, hair loss, and changes in speech and deglutition. Secondary cancers induced by radiation and osteoradionecrosis of the mandible might appear many years following radiotherapy, however this is rare (Day et al, 2003). One of the optimisation method is altered fractionation regimens (fractionation radiotherapy), which has been introduced in the past few years including accelerated fractionation and hyper-fractionation with the goal of rising the intensity of the dose and lessening treatment time, thereby decreasing cancer cell re-population chances between sessions (Bernier, 2005). Accelerated fractionation designed to rise the intensity of the radiation dose by delivering 1.5-1.8 gray (Gy) fractions more than once daily with a total dose of 10 Gy weekly. Hyper-fractionation delivers two or three fractions daily with a reduced dose/fraction ranging from1.0–1.2 Gy/fraction to a total of 81.6 Gy, with reduction in toxicity and improve effectiveness has been reported (Argiris, 2005).

Patients receiving treatment at the primary cancer site must receive standard doses of radiotherapy of 2 Gy conventional fractions ranging from 66-70 Gy. Radiation dose in postoperative setting varies from 56-66 Gy that depends on risk factors with gross residual disease receives 70 Gy (Day et al, 2003).

Other novel techniques include intensity-modulated radiotherapy (IMRT) that targets to optimise the dose to primary site of the tumour and draining nodes and to significantly reducing the dose of the radiotherapy to vital neighbouring structures such as salivary glands, mandible, middle ear and spinal cord. Chao and coworkers (2001) in a study have reported that the possible advantage for patients through toxicity reduction, locoregional recurrence, long-term survival, and functional outcomes applying IMRT have not been determined. However, Nutting and associates (2011) in a recent phase III randomised clinical trial have showed that salivary glands sparing by using IMRT will considerably decreases xerostomia incidence in patients with cancers of the pharynx.

In definitive radiotherapy or chemoradiation therapy the duration of total treatment must stay from 8-10 weeks, while in the adjuvant setting, the total treatment duration from surgery to the termination of radiation therapy should not surpass 12 weeks since extension of total treatment time results in high rates of locoregional failure (Day et al, 2003).

1.13.3 Chemotherapy

Previously systemic antineoplastic drug therapy (chemotherapy) had been used as a monotherapy in cancers of the oral cavity with somewhat poor results; nonetheless, currently the role of chemotherapy becoming well defined. Cisplatin, fluorouracil and methotrexate were the most frequently used chemotherapeutic agents. Generally, good responses (although transient) with monotherapy are seen in around 15–30% of cancer cases (Vermorken, 2005). The most established chemotherapy role in OSCC is the concurrent use of radiotherapy and cisplatin post-operatively or for treatment of un-resectable cancers (Cohen et al, 2004; Vokes et al, 2000). Many researchers in several clinical trial studies showed that better results were yielded by chemoradiotherapy than radiation therapy alone plus the locoregional tumour control has improved (Calais et al, 1999**;** Cooper et al, 2004, 2006; Adelstein et al, 2000; Lamont & Vokes, 2001).

In other head and neck cancer primary sites, the synchronous use of chemotherapy plus radiation therapy is encouraging. A study by Bourhis and colleagues (1998) indicated that survival rate of patients with HNSCC has improved when chemotherapy has been used in the treatment regimen. Concurrent and sequential chemoradiotherapy are proven substitutes to radical surgery and

radiotherapy for patients with laryngeal and hypopharyngeal malignancies and to radiotherapy for patients with cancer of the oropharynx (Lefebvre et al, 1996; Brizel et al, 1998; Calais et al, 1999).

Cisplatin is a standard chemotherapeutic agent in combination with radiotherapy, however taxanes-based compounds have also proven to be active (Argiris, 2005). Recently, an international consensus has been reached supporting the 'TPF' (taxanes, platinum, and fluorouracil) regimen (Vermoken et al, 2007). In HNSCC trials, a number of epidermal growth factor receptor (EGFR) inhibitor drugs have been used, however Cetuximab is regarded as less toxic for chemoradiotherapy combination (Bonner et al, 2006; Karamouzis et al, 2007).

Chemotherapy alone for patients with recurrent OSCC is palliative. The majority of the regimens have used cisplatin plus fluorouracil or paclitaxel. Hydroxyurea, carboplatin, and docetaxel have also used combined with radiotherapy. Chemotherapy might be used as palliative for symptoms in patients with distant metastases, particularly those without previous systemic therapy (Forastiere, 1992).

Chapter 2

Literature review concerning visual aids in oral cancer diagnosis

Chapter 2

Visual aids in oral cancer diagnosis

2.1 Knowledge gap and research need

In spite of the great improvement and the prognosis of a number of malignancies, parallel enhancement has not been observed with oral cancer (Silverman, 2001; Swango, 1996; Goldberg et al, 1994). As five-year survival rate is closely associated with stage at diagnosis, research on prevention and early detection has the potential for declining the incidence and also for survival improvement in those patients who develop this disease. Early diagnosis currently relies on skilled clinicians who could identify mucosal abnormalities while is still at an early stage. Nonetheless, it is obvious that many clinicians are not doing routine oral cancer examinations and/or might not be well-informed concerning early detection, risk factors, and diagnosis of these malignancies (Yellowitz & Goodman, 1995; Arvidson-Bufano et al, 1996; Blank et al, 1996; Yellowitz et al, 1998, 2000; Horowitz et al, 2000, 2001).

Premalignant and early oral malignant lesions are usually asymptomatic and subtle. Hence, maintaining the highest index of suspicion by the clinician is imperative, particularly where risk factors are existed, for example tobacco use or heavy alcohol consumption. Invasive OSCC is frequently preceded by the occurrence of clinically recognisable precancerous changes of the oral mucous membrane (Neville & Day, 2002). Annual cancer-related check-up has been recommended by the American Cancer Society (ACS) for all individuals aged 40 years and older, while every three years for those whose ages ranging from 20-39 years. This must involve health counselling and, depending upon an individual's age, may include examinations for oral cancer and cancers of the skin, lymph nodes, thyroid, testes, and ovaries (Smith et al, 2002).

Regrettably, little improvement in the early detection of cancer of the oral cavity has been observed. Patient delay can be defined as the amount of time taken by patients to request the initial professional advice since becoming aware of symptoms. Patients are considered to have delayed if more than 3 weeks had elapsed between first observing signs or symptoms and requesting a

professional advice, as the recommendation from public health promotion literature explains that patients must request professional medical advice, who complaining of symptoms, such as oral ulcers that do not heal for 2 weeks (Neville & Day, 2002; Pitiphat et al, 2002; Llewellyn et al, 2004c).

Public education is as yet cardinal in rising public knowledge of OSCC from an early age. Wanakulasuriya and associates (1999b) in a research have pointed to an alarming shortage of public awareness of symptoms of oral malignancies amongst the general public in Britain. It is essential for continued education amongst health care professionals, for example general medical practitioners and general dental practitioners if cancer of the oral cavity is to be detected early and diagnosed without delay (Schnetler, 1992). It would be judicious though, to state that research from the US indicate that general dentists are not as well-informed as they could be concerning prevention and early detection of oral malignancy, notwithstanding that most of the dentists report that they achieve examinations for oral cancer (Yellowitz et al, 2000; Horowitz et al, 2001). Contrasting to this, a study by Horowitz and Nourjah (1996) in a national survey reported that only about 14% of US adults recalled ever having mouth cancer examination, and in another study from New York, Cruz and coworkers (2002) have found that only around 12% of adults reported ever having mouth cancer examination. Thus, burden is on both professional development and raising people's awareness (public education) so as to improve early detection of oral malignancies plus encouraging patients to eschew high risk behaviours and to request their health care providers concerning regular screening of oral cancer examinations (Neville & Day, 2002; Llewellyn et al, 2004c).

Various new and emergent optical diagnostic techniques are becoming available to clinicians, to assist them in early recognition and diagnosis of oral premalignant and malignant lesions, with a range of desirable features including: in vivo and in real-time information, non-invasiveness, absence of ionising radiation, patient friendliness, repeatability, and high-resolution surface and subsurface images (Wilder-Smith et al, 2010). Existing visual diagnostic aids developed for the early recognition of oral malignancy include tolonium chloride or toluidine blue (TB) dye, ViziLite Plus; Microlux/DL, and numerous imaging techniques, for example VELscope and multispectral optical imaging systems. None of these methods to date have revealed equivalency or been

established to be superior to clinical examination (Lingen et al, 2008; Trullenque-Eriksson et al, 2009).

2.2 Toluidine blue

Toluidine blue (TB) or tolonium chloride staining is an inexpensive and simple diagnostic aid, which uses a vital blue dye that is thought to stain nucleic acids and highlight abnormal regions of oral mucosa. TB for many years has been used as a tool to identify clinically ambiguous oral mucosal abnormalities and as a helpful method for demarcation of the potentially malignant lesion (PML) extension before excision. TB is staining nuclear material of PML and cancerous lesions, while normal oral mucosa is not stained (Mashberg, 1983; Epstein et al, 2003; Warnakulasuriya & Johnson, 1996; Onofre et al, 2001; Martin et al, 1998; Gandolfo et al, 2006; Scully et al, 2008). Patient first rinse the mouth with 1% acetic acid for 20 seconds, then rinsing with water twice for 20 seconds; followed by rinsing the mouth with 1% toluidine blue solution; and rinsing with 1% acetic acid solution for around one minute and after that a water rinse (Scully et al, 2008).

A recent study by Lingen and colleagues (2008) suggests that TB sensitivity is considerably lower in detecting dysplasia than in detecting carcinoma (Epstein et al, 2007; Lingen et al, 2008). Moreover, the high proportion of TB false positive stains weakens its application as a valid screening method in primary care settings (Lingen et al, 2008; Patton et al, 2008). Additionally, debate exists about the subjective mucosal staining interpretation and criteria for positive results, for example pale royal blue versus dark royal blue staining (Lingen et al, 2008).

False positive staining (lesions take the blue stain, however no malignancy is recognised after taking biopsy) occurred in approximately 8-10% of cases related with regeneration of ulcers and erosions edges and keratotic lesions (Epstein et al, 2003). Rosenberg & Cretin (1989) in a meta-analysis evaluating TB for identifying oral cancer have reported a sensitivity ranging between 93-97% and specificity between 73-92%. However, other researchers in a recent study suggested that the sensitivity in detecting OSCC by TB staining ranging from 78-100%, while the specificity is between 31-100% (Lingen et al, 2008).

Many investigators in several study reported that TB stain might recognise high-risk PMLs that have poor outcome (Zhang et al, 2005; Guo et al, 2001; Silverman et al, 1984b) and positive TB staining might be associated with genetic changes (loss of allelomorph or loss of heterozygosity

[LOH]) which is linked to development to oral cancer even in lesions that have mild dysplasia and benign lesions on histology (Zhang et al, 2005; Guo et al, 2001).

2.3 Light-based detection systems

2.3.1 Chemiluminescence (ViziLite Plus; Microlux/DL)

It has been suggested that rinsing the mouth with a dilute acetic acid solution and performing clinical examination under a chemiluminescent blue/white light (ViziLite) (Lingen et al, 2008; Patton et al, 2008; Ram & Siar, 2005; Epstein et al, 2006; Kerr et al, 2006; Farah & McCullough, 2007; Oh & Laskin, 2007; Scully et al, 2008) could help to identify oral mucosal lesions.

This non-invasive screening technology (ViziLite system – Zila Pharmaceuticals, Phoenix, AZ) consists of rinsing for 1-minute with 1% acetic acid solution, after that the oral mucosa is examined under diffuse blue/white light with a moderately short wavelength with peak outputs near 430, 540 and 580 nm for illuminating the oral cavity. The dilute acetic acid in this technique dries the oral mucous membrane slightly plus eliminating the glycoprotein barrier, the blue/white light then absorbed and reflected by the abnormal mucosal cells in a different way in compare to normal cells (Lingen et al, 2008; Patton et al, 2008; Ram & Siar, 2005; Epstein et al, 2006; Kerr et al, 2006; Farah & McCullough, 2007; Oh & Laskin, 2007; DeCoro & Wilder-Smith, 2010). Consequently, light reflected by abnormal squamous epithelial sites (because of higher nuclear/cytoplasmic ratio of epithelial cells) and appear white when viewed under a diffuse low- energy wavelength light with distinct margins that appear sharper and brighter, while normal epithelium will absorb the light and appear dark (blue) (Ram & Siar, 2005; Epstein et al, 2006; Kerr et al, 2006; Farah & McCullough, 2007; Oh & Laskin, 2007; DeCoro & Wilder-Smith, 2010).

Lately both TB and ViziLite systems have been combined and a new device (MicroLux/ DL, AdDent Inc., Danbury, CT, USA) has been introduced (Poate et al, 2004; Epstein et al, 2008). McIntosh et al (2009) in a prospective study reported that Microlux DL sensitivity were 77% in detecting pre-malignant and malignant oral lesions while specificity were 70%.

It must be emphasised that no study has revealed that the chemiluminescence could assist in discrimination between benign lesions and dysplasia/malignancy (Lingen et al, 2008; Patton et al, 2008). Therefore, most of the studies have considered how chemiluminescence improves subjective clinical evaluation of lesions in the oral cavity including sharpness, brightness, and texture in compare to conventional clinical examination. The results have been paradoxical due to highly subjective of these parameters (Lingen et al, 2008; Patton et al, 2008). Although some researchers reported that ViziLite might increase oral mucosal abnormalities detection irrespective to their nature, other authors have reported that there was no significant improvement in the general detection rate and that the reflection produced by the chemiluminescent light had made visualisation more challenging in contrast to normal incandescent light (Lingen et al, 2008; Patton et al, 2008; Ram & Siar, 2005; Epstein et al, 2006, 2008; Kerr et al, 2006; Farah & McCullough, 2007; Oh & Laskin, 2007). Many authors in some studies reported that chemiluminescence might assist in detecting ambiguous lesions undetectable with incandescent light, yet there is no strong evidence to support that (Lingen et al, 2008; Patton et al, 2008).

2.3.2 Tissue fluorescence imaging

Early recognition of oral mucosal lesions can be improved by fluorescence use. In the dark, all tissues tend to glow (fluoresce), either spontaneously (auto-fluorescence) or by application of an external sensitiser to the tissues. The tissue fluoresces because the cells contain fluorescent chromophores (also known as fluorophores). Fluorophores that are most commonly detected include flavin adenine dinucleotides (FAD), nicotine adenine dinucleotide hydrogenase (NADH), collagen, elastin, haemoglobin and vascular supply and oral microbial flora, and they differ in dissimilar tissues including different regions in the oral cavity. Changes in the tissue might influence both the fluorophores and tissue fluorescence, and this in turn could aid in the detection of lesions undetectable with the unassisted eye under normal incandescent white light (Gillenwater et al, 1998a; Gillenwater et al, 1998b; Schantz et al, 1998; Heintzelman et al, 2000; Muller et al, 2003; Ingrams et al, 1997; Inaguma & Hashimoto, 1999; Kulapaditharom & Boonkitticharoen, 2001; de Veld et al, 2005a, 2005b, 2005c; Svistun et al, 2004).

Tissue autofluorescence for decades has been described in the premalignant and early cancer screening and diagnosis of uterine cervix, lung and skin. Lately, it has also extended into the oral cavity field (Farrell et al, 1992; Poh et al, 2006; Poh et al, 2007; Roblyer et al, 2009; Rosin et al, 2007; de Veld et al, 2005c). The notion of tissue autoflorescence is that changes happening in the metabolism, for example flavin adenine dinucleotide concentration (FAD) and nicotinamide adenine dinucleotide hydrogenase (NADH) and structure of the epithelium, for instance hyperkeratosis, hyperchromatin and increased cellular/nuclear pleomorphism, as well as changes of the subepithelial stroma, for example elastin and collagen matrix composition, alter their interaction with light (Lingen et al, 2008; de Veld et al, 2005c). These epithelial and stromal changes precisely could alter tissue fluorophores distribution and consequently the way that tissue produce fluorescence after stimulating the tissue with intense light, which is usually excitation with blue light with a wavelength ranging from 400 to 460 nm. The clinician can visualised directly the autoflorescence signal. The normal mucosa in the oral cavity emits a pale green autofluorescence when observed through the instrument handpiece, while abnormal tissue reveals reduced autofluorescence and looks darker than the surrounding healthy tissue (Poh et al, 2006; Roblyer et al, 2009; Rosin et al, 2007). One of the examples of tissue fluorescence imaging systems that has been marketed is VELscope system (Visually Enhanced Lesion Scope) (Lingen et al, 2008; Patton et al, 2008; de Veld et al, 2005c).

The efficiency of the VELscope system has been investigated by some studies as an aide to visual examination for improving the discrimination between normal and abnormal tissues (benign and malignant changes), distinguishing between benign and dysplastic/malignant changes, and detecting dysplastic/malignant lesions or margins of the lesion, which are under white light invisible to the naked eye. Generally, the quality of available studies is considerably superior in compare to TB and chemiluminescence studies since the sensitivity and specificity of VELscope system in all patients studied was compared to gold standard histopathology (Lingen et al, 2008; Patton et al, 2008; de Veld et al, 2005c; Onizawa et al, 1996; Schantz et al, 1998; Onizawa et al, 1999). In a study de Veld and colleagues (2005c) reported that lesions contrast has been probably improved by autofluorescence imaging of the oral cavity, hence increase the capability to differentiate healthy oral mucosa from mucosal lesions, though additional research are required in diverse populations.

Furthermore, the ability of autofluorescence has been examined in a few studies to discriminate between different lesion types and in general the technique appears to demonstrate high sensitivity, but low specificity (de Veld et al, 2005c). Still, the VELscope technique appears to be very encouraging because of its capability and efficiency in recognising lesions and margins of the lesion, which are unclear to visual examination performed under white light. VELscope showed high sensitivity and specificity in detecting dysplasia and cancer areas that extended beyond the clinically evident tumours were histopathology applied as the gold standard (Lingen et al, 2008; Patton et al, 2008; de Veld et al, 2005c; Onizawa et al, 1996; Schantz et al, 1998; Onizawa et al, 1999).

Nevertheless, it must be emphasised that these results are not from clinical trials and that the results generated from case reports and series and that no published studies on VELscope system assessment to be regarded as a diagnostic adjunct in screening individuals at lower-risk, for instance patients seen by primary care providers or those individuals without a history of dysplasia/OSCC (Lingen et al, 2008; Patton et al, 2008; de Veld et al, 2005c; Onizawa et al, 1996; Schantz et al, 1998; Onizawa et al, 1999; Poh et al, 2007; Rosin et al, 2007).

2.3.3 Tissue fluorescence spectroscopy

Lately a technique called autofluorescence spectroscopy been tested in the research of oral oncology. The autofluorescence spectroscopy system comprises of a small optical fibre that creates different excitation wavelengths and a spectrograph, which receives and records on a computer and analyses by the aid of dedicated software the spectra of the fluorescence that are reflected from the tissue (Lingen et al, 2008; Patton et al, 2008; de Veld et al, 2005c; Inaguma & Hashimoto, 1999). The subjective interpretation of the changes in tissue fluorescence can be eliminated by applying autofluorescence spectroscopy system, which is the main advantage of this method. Still, the disadvantage is that more variables, for instance methodology for analysing fluorescence, combination of wavelengths etc. required consideration and testing and this in turn has resulted in debatable and frequently unclear results. Generally, autofluorescence spectroscopy appears to be very accurate for differentiating healthy oral mucosa and abnormal mucosal lesions with high percentage of sensitivity and specificity, particularly when healthy mucosa is contrasted to

malignant tumours. Nevertheless, it has been reported by many authors that the ability of the technique is low in discriminating and categorising various types of lesion (Lingen et al, 2008; Patton et al, 2008; de Veld et al, 2005c; Inaguma & Hashimoto, 1999). Besides, autofluorescence spectroscopy is not suitable for practical reasons to demarcate sizeable lesions or distinguish new lesions as only small mucosal area can be sampled by the optical fibre (Lingen et al, 2008; Patton et al, 2008; de Veld et al, 2005c; Inaguma & Hashimoto, 1999). This bounds the application of spectroscopy modality to the assessment of a small well-defined mucosal lesion, which has been previously recognised through visual inspection, with an effort to elucidate its benign or precancerous/cancerous nature. Further investigation is required for backing this clinical application of autofluorescence spectroscopy (Fedele, 2009).

2.3.4 Optical coherence tomography

Optical coherence tomography (OCT) is an emerging imaging technique that use broadband light and based on low coherence Michelson interferometry and provide non-invasively and in real time a cross-sectional, high-resolution subsurface biological tissue images (Izatt et al, 1994a; Fercher, 1996; Schmitt, 2001; Wilder-Smith et al, 2009b). It has been demonstrated in preliminary studies that detection and diagnosis of oral precancerous lesions can be achieved by using OCT (Wilder-Smith et al, 2009b). This topic will be discussed in depth in the next chapter. Some other potential diagnostic systems are listed in table (2.1).

Table (2.1) Other potential future diagnostic technologies (Scully et al, 2008).

Laser-induced fluorescence spectroscopy
Light-induced fluorescence spectroscopy
Elastic scattering spectroscopy (ESS)
Raman spectroscopy
Photoacoustic imaging
Photon fluorescence
Orthogonal polarisation spectral (OPS) imaging
Quantum dots
Trimodal spectroscopy
Doppler OCT
Nuclear magnetic resonance spectroscopy
Chromoendoscopy
Narrow band imaging (NBI)
Immunophotodiagnostic techniques
Differential path length spectroscopy
Two-photon fluorescence
Second harmonic generation
Terahertz imaging

Chapter 3

Optical coherence tomography

Chapter 3

Optical coherence tomography

3.1 Historical aspect of OCT

In the last 10-15 years, optical coherence tomography (OCT) has evolved from a promising biomedical imaging method to a standard technique in some fields of medicine. OCT is a non-invasive imaging modality that permits in-situ and in real-time a cross-sectional evaluation of transparent (retina of the eye) and turbid (skin or oral mucosa) biological tissues. Based on low coherence interferometry (LCI), OCT produce depth profiles that are parallel to the ultrasound A-scans (Gambichler et al, 2011). This A-scan technique has been developed and applied for eye length measurements (Fercher & Roth, 1986; Fercher et al, 1988). Fercher (1993) has revealed the initial 2-dimensional (2-D) structure B-scan images. Other groups have picked up this concept and were further sophisticated through cooperation between Lincoln Laboratory, Massachusetts Institute of Technology (MIT) and the New England Eye Centre, Tufts University School of Medicine, the Department of Electrical Engineering and Computer Science at MIT. In the past two decades, Huang and colleagues (1991) in a study reported the first in vitro tomography of the human eye. In 1993, many authors have claimed the first in vivo tomography images of the human macula and optic disc (Fercher et al, 1993; Swanson et al, 1993). The OCT application in ophthalmology resulted in the advanced diagnostic abilities and in 1996, OCT technology presented commercially for ophthalmic diagnostics (Humphrey Systems, Dublin, CA, later acquired by Carl Zeiss Meditec) (Gambichler et al, 2011; Fujimoto et al, 2000). Since then OCT clinical and experimental applications have exponentially been established in the medical fields. OCT is applied in many areas of medicine: gastroenterology, urology, surgery, cardiology, neurology, gynaecology, pneumology, rheumatology and dentistry for research and clinical practice (Cahill & Mortensen, 2010; Chu et al, 2007; Drexler, 2004; Fujimoto, 2003; Lamirel et al, 2009; Schmitt, 1999; Tearney et al, 1997; Unterhuber et al, 2004).

OCT was introduced in 1997 in dermatology and currently there is increase in application of this technology in clinical skin studies (Welzel et al, 1997). With application of OCT, the stratum corneum (horny layer) of glabrous skin (palmo-plantar region), the epidermis and the upper dermis

can obviously be recognised. Besides, blood/lymphatic vessels and skin appendages, for example hair and sweat glands can be identified. For micro-morphological analysis histopathology still represents the gold standard, but skin biopsies are traumatic and cannot be repeated on identical skin location. Consequently, diagnosis and monitoring of skin changes by application of in-situ and in real time non-invasive imaging modalities might improve dermatologic practice and research (Gambichler et al, 2007a, 2007b; Altintas et al, 2009; Treu et al, 2011). Examples of some OCT instruments for dermatological purposes that are already existing on a commercial basis includes Michelson Diagnostics, Kent, United Kingdom; IMALUX, Cleveland, OH, USA; Bioptigen, Durham, North Carolina, USA; and Thorlabs, Newton, NJ, USA (Gambichler et al, 2011).

3.2 OCT technology

3.2.1 Principles and operation

The principle of OCT imaging technique is corresponds to that of B-mode ultrasonography imaging except that OCT uses near infrared (NIR) light rather than sound waves. Generation of cross-sectional image is achieved by scanning an optical beam across the sample of interest (biological tissue) and measuring the time of flight delay (echo time delay) and intensity of backscattered or backreflected light (Fig. 3.1 a, b). Since the light velocity is extremely high, the echo time delay of light cannot be measured directly by electronic detection as in ultrasound. Sound velocity in water is nearly 1500 metre/second, while light velocity is approximately 3×10^8 metre/second or 3×10^5 kilometre/second. OCT is based on more than a century old principle of Michelson interferometer (low coherence interferometry) that is akin to white-light interferometry (Fig. 3.1c), first described by Sir Isaac Newton (Fujimoto et al, 2000; Fujimoto, 2003). In low-coherence interferometry, the backscattered or reflected light from inside the sample is measured by correlation with light that travelled for a known reference path. Opto-electronic devices (optical-to-electrical or electrical-to-optical transducers) have been applied this technique to accomplish micrometre resolution optical ranging and measurement (Youngquist et al, 1987; Takada et al, 1987; Gilgen et al, 1989). Measurements of corneal thickness and axial eye length are examples of some of the first biomedical applications of low-coherence interferometry (Fercher et al, 1988; Huang et al, 1991).

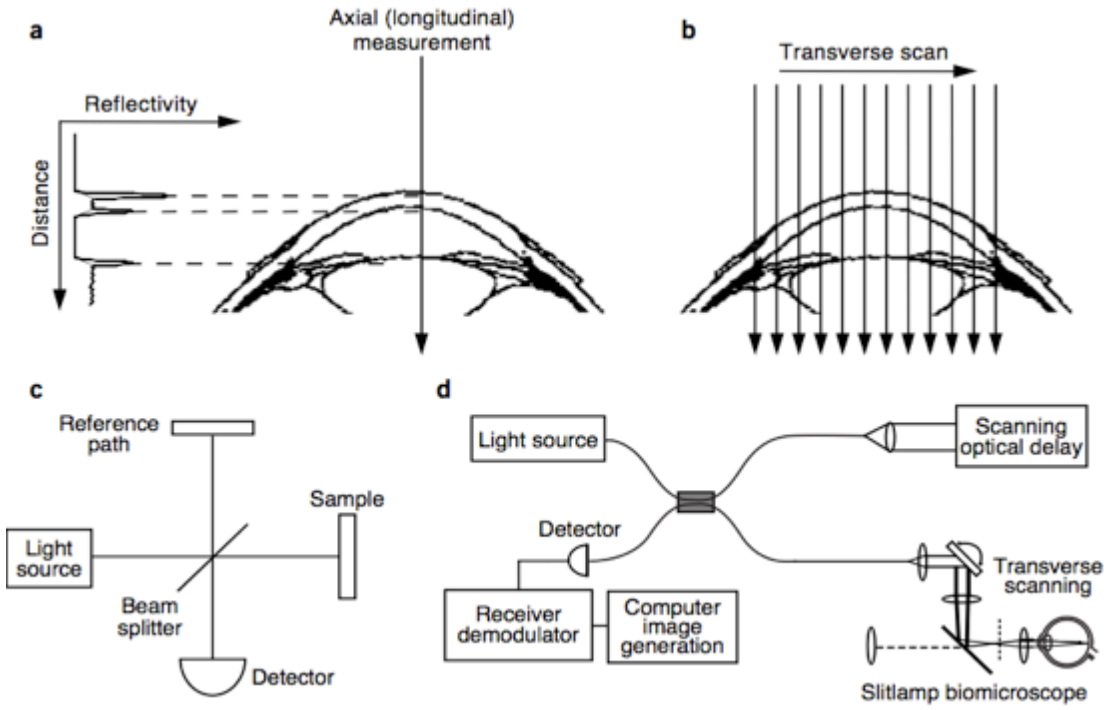

Figure (3.1) Principles of OCT imaging. (**a**) OCT performs cross-sectional imaging of internal microstructure in tissue by measuring the echo time delay and magnitude of reflected light. (**b**) Cross-sectional images are generated by scanning the incident light beam at different transverse positions. The resulting two-dimensional data set can be displayed as a gray-scale or false-colour image. (**c**) Echo time delays of light are measured using low coherence interferometry with a Michelson-type interferometer and low-coherence light source. (**d**) Fibre-optic implementations provide a compact and robust system that can be interfaced to a wide range of imaging instruments. (Fujimoto, 2003).

OCT imaging is performed using a fibre-optic Michelson interferometer with a low-coherence-length light source. The application of fibre-optic provides a robust and compact system, which can be integrated to a numerous clinical imaging instruments. Light sources that generate low coherence light in OCT instrument include compact superluminescent semiconductor diodes (SLD) or other sources, for example solid-state lasers. One arm of the interferometer contains a modular probe (called sample arm) that focuses and scans the light onto the specimen plus collecting the backreflected light. The second arm of the interferometer is a reference path with a revolving mirror or scanning delay line. Optical interference occurs between the light from both the reference and sample paths only when the distance travelled by the light in both paths matches to within the coherence length of the light (Swanson et al, 1992). The interference fringes are detected and

demodulated to generate a measurement of the magnitude and echo delay time of backscattered or backreflected light from microstructures inside the tissue sample of interest. Therefore, low coherence interferometry allows femtosecond time resolution of optical echoes, matching to micron-scale distance measurement.

In OCT system, the 2-D cross-sectional images of the microstructure inside the sample are made by scanning the optical beam and performing multiple longitudinal (axial) measurements of backreflected light at different transverse locations. The developing data set is a 2-D array that represents the optical backreflecting within a cross-sectional slice of the tissue sample of interest. These data can be filtered digitally, then processed and displayed as a 2-D false colour or grey scale image. In addition to cross-sectional plane imaging, it is also possible to image in en face planes at a given depth (Izatt et al, 1994b; Podoleanu et al, 1998, 2000).

The longitudinal (axial) resolution of the image is independent of numerical aperture and beam focusing conditions, while it depends upon the coherence length of the light source. For OCT imaging SLDs are commonly used that typically have 10-15μm longitudinal resolution. To identify individual cells or evaluating subcellular structures, for example nuclei, this resolution is insufficient to achieve that (Drexler et al, 1999). The transverse (lateral) resolution for OCT image depends on the beam spot size that focuses on the tissue sample (imaging aperture), as in microscopy (Swanson et al, 1992). OCT instruments with ultrahigh depth resolution of around 1μm have been developed (Wang et al, 2003b). Though, the more common depth resolution is on the order of around 5–10 μm (Alex et al, 2010). For typical image resolutions and sizes, OCT techniques have a high sensitivity reaching around –100 dB. This means that backreflected signals as small 10^{-10} might be identified (Fujimoto, 2003). The OCT technique applies low energy of the order of 5-8 mW; hence no damage to the scanned biological tissue has been observed (Regar et al, 2003).

Strong scattering is limiting the OCT penetration depth ability in biological tissue (Brezinski et al, 1996). Scattering arises from changes in the refractive index between different constituents of the tissue and the surrounding medium. It is reliant on present scatterers shape and size; accordingly the macroscopic scattering properties of different types of tissue can differ significantly. Absorption of the light waves by water, lipids, protein and haemoglobin could mainly be prevented by appropriate selection of the wavelength band. The absorption of water and other typical constituents of the

tissue such as haemoglobin or melanin between 600-1300 nm are low, which result in an optical window (also known as NIR or therapeutic window or window of transmission) (Parrish, 1981). Requirements of the OCT application influence the selection of the operating wavelength within the NIR window. Wavelength light at the range of 1300 nm permits for the deepest penetration into most non-transparent tissues such as skin or mucosa, because absorption in melanin and scattering reduce with rising wavelength (Brezinski et al, 1996). Deeper penetration for applications in the tissue may be achieved by using longer wavelengths, for example around 1700 nm where absorption of water has no substantial effect (Sharma et al, 2008). Nevertheless, examination of the posterior eye segment in vivo with these long wavelengths are not suitable because of strong attenuation of the signal in the vitreous that largely comprises of water. Therefore, for retinal imaging the commonly utilised range is about 800 nm wavelength that exhibits low water absorption (Považay et al, 2003), while wavelengths around 1050 nm allows deeper penetration into the subretinal layers (Považay et al, 2003) and at the same time performing marginal chromatic dispersion in water (Wang et al, 2003a). Although penetration depth of imaging is restricted by optical attenuation from tissue microstructure absorption and scattering, imaging up to 2-3 mm deep can be attained in most biological tissues. This imaging depth is identical to the scale that typically imaged by conventional biopsy and histolopathologic analysis. Though imaging depths are not as deep to that obtained with ultrasound, the OCT image resolution is in excess of 10-100 times finer than standard clinical ultrasonography (Fujimoto et al, 2000; Brezinski et al, 1996, 1997).

A phenomenon called speckle can be observed when imaging highly scattering biological tissues with OCT such as skin or mucosa. Usually speckle pattern appears in OCT images as a grainy fine structure, which is resulted from the interference of reflected light from many scatterers that are randomly distributed within the scanning volume (Schmitt et al, 1999). Speckle characteristics, for example the size and the intensity distribution, can deliver further information concerning the underlying scatterers (Gossage et al, 2003; Hillman et al, 2006). On the other hand, the texture of speckle masks small features in the OCT images and is generally considered a source of noise. Consequently, various methods for decreasing speckle phenomenon have been developed and applied to OCT (Schmitt et al, 1999). Some of the methods are grounded on the incoherent addition of numerous signals from the identical position under varying conditions, for instance spatial

compounding (Sander et al, 2005; Jørgensen et al, 2007), frequency compounding (Pircher et al, 2003), and angular compounding (Schmitt, 1997). Different methods for image processing can be used to quell speckle where compounding is unfeasible, like different types of smoothing filters, wavelet analysis (Xiang et al, 1998), anisotropic diffusion (Wang, 2005), deconvolution (Kulkarni et al, 1997; Schmitt, 1998), and rotating kernel transformation (Rogowska & Brezinski, 2000).

3.2.2. OCT imaging modalities

OCT imaging techniques separated into different concepts. The most important modalities are OCT in the time domain (TD-OCT) and in the frequency domain (FD-OCT) (Gambichler et al, 2011).

3.2.2.1 Time domain OCT (TD-OCT)

In TD-OCT the reference arm is furnished with a revolving (translating) mirror or scanning delay line. Figure (3.2) shows a typical TD-OCT system.

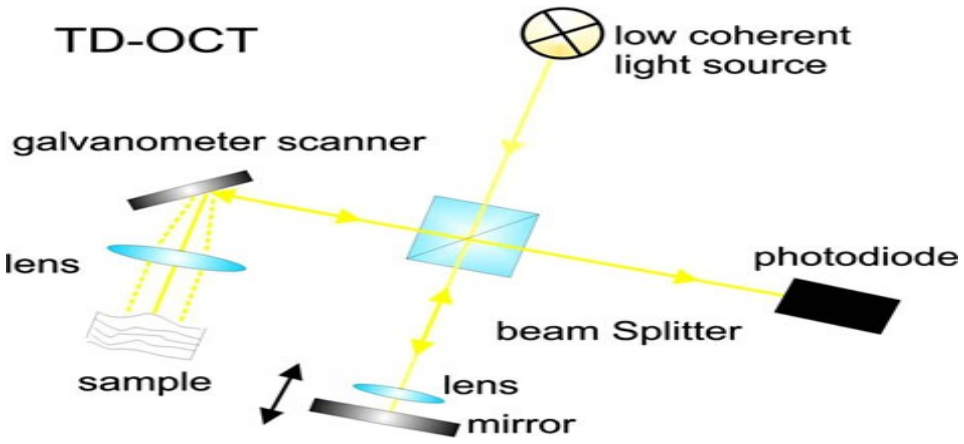

Figure (3.2) Time domain OCT system, A-scans are obtained by movement of the mirror in the reference arm. (Gambichler et al, 2011).

The distance between two points in space is determined by the coherence length of light source where interference is probable. Therefore, when the distance between a point inside the tissue and the reference arm, where the backreflecting or backscattering occurs is longer than the coherence length, no interference fringes are observed on the photodiode (detector). Accordingly, depth

filtering could be achieved by this coherence gate that limits the imaged region to the coherence length. For imaging the internal tissue microstructure as a function of depth, periodic shift of the reference arm mirror take place and the time-dependent signal is recorded. The interference fringes that are detected subsequently demodulated and form the axial (A-scan) measurement. The combination of several A-scans (one-dimensional depth scan) from various positions result in two or three cross-sectional images production. To attain high resolution over the entire imaging depth, the reference mirror and lens that focuses the light into the sample of interest can be moved with each other. Therefore, the focal gate and coherence is matched across the entire depth of the scanning (Gambichler et al, 2011).

3.2.2.2 Frequency domain OCT (FD-OCT)

In FD-OCT, there are two chief approaches where the mirror is fixed in the reference arm in both approaches. In the first approach, which is called spectral domain OCT (SD-OCT) a spectrometer is replacing the photodiode (photodetector). A typical FD- OCT system is shown in figure (3.3). The axial (longitudinal) depth scan can be achieved by reading out the diode array of the spectrometer without mechanical movement of the reference arm mirror. The light that reflected back from different depths in the sample and superimposes (interferes) with the reflected light from the reference arm, modulates the spectra. The frequency of the modulation is directly proportional to the depth of the sample microstructures. Fourier transform of the spectra is therefore provides direct access to the depth information (Gambichler et al, 2011).

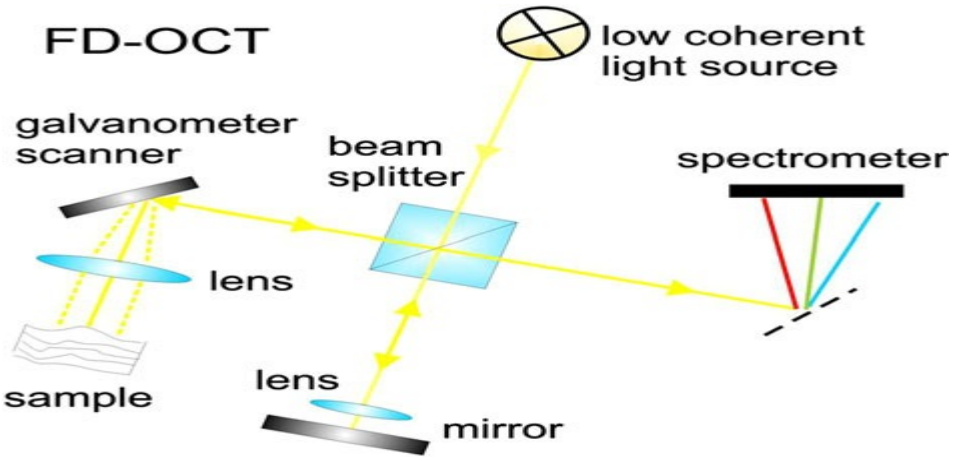

Figure (3.3) Frequency domain OCT system, A-scans are obtained when the spectra, which are recorded by the spectrometer, are Fourier transformed. (Gambichler et al, 2011).

The second approach is known as swept source OCT (SS- OCT). SS-OCT systems are working with a similar principle, which is shown in figure (3.4). Here, a tunable narrowband light source is replacing the broadband light source that scans over a time interval the wavelengths of the spectrum. Therefore, a simple photodetector can replace the spectrometer that permits high-speed detection. The photodetector is recording one-dimensional depth scan (A-scan) when the laser light is scanning over one wavelength interval. The recorded data are corresponding to the recorded data by the spectrometer. Therefore a Fourier transform provides access to the depth information (Marschall et al, 2011; Gambichler et al, 2011).

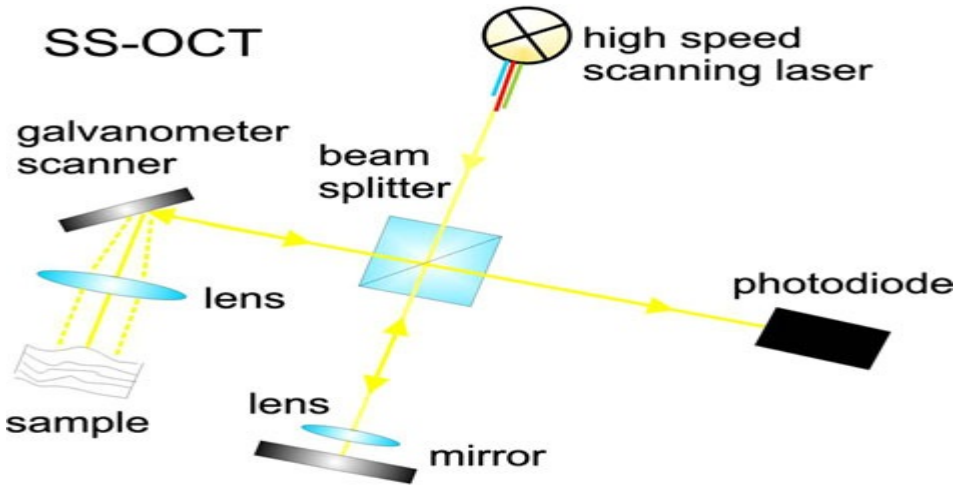

Figure (3.4) Swept source OCT system. An A-scans is recorded when the laser scans over the wavelength range and the recorded spectrum is Fourier transformed. (Gambichler et al, 2011).

Many authors in several studies have reported the faster image acquisition rate and higher sensitivity of FD-OCT techniques in contrast with TD-OCT systems (Choma et al, 2003; de Boer et al, 2003; Leitgeb et al, 2003). Typical fast SS-OCT techniques of about 50 kHz record three-dimensional data sets in about one second, while some investigators in a recent research reported line scan rates of 20.8 million A-scans/second (Wieser et al, 2010).

3.2.2.3 Functional OCT

Polarisation-sensitive OCT (PS-OCT) has the capability for visualising and quantifying the skin birefringence properties (Fan et al, 2007; Mogensen et al, 2008, 2009a, 2009c; Pierce et al, 2004; Sakai et al, 2009; Saxer et al, 2000; Strasswimmer et al, 2004) and has been applied as a useful instrument for tissue segmentation (Gotzinger et al, 2008). In PS-OCT numerous types of tissue are discernible, especially those with a high content of collagen, for example the skin. Defect or loss of collagen integrity and structure is frequently related with abnormalities of the skin, such as neoplasms and diseases of connective tissue. This proposes that evaluation of birefringence might prove useful as a diagnostic guide of certain cutaneous pathologies (Gambichler at al, 2011).

Optical Doppler Tomography (ODT), which is also known as Doppler OCT, uses the Doppler frequency shift. When an object is moving inside the sample such as blood, this frequency shift is introduced. The most common method in FD-OCT to measure flow velocities is termed phase-resolved Doppler OCT. Applications of this method for observing changes in blood flow dynamics and vessel structure subsequent to pharmacological intervention and PDT have been exhibited (Aalders et al, 2006; Chen et al, 1997; Izatt et al, 1997; Leitgeb et al, 2003b; Nelson et al, 2001; Vakov et al, 2005; Wang et al, 2004; Zhang & Chen, 2005; Zhao et al, 2000).

Spectroscopic OCT (S-OCT) is another region of investigation. In all methods that exploit reflected and backscattered light for tissue imaging, the spectral properties of light that is detected from each position inside the tissue is determined by the specific absorption and scattering properties of the intermediate tissues. Image contrast is improved by applying S-OCT and makes it probable to distinguish pathologies of the tissue by their functional state or spectroscopic properties. S-OCT may accordingly act as a type of 'spectroscopic staining', equivalent to histopathology staining, and with a single measurement it has the possibility for detecting spatially resolved functional and bio-chemical tissue information over the whole area of emission wavelength of the light source (Drexler & Andersen, 2009).

3.3 Applications of OCT

3.3.1 Ophthalmology

In ophthalmology, direct imaging of the ocular structure of human eyes in both anterior and posterior segments utilising OCT has been performed in vivo and in vitro (Fercher et al, 1993; Swanson et al, 1993; Izatt et al, 1993). A cross-sectional image of the retina can be produced by using OCT that possess a resolution comparable to a histologic section in light microscopy (Tanno & Kishi, 1999) and retinal structures are visualised with this method that are unapproachable with any other technique (Fig. 3.5). OCT is non-invasive in contrasting to fluorescein angiography, and no physical contact is required with the eye, as opposed to ultrasound imaging that may result in a significant discomfort to the patient. These advantages were behind the fast success of OCT technique in ophthalmology.

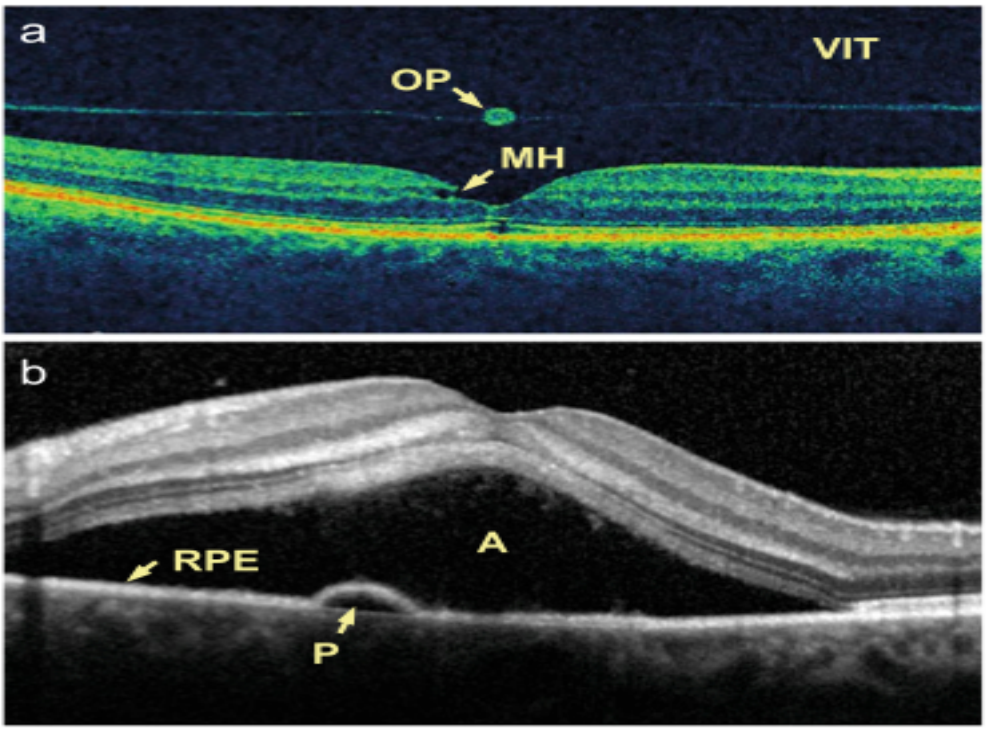

Figure (3.5) OCT images of diseased human retinas. (**a)** Macular hole (MH) has developed after the detachment of the vitreous humour from the retina. The OCT image clearly shows the posterior surface of the vitreous (VIT) and reveals the presence of an operculum (OP). (**b**) Central serous chorioretinopathy has led to a large fluid accumulation anterior (A) and a smaller one posterior (P) to the retinal pigment epithelium (RPE). (Marschall et al, 2011).

A number of retinal diseases have investigated by OCT imaging as a clinical standard and is being applied increasingly in the diagnosis, monitoring, and treatment control of glaucoma (Tan et al, 2008), age-related macular degeneration (Kaiser et al, 2007), vitreo-retinal traction and macular holes (Larsson et al, 2006), and diabetic retinopathy (Soliman et al, 2008; Gaucher et al, 2008).

Imagining of retinal morphology and measurement of thickness of the retina has become essential so as to evaluate patients with age-related macular degeneration. This condition if untreated will leads quickly to a considerable loss of vision. The condition can be treated by monthly application of vascular endothelium growth factor (VEGF) inhibitors until the disease is inactive (Chang et al, 2007; Brown & Regillo, 2007). Because intra-vitreal injection of VEGF inhibitor into the eye is required for treatment, retreatment frequencies should be kept as low as possible. The existence of fluid inside or beneath the retina (intra-retinal or sub-retinal fluid respectively) and the related

thickness in retina have major influence on the decision to administer retreatment, and OCT imaging is applied for assessing these conditions in most major hospital clinics (Marschall et al, 2011).

Patients with type 1 or 2 diabetic retinopathy frequently develop retinal thickening and among those patients nearly 15% develop macular oedema, which is slowly developing and the patient may be unaware of the condition for a long time. Treatment will be crucial when the oedema is large or close to the fovea (the very centre of macula, which in turn is the centre of the retina), which is the area of maximal visual acuity. OCT modality has become a prevailing method for clinical studies investigating the treatment of oedema, especially the injection of intra-vitreal steroid and VEGF inhibitors. The main risk factors for the diabetic retinopathy progression are blood pressure and blood glucose, and OCT imaging has been applied to analyse the association between acute changes in blood glucose, thickness in retina and blood pressure (Jeppesen et al, 2007). The visualisation of fluid accumulation patterns might be an important tool for identifying patients who have more severe stages (Soliman et al, 2008; Gaucher et al, 2008). OCT is most probably will not replace invasive techniques completely, for example fluorescein angiography, however it might lessen their application and consequently the burden of repeated eye examinations for patients and clinics would be decreased (Kaiser et al, 2007; Bolz et al, 2009).

Glaucoma is a leading cause of visual impairment, a disease that involves retinal nerve fibres layer atrophy. The diagnosis of glaucoma in the early stages is difficult as it based on defects in visual field, that is, the diagnosis of glaucoma is confirmed when the retinal nerve fibre damage has already occurred. Many investigators in recent studies have shown that the thinning of the retinal nerve fibre layer can be detected by OCT imaging that usually precedes the visual field loss (Hougaard et al, 2007; Tan et al, 2008; Gyatsho et al, 2008). With ongoing enhancements in both resolution and speed of OCT, it will possibly become a valuable apparatus for detecting glaucoma in its early stages (Marschall et al, 2011). In addition to the major diseases, OCT imaging technique is applied in almost all fields of eye diseases, for instance eye surgery monitoring and follow-up, vascular occlusions, macular holes, and examination of the anterior segment of the eye (Larsson et al, 2006; Kovacs et al, 2007; Kalev-Landoy et al, 2007; Doors et al, 2010).

Clinical applications of OCT have up till now been established on structural images. Still, functional imaging offers many chances for attaining further information that assists in detection of

diseases. Polarisation-sensitive OCT (PS-OCT) facilitates quantitative measurements of the birefringence of the retinal nerve fibre layer (RNFL) (Chen et al, 2004). The detection of changes resulted from early stage glaucoma can advance diagnostic precision. PS-OCT is also helpful for a more accurate demarcation of different layers of retina based on their polarisation properties (Pircher et al, 2004; Baumann et al, 2010). Retinal pigment epithelium (RPE) for example can be recognised by its depolarising nature that might prove beneficial for the detection and monitoring of diseases that affects RPE layer (Michels et al, 2008). Blood flow in retinal vessels can be visualised by applying Doppler OCT (Yazdanfar et al, 2000). In combination with a 3-dimensional fast imaging, a new procedure can be employed for non-invasive angiography (Makita et al, 2006), which might improve the diagnosis and monitoring of some diseases like diabetic retinopathy and glaucoma.

OCT in comparison with other methods, such as electro-retinography, provides non-invasive and uncomplicated approach for examining the physiology of the retina and could open new likelihoods for studying pathology of the retinal structures (Bizheva et al, 2006; Srinivasan et al, 2009).

Because of ocular aberrations, there is difficulty in achieving high lateral (transverse) resolution in imaging of the retina. Adaptive optics can compensate these ocular aberrations to a certain range, thereby allowing transverse resolutions of a few micrometres as well as signal-to-noise ratio (S/N) improvement (Hermann et al, 2004; Zawadzki et al, 2005).

Drexler and colleagues (2001) have reported that light source in the range of 800 nm wavelength allows ultrahigh resolution imaging of the retina. Yet, it can hardly penetrate retinal pigment epithelium (RPE), a structure that strongly absorbs the light and therefore the 800 nm wavelength is not sufficient enough for deep penetration into the choroidea (choroid coat), which is located under the retina. Imaging at a wavelength of around 1300 nm undergoes strong water absorption in the vitreous. The light source of 1050 nm wavelength band for this special purpose is therefore interesting as it demonstrates a local minimum of absorption and disappearance of chromatic dispersion in water. Since some researchers in the last decade have showed the potential for deep penetration into the choroid (Považay et al, 2003), a number of research have started application of

light source with a wavelength of around 1050 nm range (Yasuno et al, 2007; Hammer et al, 2010). Depending on the choroid OCT images diagnostic value (utilising 1050 nm wavelength), it might become an extra standard tool for ophthalmology (Marschall et al, 2011). In order to prevent motion artefacts, high data acquisition speed rates are essential for in vivo imaging (Yun et al, 2004), as the eye in particular is continuously moving (Leitgeb et al, 2009).

3.3.2 Cardiology

Cardiovascular disease is the leading cause of death worldwide, resulting in millions of deaths annually (World Health Organisation, 2010). Hence, early recognition and detection of vulnerable atherosclerotic plaques (VP), the most predominant condition that lead to myocardial infarctions, is highly pertinent. These lesions characterise by the existence fibrous cap thinner than 65 μm that covers a lipid-rich and infiltrating activated macrophages (Davies et al, 1993; Burke et al, 1997; Virmani et al, 2000, 2002; Kolodgie et al, 2004). Post-mortem analyses exhibit that the majority of fatal acute coronary events appear at the location of a ruptured, macrophage-rich, thin-capped fibro-atheroma (TCFA) with a minority because of erosion of the endothelium (Arbustini et al, 1991; Farb et al, 1996; Davies et al, 1993; Burke et al, 1997; Virmani et al, 2000; Kolodgie et al, 2004). All TCFA will not rupture and the factors that initiate plaque rupture in one place in contrast to another place is unknown (Pinto & Waksman, 2006). Intra-vascular ultrasound imaging (IVUS) has been applied previously for visualising plaque lesions, although dependable characterisation was not performed adequately due to insufficient resolution of US images (Jang et al, 2002). Application of intra-vascular OCT (IV-OCT) can assist in resolving small details (Fig. 3.6), and thus IV-OCT is more likely to become a vital tool that enables clinicians in classifying atherosclerotic plaques (Low et al, 2006).

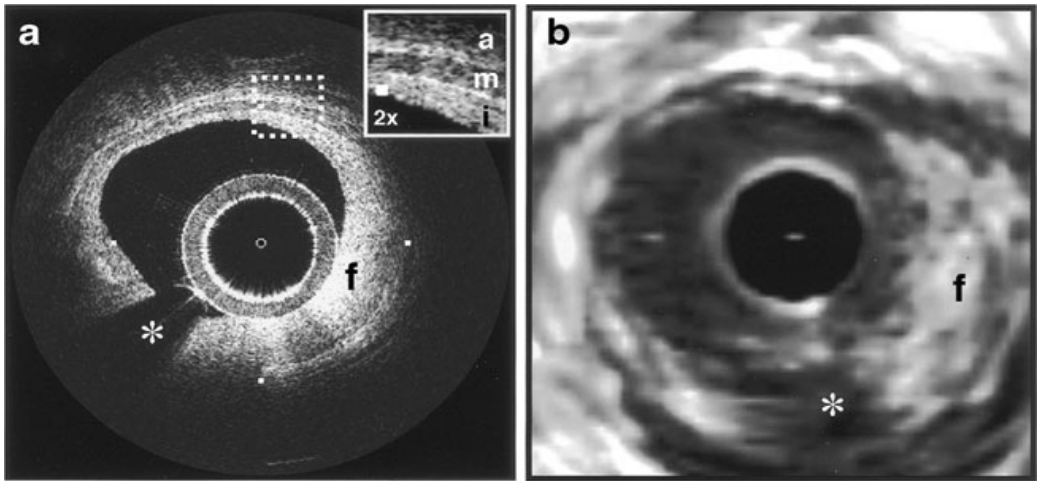

Figure (3.6) Images acquired with intravascular OCT (**a**) and 30 MHz ultrasound (**b**) for comparison. Due to its higher resolution, OCT has a clear advantage for visualising the structural details of the vessel walls. (i) Intima with intimal hyperplasia, (m) media, (a) adventitia, (f) fibrous plaque, (asterisk) guidewire shadow. (Jang et al, 2002).

A number of non-invasive imaging techniques like multidetector-row computed tomography, coronary angiography, or magnetic resonance imaging (MRI) have been limited in resolution in comparing to invasive modalities such as IVUS, in addition their capability at imaging distal vessels are poor (Brezinski et al, 1996a, 1997; Jang et al, 2002). Similarly, angiography has a resolution of around 500 μm, which is not sufficient to permit visualisation of atherosclerotic plaque components (Brezinski, 2002).

Brezinski and associates (1996b) in an in vitro study have first showed that OCT is feasible instrument for vascular imaging of blood vessels when they successfully scanned left anterior descending coronary artery from a cadaver, and the images acquired resembled the histology. Comparing IVUS images to OCT images and histopathology of post-mortem stenotic coronary arteries and aortas demonstrated several advantages (Brezinski et al, 1997; Patwari et al, 2000). OCT images had a greater resolution, a sharper demarcation between the plaque and tunica intima, capability to reveal beyond calcified tissue, and a higher capability to visualise lipid pools not demonstrated by IVUS images (Pinto et al, 2006). Ex vivo IV-OCT measurements revealed the ability to discriminate between different structures in the tissue (Brezinski et al, 1996) and types of VP (Yabushita et al, 2002; Levitz et al, 2004), and were followed by in vivo OCT studies that targets at VP identification (Jang et al, 2005;Tearney et al, 2006; Brezinski, 2007). Typical

characteristics can be quantified by OCT imaging, for instance the thickness of the fibrous cap (Kume et al, 2006), presence of macrophage infiltration (Tearney et al, 2003) or lipid (van der Meer et al, 2005). The application of PS-OCT could help in detecting the degradation of organised collagen fibres (Giattina et al, 2006; Nadkarni et al, 2007), and local attenuation coefficients extraction permits the automated identification of dissimilar tissue microstructures (van Soest et al, 2010). The high-resolution IV-OCT imaging capabilities and extraction of information with regard to the tissue composition, it has become an important research method in playing an important role for examining cardiovascular diseases (Raffel et al, 2008; Li et al, 2010; Yamada et al, 2010) and possible treatments (Yu, 2009).

While atherosclerotic plaques classification is the subject of ongoing investigations, the chief clinical IV-OCT application is for percutaneous coronary interventions (PCI) monitoring and follow-up (Diaz-Sandoval et al, 2005), particularly in coronary stents deployment (Gonzalo et al, 2009). All stent struts when implanted must be adequately apposed to the wall of the vessel (Fig. 3.7), and in the consequent healing process the stunt is covered by neointimal tissue layer. Lack of neointimal tissue layer coverage and inadequate stent apposition are suspected to rise the danger of probably fatal late stent thrombosis (Murata et al, 2010; Ozaki et al, 2010). Long-term follow up by IV-OCT is feasible so as to monitor the stent deployment outcome (Guagliumi & Sirbu, 2008), and as revealed by comparative studies, the superior resolution provides IV-OCT a strong advantage over IV-US (Bouma et al, 2003; Diaz-Sandoval et al, 2005; Ozaki et al, 2010).

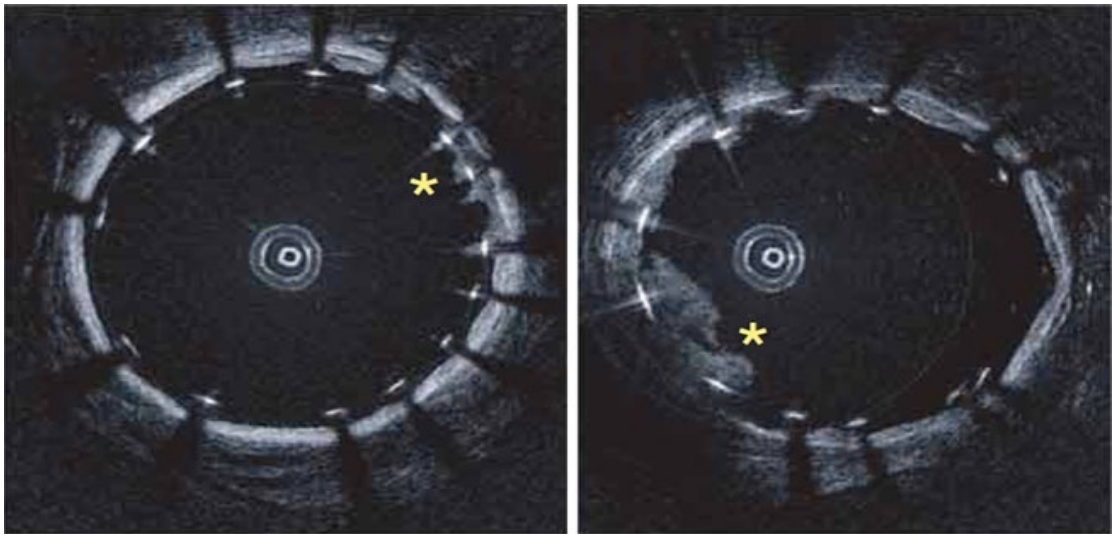

Figure (3.7) OCT images of a stented porcine coronary artery in vivo. The stent struts appear as highly reflective objects casting radial shadows. The images reveal tissue prolapses between the struts (asterisks). (Yun et al, 2006).

When comparing to other invasive imaging techniques such as IVUS, it has two chief disadvantages. First is weak penetration depth in nontransparent highly scattered tissues, with a 2–3 mm visualisation limit (Brezinski et al, 1997; Stamper et al, 2006). Penetration depth is sufficient to assess the tunica intima and composition of plaque and to measure thin cap, however this limited depth does not permit evaluation of positive or negative remodelling and the total lipid pool cannot be completely imaged in deep plaques that have large necrotic cores. Nevertheless, the depth of penetration is adequate for the purpose of evaluating VP and for coronary pathology and microstructure imaging for most lesions. Notwithstanding the better penetration depth of IVUS (approximately 5 mm), it has not been revealed to detect VP dependably most likely because of its low resolution. In general, for the purpose of detecting unstable plaque, IV-OCT is more sensitive and specific in compare to IVUS (Brezinski, 2002; MacNeill et al, 2003). Signal attenuation by RBCs is more challenging problem that is thought to be due to mismatch in index of refraction between red blood cell (RBC) cytoplasm and serum. Furthermore, this has been supported in a study done by Brezinski and colleagues (2001), and they showed that lysed blood does not interfere with OCT imaging.

To overcome the blood opacity for near-infrared light is the main difficulty for in vivo IV-OCT imaging that occurs because of scattering by RBCs. Clearing the blood vessel by saline flushing for a short time has been successfully showed in both animals (Fujimoto et al, 1999) and humans (Jang et al, 2002), and has become a common practice at present. Many investigators in initial patient studies have demonstrated the general safety of this technique (Prati et al, 2007; Yamaguchi et al, 2008). Though, research continues to totally remove the risk of ischemia, for example by matching blood serum refractive index with that of the RBCs (Brezinski et al, 2001), or by utilising oxygen-carrying flushing liquids (Villard et al, 2002; Hoang et al, 2009). The introduction of high-speed FD-OCT instruments was an important stride as it enables in a relatively short flushing periods the acquisition of large sampling volumes (Yun et al, 2006; Bouma et al, 2009).

3.3.3 Dermatology

The OCT technique seemed promising for examination of skin abnormalities, particularly lesions or conditions that are challenging to be assessed by visual inspection. Therefore, in the area of dermatology most OCT research has addressed non- melanoma skin cancer (NMSC), though OCT studies in relation to inflammatory diseases such as eczema and psoriasis, photo-damage, and burns has also been studied (Steiner et al, 2003; Mogensen et al, 2009a). Morsy and associates (2010) in a recent research have suggested that OCT might be applied for measuring thickness of the epidermis in psoriasis and that these measurements correlate with numerous other disease severity parameters. This indicates that assessment of psoriatic plaques by OCT imaging might offer a useful approach for non-invasive and in vivo technique to follow the development of psoriatic lesions (Fig. 3.8). NMSC term includes mainly common skin tumours like basal cell carcinoma (BCC), squamous cell carcinoma (SCC) and actinic keratosis (AK). OCT with regard to these tumours looks to be efficient in revealing the tumour cell aggregates derivation from the epidermis (Gambichler et al, 2011). In the diagnosis of NMSC, OCT could possibly lessen the frequency of invasive skin biopsies, aid in finding an optimal biopsy sites, or measuring the thickness of tumour (Mogensen et al, 2009b). Still, in spite of many initial promising study results, OCT in clinical dermatology has not hitherto been established (Marschall et al, 2011).

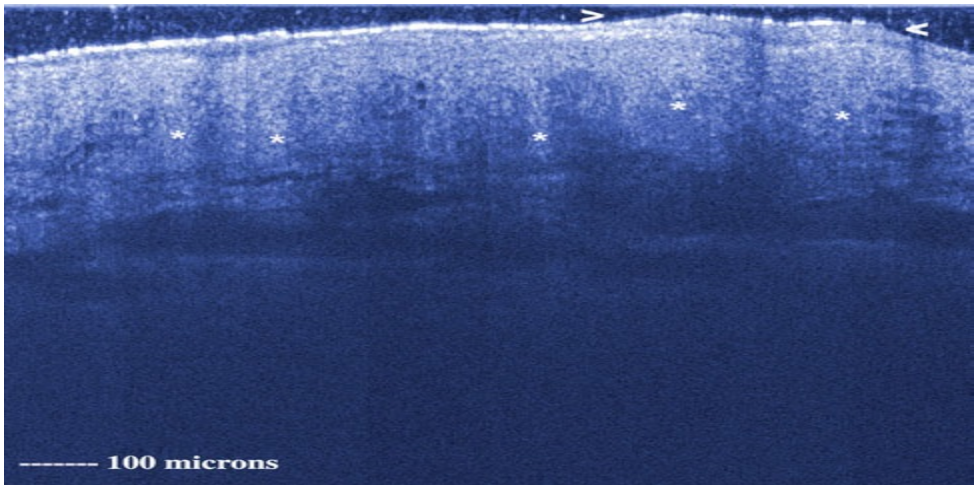

Figure (3.8) OCT of psoriasis vulgaris showing a thickened hyperreflective band (arrow heads thickened stratum corneum) and acanthotic epidermis (asterisk) with elongated rete ridges. (Gambichler et al, 2011).

The upper part of the skin can be demonstrated on OCT images. In normal skin (Fig. 3.9a), a well-defined boundary between the horny layer (stratum corneum) and the living part of the epidermis can usually be seen in palmo-planter region of skin (glabrous skin), and the upper dermis can be discriminated from epidermis in OCT images (Mogensen et al, 2008; Alex et al, 2010). Due to incapability of OCT modality in resolving single cells, diagnosis of the disease should be dependent on alteration in the morphology of skin (Fig. 3.9b), for example a separation or breaking up of tissue layers, general disarray structure, or a change in the amount of backreflected light contrasted to normal skin (Mogensen et al, 2008; Welzel, 2001). OCT, for example can recognise the loss of architecture of normal skin in malignant melanomas (MMs) that might be applied to distinguish them from benign melanocytic nevi (BMN) (Gambichler et al, 2007c).

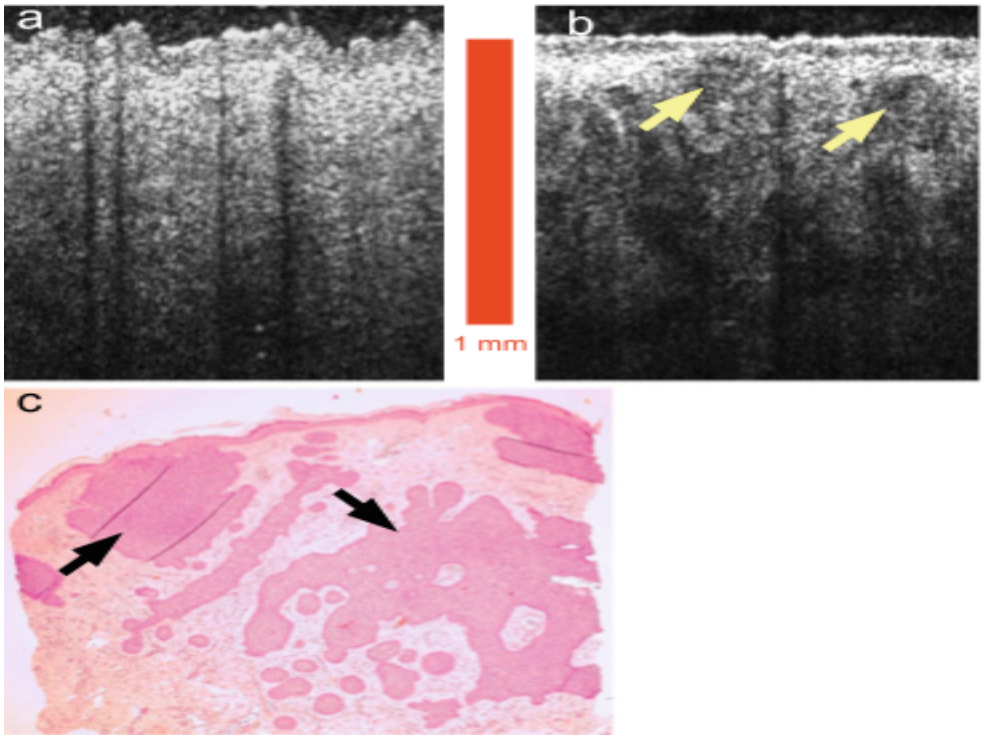

Figure (3.9) OCT images of normal skin (**a**) and basal cell carcinoma (**b**) show a clear structural difference. The basaloid carcinoma cell islands, the main features in the corresponding histological image (**c**), can also be recognised in the OCT image (arrows). (Marschall et al, 2011).

AK is an intraepithelial premalignant neoplasm and considered the precursor lesion of SCC, characterised by partial thickness epidermal dysplasia, hyperkeratosis, parakeratosis and solar elastosis (Gambichler et al, 2011). Nearly 10% of AK lesions will advance to SCC (Glogau, 2000). OCT images of AK display streaks and white dots congruent to hyperkeratosis (Jorgensen et al, 2008). It has been suggested in a pilot study by Barton and associates (2003) that OCT is beneficial in AK detection and characterisation, as well as monitoring their reaction to chemoprevention agents. According to a study by Korde and coworkers (2007), AK can be discriminated from healthy skin with 86% and 83% sensitivity and specificity respectively.

Solid tumours such as BCC are usually characterised by a consistent signal distribution (Forsea et al, 2010; Welzel et al, 2002). Subepidermal hyperreflective zones would be observed in the OCT images of BCC lesion that had analogous size, allocation and form similar to the tumour cell nests in histopathological slides. The echo-rich tumour aggregates separated from the tumour stroma by a narrow hyporeflective band. In the deeper dermis, many smaller tumour cell nests were seen as

echo poor roundish spots (Bechara et al, 2004). Gambichler and colleagues (2007d) in a more systematic study have found that on OCT images of BCCs, a loss of normal architecture of the skin and a disarray of the epidermal and upper dermal layers were seen as compared with contiguous non-lesional skin. Moreover in the upper dermis, big signal-intense plug-like structures, signal-free honeycomb-like structures and prominent cavities (signal-free) were frequently identified. The latter descriptions correlated with histopathology sections (Fig. 3.10). Olmedo and associates (2006) in a pilot study have reported that an excellent correlation between histological features of BCC and OCT images can be recognised. Consequently, the altered architecture of the skin layers that present in BCC lesion can be visualised on OCT images along with good correlation with histopathological section.

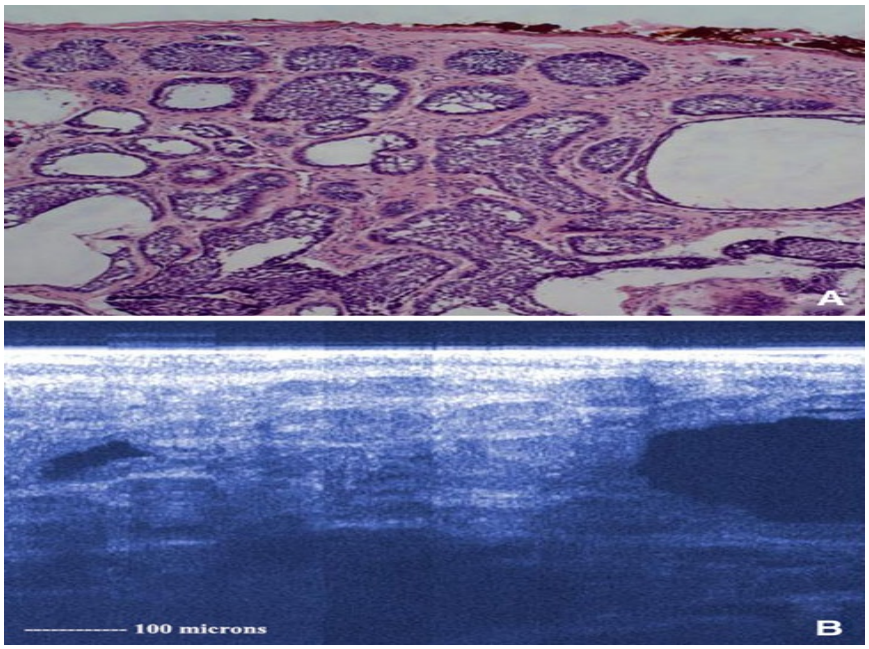

Figure (3.10) Image (**A**) showing H&E slide of infiltrative BCC with multiple adjacent oval tumour nodules. The latter histologic finding correlated with honeycomb-like signal-poor structures in the OCT image (**B**). (Gambichler et al, 2011).

Similarly, in polarisation-sensitive OCT the same is true (Strasswimmer et al, 2004). Functional

OCT can provide additional information that may be used to locate and characterise skin cancer. The highly organised structure of collagen fibres in the dermis, resulting in birefringence, breaks down in skin cancer lesions (Marschall et al, 2011). Strasswimmer and associates (2004) in a pilot study have concluded that there might be possibility for distinguishing normal skin and basal cell carcinoma by utilising PS-OCT. Nonetheless, in a recent study by Mogensen and coworkers (2009c) on more than 100 patients with various types of lesions have reported that the diagnostic precision using PS-OCT could not improve when contrasted to an evaluation based on structural OCT images.

The discrimination, in a clinical setting, between benign and malignant lesions is significantly more challenging since benign lesions frequently demonstrate similar structure in OCT images to malignant lesions. Additionally, some factors should be taken into account such as variations with age, type of the skin, anatomical location, etc. (Mogensen et al, 2008; Gambichler et al, 2006a). Nevertheless, many authors in different studies have shown a high correlation between histopathology sections and OCT images of BCCs lesion, which suggest that OCT can be applied to distinguish NMSC lesions (Gambichler et al, 2007d; Khandwala et al, 2010). Assessment of thickness of tumour is very important in non-invasive treatments of superficial BCC and AK. Mogensen and colleagues (2009b) in a study compared OCT with a wavelength around 1318 nm with 20-MHz ultrasound imaging and reported that both modalities overestimated depth of the tumour compared with histopathology, however, OCT was less partial and more accurate. Though, Gambichler et al (2007d) in an in vivo OCT study on BCC lesion have revealed that discrimination between the dissimilar BCC subtypes (nodular, multifocal superficial and infiltrative) with OCT application is not possible. Mogensen and colleagues (2009c) in another study with observer-blinded evaluation by both pathologists and dermatologists of OCT images have pointed out that discrimination of BCC and AK cannot be achieved grounding on the OCT images alone. Nevertheless, though OCT is less accurate in diagnosing NMSC than clinical differential diagnosis, it has a relatively high accuracy in tumour borders delineation and differentiating lesions from normal skin (Mogensen et al, 2009c). Several investigators in a recent pilot study have reported that imaging of the skin by using OCT is a useful instrument for delineating BCCs on eyelids and the face (Khandwala et al, 2010). Besides, Hamdoon and associates (2011) in another recent study have showed that photodynamic therapy (PDT) guided by OCT is a promising method to differentiate

between tumour involved and non- involved margins efficiently. OCT-guided PDT has lessened the unfavourable necrosis of healthy tissue and delivers an encouraging monitoring of the process of healing.

Melanocytic naevi on OCT images frequently demonstrate elongated rete ridges and accentuated epidermal layer (Figures 3.11 & 3.12). Naevus cells nests are distinguished as areas of poor signals with a typical arrangement in the rete ridges (apical part). As the naevus cells nests are more compact, they can be better showed (Welzel et al, 1997; Gladkova et al, 2000; Welzel, 2001; Bechara et al, 2004). In compound naevi or infiltrative growing melanoma, the second intensity peak (represents the boundary between the dermis and epidermis) might disappear. The penetration depth of melanomas could only be measured in lesions that are very thin of about less than 1 mm in tumour thickness. Deeper OCT measurements in skin are hardly probable because of the limited depth of penetration owing to the absorption and scattering effects (Gambichler et al, 2011). In another study, Gambichler and coworkers (2007c) have reported the detection of important differences between MM and benign naevi with respect to micro-morphological features revealed by OCT. Large vertical, icicle-shaped structures in MM were the most remarkable OCT feature that did not appear in benign naevi OCT images. There is a good correlation between this distinct OCT features and histology findings (Figures 3.13 & 3.14). Hence, these OCT features may assist as a valuable distinguishing parameters that can be applied in future studies to explore OCT sensitivity and specificity in melanocytic skin lesions (Gambichler et al, 2007c). Systematic studies are still deficient for the diagnosis of pigmented lesions utilising OCT with respect to sensitivity and specificity.

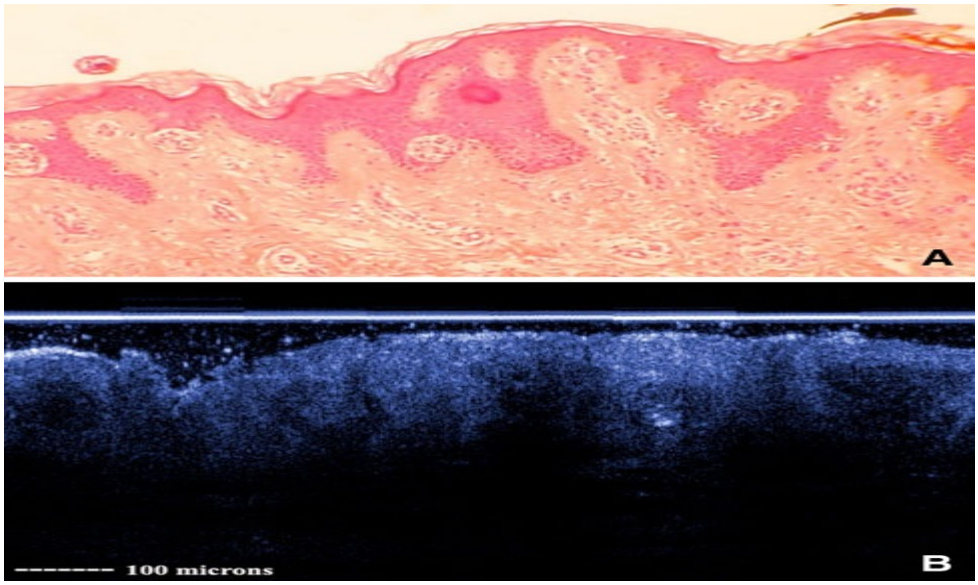

Figure (3.11) H&E slide of a melanocytic naevus (**A**) & the corresponding OCT image (**B**). OCT displays finger-shaped elongated and broadened rete ridges including dense naevus cell clusters. The dermo-epidermal junction zone is relatively clearly demarcated from the more or less dark appearing upper dermis (**B**). (Gambichler et al, 2011).

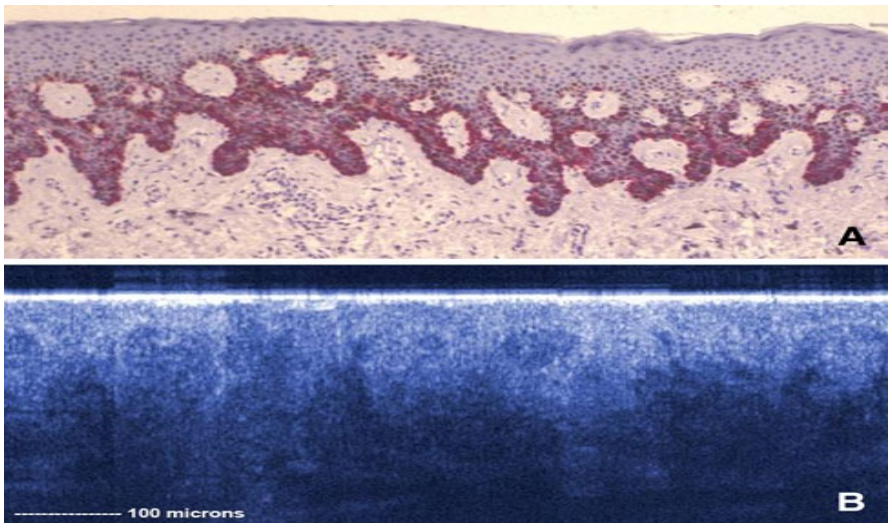

Figure (3.12) Immuno-histology showing MART-staining of a melanocytic naevus (**A**). On OCT image (**B**), the quite regularly arranged naevus cell nests are visualised. (Gambichler et al, 2011).

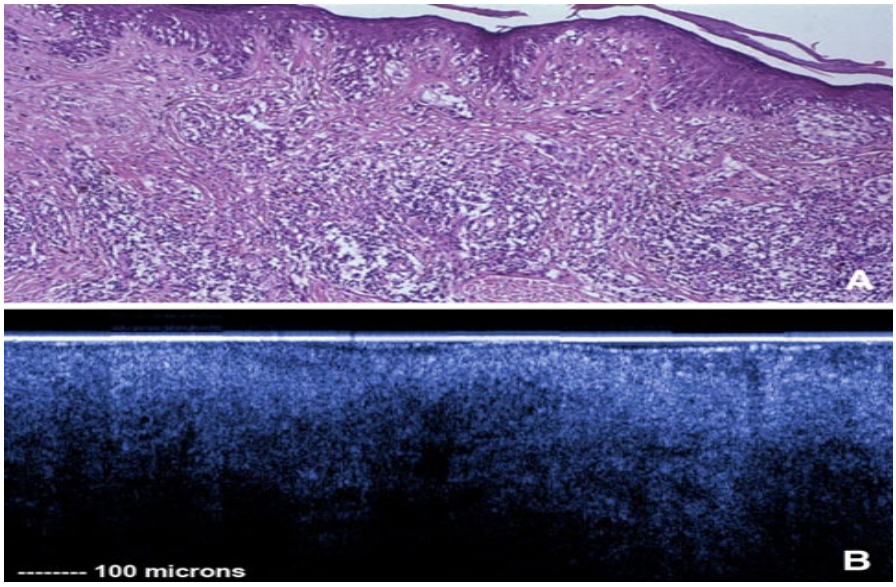

Figure (3.13) Histology (**A**, haematoxylin–eosin) a superficial spreading melanoma including the corresponding OCT image (**B**). OCT displays marked architectural disarray including large vertically arranged icicle-shaped structures (**B**). (Gambichler et al, 2011).

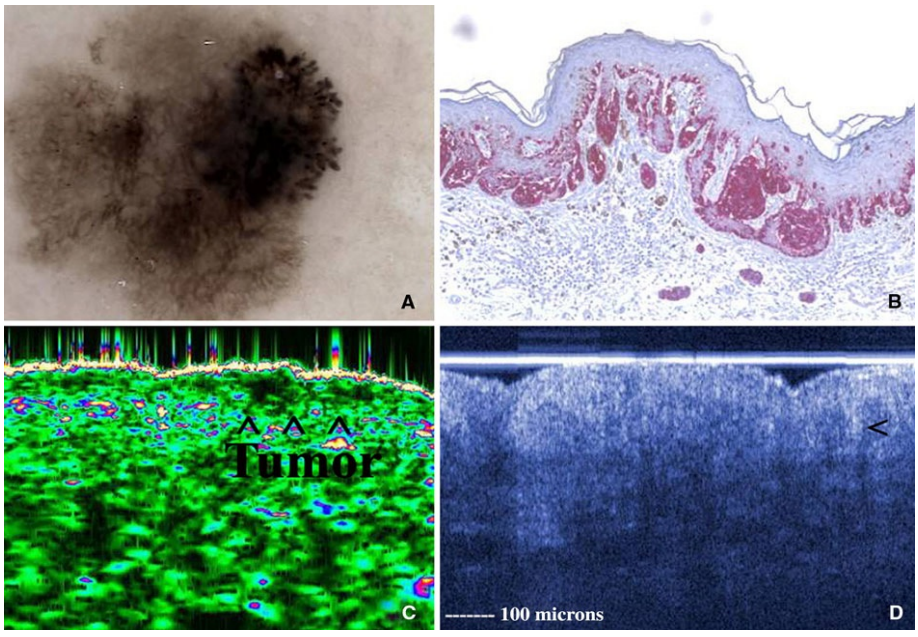

Figure (3.14) Showing corresponding images of a superficial spreading melanoma on digital dermoscopy (**A**), immunohistology (MART-staining, **B**), 20 MHz ultrasound (**C**), and OCT displaying elongated rete ridges and tumour cell nests in the upper dermis (**D**). (Gambichler et al, 2011).

3.3.4 Application of OCT in the oral cavity

Many investigators in numerous studies have tried to explore the in vivo OCT diagnostic efficacy for the detection and diagnosis of oral pre-malignant and malignant lesions (Tsai et al, 2008a,b; Wilder-Smith et al, 2009a,b). In a study by Wilder-Smith et al (2009b) involving 50 patients with suspicious oral lesions, the evaluation of the usefulness of OCT for detecting oral dysplasia and malignancy has been investigated. The dysplastic lesions on OCT images have showed loss of stratification in the epithelium, visible thickening of the epithelium, and down-growth epithelial pattern (Fig. 3.15). In the OCT images, regions of OSCC of the buccal mucosa were recognised by discontinuity (disruption) or loss of the basement membrane, high variability in thickness of the epithelial layers, with erosion areas and extensive down-growth pattern of the epithelium and invasion into the sub-epithelial layers (Fig. 3.16). Statistical analysis of data from this research supported the capability of in vivo OCT with excellent diagnostic precision to detect and diagnose oral pre-malignant and malignant lesions. OCT sensitivity of 0.931 and specificity of 0.931 was obtained for identifying CIS or SCC versus non-cancer, while sensitivity of 0.931 and specificity of 0.973 for distinguishing SCC versus all other pathologies.

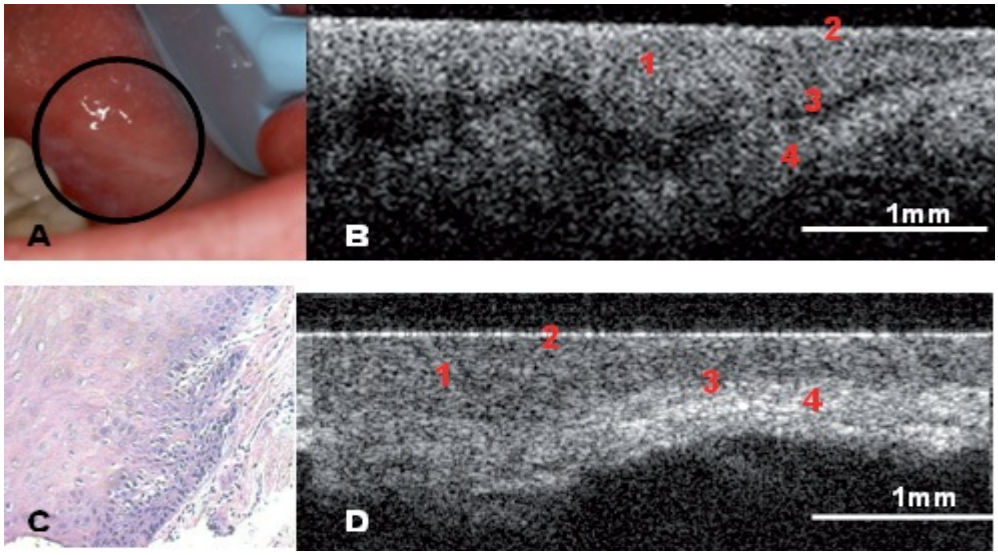

Figure (3.15) Dysplastic and normal buccal mucosa: (**A**) Photograph, (**B**) in vivo optical coherence tomography (OCT) image, and (**C**) H&E (10X) of dysplastic buccal mucosa. (**D**) In vivo OCT image of normal buccal mucosa. 1: stratified squamous epithelium; 2: keratinised epithelial surface layer; 3: basement membrane; 4: submucosa). (Wilder-Smith et al, 2009b).

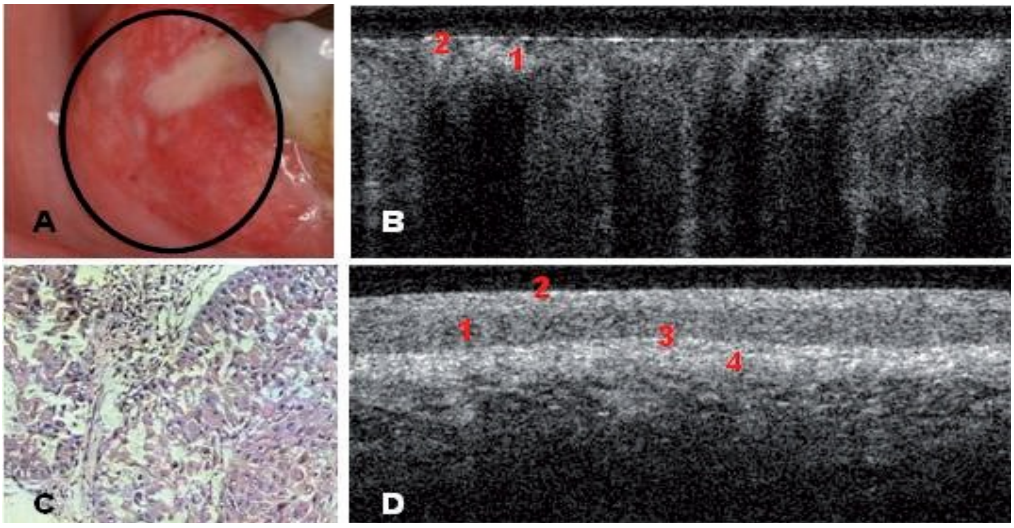

Figure (3.16) SCC of the buccal mucosa: (**A**) photograph, (**B**) in vivo OCT image and (**C**) H&E (10X) of buccal mucosa with SCC. (**D**) In vivo OCT image of normal buccal mucosa. 1: stratified squamous epithelium; 2: keratinised epithelial surface layer; 3: basement membrane; 4: submucosa). (Wilder-Smith et al, 2009b).

Tsai and colleagues (2009) in a study involving 97 patients applying OCT imaging for the detection of oral neoplasia have reported that the principal diagnostic criterion for high-grade dysplasia/CIS was absence of a layered structural arrangement. Diagnosis for dysplastic and or malignant versus benign and or reactive conditions established on this criterion accomplished a sensitivity and specificity of 83% and 98% respectively with about 0.76 inter-observer agreement value. This OCT study has concluded that with high sensitivity and specificity combined with good inter-observer agreement, is a promising imaging modality which is non-invasive, real time, and evaluates tissue sites that may have high-grade dysplasia or malignancy.

In other studies by Tsai and associates (2008a,b) have applied direct evaluation of OCT scan profiles instead of image-based criteria, as a method of demarcating the location and margins of oral malignant lesions. Applying numerical parameters from A-scan profiles as diagnostic criteria, the decay constant in the exponential fitting of the OCT signal intensity along the depth of the tissue reduced as the A-scan point moved across the lesion margin laterally. Furthermore, the standard deviation of the OCT signal intensity fluctuation considerably increased across the transition region between the abnormal and normal portions. The investigators concluded that such parameters might

be beneficial for determining an algorithm for identifying and mapping of oral cancer lesion margins. Such a capability has massive clinical importance, because of the demand to better define excisional margins during surgical removal of precancerous and cancerous oral lesions (Tsai et al, 2008b).

Since subtle changes in epithelial thickening, stratification, sub-epithelial integrity and continuity can be delineated by utilising OCT instrument, this imaging modality has potential wide applications in other mucosal lesions related with immune or inflammatory diseases, such as pemphigus, pemphigoid, lichen planus, lupus erythematosus, graft versus host disease, or anomalies like vascular lesions (Wilder-Smith et al, 2010).

OCT images of oral vascular anomalies have been reported in two cases in a recent study by Ozawa and colleagues (2009), one with a capillary–venous malformation located on the lower lip and the other with a reddish mass situated on the buccal mucosa. OCT images in the reported cases are correlated well with histopathological structures, satisfactorily displaying defined capillary vessel lumina and endothelial lining. Information about the vascular lesion area, size, and borders can be advantageous for the diagnosis and for surgical treatment options especially for vascular anomalies and hemangiomas in the oral and facial region. The high resolution in real-time and in situ, non-invasiveness, and its ease of use deliver a safe ways of oral structure imaging at a level that is otherwise only attainable by histo-pathological analysis of a biopsy specimen (Wilder-Smith et al, 2010).

Most interest in the application of OCT in the head and neck area has concentrated on early recognition and monitoring of dysplasia and malignancy to aid in less destructive treatment and also in a better prognosis as well. Jerjes and associates (2009) in a recent study have carried out a comparison between OCT images and histological findings of suspicious oral lesions to establish whether this method would assist in clinical examination and monitoring of these lesions that would not usually necessitate a biopsy. The researchers based on four variables for assessment; changes in keratin, epithelial, sub-epithelial layers, and identification of the basement membrane and from these variables they calculated whether or not there were architectural changes. 34 oral lesions were assessed applying OCT and compared with histopathological results. In only 15 oral lesions the

basement membrane was identified. OCT could distinguish diseased areas, however it could not offer a diagnosis or discriminate between lesions.

Fluid-filled vesicle on the lower lip was one of the lesions that perfectly demarcated by OCT with defined keratin, epithelial layer, and lamina propria. Vesiculo-bullous lesion of the buccal mucosa was another case where OCT image showed the basement membrane with unclear outline, which correlated with the histological descriptions of the disease. There was break in the keratin layer with ulceration of the epithelium and areas of keratosis and thickening when plaque lesion on the cheek mucosa has been OCT imaged, which is suggestive of submucous fibrosis. Jerjes and coworkers (2009) pilot study approves the practicability of applying OCT as an imaging technique for the diagnosis and monitoring of some benign and potentially malignant oral lesions without the necessity for many biopsies. This real time, non-invasive, and in situ modality is less morbid for patients and permits preventive screening of at-risk populations (Wilder-Smith et al, 2010).

In a recent ex vivo study, Hamdoon and colleagues (2010) assessed the tumour resection margins utilising OCT on 24 patients with diagnosed T1-T2 OSCC. The surgical margins of the specimens have been interrogated by OCT and the acquired images were compared with histopathology slides. Recognition of the junctional epithelium between negative and positive margins has been observed by gradual change in thickness of the epithelium and basement membrane integrity or organisation from the normal to pathological margins. Recognisable changes in the positive margins of the resected tumour include hyperkeratinisation, break or discontinuity of the basement membrane and disarray of the epithelial structure. Calculation of sensitivity and specificity in this study have showed to be encouraging and the authors suggested that OCT imaging modality is feasible in discrimination between negative and positive surgical margins.

Chapter 4

Validation of the modified OCT oral instrument compared to the commercial standard OCT dermatology instrument

Chapter 4

Validation of the modified OCT oral instrument compared to the commercial standard OCT dermatology instrument

4.1 Introduction

The Michelson Diagnostics VivoSight® topical OCT instrument (version 2.0), which is CE-certified (Conformité Européene) for clinical dermatological imaging, has a handheld probe (Fig. 4.1) designed for imaging skin. The large size, imaging head bulk and the short working distance of the dermatology probe makes it practical only for scanning the anterior region of the oral cavity including lips, anterior part of the tongue and a small area of the inner side of the cheek. In order to enables the clinician to examine different and distant oral mucosal surfaces, for example hard palate, lateral and ventral surfaces of the tongue, etc. the Michelson company have adapted the probe with an additional oral extension tube to reach anatomical locations where it was previously impossible to image. The new oral instrument (Michelson Diagnostics VivoSight® OCT oral scanning instrument, version 2.1) is a one-off, non-CE certified, uncalibrated and consequently non-standard modification of the existing CE marking instrument. Therefore, prior to any clinical application or use, the new oral instrument required confirmatory calibration and comparison with the conventional skin instrument to assess and confirm performance in image quality and resolution in X, Y, and Z-planes (Fig. 4.3), equates to the existing instrument.

The oral probe (Fig. 4.1) comprising a metal tube extension of about 12.5cm in length and 1.4cm in diametre, has a glass window at the patient imaging end at 90°degrees to the axis of the probe to facilitate access to anterior-posterior orientated surfaces within the oral cavity.

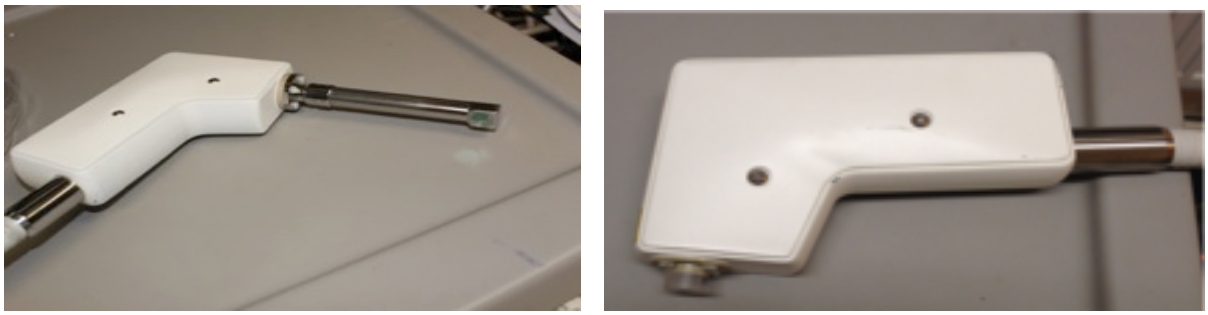

Figure (4.1) OCT oral instrument probe (left) and dermatology probe (right).

In this study, we used a commercial frequency domain swept source optical coherence tomography (SS-OCT, VivoSight® Michelson Diagnostics Ltd, Orpington, Kent, UK) as a standard for calibrating the modified oral instrument. The light source utilised by this instrument is Santec HSL-2000 swept laser with a centre wavelength of 1.305± 15nm, and sweep range of 150nm. In standard configuration, the instrument achieves axial and lateral resolutions of < 10μm over a depth range of 2mm and image width up to 6mm. The tissue penetration depth is around 1-2mm depending on the optical absorption and scattering properties of the object being imaged. In addition, the system can generate both two-dimensional and three-dimensional images by reconstruction of serial two dimensional slice data (www.michelsondiagnostics.com).

From our initial observation, the image produced by scanning with the OCT oral instrument has a convex white line (Fig. 4.2) at the top of the image. This line is not apparent when the skin instrument is used to scan the same sample.

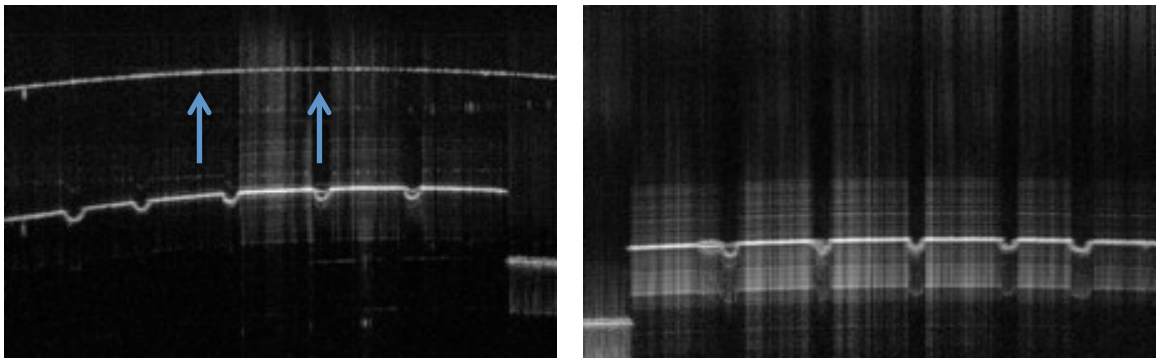

Figure (4.2) OCT oral instrument image (left) reveal the convex white line (arrows), when compared with more uniform OCT skin instrument image (right). Maximum of 56μm rise in the curvature over the 6000μm imaging width field.

To find out the degree of the convex line curvature, a line drawn from one end of the arc to the other end and the distance (in the middle of the image) between the arc and the straight line drawn has been measured by utilising image J programme. Over the 6mm (6000μm) imaging width field the curvature allowed a maximum rise of 14 pixels (56μm) where the scale set on 250 pixels/mm. This has raised concern about the new OCT oral instrument images in providing accurate

measurements in X, Y, and Z-planes in comparing with OCT skin images. Therefore, achieving the following objectives need to be achieved in order to make sure that OCT oral instrument can be used as a surrogate for the CE certified OCT skin instrument. The objectives of this study are:

1. Comparison of OCT oral and skin instruments by calibrating NPL Optical Dimensional Standard and metric slip gauges in air.

2. Comparison of OCT oral and skin instruments by calibrating metric slip gauges Z step height model and Perspex plate slopes phantom in liquids (effects of change in medium refractive index).

4.2 Materials and methods

4.2.1 Materials

1. National Physical Laboratory (NPL) Optical Dimensional Standard (Fig. 4.3B).
2. Metric slip gauges blocks, Mitutoyo Corporation, Japan.
3. Purpose-built phantom comprising Petri dish containing Perspex plates fixed to the upper border of the dish in different and ascending slope angles.
4. Collagen matrix gel block (Fig. 4.7).

4.2.2 Methods/ study design

4.2.2.1 Calibration of instruments using NPL and slip gauges step height phantoms:

4.2.2.1.1 Calibration in X and Z planes

To measure the instruments' accuracy in X-axis, NPL Optical Dimensional Standard has been utilised to achieve this experiment (Fig. 4.3 A&B). Images of a standard known dimension reflecting panel were taken across its known 1200μm linewidth, with each instrument. The linewidth (rectangular-shaped) was first imaged in the centre of the 6mm imaging field, then in the right and left side of the field to measure the accuracy across the field in both OCT systems. Six measurements or readings were obtained for the scanned rectangle width in the centre, right, and left side of the imaging field and the mean and standard deviations (SD) were calculated for both oral and skin instruments (Table 4.1). The same NPL linewidth was re-imaged by both OCT instruments under the water and water adulterated with surfactant.

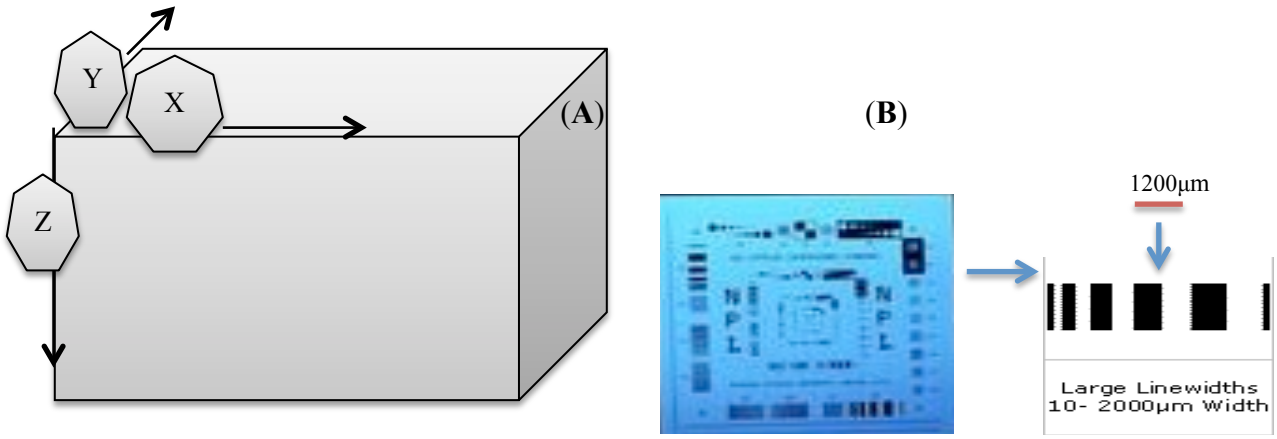

Figure (4.3) (**A**) Diagram show X, Y, and Z-planes. (**B**) Calibration of X-plane utilising an NPL set of standard sized shapes.

To assess the Z dimension measurements, a series of calibrated engineering standard depth gauges (slip gauges) were arranged as a series of steps, imaged in the vertical axis, normal to their combined width and length axes, ensuring a uniform image plane orientated to the centre line of the step intervals of the ladder phantom (Fig. 4.4A&B). Each imaging measurement was taken 6 times, and all images were measured in "image J programme" integrated in the OCT system yielding mean, SD and Bland and Altman plots for variation compared to known laboratory standards for each instrument. Vertical step heights were difficult to assess as the machined edges were rounded rather than right angle sharp. The end of the bright reflections of each surface were joined by construction lines in image J – their angle to the horizontal face of each slip gauge was found to be a reliable surrogate for vertical height by construction lines using the option 'angle measure' in image J (Fig. 4.4B).

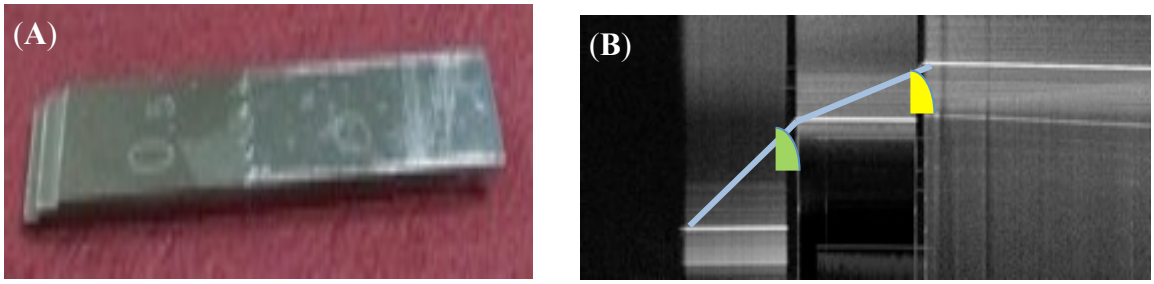

Figure (4.4) (A) Metric slip gauges Z step height model. (**B**) OCT image of the metric slip gauge steps. In many of the images it was difficult to determine the edge of the slip gauge because it was rounded. To overcome this problem we used Image J software to add construction lines, shown in blue, and then calculated the step height by measuring the angles.

To assess the effects of imaging environment refractive index (RI) change on the Z-axis imaging, the same slip gauge step phantom was re-imaged by both instruments as before, but the phantom was serially immersed in transparent media with RI's higher than water [RI of water=1.333 (www.physicsclassroom.com)], such as surfactant RI=1.359 (Lee et al, 2005) and microscopist's imaging immersion lens oil RI=1.515 (Abramowitz et al, 2002) and an aqueous scattering medium, milk RI=1.344-1.348 (Hui et al, 2007; www.iftbu.org/milk.htm), to assess the changes in depth measurement due to dissimilar media with different RIs. Changes in included angle measurements reflect altered apparent Z step heights in the resulting images, introduced by the imaging environment as the only variable. Six measurements were taken for each angle in each medium and the mean and SD of the angles calculated for both instruments for statistical analysis (Table 4.3).

4.2.2.1.2 Calibration in X, Y, and Z-plane (3-D object measurement)

A slip gauge block (1.5mm) was taken and arranged on a suitable stage so that its edge would be scanned and 3-D data can be obtained. Both OCT skin and oral instruments were applied to obtain 3-D 500 multislice images (Fig. 4.11). After that, the 3-D multislice images were analysed and the width of the slices were measured using image J programme. Six measurements were taken for the first slice width, then followed by measuring slice number 100, slice 200, slice 300, slice 400 and finally the last slice was measured. The mean and SD of the readings were calculated for each slice. This was repeated for the 3-D images taken by the OCT oral instrument and measurement done using the same procedure. The purpose of measuring the width of the first and last slice as well as selected slices in between was to establish whether or not any distortion was occurring in OCT oral instrument images across Y scan aspect, which could progressively alter volumetric (3-D) OCT data and compare that to the known standard OCT skin instrument. All the measurements are illustrated in table (4.4) for OCT skin and oral instruments respectively.

4.2.2.2 Effects of change in medium refractive index on the Perspex plate slopes phantom

The definition of refraction is "the bending of the path of a light wave as it passes across the boundary separating two media" (www.physicsclassroom.com). Refraction is a result in the change of speed in the progression from one medium to another (Fig. 4.5).

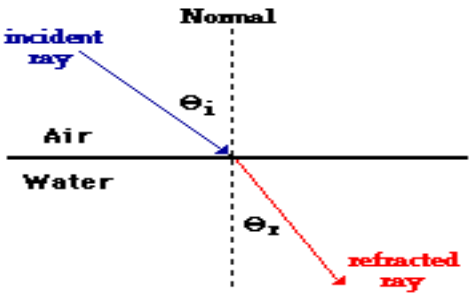

Figure (4.5) Diagram illustrates angles of incidence & refraction.

The diagram illustrates the light ray undergoing refraction as it passes from one medium to another as in this paradigm from air into water below. As the light ray travels to the boundary from one medium to another, is referred to as the incident ray and the refracted ray is the direction that light travels after hitting the boundary. In the above diagram, a normal line (dashed line) at the point of incidence is drawn to the surface, which always drawn perpendicular to the boundary. The angle of incidence, which is denoted by the symbol (θi), produced by the angle formed between normal line and incident ray. Likewise, the angle of refraction, which is denoted by the symbol (θr), produced by the angle formed between normal line and refracted ray. The angle of refraction is a quantifiable assessment of the amount of refraction that is taking place at any boundary. With any angle of incidence, the angle of refraction is dependent upon the speeds of light through the two materials. This speed is dependent on the index of the refraction values and optical density of the two materials. The relationship between the angles of incidence and refraction and the indices of the refraction of two media is referred to as Snell's Law (www.physicsclassroom.com). Snell's law allows assessing the angle of refraction provided the refractive indices of the materials of interest and the angle of incidence are known. Snell's law is demonstrated mathematically as:

$Ni \times Sin(\theta i) = Nr \times Sin(\theta r)$

Ni = index of refraction of the incident medium

Nr = index of refraction of the refractive medium

θi("theta i") = angle of incidence

θr("theta r") = angle of refraction

As the OCT instruments employ near infrared (NIR) scanning wavelengths and only a visible red line to indicate the approximate orientation of the imaging beam for operator alignment purposes, it is very difficult to measure RI or effects directly with the Michelson OCT instruments.

Not all Z-axis measurements are taken on step heights arranged perpendicular to the imaging axis in clinical medical imaging. To investigate subject tissue RI changes on an obliquely orientated phantom, effects of a change in RI of the imaging environment were investigated using a simple oblique flat plane surface phantom, entering a different RI environment. For simplicity, an air-liquid interface phantom was constructed (Fig. 4.6) and serial 6 images of each air-fluid interface at the point of penetration by an oblique surface (of known angulation) were taken. The oblique plane was bright reflecting polished Perspex, visible on both sides of the air-fluid interface. Distortion of the planar surface geometry would reflect interference by environmental RI. Scattering and non-scattering media were employed to transparent media (water) were compared, along with scattering media (milk) to assess impact of a more translucent (surfactant) or scattering environment (milk) representing variations in tissues within the body. Environments chosen were water adulterated with surfactant and milk.

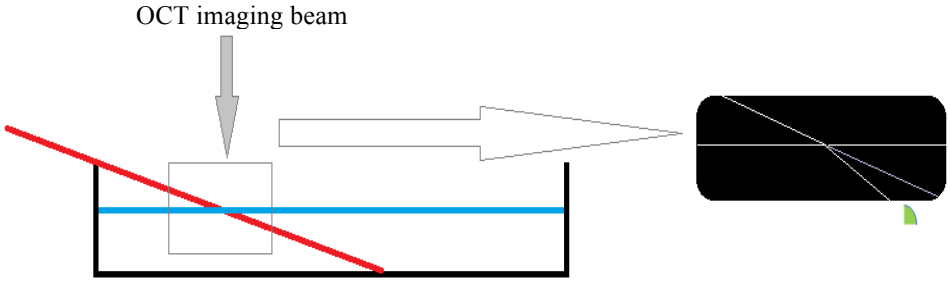

Fig. (4.6) Schematic shows how OCT scanning performed to scan the air-aqueous boundary of the Perspex plate in water adulterated with surfactant/milk. The solid red line represents the Perspex plate slope undistorted (if scanned dry) (left panel). Measurement of distortion angle (θ D) illustrated on OCT image (right panel).

Serial Perspex slope angles were imaged at the air-fluid interface and the difference in plane angle from the air to the fluid interface was measured. In air no change would exist. Water represents the lowest RI interface. OCT images obtained for each Perspex slope and by utilising image J software the angle for each slope has calculated. Slope angles ranged from 4.62°-11.44°. θ D was used as a representation of the effect of RI change in the media utilised to scan the Perspex slopes for both OCT instruments and consequently comparing the imaging behaviour between the systems. Using the 4.62° slope as a constant, aliquots of 1ml of surfactant (teepol) were added and the slope distortion θ D was reassessed six times after each of six additional 1ml teepol aliquots were added. To establish influence of scatter, the θ D assessments were repeated for milk dilutions to demonstrate any scattering influence on the altered image, again using image J programme.

4.2.2.3 Investigation of OCT skin and oral instruments using tissue mimics (collagen gel block)

A block of collagen gel was prepared and used as a connective tissue substitute model to observe the effect of RI change of the collagen medium on the OCT laser light beam by observing a known flat reflective plane (Surgical Scalpel Blade No. 15, Swann-Morton, Sheffield, UK) inserted into the collagen block (Fig. 4.7). The collagen gel was prepared as follow; acid solubilised rat-tail collagen (First Link, UK) was neutralised using 10X Minimum Essential Medium (MEM) from Invitrogen™ as an indicator and dropwise addition of sodium hydroxide [NaOH (5Molar and 1Molar)]. This was then poured into a casting reservoir (2ml capacity, 13mm x 43mm) and allowed to set at room temperature for 30 minutes. The samples of collagen block were prepared in the laboratories of the Biomaterials and Tissue Engineering Department at UCL, Eastman Dental Institute, UK.

The block of wet collagen matrix placed inside a suitable Petri dish. A convenient reflective and reliably flat plane that could be inserted into the tissue was a scalpel blade. Images were acquired for the scalpel blade penetrating the collagen block utilising OCT skin instrument. Extreme difficulty was experienced in scanning and obtaining images for the scalpel blade penetrating the collagen block by using the OCT oral instrument because of the geometry of the oral probe that require to be in close proximity to the object to be imaged. Therefore, it was not possible to obtain a good quality image that could be trustworthy and comparable with the image obtained by OCT skin

instrument in order to demonstrate the similarity in θ D changes.

Figure (4.7) OCT skin instrument used to scan the scalpel blade inserted into the collagen gel block.

4.3 Statistical analysis

Data were analysed by Stata statistical software for the Bland-Altman analysis (StataCorp. 2013. Stata Statistical Software: Release 13. College Station, TX: StataCorp LP.), whereas for the scatter diagram SPSS statistical software was utilised (IBM Corp. Released 2013. IBM SPSS Statistics for Windows, Version 22.0. Armonk, NY: IBM Corp.). $P < 0.05$ was considered statistically significant.

4.4 Results

4.4.1 Calibration in X and Z planes

The mean and SD of the six measurements of the NPL linewidth (1200μm width, which is equal to 300 pixels) that was scanned crosswise by both OCT instruments in the centre, right and left side of the 6mm imaging field to compare the accuracy in X-plane (Fig. 4.8) are illustrated in table (4.1) below. The reason behind measuring the 1200μm linewidth on both sides of the imaging field was to observe whether the convex distortion of the oral instrument had any influence on the accuracy of measurement across the field of image. By comparing the mean and SD for the linewidth imaged by both instruments across the imaging field, there is consistency between OCT skin and oral instruments in measurement in X-plane both in air and liquids that possess dissimilar RI.

Table (4.1) Calibration of NPL rectangle shape in X-plane scanned crosswise by OCT skin & oral instruments in the centre, right, and left side of the imaging field (measurements in pixel and scale set on 250 pixels/mm).

Types of OCT	Centre (Mean± SD)	Right (Mean ± SD)	Left (Mean ± SD)
Skin	300.03± 0.17	300.02± 0.09	300.04± 0.15
Oral	300.04± 0.22	300.03± 0.22	300.00± 0.06

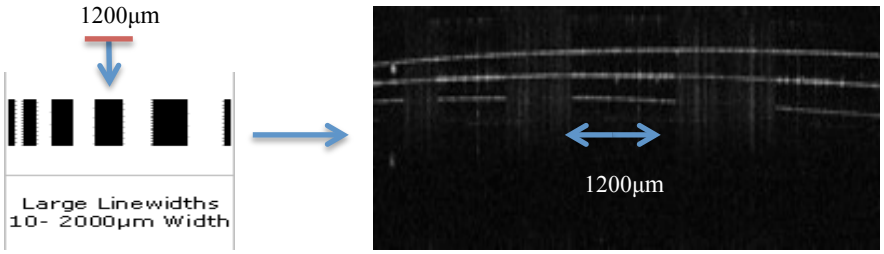

Figure (4.8) OCT oral image for the NPL linewidth in the centre of the 6mm imaging field (arrowed).

With regard to calibration in Z-plane, table (4.2) illustrates all the angle measurements between the metric slip gauges Z steps phantom in air and it shows that although the readings were not identical between both instruments, it still demonstrates consistency and similarity in trends between both instruments in measuring the angles between the steps when the mean and SD of the OCT skin and oral instrument measurements are compared with each other.

Table (4.2) Mean and standard deviation of 1st and 2nd angle readings of the metric slip gauges Z steps height model produced on images scanned by both OCT skin and oral instruments in air.

OCT Type	Angles	Mean ±SD
Skin	1st angle	160.54°± 0.33°
	2nd angle	151.39°±0.41°
Oral	1st angle	162.10°±0.30°
	2nd angle	152.25°±0.33°

After examining metric slip gauge Z height model by both OCT skin and oral instruments in different liquids, the obtained images were analysed and by using image J software all the angles between the steps were measured in the same way followed for measuring angles of the steps of the Z phantom in air. Table (4.3) shows the mean and SD of the readings.

Table (4.3) Mean and SD of the metric slip gauge step angles measurements produced on images scanned by both OCT skin and oral instruments in different liquids. 2nd angle measurements for phantom in milk (both OCT systems) & 2nd angle for phantom in immersion oil (OCT oral only) were not recorded due to invisibility of the lower step of the phantom.

Types of media	Angles	(Mean ± SD) OCT skin	(Mean ± SD) OCT oral
Water	1st angle	152.43° ± 0.40°	153.68°± 0.33°
	2nd angle	139.90°± 0.36°	141.44°± 0.32°
Milk	1st angle	151.64°± 0.26°	152.62°± 0.37°
Surfactant	1st angle	151.18°± 0.34°	152.35°± 0.38°
	2nd angle	138.78°± 0.37°	141.01°± 0.31°
Immersion oil	1st angle	149.54°± 0.42°	150.53°± 0.40°
	2nd angle	136.79°± 0.39°	

Moreover, the table displays increases in the step height distances (represented as reduction in 1st and 2nd angles) between metric slip gauge steps when scanned in water and progressively increasing RI media as described. Similarly, the table also illustrates the same trend in the increase of the step height distances between the slip gauge steps using OCT oral instrument to scan the steps (Fig. 4.9). The 2nd angle in both OCT skin and oral images of steps in the milk were not measured due to difficulty in viewing the lower slip gauge in the images shown below. Besides, the 2nd angle for OCT oral images of steps in microscopist's immersion lens oil was invisible as well (Fig. 4.9).

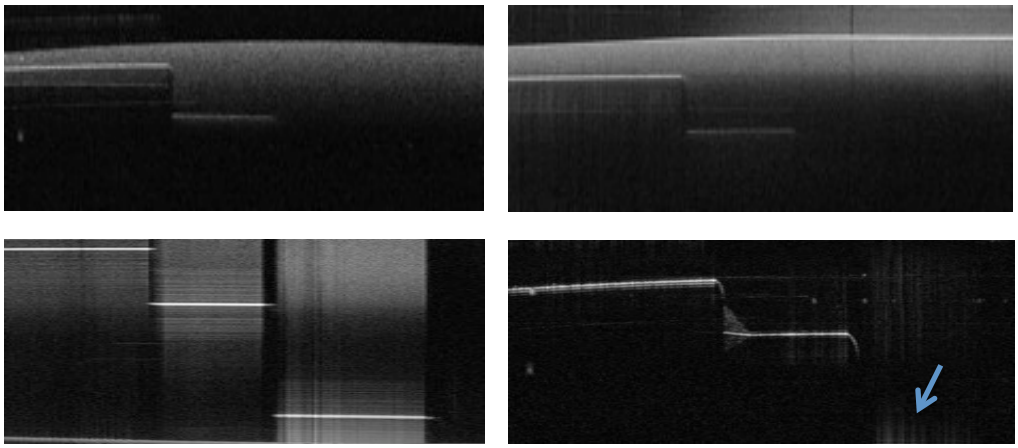

Figure (4.9) OCT images show distances between the steps is increased due to change in RIs of the media (RI of milk = 1.344-1.348, RI of immersion oil = 1.515). OCT skin (left) and oral (right) instrument images are acquired for ladder phantom in milk and microscopist's immersion lens oil respectively**.** Arrow indicates reflection from the lower step.

It can be perceived from the table (4.3) that as the RI of the medium is increased (from lowest 1.333 of water to the highest 1.515 of immersion lens oil) the angles between the tip of the slip gauges is decreased, demonstrating that the distance between the steps is increased as a result of reduction in light speed (or increased time of flight) due to optical density and RI of the medium (Fig. 4.9). The plot in Fig. (4.10) below illustrates similarity in behaviour between both OCT instruments.

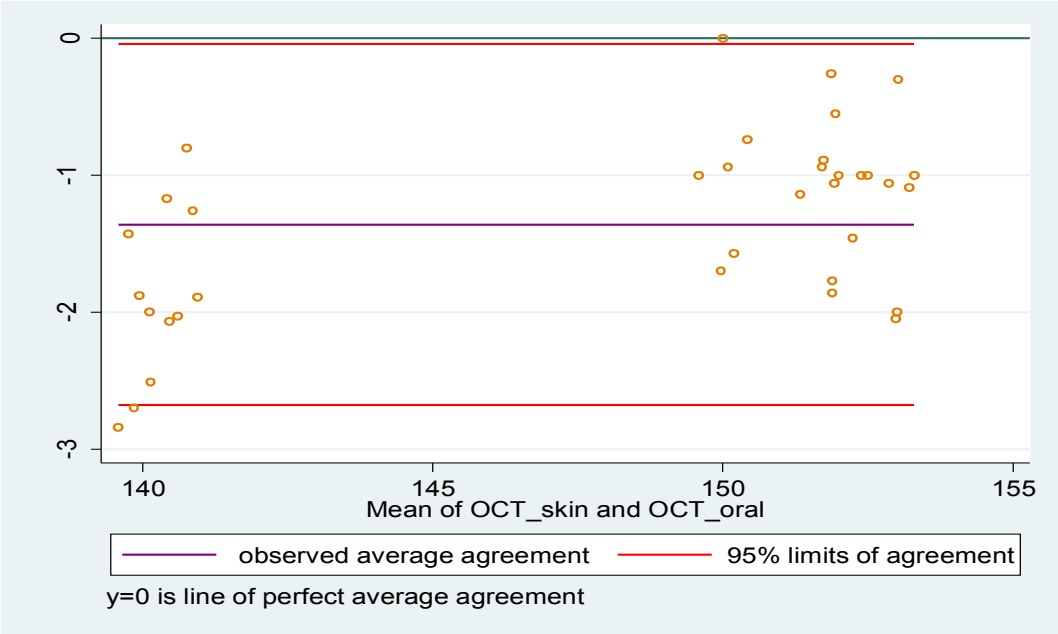

Figure (4.10) Bland and Altman (1986) plot (n=36) of the mean of 1st and 2nd angle readings for both OCT skin and oral instruments (horizontal axis), while vertical axis represents the difference between the mean angles (in degrees) measured by OCT skin and oral systems (mean of OCT skin readings- mean of OCT oral readings). The green line represents zero bias (mean of OCT skin reading- OCT oral reading = 0). Apart from bias of nearly -1.30° degrees [$P < 0.001$ from a paired *t*-test (the purple line below the zero bias line)], there is good agreement between OCT skin and oral instruments with expected discrepancies ranging from just below zero bias to nearly -2.70° degree (95% limits of agreement represented by the top and bottom red lines).

4.4.2 Calibration in X, Y, and Z-plane (3-D object measurement)

Assessment of the volumetric (3-D) OCT oral instrument capability was undertaken by scanning a laboratory calibration standard (metric slip gauge block, 1.5mm in width) in serial Y-axis slices, to obtain a 3-D image of the object (Fig. 4.11) and assess any distortion. Direct comparison with the 3-D images produced by the OCT skin instrument (Fig. 4.11) allowed an assessment of the impact of the altered scanning geometry in the new instrument. Six readings were obtained for each slice site in a 500-slice reconstruction and the mean and SD of the readings calculated. Table (4.4) show that the mean of the readings for all the examined slices are either 375 pixels or slightly above or below this figure (375×4= 1.5mm) for both OCT skin and oral instruments slice measurement. This indicates congruence between both systems in producing 3-D sample volume, which can be observed in the scatter plot in (Fig. 4.12) below.

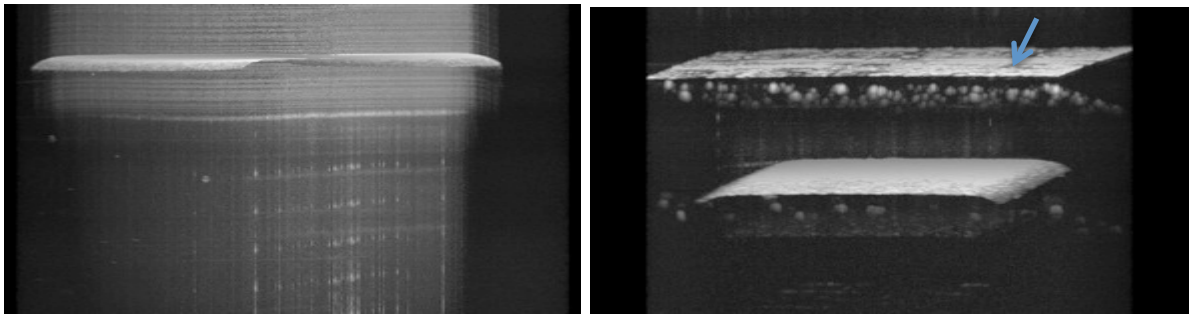

Figure (4.11) 3-D OCT images of slip gauge block (1.5mm in width) by skin (left) and oral instruments (right). Arrow indicates the glass window of the oral probe that represent 3-D of the convex white line.

Table (4.4) Measurement of 3-D multislice images of slip gauge (1.5mm in width) produced by both OCT instruments using image J software. All measurements are in pixels where scale set on 250 pixels/mm.

Types of OCT	**OCT skin (Mean± SD)**	**OCT oral (Mean ± SD)**
Slice 1	374.98± 0.10	375.00± 0.08
Slice 100	375.01± 0.15	375.00± 0.11
Slice 200	374.98± 0.13	375.02± 0.10
Slice 300	374.98± 0.12	375.01± 0.12
Slice 400	375.01± 0.10	374.99± 0.09
Slice 500	374.99± 0.11	374.98± 0.10

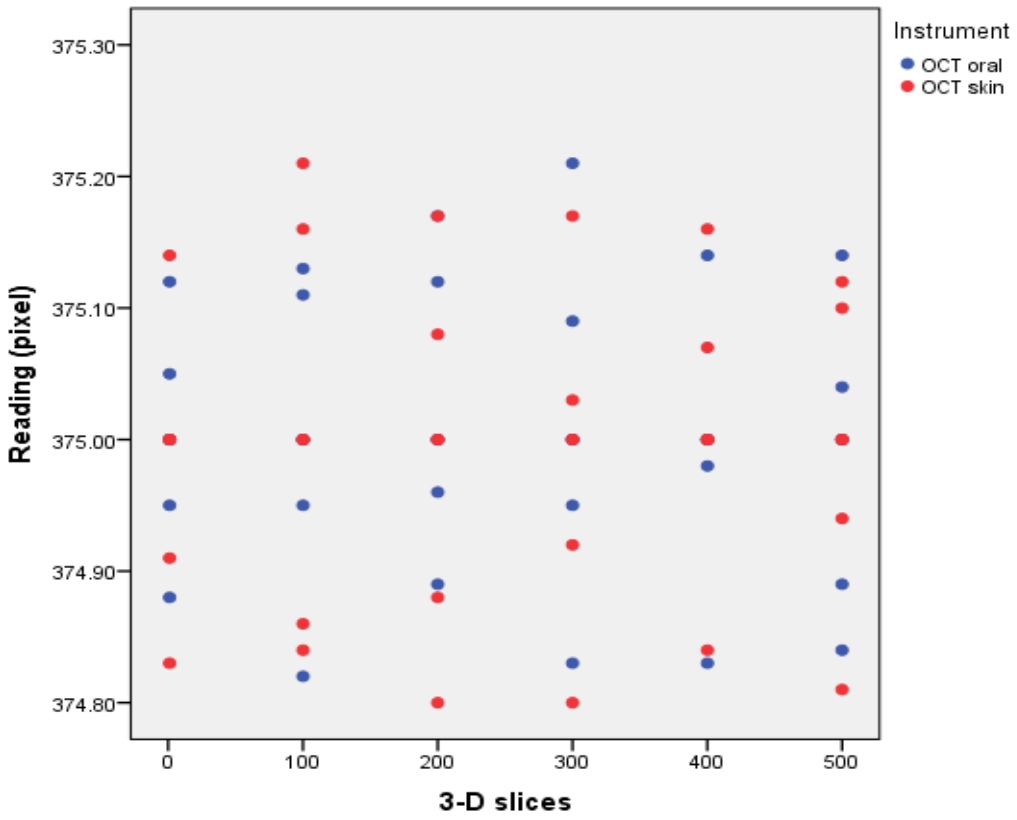

Figure (4.12) Scatter plot illustrates parity between both OCT systems in measuring the 3-D multislice images of slip gauge (1.5mm in width) using image J software programme. All measurements are in pixels where scale set on 250 pixels/mm.

Bland and Altman (1986) statistical analysis was applied to evaluate the agreement between both OCT instruments. Bland and Altman plot in figure (4.13) shows random scatter around the mean difference between slices width determined using OCT skin and oral instruments. There is no evidence of systematic effect between the two instruments with the mean of the differences being 0.008 (SD= 0.025) and P value equal to 0.44 from a paired *t* test. Lin's concordance correlation coefficient equal to -0.40 (95% CI from -0.87 to 0.44). In addition, the maximum likely difference between the two instruments is approximately 0.05 pixel, which is clinically acceptable.

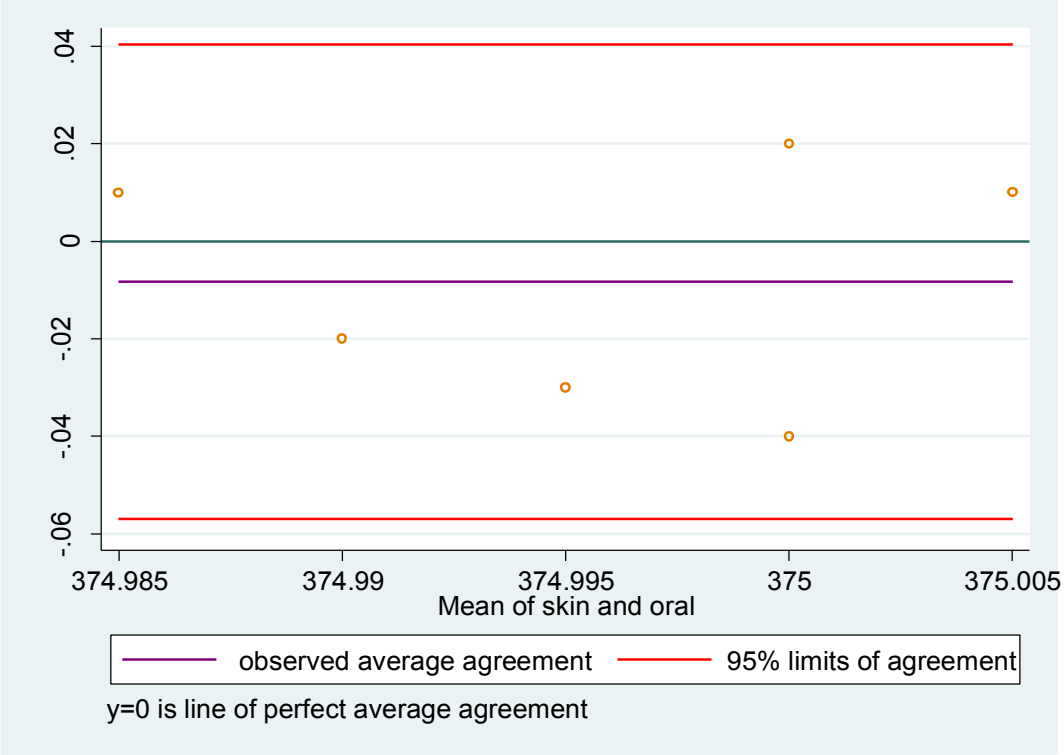

Figure (4.13) Bland and Altman (1986) plot (n=6) of the mean of slices width for both OCT skin and oral instruments (horizontal axis), while vertical axis represents the difference between the mean of the slices width measured by OCT skin and oral systems (mean of skin- mean of oral). The green line represents zero bias (mean of OCT skin- OCT oral = 0). Apart from bias of nearly -0.01 pixel [P = 0.44 from a paired *t*-test (the purple line below the zero bias line)], there is very good agreement between mean of OCT skin and mean of OCT oral with expected discrepancies ranging from just below -0.06 to 0.04 pixel (95% limits of agreement represented by the top and bottom red lines).

4.4.3 Effects of change in medium refractive index on the Perspex plate slopes phantom

In this experiment it can be observe that θ D is increasing gradually as the RI of the medium (water+ surfactant or water+ milk) is increased by adding more surfactant or milk to the medium. In addition, θ D is also increasing when the angulation of the Perspex slopes are increasing. Figure (4.14) below show how θ D was increased as a result of increasing the Perspex slope angulation and also increase in the RI of the medium by adding more milk to the water. Similarly, the same change or increase in θ D has been observed when surfactant was added to the water confirming that the

behaviour of milk and surfactant solutions is similar and that once again behaviour of the OCT oral instrument is similar to the OCT skin instrument. Six times repeat of this experiment led to generation of six readings in order to obtain accurate measurement by calculating the mean of the readings and also for the purpose of statistical analysis (Raw data can be found in tables in appendix 1). The Bland-Altman plot in figure (4.15) below shows congruency between both OCT instruments.

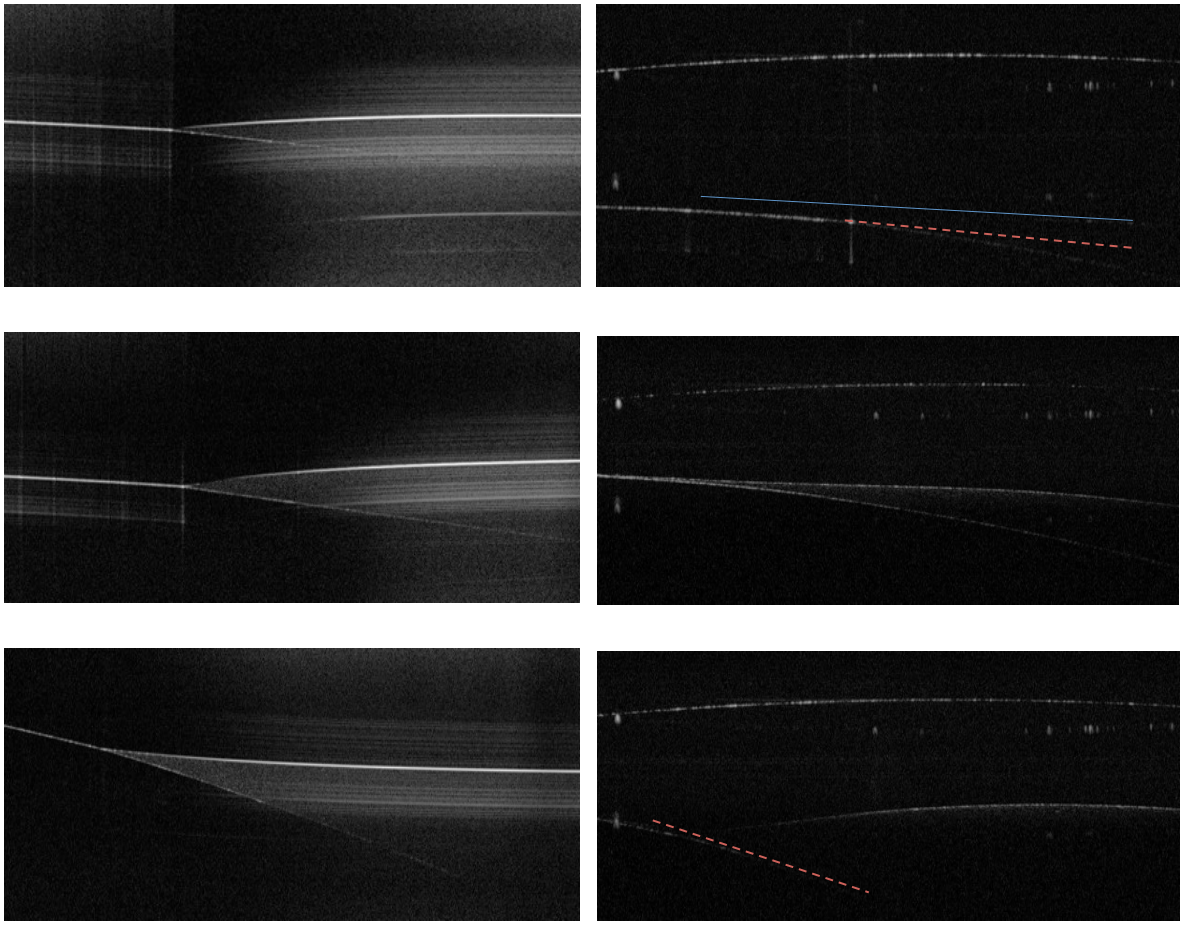

Figure (4.14) Images for both OCT skin (left) and oral (right) instruments show increase in the distortion angle (θ D) subsequent to increase in the index of refraction of the medium as well as increase in the Perspex slope angulation. Top image represents Perspex slope 4.62° in water+1ml milk (θ D= 3.67°, θ D= 2.99° for OCT skin and oral respectively), middle image represents Perspex slope 4.62° in water+4ml milk (θ D=4.28°, θ D=3.43° for OCT skin and oral respectively), while lower image represents Perspex slope 11.44° in water+6ml milk (θ D=6.93°, θ D=5.35° for OCT skin and oral respectively). It can be noted that changes in θ D are introduced by both slope angle and solution RI together, the slope angle having a more pronounced effect in this model. Furthermore, the behaviour of the OCT oral instrument is similar to the OCT skin instrument. The blue line represents air-liquid boundary. Blue and dashed red lines have been drawn on OCT oral images due to difficulty in observing the original lines.

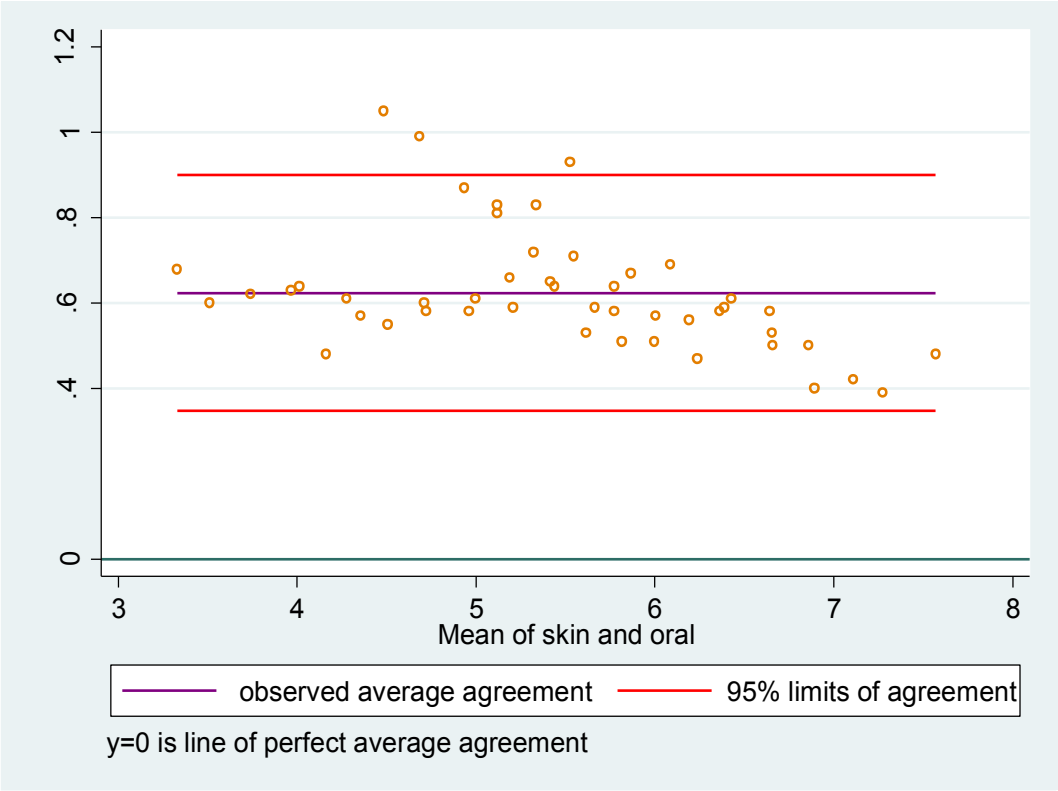

Figure (4.15) Bland and Altman (1986) plot (n=48) of the mean of θ D for both OCT skin and oral instruments [both water+ surfactant and water+ milk (horizontal axis)], while vertical axis represents the difference between θ D measured by OCT skin and oral systems (mean of OCT skin-OCT oral). The green line represents zero bias or perfect average agreement (no difference between both OCT systems). Aside from the bias of just above 0.60° [$P < 0.001$ from a paired *t*-test (the purple line above the zero bias line)], there is a very good agreement between mean of OCT skin and mean of OCT oral with expected discrepancies ranging from just below 0.40° to 0. 90° (95% limits of agreement represented by the top and bottom red lines).

4.4.4 Investigation of OCT skin and oral instruments using tissue mimics (collagen gel block)

With regard to collagen matrix block experiment, figure (4.16) below displays the refraction (bending) of the scalpel blade when it crosses two different media with different indices of refraction (air-water boundary). A marked second distortion can be observed when the blade passes from the simple aqueous to the hydrated collagen environment (collagen gel), which is more turbid and optically denser than the water.

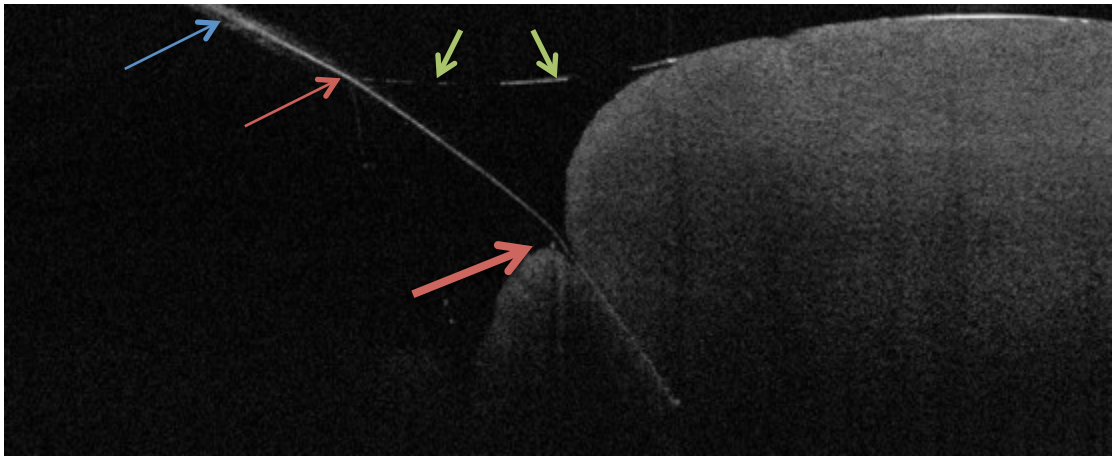

Figure (4.16) OCT skin image showing that a scalpel blade (blue arrow) undergoes first bending (red arrow) as it crosses air-water boundary (green arrows), then second refraction (bold red arrow) when it crosses water-collagen boundary.

4.5 Discussion

Convex white line on the top of OCT oral instrument image

The adaptation from the original OCT skin instrument to the new OCT oral instrument involved the application of a long imaging tube with a 45 degree planar surface scanning mirror to facilitate side viewing. The optical path length increase was matched by the reference path to sustain the interferometric imaging technique. However over such an elongated path, the tendency for a radial scanning effect in X- plane across a flat planar mirror introduced an immediately apparent distortion in the X plane (the apparent convexity of the planar viewing window), which is visible in all scans. Although Z scanning is relatively unaffected by this geometry, there was a real concern that serial Y-plane scans to build a 3-D model might demonstrate a serial amplification or reduction of the effect, thus compromising the integrity of any volumetric data (for example, tumour volume change data) derived from the instrument. This curvature allowed a maximum rise of 14 pixels (56μm) over the 6mm (6000μm) imaging width field. Comparison of standards measured across the field width failed to show additional distortion from one side of the image to the other.

Calibration of NPL and metric slip gauges in X-plane, Z-plane, & X, Y, and Z-planes (3-D)

Despite the apparent arc distortion of the plane viewing window in the OCT oral instrument, measurements of the linewidth (rectangle width) on the NPL standard at both extremes and centre of the imaging field in the OCT oral instrument and comparing that with the measurements obtained by the CE certified OCT skin instrument failed to demonstrate any significant error in object dimension. This is encouraging, suggesting that the distortion observed (56μm height in a 6 mm wide field) is tolerable in clinical feature size assessment, as a cell is approximately 10μm in diametre and the instrument resolution in clinical practice is limited to several cell width equivalents. Moreover, no distortion of the linewidth sample was observed when re-imaged under aqueous imaging environments that have dissimilar RIs. This indicates the stability of the OCT scan X dimension regardless of environmental RI change. This also confirms that the distortions of the planar surface phantom were mainly induced by time of flight delays, reflecting the differing RI of the surrounding media. This enhances our confidence in the reliability of width measurements (X axis) in OCT if applied to human in vivo/ ex vivo research.

Calibration in Z-plane in air and in different liquid environments that possess dissimilar RIs revealed that OCT oral system is performing identically to OCT skin instrument in measuring the distance between the metric slip gauges steps by measuring the angles between the tips of the steps, although the angles were not identical from both OCT oral and skin instruments. Both OCT systems revealed the same reduction in the angles across different RI media reporting increases in the distance between steps with higher RI, for instance in immersion oil (RI=1.515) compared to milk (RI=1.344-1.348). Furthermore, the distance is also increased gradually when the difference in the RI between the media were slight, for example RI of milk and surfactant (RI=1.359). One indicator of the material optical density is the RI value of the material. RI values are numerical index values that are expressed in relation to light speed in a vacuum. The index of refraction value of a material is a number that indicates the number of times slower that a light wave would travel in that material than if it were in a vacuum. The least optically dense materials are those through which light travels fastest, while the most optically dense materials are those through which light travels slowest. So as the RI value increases, the optical density increases, and the light speed in that material decreases. The optical density of a material refers to the sluggish tendency of the atoms of a material to

maintain the absorbed energy of the light wave in the form of vibrating electrons before reemitting it as a new electromagnetic disturbance (www.physicsclassroom.com). Statistical analysis using Bland and Altman (1986) method has displayed good consistency in measuring the angles of step height model in liquid between both OCT systems.

The images obtained by both instruments for the step height model in milk and immersion lens oil has demonstrated that increase in RI has minimal influence on the penetration depth of the OCT light beam, but the optical scattering properties of milk has influenced (reduced) the depth of OCT light beam where the lower step was invisible in both OCT skin and oral images. In immersion oil, the lower step was visible in the OCT skin image, while in the OCT oral image, although it was invisible, the reflection from the step can still be observed (Fig. 4.9). This reflects the reduction of imaging depth when changing from a transparent to a scattering environment such as skin or oral mucosa compared to relatively deeper imaging depth when scanning through more transparent media, for example the humours, anterior to the retina of the eye.

The volumetric (3-D) measurement of the standard slip gauge (1.5mm) was demonstrating an excellent congruence in performance between the OCT skin and oral systems. The width measurement X orientation of the slip gauge slices through the entire multislice scan Y-plane demonstrate that the OCT oral instrument is scanning the sample of interest without producing additional distortions in any planes of the obtained image. The Bland and Altman (1986) statistical method confirmed that the width measurement identified throughout the 500 slice Y-scans in both instruments was the same (~ 375 pixels × 4μm = 1,500μm) confirming the known width of the slip gauge block.

Perspex plate slopes phantom in liquids (effects of change in medium refractive index)

The Perspex slope phantom experiment also exhibited concordance between both OCT instruments performance in observing the effect of RI change of the material or medium on the distortion angle (θ D). Surfactant was used to adulterate water and obtain media with gradually increasing index of refraction, that is, more optically dense media and assess the effect of that on the change of θ D. Human tissues have variable RI and scattering properties, so milk was used for second comparisons

to assess affects of media with different refractive indices plus adding scattering properties. The fat component (4%) of milk is present as 1-10μm diametre globules (Hui et al, 2007; Mulder & Walstra, 1974; Michalski et al, 2001) that act as light scattering surfaces, along with casein micelles, and colloidal calcium phosphate (Hui et al, 2007). Our transparent surfactant experiments showed a similar increase in RI effect to the milk provides valuable evidence that the apparent RI change and distortion (θ D) of a known planar object passing into that medium, is principally a feature of RI and not scattering. This offers a potential mechanism for RI description of dissimilar tissues in surface structures by θ D type distortion. One possible application of this could be the assessment of a suspect lesion by following needle distortion during fine needle aspiration (FNA) and confirmation that the target tissue had been breached by the FNA needle prior to sampling. At present still theoretical, this could offer a useful tissue assessment, biopsy confirmation or guidance mechanism in the future.

The tables in appendix 1 show that as the Perspex slope angle is increased and as the RI of the medium increased by adding more surfactant or milk to water, this has influence in increasing θ D. There were consistencies of behaviour between both OCT systems in detecting the change in θ D, which suggest that the OCT oral instrument is performing in similar ways to the standard OCT skin instrument. This validation is essential, as National Research Ethics Service (NRES) have been granted to allow the first application of this new instrument to human lesion imaging in vivo (12/LO/0371). As both instruments run the same display and calibration software, it is an essential first step to assess the performance of the new instrument against the CE marked standard to ensure the 2D and 3D scan measurements and volumetric analyses are the same and consistent. It is encouraging that the planar X distortion that introduced by an elongated final optical path to the head of the instrument and an arc scan across a planar mirror final geometry, is not significantly amplified in sequential Y-slices, amplifying the effect throughout a 3-D volume scan. Thus 3-D datasets and 2-D tissue slice images can be interpreted in the same way and considered similarly reliable whether from the oral or the skin instruments.

Investigation of OCT skin & oral instruments using tissue mimics (collagen gel block)

Collagen matrix gel block were prepared to act as connective tissue substitute model. Collagen is the principal constituent of connective tissue, making up approximately 25-35% of the total body protein content. Collagen, in the form of elongated fibrils, is mainly found in fibrous tissues, for example tendon, ligament and skin (Di Lullo et al, 2002).

The collagen gel block models were selected to evaluate and observe the refraction of the OCT light beam in a medium that model connective tissues. The double refraction of the scalpel blade at air-aqueous boundary, then aqueous-collagen boundary serves as a clear demonstration of serial image distortions with serial RI changes. In this case the interfaces were the air-water/water-wet collagen boundaries where the light wave slows down upon crossing the boundary due to higher optical density of the water/collagen compared with air.

4.6 Conclusion

This study revealed that changes in RI of the imaging environments for scanning objects in the X plane has no apparent influence upon the measurement and thus no effects on the accuracy of data of both OCT systems. However, for the Z plane, changes in RI media have resulted in decelerating and scattering of the OCT light beam, which was obvious in the step phantom experiment when scanned in different liquids having dissimilar RIs. Furthermore, there was refraction of the OCT light beam when scanning obliquely orientated objects with refraction increasing or decreasing with the RI value of the medium.

This series of laboratory experiments would suggest that despite a small arc distortion in the X scan plane due to the final right angle turn geometry in the scanning system, the non-CE certified OCT oral instrument offers comparable images and measurement data in X, Y, and Z parameters compared to the clinically available CE certified OCT skin instrument marketed for dermatological imaging applications. Notwithstanding the initially concerning distortion in the single X-plane scan of the oral instrument, there is consistency in measurement of 3-D objects. Conformity in measuring small object dimension, on standard phantoms such as NPL microscopy and engineering standards to the level of pixel precision, render the convex X distortion negligible. Of greater significance is

that the distortion is consistent throughout serial Y scans (3-D volume scans), rendering the volumetric analyses trustworthy. The investigators were concerned that a radial X scan geometry against a planar mirror could introduce additional and progressive distortions by use of same mirror in serial Y scans, but this was not identified in the reported single media serial slice studies.

Consequently, we suggest that the OCT oral system can be used as direct surrogate for the CE certified OCT skin instrument in measurement of cutaneous and oral tumour thickness and depth with confidence and accuracy. NRES ethical approval for these studies (12/LO/0371) has now been granted for this purpose.

In order to be able to apply a new or modified OCT instrument from existing standard and calibrated instrument, it was fundamental to assess and validate the modified instrument before starting to examine ex vivo and in vivo human cutaneous and oral tissue to evaluate OCT oral instrument in diagnosing and monitoring premalignant and malignant lesions in the head and neck region especially in the oral cavity. The series of laboratory experiments have paved the way for application of the oral instrument into ex vivo and in vivo human clinical research.

Chapter 5

Evaluation of effects of refractive index change on the OCT oral instrument using different porcine tissue models

Chapter 5

Evaluation of effects of refractive index change on new OCT oral instrument using different porcine tissue models

5.1 Background and objectives

Propagation of light through an optical system can be attenuated by absorption, reflection and scattering (Fox, 2002 & Smith, 1972). Optical scattering occurs because of mismatches in the index of refraction of the different components of the tissue, varying from cell membranes to whole cells. The most important scatterers are cell nuclei and mitochondria (Wang & Wu, 2007). Their dimensions range from 100nm to 6μm. Most of these organelles exhibit highly forward-directed scattering (Vo-Dinh, 2002).

Strong scattering limits the OCT penetration depth ability in biological tissue (Brezinski et al, 1996). Scattering arises from changes in the refractive index (RI) between different constituents of the tissue and the surrounding medium. It is reliant on the shape and size of scattering components in the area and material of interest; accordingly the macroscopic scattering properties of different types of tissue can differ significantly. Absorption of the light waves by water, lipids, protein and haemoglobin could mainly be prevented by appropriate selection of the wavelength. The optical absorption of water and other typical constituents of tissues such as haemoglobin or melanin between 600-1300 nm is low (Parrish, 1981; Brezinski et al, 1996), which results in an optical window [also known as near infrared (NIR) or therapeutic window or window of transmission] (Parrish, 1981).

The depth of OCT imaging influences the selection of the operating wavelength within the NIR window. Light at approximately 1300nm permits deepest penetration into most translucent tissues such as skin or mucosa, because absorption in melanin and scattering reduce with rising wavelength (Brezinski et al, 1996). Deeper penetration for applications in the tissue may be achieved by using even longer wavelengths, for example around 1700nm in applications where there is a low concentration of water so water absorption has no substantial effect (Sharma et al, 2008). However, these long wavelengths are not suitable for in vivo examination of the posterior eye segment because of strong attenuation of the signal in the vitreous humour, which largely comprises of water and is situated between the lens at the front and the retina at the back. Therefore, for retinal imaging

the commonly utilised range is about 800nm wavelength that exhibits very low water absorption (Považay et al, 2003), while wavelengths around 1050nm allows deeper penetration into the subretinal layers plus provides the best compromise between these factors (Považay et al, 2003) and at the same time featuring slight chromatic dispersion in water (Wang et al, 2003a).

In this study we aimed to evaluate human skin/oral mucous membrane layers for differing RI, depending on the constituents and properties of each layer. Based on morphological and functional data, porcine skin appears to be the closest to human skin (Meyer et al, 1978; Monteiro-Riviere and Riviere, 1996; Barbero and Frasch, 2009), and is frequently used as a substitute in numerous human skin studies (Barbero and Frasch, 2009; Godin and Touitou, 2007). Therefore, porcine skin and subcutaneous tissue models were selected to evaluate and observe the refraction of the OCT imaging beam.

In transparent media, the direction of the imaging beam can be demonstrated simply in figure (5.1) below. However, in translucent animal tissues this form of RI interrogation is not possible. An alternative mechanism had to be developed showing optical distortion, based upon the previous slope imaging experiments (Chapter 4), examining the distortion of a known linear reference plane as tissue type boundaries are traversed.

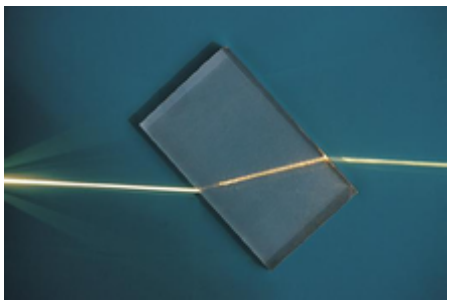

Figure (5.1) A ray of light being refracted in a plastic block.

5.2 Materials and methods

Fresh porcine skin samples with the underlying subcutaneous fat and muscle were obtained from a local abattoir and each tissue type was separated and put separately in suitable Petri dish. Ten shortened surgical scalpel blades (No. 15, Swann-Morton, UK) were placed into each tissue type at 40-60° angle, allowing scanning by the OCT oral instrument of the aforementioned tissues with the scalpel blades penetrating the tissues (Fig. 5.2).

Direct simple imaging of the distortion of the known flat bright steel surgical blade upon change from air-tissue interface allowed calculation of distortion angle (θ D) as in previous chapter by observing apparent image distortion as a result of differing indices of refraction. This was repeated for both OCT instrument types. Images of the air-tissue interface were captured using software with the beam perpendicular to the tissue surface and scanning parallel to the long axis of the blade inserted.

To measure (θ D), 10 measurements were obtained for each tissue sample and the mean and standard deviation (SD) calculated (Tables 1 & 2 in appendix 2) for statistical analysis using "Three way Analysis of Variance" method.

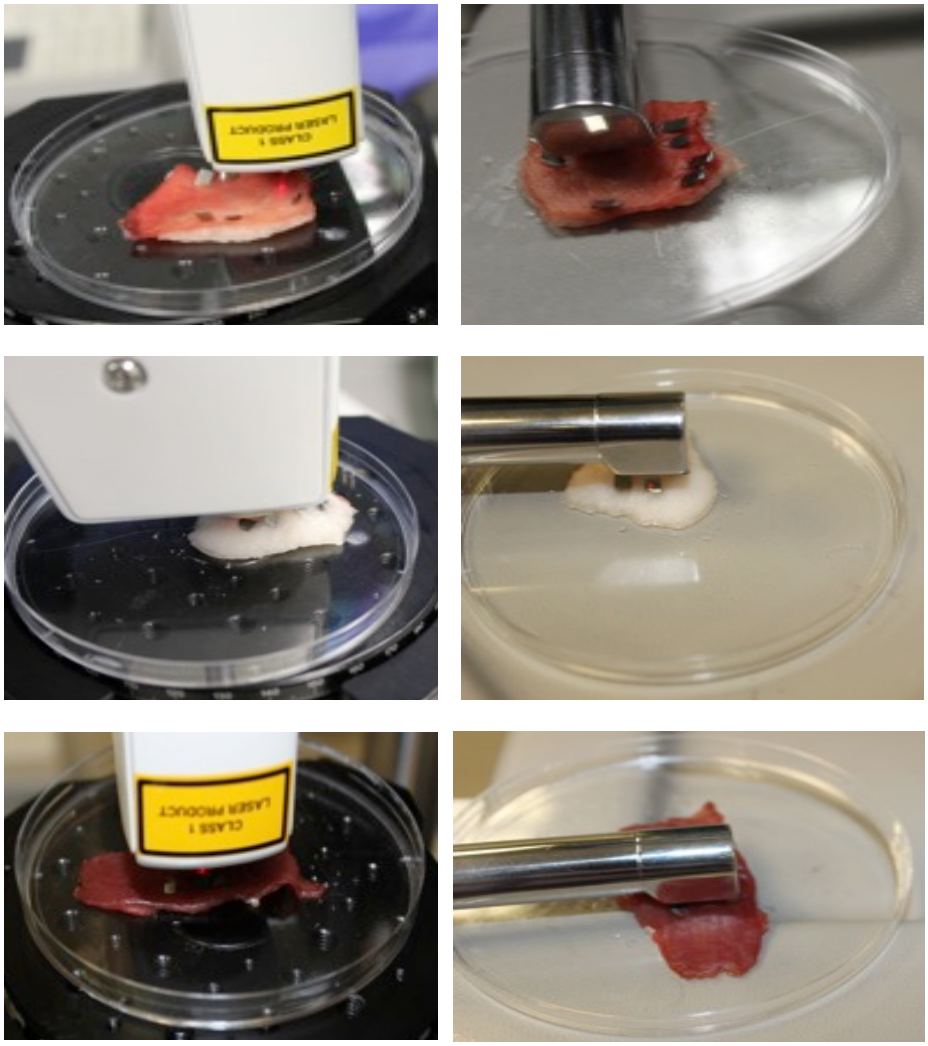

Figure (5.2) Images of fresh porcine skin, subcutaneous fat, and muscle scanned by OCT dermatology (left) and oral instruments (right), respectively.

After scanning each of the three fresh porcine tissues, the samples were immersed in isotonic phosphate buffered saline (PBS) solution for three days, to rehydrate the tissues in an isotonic environment. All scalpel blades were kept in their positions. Repeat imaging was conducted using both instruments after decanting the hydration fluid. Again, ten images were taken for each tissue type and analysed in the same way (Tables 3 & 4 in appendix 2). Direct pre- and post-hydration comparison demonstrated change in the distortion angles (θ D) as a result of the isotonic solution.

As a third environmental change, each series of tissue / blade samples were then deep frozen for three days at a temperature of -20° C. On day 4 the same samples were thawed for 30 minutes prior

to re-imaging in the same fashion, looking for freeze-thaw damage effects. Images of the blades penetrating the frozen samples were acquired by both OCT skin and oral systems to evaluate the distortion angle (θ D) by utilising image J programme (Tables 5 & 6 in appendix 2).

5.3 Statistical analysis

Statistical study was performed using "Three way Analysis of Variance" method for three factors: OCT skin and oral instruments, conditions of the porcine tissue samples (fresh samples, samples in PBS, and samples after freezing) and types of tissue (skin, fat, and muscle). "Bonferroni Post Hoc Tests" method was used to compare between the three porcine tissue types. $P < 0.05$ was considered statistically significant.

5.4 Results

With regard to fresh porcine tissue samples, the refraction of the apparent image of the scalpel blade was observed as the blade entered into different tissue samples that have different indices of refraction, which affected the degree of the bending of the blades (i.e. the apparent distortion of the image we are looking for) because of optical density of the medium that has been observed in the Perspex plate slope phantom experiment in previous chapter. Images of the fresh skin, adipose tissue, and muscle samples were acquired by both OCT systems, which can be seen in figures (5.3, 5.4 & 5.5) below.

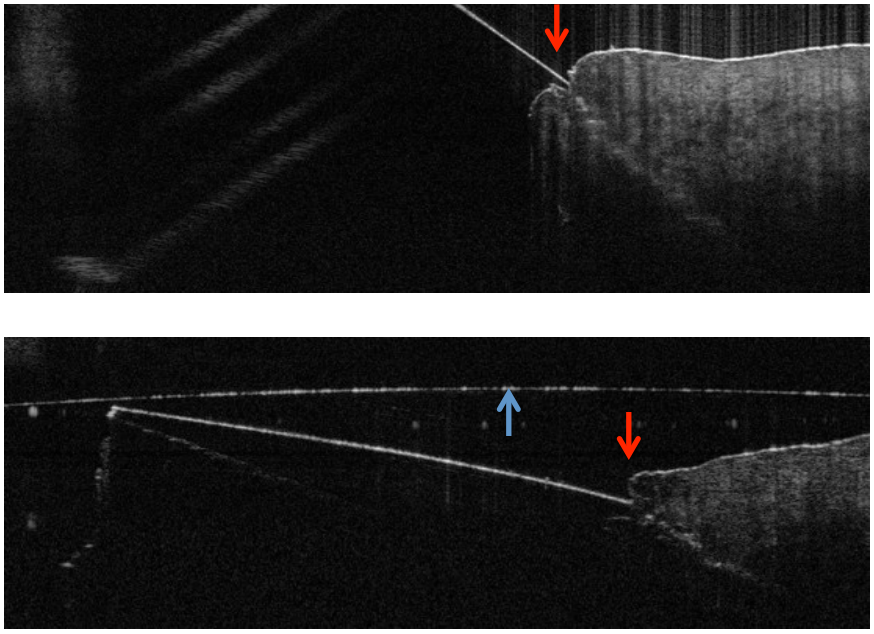

Figure (5.3) OCT images of scalpel blade refraction in porcine skin sample (fresh) scanned by OCT dermatology (above) and oral instruments (below). Red arrows indicate air-tissue interface, whereas the blue arrow indicates the glass window of the oral probe.

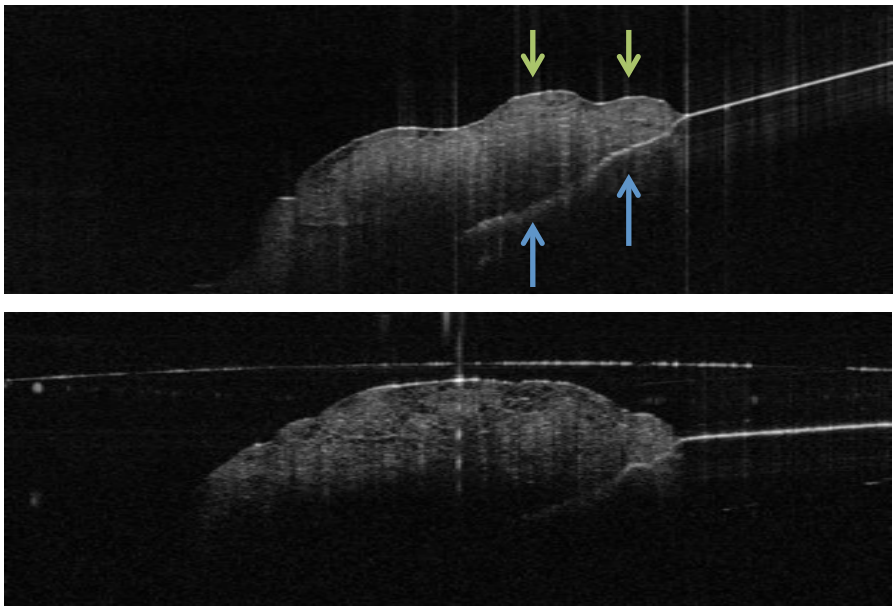

Figure (5.4) OCT images of scalpel blade refraction in porcine fat sample (fresh) scanned by OCT dermatology (above) and oral instruments (below). Undulation of the blade bend (blue arrows) can be noted, which corresponds with the undulation in the superficial layer of the sample (green arrows).

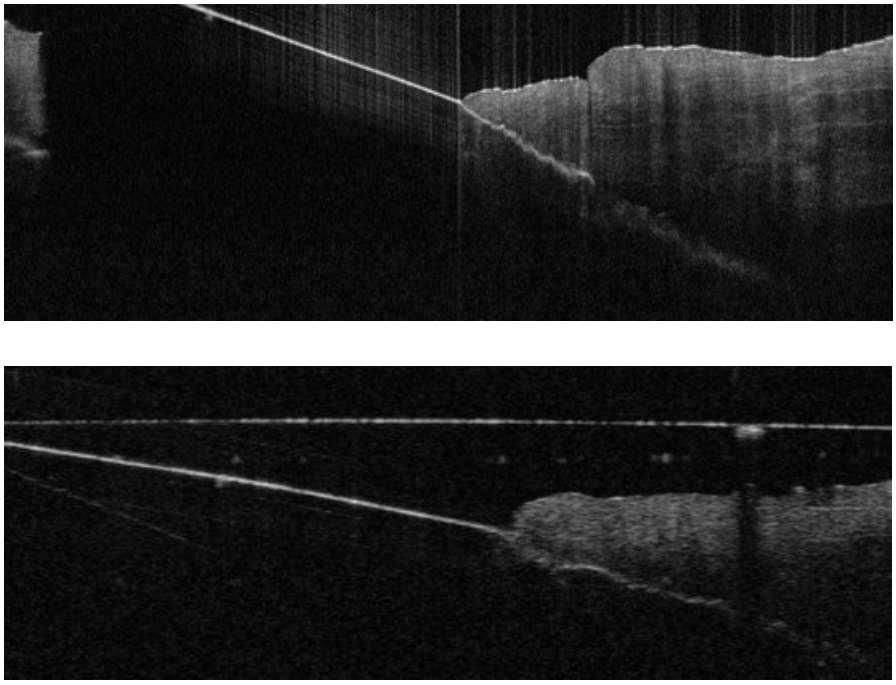

Figure (5.5) OCT images of scalpel blade refraction in porcine muscle sample (fresh) scanned by OCT dermatology (above) and oral instruments (below).

Table (5.1) below shows the summary mean and SD "angle of distortion **(**θ D)" data for all images obtained by scanning the porcine skin, fat, and muscle samples (fresh, in PBS and after freezing) using both OCT instruments. Raw data can be found in tables 1-6 in appendix 2. It appeared that there were similarities between the OCT skin and oral instruments data in different tissues that have dissimilar indices of refraction. The table illustrate that θ D is increased as the optical density of the media is increased, for e.g., muscle was the least optically denser (mean of θ D= 11.51°) in comparison to fat (mean of θ D= 15.52°) and skin (mean of θ D= 19.53°) confirming the findings of the Perspex slopes model experiment in previous chapter.

(Table 5.1) Summarise and illustrate the mean of θ D and SD for all the porcine tissue types (fresh, in PBS, and after freezing) for both OCT skin and oral instruments.

Type of tissue	**Mean of θD ± SD (OCT skin)**	**Mean of θD ± SD (OCT oral)**
Skin (Fresh)	19.53° ± 0.25°	19.53° ± 0.28°
Fat (Fresh)	15.52° ± 0.21°	15.54° ± 0.23°
Muscle (Fresh)	11.51° ± 0.23°	11.52° ± 0.23°
Skin (in PBS)	20.65° ± 0.35°	20.66° ± 0.26°
Fat (in PBS)	16.57° ± 0.21°	16.59° ± 0.36°
Muscle (in PBS)	12.58° ± 0.34°	12.55° ± 0.33°
Skin (after freezing)	19.47° ± 0.33°	19.33° ± 0.28°
Fat (after freezing)	15.30° ± 0.22°	15.27° ± 0.19°
Muscle (after freezing)	11.21° ± 0.13°	11.20° ± 0.11°

Table (5.1) above demonstrates the mean of θ D for all the images obtained by scanning the porcine skin, fat, and muscle samples after they have been immersed in PBS for three days using both OCT skin and oral systems. By looking at the table, it can be noted again that there were resemblance between the OCT skin and oral instruments data in different tissues (PBS) that have different indices of refraction. The table illustrates that mean of θ D is increased by about 1 degree or so for each tissue type in comparison to fresh tissues as the PBS resulted in altering the index of refraction of each porcine tissue samples.

The above table (5.1) reveals mean of θ D for all the images attained by scanning the porcine skin, adipose tissue, and muscle samples after being frozen for three days using both OCT skin and oral instruments. By observing the table, it can be noticed again that there were parity between the OCT skin and oral instruments data in different tissues (after freezing) that have different indices of refraction. The table illustrates that mean of θ D is dropped by about 0.20°-0.30°or so for each tissue type in comparison to fresh porcine tissues as the freezing result in slight decrease in the index of refraction of each porcine tissue samples, though the change is lesser when compared to the tissue samples in PBS.

The assumption of the analysis were checked by the study of the residual and found to be satisfied. There were no significant differences between the two instruments ($P = 0.059$). Furthermore, there were highly significant differences between the three tissue types ($P < 0.001$), and there were significant difference between the conditions of the porcine tissue samples ($P < 0.001$).

A comparison of the three tissue types using "Bonferroni Post Hoc Tests" method indicated significant difference between each porcine tissue types ($P < 0.001$), and between all the three conditions of the porcine tissues ($P< 0.001$). These statistical findings can be observed in the below plots (Figures 5.6, 5.7 & 5.8).

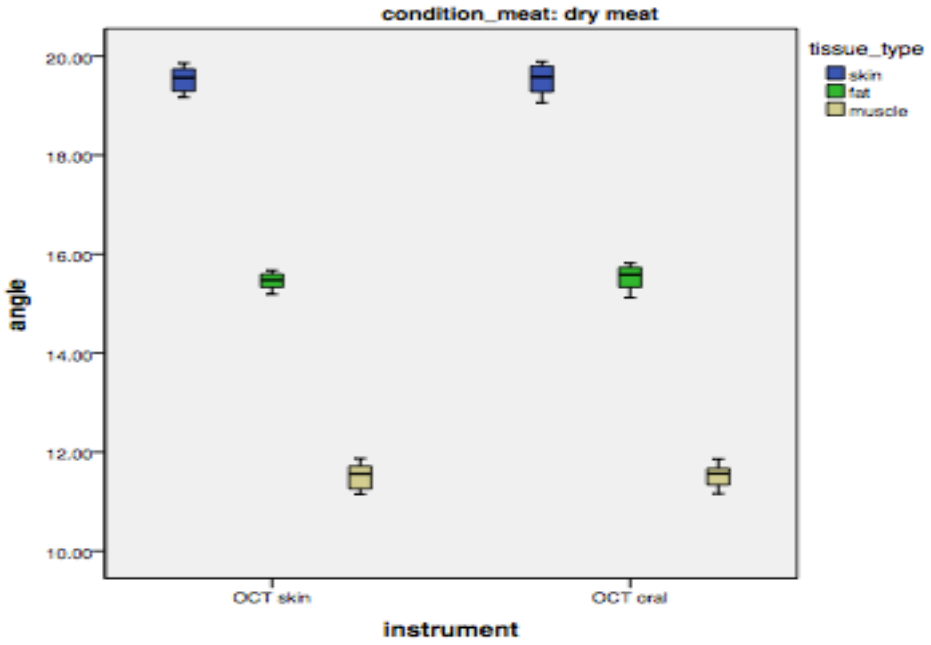

Figure (5.6) Box and whisker diagram illustrates congruency between both OCT skin and oral systems in scanning different porcine tissue samples (**fresh**) that have dissimilar RI.

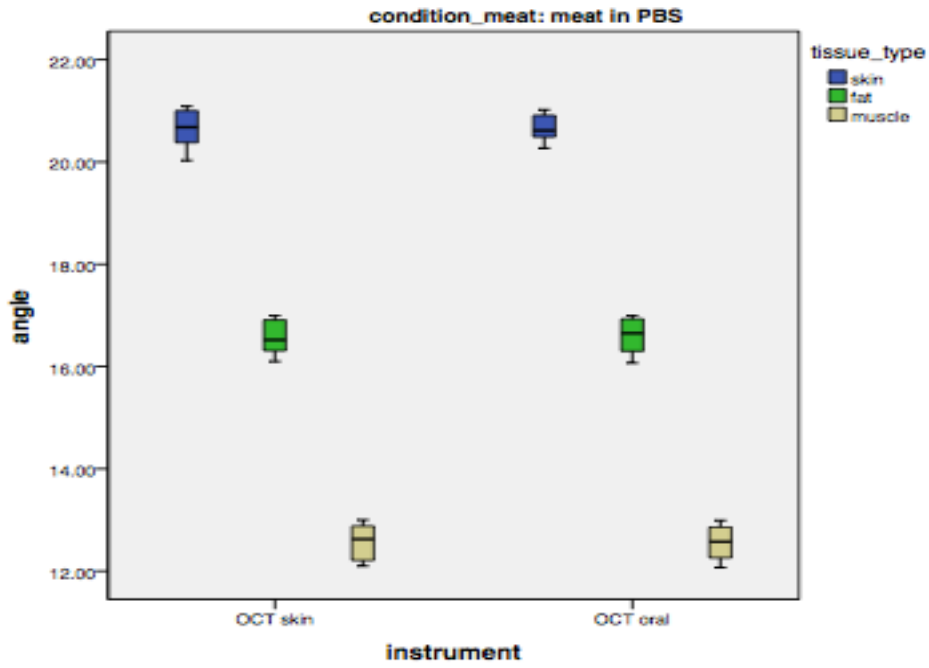

Figure (5.7) Box and whisker diagram illustrates congruency between both OCT skin and oral systems in scanning different porcine tissue samples (**PBS**) that have dissimilar RI.

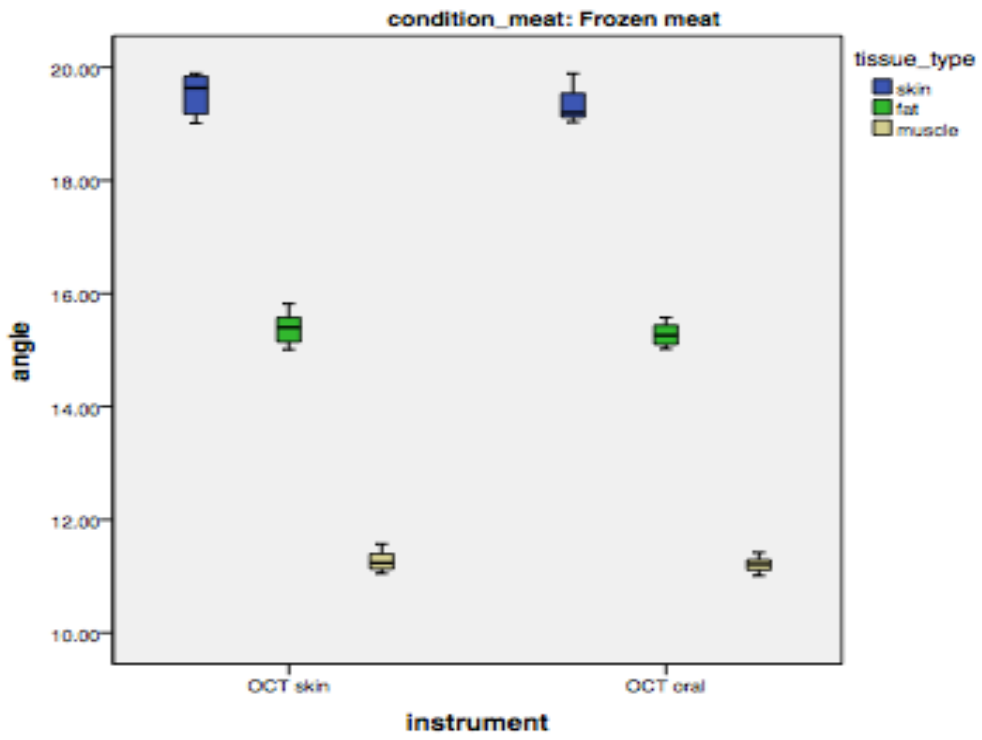

Figure (5.8) Box and whisker diagram illustrates congruency between both OCT skin and oral systems in scanning different porcine tissue samples (**after freezing**) that have dissimilar RI.

5.5 Discussion

Scanning of porcine tissue samples (skin, fat, and muscle) in different conditions (fresh or dry, soaked in PBS for 3 days, and finally freezing the samples for 3 days) with the scalpel blades inserted into the tissues, aid in evaluating the effect of RI of each tissue type on the distortion angle (θ D) and whether it will be affected by changing the condition of the fresh porcine tissue types. From observing and comparing the obtained data pertaining the measurements of θ D in different porcine tissues that possess dissimilar RIs and in different conditions for both OCT skin and oral instruments (Table 5.1), it appears that hydrating the tissues in isotonic PBS for 3 days, has mimicked replacement of tissue fluids, which in turn has increased the apparent RI of the tissue samples. This can be observed from the summary table (5.1), where the mean of θ D has increased by about 1° or so. A freezing cycle imposed upon the same fresh tissues had lesser effects on the RI of the different types when compared to hydration. The mean of θ D that dropped by an additional 0.20°-0.30° due to the freeze-thaw damage. There were highly significant differences between the

three tissue types ($P < 0.001$), and there were significant difference between the conditions of the porcine tissue samples ($P < 0.001$).

Comparison of the data obtained for both OCT systems in table (5.1) as well as the statistical diagrams in the figures (5.6, 5.7 & 5.8), were clearly displayed the conformity in behaviour between the CE marked OCT skin instrument and the modified non-CE certified OCT oral instrument. There were no significant differences between the two instruments ($P = 0.059$). It is of interest that the apparent surface of the scalpel blade was uniformly altered by θ D depending on the tissue type, but the ragged tissue surfaces introduced multiple parallel segments to the distorted plane (Fig. 5.4), reflecting the effect of distance travelled through a material of increased optical density as well as its RI on the final image, disrupting the apparent plane's continuity, but not the apparent image distortion (θ D). So time of flight mechanism gives additional distortion. These results point to a clear need for caution with navigation or tissue sampling proposals guided by markers not positioned within the tissue, or RI of similar value. Apparent angulation changes and distortions could lead to tissue sampling errors and guidance errors for the unwary.

Based on theta D (effect of RI) obtained in each porcine tissue, we can infer that cutaneous/ oral premalignant or malignant tissues could possess higher RI than benign and normal tissues due to the change in histopathological features, for instance increased N/C ratio, nuclear hyperchromatism, fluid content etc. altering the apparent optical density of adjacent malignant tissues. One possible application of this could be the assessment of a suspect lesion by following needle distortion during fine needle aspiration (FNA) and confirmation that the target tissue had been breached by the FNA needle prior to sampling, as monitored by intra-operative OCT guidance. At present still theoretical, this could offer a useful tissue assessment, biopsy confirmation or guidance mechanism in the future. Figure (4.16) in chapter 4 clearly demonstrates multiple theta D effects of each medium, i.e. first refraction in water followed by second refraction in collagen.

5.6 Conclusion

The series of the porcine skin and subcutaneous tissue scanning while penetrated by the scalpel blades using both OCT systems to observe the effects of different tissue types that possess dissimilar RIs on the distortion angle (θ D) of the OCT light beam has clearly revealed that the modified non-CE certified OCT oral instrument is performing similarly to the standard CE certified OCT skin instruments and offered comparable and trustworthy images when compared to OCT skin system images.

Chapter 6

Utilising OCT for tissue dimensional changes measurements: Shrinkage of porcine cutaneous specimens after formalin fixation and histopathology preparation

Chapter 6

Utilising OCT for tissue dimensional changes measurements: Shrinkage of porcine cutaneous specimens after formalin fixation and histopathology preparation

6.1 Background and objectives

It is widely accepted that tissue samples will shrink after excision and through histopathological processing (Ma et al, 2004; Goldstein et al, 1999; Quester & Schroder, 1997; Schned et al, 1996; Ladekarl, 1994; Lum & Mitzner, 1985; Boonstra et al, 1983), though there is a paucity of data concerning cutaneous specimen responses. As most close margins are reported in millimetre by pathologists, the meaning of that figure is debatable in direct translation into life. Cutaneous tissue shrinkage during processing is a source of debate (Kerns et al, 2008). A few studies have examined shrinkage of cutaneous tissue with contradictory results (Hudson-Peacock et al, 1995; Gardner et al, 2001; Golomb et al, 1991; Silverman et al, 1992). Yet, most previous studies have not stressed the significance of shrinkage as an element in settling inconsistencies in the medical record (Kerns et al, 2008).

Malignancies of the head and neck, including cancers occurring in the oral cavity, oropharynx, hypopharynx and larynx, represent globally the sixth most common type of cancers (Chang et al, 2008). One of the most prognostic factors in head and neck cancer is tumour size. According to the American Joint Committee on Cancer (AJCC) staging system, the pathological classification of a carcinoma is determined by evidence gained prior to treatment, then supplemented and modified by further evidence acquired during surgery, especially examination of the specimen by a pathologist. The pathological T (tumour size) category is derived from the actual measurement of the unfixed tumour in the resected specimen since up to 30% shrinkage of soft tissue might occur in a resected specimen after fixation in formalin (Edge et al, 2009).

In this study we utilised a porcine model in order to evaluate and measure the percentages of both horizontal and vertical dimensional changes, using our modified OCT oral instrument and the standard OCT skin instrument, before and after 48-hour formalin fixation. In addition, we re-measured the dimensions on the histopathology slides that corresponded to the same measured sites.

6.2 Materials and methods

Fresh full thickness epidermis, dermis and muscle porcine tissue samples were obtained from a local abattoir. Two parallel rows of six identical holes were cauterised into the skin tissue by heating the working end (smooth-faced) of an amalgam condenser in a Bunsen burner and applying the condenser firmly on the skin sample to (burn) create a sufficient and as uniform a depth hole as possible, the depth being regulated by the shape of the cylindrical instrument. We ensured that each parallel pair of holes remained within the maximum 6mm scan width of each OCT instrument by drawing parallel lines on the skin sample prior to creating the holes (Fig. 6.1).

Samples were retained in suitable Petri dishes and scans were conducted with both dermatological and oral OCT instruments, across the maximum diametre of each hole pair. Image J software was used to analyse all the images obtained by both OCT skin and oral systems to attain different measurements between the holes (X-plane) as well as between the walls of the holes (depth or Z-plane), see table (6.1).

Directly after first measurement, the tissues were fixed in 10% NBF (neutral buffered formalin) within the same Petri dish to minimise tissue disturbance. It was essential to ensure the tissues were completely immersed in 10% NBF and the cover of the Petrie dish were secured with adhesive tape for vapour control.

After 7 days the 10% NBF solution was decanted and the tissue sample were gently dried with a piece of tissue paper before commencing scanning, to avoid fluid collection in the perforated holes, distorting the measurements further. Again both OCT instruments were used to scan the six sets of the parallel holes across their maximum diametres to allow as best an approximation of co-

localisation that was possible. Images were further analysed and measurements taken using image J software.

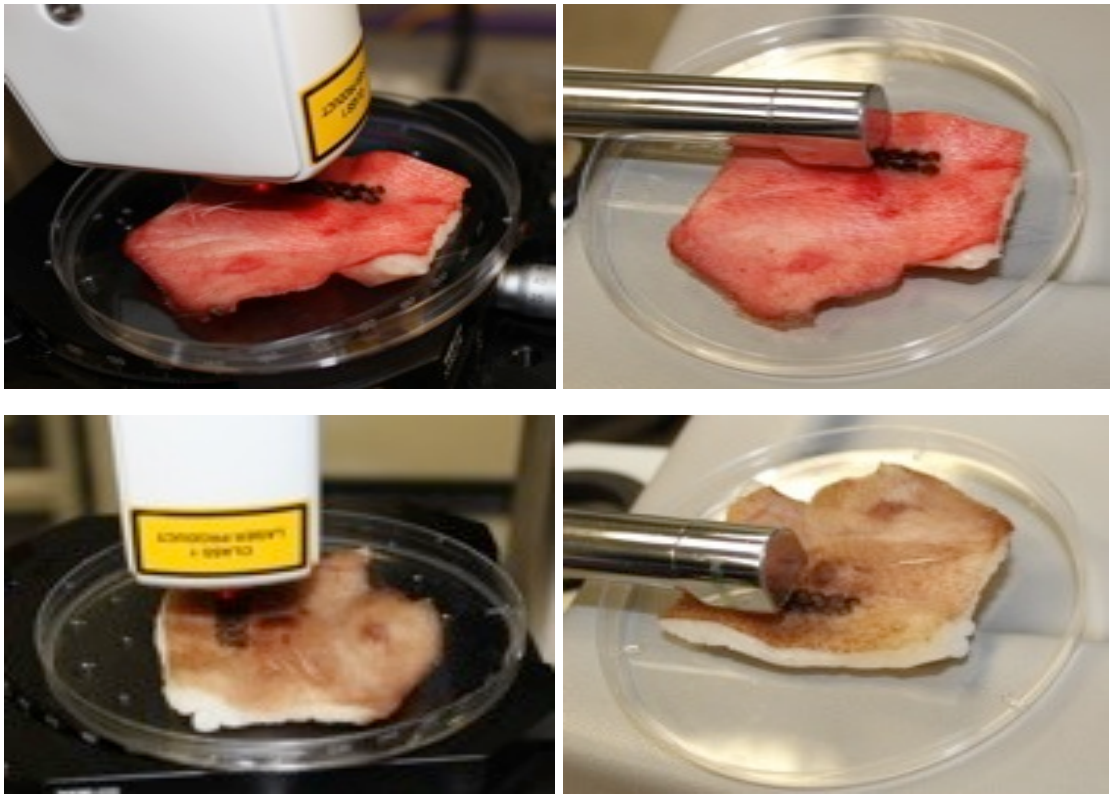

Figure (6.1) Images of fresh (upper set) and formalin-fixed (lower set) porcine skin parallel holes scanned by OCT dermatology (left) and oral instruments (right).

Once scanning was completed, the tissue were sent to the Core-Pathology laboratory department at Blizard Institute/Queen Mary University of London (QMUL) for routine paraffin embedding, sectioning and H&E staining according to a standard histopathological reference laboratory protocol. Outsourcing avoided any direct bias in sectioning / processing by the author. Care was taken by the laboratory to cut the sections at the middle of the circles (parallel holes) to match with nearly exact area of tissues that underwent scanning by both OCT instruments. All the measurements obtained for the porcine skin H&E slides in X and Z planes can be found in table 1, appendix 4.

6.3 Statistical analysis

The data were analysed by Stata statistical software for the Bland-Altman analysis (StataCorp. 2013. Stata Statistical Software: Release 13. College Station, TX: StataCorp LP.). $P < 0.05$ was considered statistically significant.

6.4 Results

All the images obtained from scanning the fresh porcine skin parallel holes, utilising both OCT skin and oral instruments, were subjected to analysis using image J programme to measure the distance between the holes as well as each hole separately (X-plane). In addition, the distance from the top of the holes to the bottom was measured (Z-plane). Figure (6.2) below illustrates how image J software was utilised to obtain all the measurements in both X and Z planes for the first parallel holes of the OCT skin instrument image. The same procedure was followed for measuring the remaining five parallel holes for the images attained by both OCT systems.

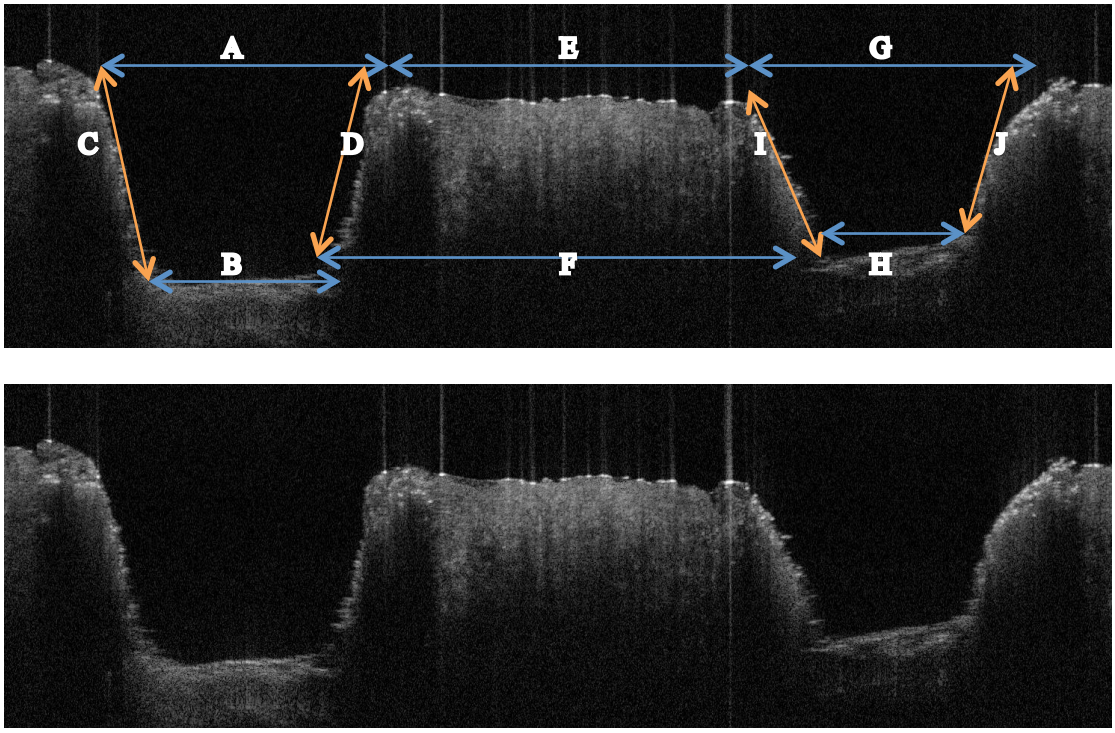

Figure (6.2) OCT images of fresh porcine skin **first** parallel holes scanned by OCT dermatology (above) and oral instruments (below). Double head blue arrows represent measurements in X-plane, while orange arrows represent measurements in depth plane (Z-plane).

Table (6.1) below demonstrates all the measurements in X and Z planes for the first set of the parallel holes for both OCT skin and oral images. The letters C, D, I, and J represent measurements in Z-plane, while the other letters represent measurements in X-plane. By comparing the data obtained for both OCT systems, it appear that there is congruency between both OCT instruments in measurements in both X and Z planes confirming the findings of measuring the linewidth (rectangle shape) on the NPL Optical Dimensional Standard and Z step height slip gauges model in the aforementioned planes, which can be found in chapter 4. Raw data for the remaining five sets of the parallel holes can be found in tables (1-5) in appendix 3.

(Table 6.1) Fresh porcine skin first parallel holes measurements by both OCT skin & oral instruments. Letters from A-J stands for the different measurements in Z (highlighted in green) & X planes in millimetre using image J programme.

Type of OCT	**A**	**B**	**C**	**D**	**E**	**F**	**G**	**H**	**I**	**J**
Skin	0.77	0.47	0.58	0.51	1.02	1.18	0.77	0.43	0.42	0.43
Oral	0.77	0.46	0.58	0.52	1.01	1.18	0.78	0.45	0.42	0.43

All the repeat images obtained from scanning the formalinised sample were analysed in the same way using image J programme (Fig. 6.2) to measure the distance between the holes (X-plane) as well as the depth of the holes (Z-plane).

It can be noted again that there is parity in behaviour between both OCT skin and oral systems when comparing the measurements from A-J in table (6.2) for the first parallel holes (raw data for the remaining five sets of the parallel holes can be found in tables 6-10 in appendix 3). However, the measurements in X and Z planes, which represented by letters from A-J, for the six sets of the parallel holes for both OCT skin and oral images appears to be smaller compared to the tables pertaining fresh porcine skin parallel holes. These reductions in the measurements are due to the resultant shrinkage of the skin sample after fixing it in 10% NBF for one week. The findings of

calibrating the NPL and Z step height slip gauges phantoms in X and Z planes using both OCT skin and oral instruments (chapter four) are confirmed again by the similarity in the data obtained for both OCT systems.

(Table 6.2) Porcine skin (formalin-fixed) first parallel holes measurements by both OCT skin & oral instruments. Letters from A-J stands for the different measurements in Z (highlighted in green) & X planes in millimetre using image J programme.

Type of OCT	**A**	**B**	**C**	**D**	**E**	**F**	**G**	**H**	**I**	**J**
Skin	0.87	0.43	0.52	0.45	0.90	1.20	0.87	0.39	0.41	0.42
Oral	0.88	0.43	0.51	0.45	0.90	1.20	0.89	0.39	0.41	0.42

Table (6.3) below shows the mean of A-J tissue dimensional changes in both X (A, B, E, F, G, and H) and Z planes (C, D, I, and J) for all the six set of the parallel holes. The means of tissue dimensional changes were obtained by subtracting A-J figures of the fresh porcine tissue from A-J figures of the formalin-fixed porcine tissue for all the six holes.

(Table 6.3) Illustrate the mean ± SD of A-J tissue dimensional change after formalin-fixed for all the six set of the parallel holes, highlighted figures underwent expansion, while the rest underwent shrinkage. All the measurements are in millimetres.

OCT	A	B	C	D	E	F	G	H	I	J
Skin	0.061± 0.02	0.025± 0.08	0.041± 0.02	0.031± 0.02	0.053± 0.035	0.036± 0.018	0.061± 0.049	0.045± 0.042	0.021± 0.014	0.021± 0.014
Oral	0.060± 0.03	0.028± 0.009	0.040± 0.03	0.036± 0.026	0.055± 0.03	0.036± 0.016	0.065± 0.050	0.043± 0.031	0.023± 0.015	0.025± 0.013

The mean percentage of tissue expansion and shrinkage in horizontal (X) plane as a result of formalin fixation was about 7.2% for OCT skin instrument, while for OCT oral system was about 7.4%, whereas in vertical (Z) plane the mean percentage of tissue shrinkage was 7.01% and 7.4% for OCT skin and oral systems respectively (raw data can be found in tables 1 & 2 in appendix 5). Figure (6.3) below explain the mean % tissue dimensional changes of both X & Z planes from A-J for both OCT instruments.

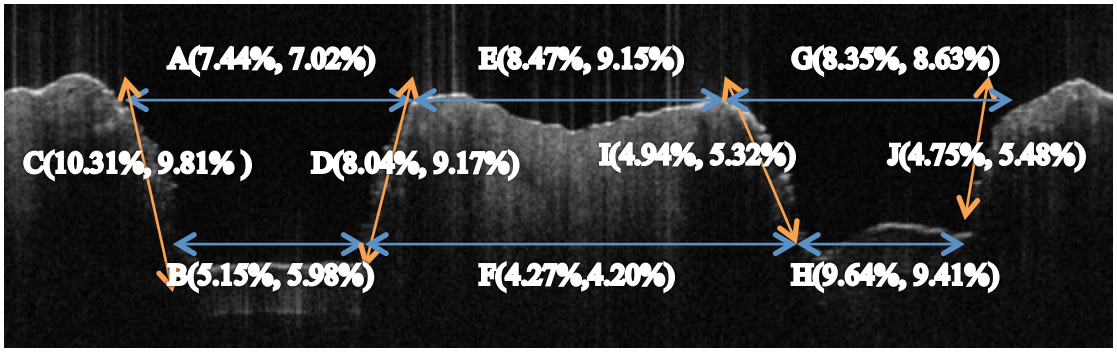

Figure (6.3) OCT image of formalin-fixed porcine skin illustrates the mean % change of both X & Z planes dimensions A-J. Double head blue arrows represent measurements in X-plane, while orange arrows represent measurements in depth plane (Z-plane). Percentages between brackets represent tissue contraction and expansion (A, F, & G) measurements for OCT skin and oral instruments, respectively.

The statistical results for evaluating the mean difference between both OCT skin and oral instruments in measuring the distances in both X and Z planes for the porcine skin parallel holes, which is illustrated in figure (6.4) were as follows: the mean of the differences being -0.001(SD= 0.007) and P value equal to 0.208 from a paired *t* test indicating no systematic difference between OCT skin and oral instruments. "Lin's concordance correlation coefficient" equal to 1.000 (95% CI from 0.99 to 1.00) suggesting good agreement. Additionally, the maximum likely difference between the two instruments is approximately 0.014 mm, which is clinically acceptable.

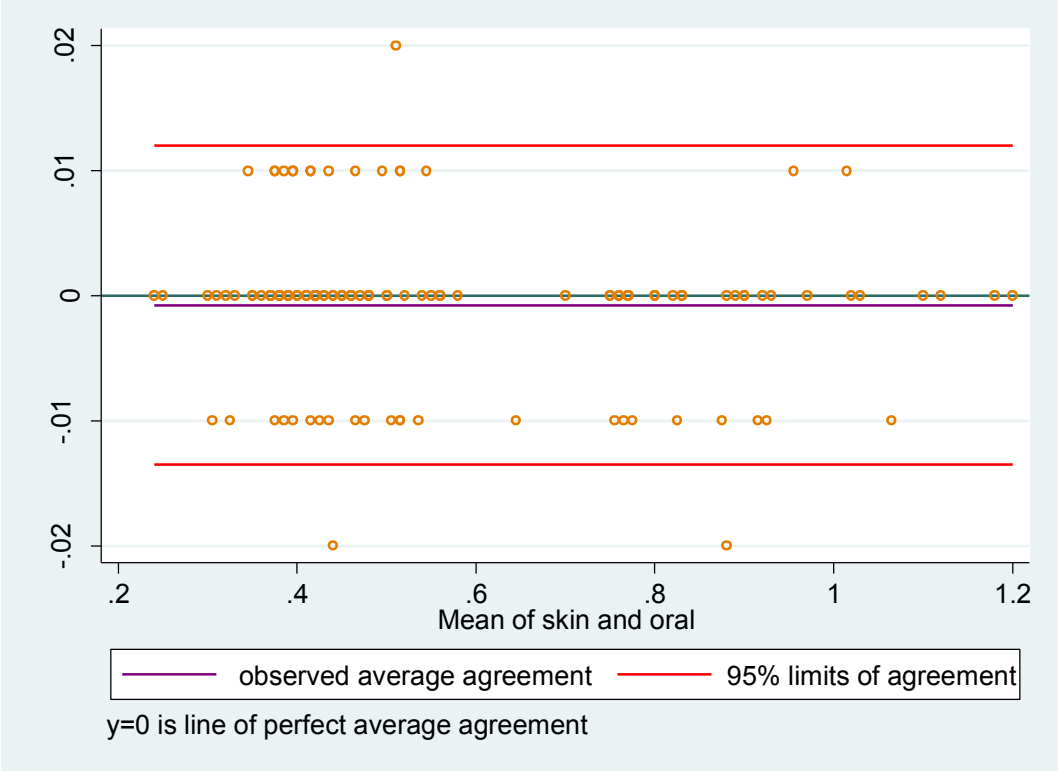

Figure (6.4) Bland and Altman (1986) plot (n=82) illustrates the measured distances (in millimetre) in X and Z planes (mean of A-J) represented by the orange circles for both skin and oral instruments (horizontal axis), while vertical axis represents the difference of measurements for both OCT skin and oral systems (measurements of OCT skin- measurements of OCT oral). The green line represents zero bias or perfect average agreement (no difference between both OCT systems). The purple line below the zero bias line represent bias, which indicates a very good agreement between mean of OCT skin and mean of OCT oral with expected discrepancies ranging from just below -0.01mm to just above 0.01mm (95% limits of agreement represented by the top and bottom red lines).

The parity in behaviour between both OCT skin and oral instruments, in scanning porcine skin (fresh and formalin-fixed) parallel holes in both X and Z planes, can be observed in figure (6.5) below.

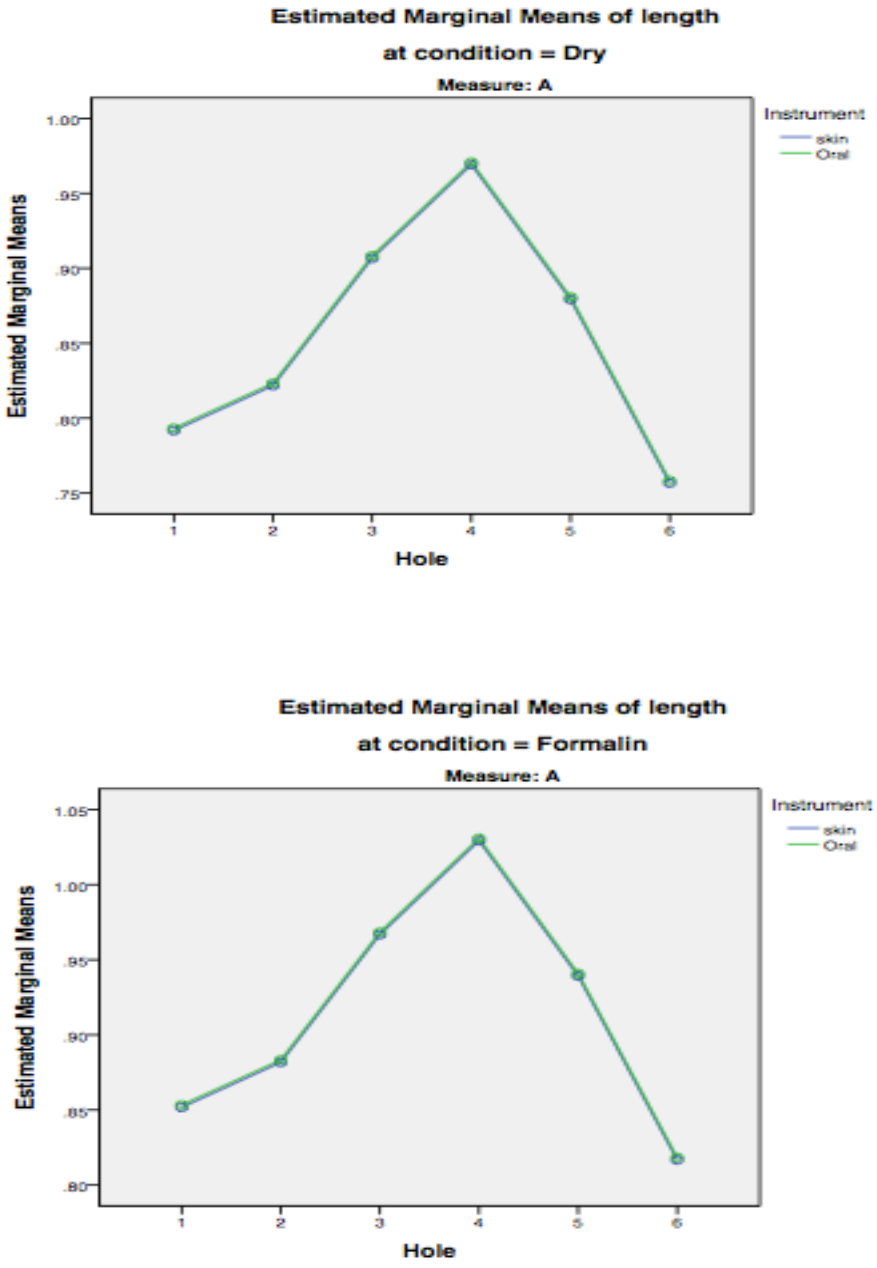

Figure (6.5) Diagram illustrates parity in behaviour between OCT skin and oral instruments in scanning fresh or dry porcine skin (above) and formalin-fixed porcine skin (below) for measure A of all the six set of the parallel holes.

After obtaining the H&E slides/images of the six sets of the parallel holes, all the images were underwent analysis using the "NanoZoomer Digital Pathology" programme (Hamamatsu Photonics K.K., Japan) with an integrated scale to measure the distance between the holes (X-plane) as well as the depth of the holes (Z-plane), represented by the letters from A-J (Fig. 6.6), to find out the degree of shrinkage on the porcine skin sample as a result of the steps that followed for processing the tissue for obtaining the histology sections.

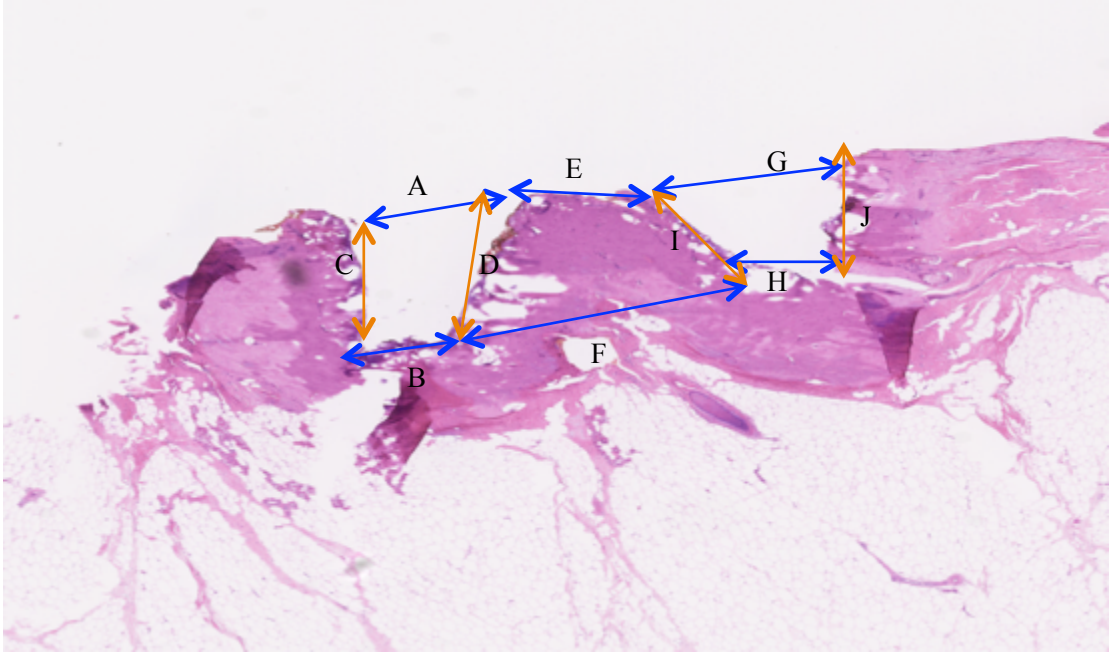

Figure (6.6) Haematoxylin and Eosin (H & E) slide of the porcine skin first parallel holes. Double head blue arrows represent measurements in X-plane, while orange arrows represent measurements in depth plane (Z-plane).

Table 1 in appendix 4 shows all the measurements obtained for the porcine skin H&E slides in X and Z planes. When comparing these data with the data obtained for fresh porcine skin sample scanned by both OCT instruments, it demonstrates the reduction in both X and Z plane measurements due to the resultant tissue dimensional change. The exception are axes A, F, and G where the measurements increased, which is due to contraction of the tissue bulk at both the upper and lower ends of each hole.

Table (6.4) below demonstrates the mean of A-J histopathology tissue dimensional change in both X and Z planes for all the six set of the parallel holes. The mean of tissue dimensional change was obtained by subtracting A-J figures of the fresh porcine tissue from A-J figures of the histopathology porcine tissue slides for all the six holes.

(Table 6.4) illustrate the mean± SD of A-J histopathology tissue dimensional change for all the six set of the parallel holes, highlighted figures underwent expansion, while the remainder underwent shrinkage. All the measurements are in millimetres.

OCT	**A**	**B**	**C**	**D**	**E**	**F**	**G**	**H**	**I**	**J**
Skin	0.100± 0.02	0.046± 0.05	0.066± 0.017	0.053± 0.018	0.076± 0.01	0.063± 0.016	0.093± 0.04	0.065± 0.042	0.040± 0.009	0.046± 0.001
Oral	0.096± 0.016	0.046± 0.08	0.063± 0.02	0.056± 0.021	0.078± 0.01	0.061± 0.013	0.090± 0.04	0.065± 0.034	0.041± 0.03	0.048± 0.08

The mean percentage of tissue expansion and shrinkage in horizontal (X) plane for the histopathology sections/images was greater compared to formalin fixation of the porcine skin tissue and was approximately 11.3% for OCT skin instrument, while for the oral system was 11.2%. In the vertical (Z) plane the mean percentage of tissue shrinkage was 12.4% and 12.8% for OCT skin and oral systems respectively (raw data in tables 3 and 4 in appendix 5). Figure (6.7) below explain the mean % tissue dimensional changes of both X & Z planes from A-J.

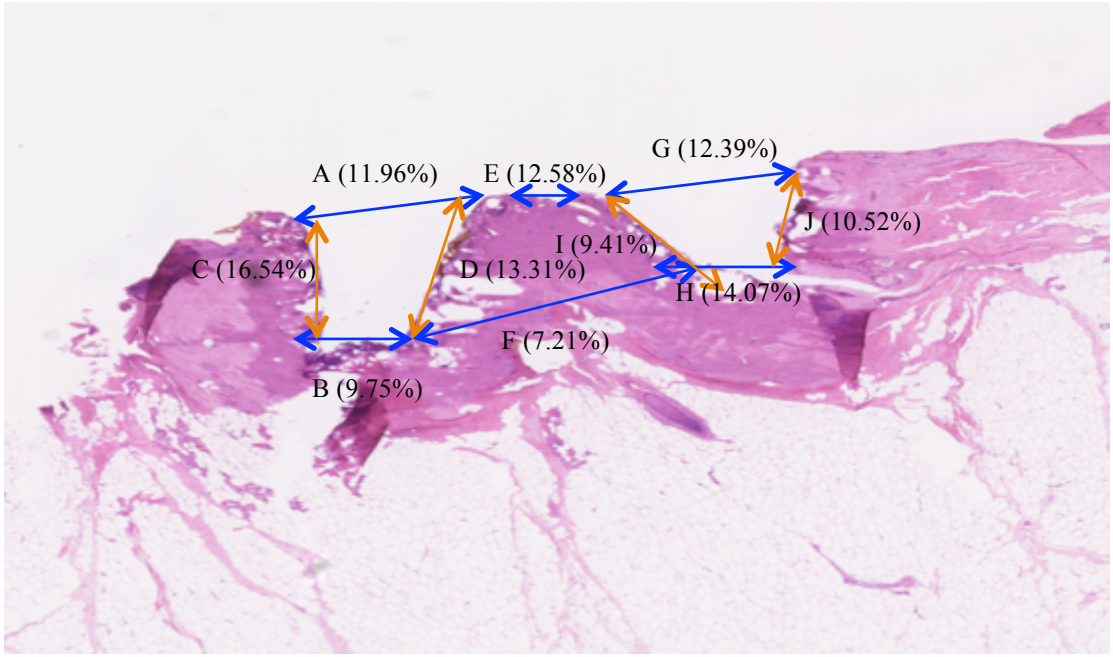

Figure (6.7) H & E slide of porcine skin illustrates the mean % change of both X & Z planes dimensions A-J. Double head blue arrows represent measurements in X-plane, while orange arrows represent measurements in depth plane (Z-plane). Percentages between round brackets represent tissue contraction and expansion (A, F, & G).

6.5 Discussion

Porcine skin (fresh and formalin-fixed) parallel holes

The measurements of the distances between the sets of the parallel holes (both X and Z planes) using both OCT skin and oral systems for scanning porcine skin (both fresh and formalin-fixed) demonstrate similarity in behaviour by comparing the figures, which represented by the letters from A-J, in the tables (6.1 & 6.2). Moreover, the results of the statistical analysis represented by the diagrams in figure (6.5) demonstrate that both OCT instruments are performing in the same way and are reporting the same dimensional changes in horizontal (X) and vertical (Z) planes. This confirms the findings of calibrating the NPL and Z step height slip gauges phantom in the aforementioned planes in chapter 4.

The NBF fixation of the porcine skin sample in a formalin-containing solution for 7 days resulted in tissue dimensional change in both X and Z planes (Table 6.3). For example, the mean of E shrinkage (shrinkage in X plane) for all the six set of the parallel holes were 53µm and 55µm for OCT skin and oral instruments respectively. Taking a closer look at the table, one can notice that figures of A, F, and G were increased as the tissue shrank at both the upper and lower ends of each hole and resulted in stretching the tissue at these locations. While for the shrinkage in Z plane, for example, the mean of I shrinkage for all the six set of the parallel holes were 21µm and 23µm for OCT skin and oral instruments, respectively. Moreover, the mean percentage of tissue dimensional change in horizontal (X) plane as a result of formalin fixation was about 7.2% for OCT skin instrument, while for OCT oral system was about 7.4%, whereas in vertical (Z) plane the mean percentage of tissue shrinkage was 7.01% and 7.4% for OCT skin and oral systems, respectively.

Due to creating holes in our specimen, the tissue underwent expansion in the periphery and contraction at the centre where it has surrounded by holes in both sides. Similar expansion and contraction may not occur within routine incisional/ excisional biopsies, as the tissue is usually a single piece. However, any sectioning / disturbance will have significant impacts on dimensional stability in formalinisation and tissue processing. Usually an incisional biopsy will take a complete mixture of normal and abnormal tissues, contracts in both horizontal and vertical planes and there is

no holes surrounding a lump of tissue in the middle. The sample might probably undergo various degrees of contraction depending on the type of tissue (normal or cancerous). Therefore our data pertaining to the percentage of tissue changes in both X and Z planes might not correlate exactly with biopsies taken from patients who have cutaneous or oral malignant lesions, as our porcine sample was free from malignant change. However, the work highlights the instability of tissues in formalin fixation.

Histopathology sections for the porcine skin parallel holes

The measurements and analysis of the porcine skin H&E slides/images of the six sets of the parallel holes demonstrated that tissue processing (dehydration stage using fixative, for example 10% NBF, and clearing agent such as xylene) to obtain the histopathology slides has resulted in further shrinkage of the porcine skin sample in both X and Z planes when compared to the fresh porcine tissue, which can be seen in table (6.4). This table, for instance, shows that the mean of E shrinkage for all the six set of the parallel holes were 76μm and 78μm for OCT skin and oral instruments respectively, which has been calculated by subtracting E (fresh porcine holes) from E (histopathology porcine holes). Whereas for the shrinkage in Z plane, for example, the mean of I shrinkage for all the six set of the parallel holes were 40μm and 41μm for OCT skin and oral instruments, respectively.

Furthermore, the mean percentage of tissue dimensional change in horizontal (X) plane for the histopathology sections/images was greater compared to formalin fixation of the porcine skin tissue and was 11.3% for OCT skin instrument, while for OCT oral system was about 11.2%. In vertical (Z) plane the mean percentage of tissue shrinkage was 12.4% and 12.8% for OCT skin and oral systems respectively.

Though a variety of fixatives were developed for preparation of surgical specimen, formalin fixation offers the maximum histo-morphological quality for staining of biopsied tissues and determining a pathological diagnosis (Titford & Horenstein, 2005). The most common fixative used in the laboratory is 10% NBF that contains 4% formaldehyde. The formalin effects on the biopsied tissues can be divided into two phases. Formalin in the early phase penetrates the tissue by diffusion

and accumulates to a concentration sufficient for the next phase to commence (Hsu et al, 2007). In the second phase, the molecular changes include crosslinks formation between proteins or between nucleic acids and proteins, which involve hydroxymethylene bridges. Another proposed mechanism is the creation of coordinate bonds with calcium ions. The crosslinks and coordinate bonds might alter the proteins three-dimensional structure (Werner et al, 2000). This is a slow reaction, taking 24-48 hours to complete. Fixation for a short time results in incomplete processing, hence the duration of fixation can affect the degree of tissue shrinkage (Jonmarker et al, 2006 & Hsu et al, 2007). In the current investigation, we had fixed the sample in 10% NBF for more than 48 hours in order to circumvent incomplete processing and partial tissue shrinkage as well as achieving credibility for our findings.

It is well known that tissues will shrink after fixation in a formalin-containing solution. Nonetheless, different findings have been reported from different studies (Chen et al, 2012). Boonstra & associates (1983) found that cervical tissue shrank up to 15% after formalin fixation and processing. In another study, esophageal tumours demonstrated 10% shrinkage after formalin fixation (Siu et al, 1986). Jonmarker et al (2006) also reported that prostate biopsies shrank by 4.5% in diametre and 13% in volume after formalin fixation. Different results have been reported from two researches on breast cancer specimens. Yeap et al (2007) in a study on breast cancer have reported 4.5% shrinkage in diametre after histological fixation. On the contrary, in another study by Pritt et al (2005), the authors reported no significant change between fresh and fixed states in 96% of breast cancer biopsies. Concerning the difference in shrinkage reported in the aforementioned researches, it is likely that the type and composition of the tissues, for instance amount of fat or muscle tissues could impact the overall degree of shrinkage. Thus, it is rational that researches addressing dimensional changes must be organ-specific and explain tissue constitution (Chen et al, 2012).

Formalin fixation might cause tumour to shrink and consequently lead to the underestimation of T (tumour) staging. The study by Chen and colleagues (2012) in which they examined a total of 100 head and neck cancer specimens (first study investigating head and neck cancer specimens shrinkage), have found that the maximal diametre of the head and neck cancer specimens shrank 1.5 mm (4.40%) after fixation in formalin. The authors found that there was underestimation of T

staging in eight patients according to AJCC (American Joint Committee on Cancer) guidelines, in which five patients underestimated from T3 (tumour > 4 cm) to T2 (tumour 2-4 cm) and three patients from T2 to T1 (tumour < 2 cm). Alike result was reported by Hsu et al (2007) in their research on the effects of formalin fixation on tumour size underestimation in lung cancer. The authors found tumour shrinkage and migration from T2 to T1.

There was no substantial difference in the rate of tumour shrinkage between subgroups in terms of gender, age, and site of the tumour. Sex has not been reported as an association with shrinkage after formalin fixation (Chen et al, 2012). However, Kerns and associates (2008) reported that patient age is an important factor related to shrinkage in cutaneous biopsies. The authors also found that there was 5% greater shrinkage in trunk excisions when compared to head and neck excisions. This incongruence may be because of the diverse pathological features in the different researches. Most of the patients in Chen et al (2012) study had SCC, while patients in Kerns et al (2008) study had skin malignancy. Another potential explication is that the skin biopsies shrank in length and width instantly after excision owing to intrinsic tissue contractility, not formalin fixation (Kerns et al, 2008 & Dauendorffer et al, 2009).

Consistent with the latest version of the "AJCC Cancer Staging Manual", the pathological classification of a cancer is determined by the evidence obtained prior to treatment, then supplemented and modified by further proof acquired during and from surgery, especially pathological examinations of resected tissues (Edge et al, 2009). The pathologists do not routinely measure fresh biopsies in the operating theatre, but they always measure specimens that have undergone overnight fixation in formalin solution. Not all medical facilities have their histopathologists handle the fresh biopsies directly after resecting the tumour in the operating room (Hsu et al, 2007). Hence, the surgeons must measure the fresh specimens so as to avoid erroneous determination of the tumour stage. Chen et al (2012) report a mean shrinkage of 4.40% of the greatest diametre of head and neck cancer specimens. Therefore the authors recommended that size of the tumour require measuring immediately once resection in the operation room performed so as to eschew the understaging of head and neck cancers.

It has been reported that malignant tumours shrink less than benign tumours (Hudson-Peacock et al, 1995). In frozen sections from MMS (Mohs Micrographic Surgery) specimens, shrinkage of the tissue was statistically greater during processing in those above 60 years of age, and tissue from extremities and the trunk displayed considerably more shrinkage during processing than that from the head and neck region (Gardner et al, 2001). It has been determined that tissue shrinkage is not affected by gender (Hudson-Peacock et al, 1995 & Gardner et al, 2001). The use of formalin-containing solution for preservation in some studies has been found to further increase the shrinkage seen in excised cutaneous specimens (Hudson-Peacock et al, 1995); nevertheless, in another study by Golomb et al (1991) for determination of pre-excision surgical margins of melanomas from fixed tissue specimens, the authors have concluded that formalin is non-contributory to cutaneous specimens shrinkage with the majority of shrinkage occurring at time of removal of tissue from the body.

In another study by Kerns et al (2008) indicated that the majority of post-excision cutaneous tissue shrinkage is owing to intrinsic contractile properties of the tissue itself, and not to formalin. The intrinsic contractile properties of the tissue are negatively affected (diminished) by both the aging process and the solar damage as measured by solar elastosis, both of which reduce the viable elastin in the skin leading to reduced contractility.

Shrinkage of tissue specimens in length and width occurred straightway after excision and then on average, re-expanded to some extent with formalin fixation. These results resemble other researchers' findings in a study on shrinkage of resected specimens of esophageal carcinoma where rate of tumour shrinkage was 83.59% after resection but only 80.92% subsequent to formalin fixation (Ma et al, 2004). Contrary to that, Hudson-Peacock et al (1995) previously noted that biopsied tissue shrank by 22% post-excision with a further 11% decrease in size following fixation in formalin. Other researchers also found that the majority of tissue shrinkage happened before formalin fixation (Golomb et al, 1991). The clinicians and dermatopathologists should be acquainted with the predictable shrinkage of submitted biopsies for settling inconsistencies within the medical record (Kerns et al, 2008).

6.6 Conclusion

The findings in this study demonstrated that cutaneous porcine specimen has shrunk after fixing it in formalin-containing solution. Further shrinkage occurred by subjecting the specimen to paraffin-embedding and histologic processing in order to obtain the H&E slides. Our results established that OCT oral instrument behaved similarly to the standard OCT dermatology system in measuring the dimensional changes in both X and Z planes. This was demonstrated by the statistical analyses of both OCT systems data, including the Bland-Altman plot and the P value that showed no significant differences between both OCT instruments.

Chapter 7

Epidermal & epithelial thickness measurements of normal skin and mucosa utilising OCT imaging in vivo

Chapter 7

Section I: Epidermal layer thickness measurements of normal skin imaged by the OCT oral instrument in vivo

7.1 Background and objectives

A knowledge of skin thickness in different anatomical sites of human body, especially in the head and neck region, is of huge importance in various medical and biological research areas (Gambichler et al, 2006b). Epidermal thickness (ET) of healthy human skin differs depending on the site (Whitton & Everall, 1973; Sandby-Moller et al, 2003). Detailed understanding of ET in the various anatomical facial subunits is useful when performing facial reconstructive surgery and can optimise cosmetic outcomes.

Most of the earlier studies on evaluation of ET used confocal laser scanning microscopy (CLSM) in vivo (Corcuff et al, 1993; Huzaira et al, 2001; Sauermann et al, 2002; Neerken et al, 2004). Nevertheless, the first report provided only limited data with limited depth of penetration, as the ET thickness measurement was fairly significant (Branchet et al, 1990).

In order to distinguish different cutaneous pathologies utilising OCT, it is essential to determine baseline morphological features of normal skin layers especially the thickness of the topmost layer (ET). The aim of the present clinical in vivo study was to assess the effectiveness of the OCT oral instrument in measuring the mean ET in different age groups and skin types and different anatomical sites of the body.

7.2 Materials & methods

7.2.1 Patients

Sixty healthy subjects were registered for the current study. The study protocol approved by the NRES REC London-Dulwich (12/LO/0371), and informed consents was obtained from volunteers. Inclusion criteria included patients above 18 years old, whilst any subjects with a history of dermatological disease were excluded.

7.2.2 Methods/ study design

The study protocol was explained to recruited healthy subjects before they underwent OCT imaging of their skin. Imaging was performed at 14 anatomical sites: forehead, nasal tip and lateral nose, infra-orbital skin (lower eyelid), cheek, chin, ear, back of neck, palm and back of hand, ventral and dorsal forearm, chest and calf. All OCT images were examined by a single investigator to measure the ET using image J programme. The mean ET on the OCT image was calculated from 7 measurements taken from the centre of the image and 3 lateral measures on each side at equal distances from the centre. These values were utilised in order to determine an overall mean for each site and their standard deviations.

7.3 Statistical analysis

SPSS statistical software was utilised to analyse the data (IBM Corp. Released 2013. IBM SPSS Statistics for Windows, Version 22.0. Armonk, NY: IBM Corp.). In addition, two-way analysis of variance (ANOVA) was utilised to find out differences in ET with regard to skin type and gender. For assessing the relationship between quantitative variables for ET and age, a Pearson's Correlation method was used. P value of ≤ 0.01 rather than 0.05, to adjust for multiple testing, was considered to indicate statistical significance.

7.4 Results

The mean age of volunteers was 31 years (range 19–66). Females comprised 34 subjects, while males were 26. The cohort consisted of 29 subjects with skin type I-III (Fitzpatrick skin type scale), and 31 with skin type IV-VI. The OCT images of different anatomical regions of the body revealed layered architecture of skin with a clear demarcation (represented by the DEJ) between the darker, less reflective epidermis layer compared to the brighter, more backscattering dermis layer. In some of the OCT images with subtle layering, we had difficulty in measuring the ET. Figures (7.1-7.13) show all OCT images of the anatomical regions examined. Stratum corneum layer was invisible except on the palm of the hand. Glabrous skin also showed sudoriferous (sweat) gland duct in the epidermis, which featured as hyper-reflective (high scattering) coiled structure.

The epidermal layer of back of the neck, forearm (both ventral and dorsal surface) and calf have more ragged surface in comparison to the rest of the anatomical regions scrutinised. There were difficulties in identifying and measuring ET of forehead, cheek, chin and nose in comparison to other anatomical body regions examined. In addition, the skin layering was less well-defined in these regions. This is probably because of the large number of hair follicles and sebaceous glands that reside in these anatomical regions. Interestingly, in the reticular dermis of the ear OCT scans, we noticed dark (hypo-reflective) elongated structures ranging from 1-4mm in length in the majority of the images examined.

The thinnest epidermal layer of all areas examined was infra-orbital skin (92.88μm) followed by ear (103.14μm), while the thickest was back of hand (121.90μm) followed by back of neck (121.88μm) if palm of hand is excluded from the analysis (Table 7.1 & Fig. 7.14).

Two way ANOVA was utilised to calculate P values. Skin type and gender do not affect thickness of epidermis, except the ET in cheek, back of neck and dorsal forearm. Furthermore, Pearson's Correlation method indicated no statistical significance correlation between age and ET, except the epidermis in the forehead region became thinner in the older population (old group ranged from 40-63 years, while young group from 19-39 years) compared to younger group of the cohort {P value = 0.024 (correlation is significant at the 0.05 level (2-tailed)}.

Table (7.1) Values of mean epidermis layer thickness of normal skin at different anatomical body regions of the population studied (n = 60).

Anatomical location	Mean ET thickness ± SD
Lower lid (Infra-orbital skin)	92.88± 10.99
Ear	103.14± 16.34
Cheek	105.23± 11
Forehead	106.52± 10.51
Chest	109.35± 10.63
Chin	111.23± 9.27
Nasal tip	112.95± 11.05
Lateral nose	112.95± 11.05
Forearm (dorsal surface)	114.04± 10.52
Calf	115.92± 10.65
Forearm (ventral surface)	117.85± 11.47
Back of neck	121.88± 12.02
Hand (back)	121.90± 10.36
Hand (palm)	168.07± 13.10

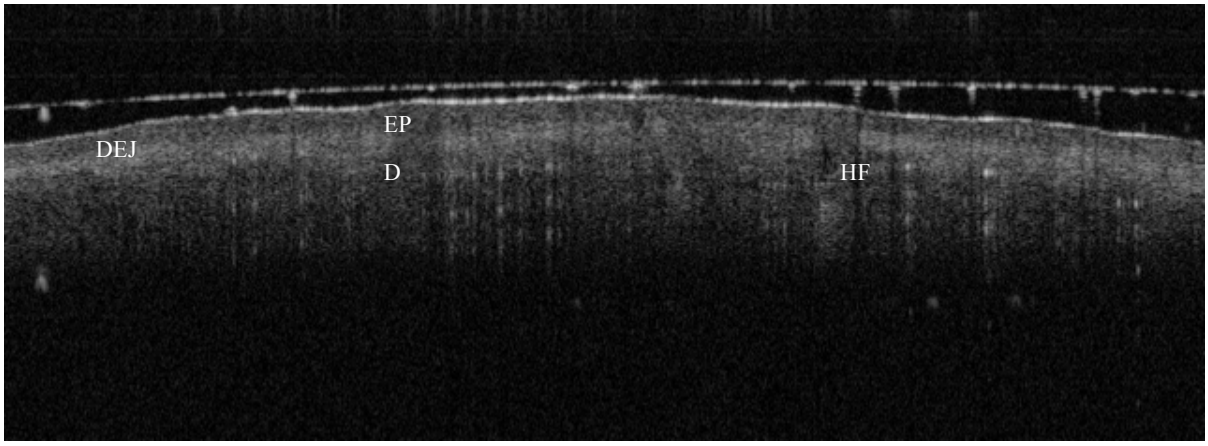

Figure (7.1) OCT image of forehead. DEJ= dermal-epidermal junction; EP= epidermis; D= dermis; HF= hair follicle. Epidermis appears dark (hypo-reflective) due to high nuclear content, while the higher reflectivity of dermis layers (papillary & reticular) is assumed to be the result of the collagen content.

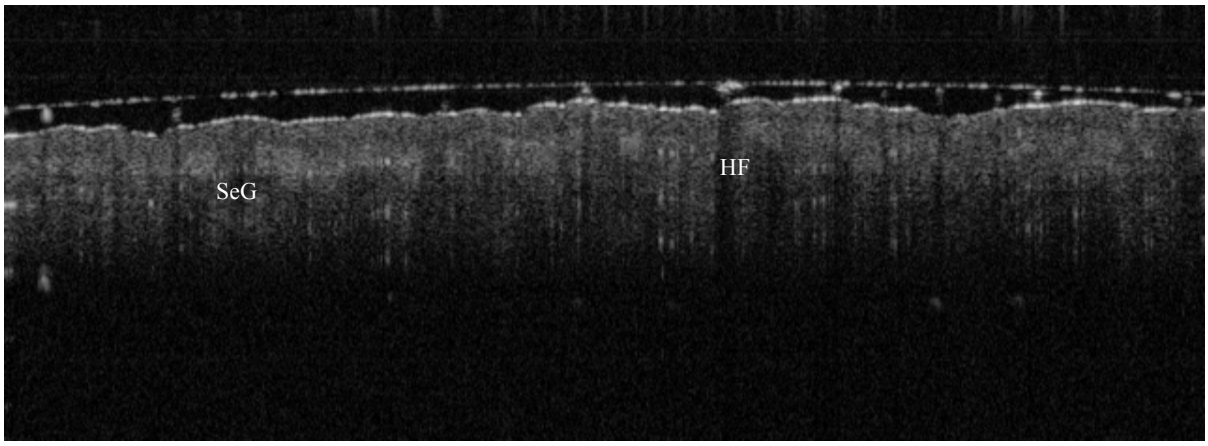

Figure (7.2) Nose. SeG= sebaceous gland.

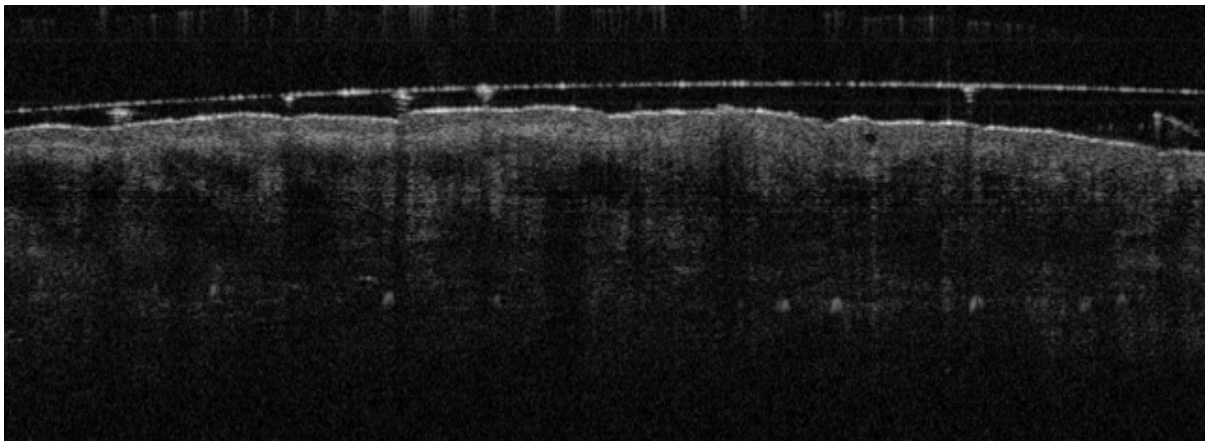

Figure (7.3) Infra-orbital skin.

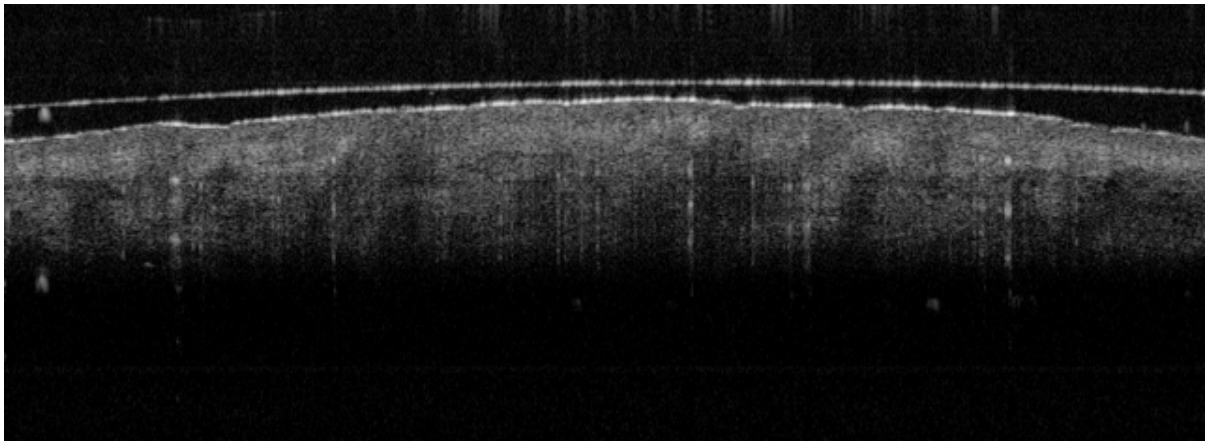

Figure (7.4) Cheek.

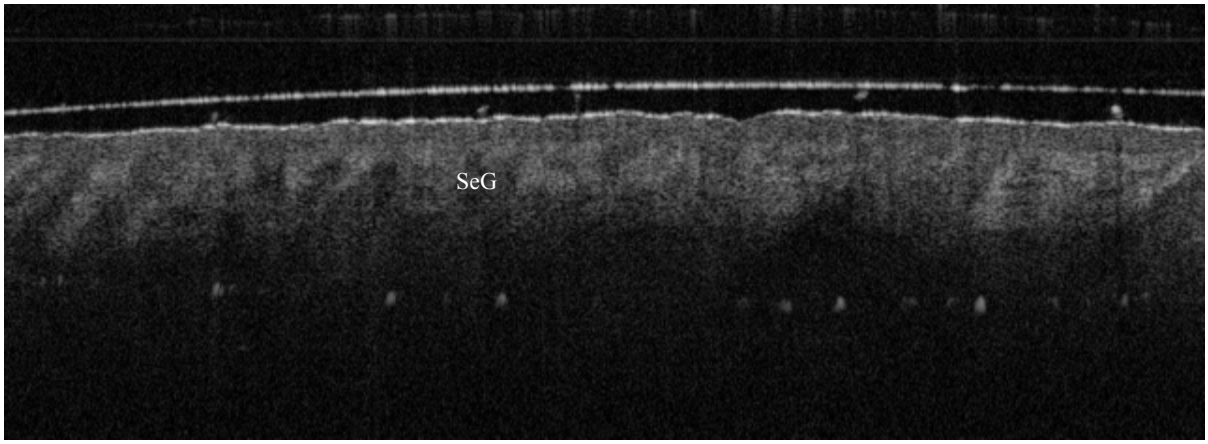

Figure (7.5) Chin.

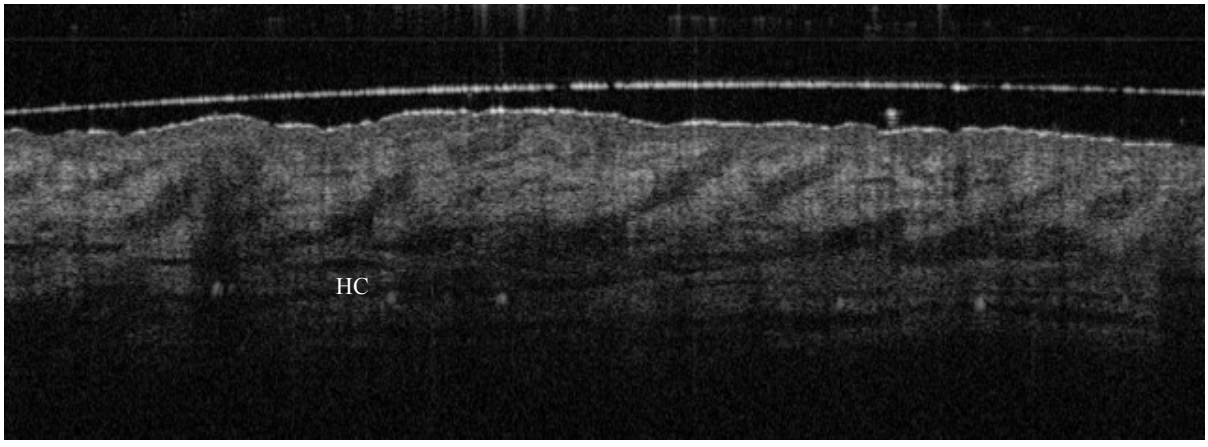

Figure (7.6) Ear. HC= hyaline cartilage

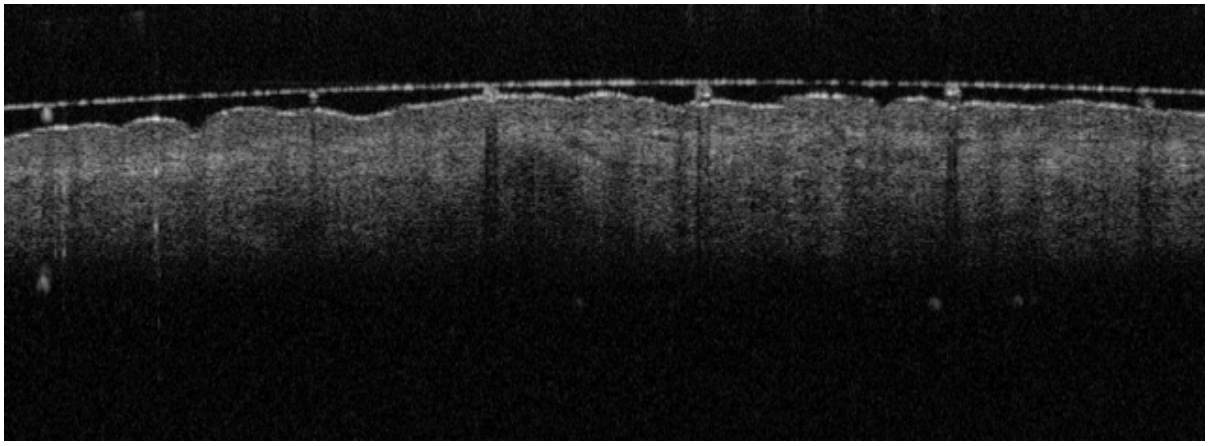

Figure (7.7) Back of the neck.

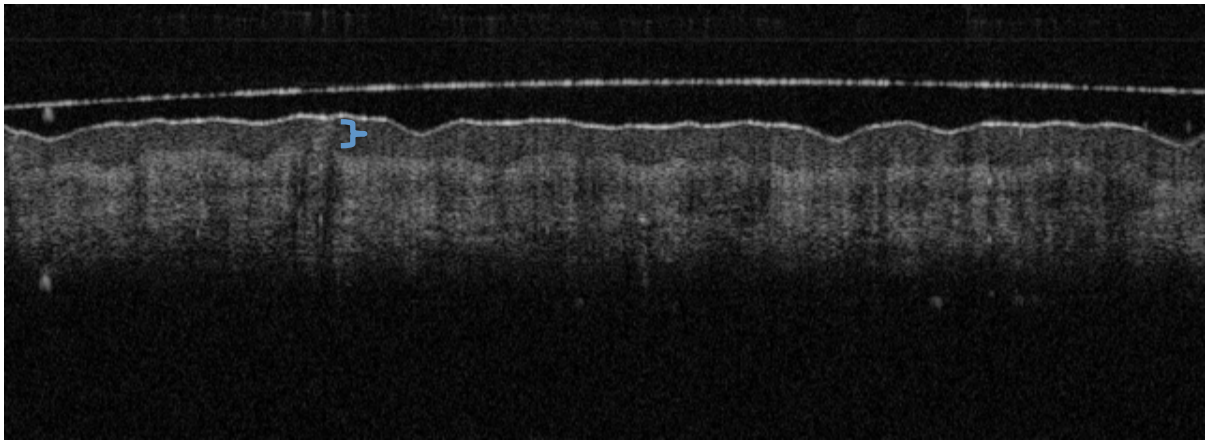

Figure (7.8) Palm of hand. Curly bracket indicates sudoriferous (sweat) gland duct present as hyper-reflective spiral structures. These ducts can only be recognised in glabrous skin regions (palm-plantar region) and are absent in follicular skin.

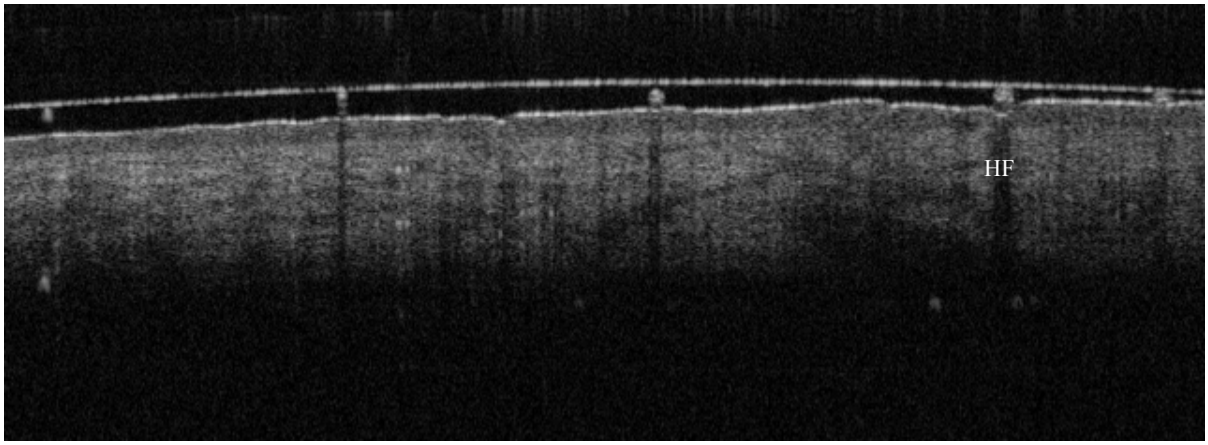

Figure (7.9) Back of hand.

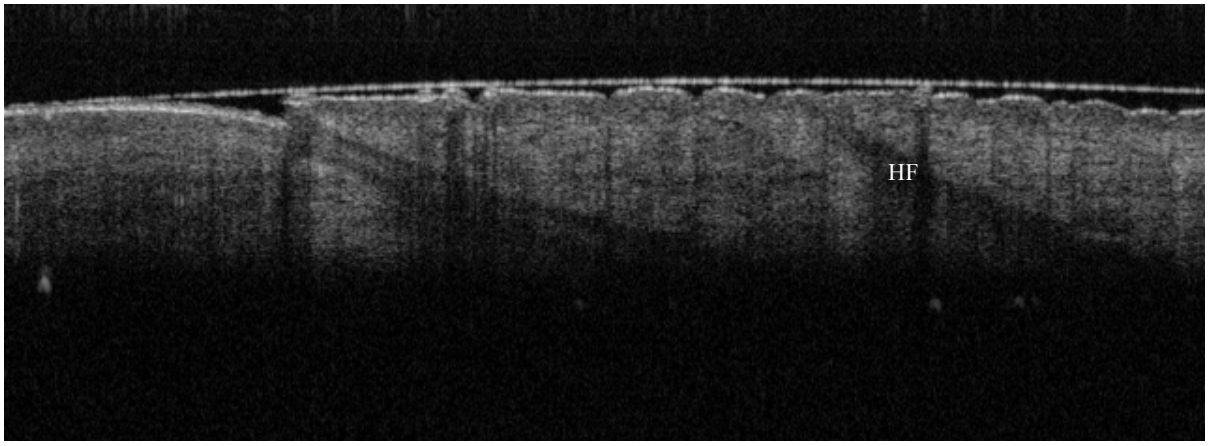

Figure (7.10) Ventral forearm.

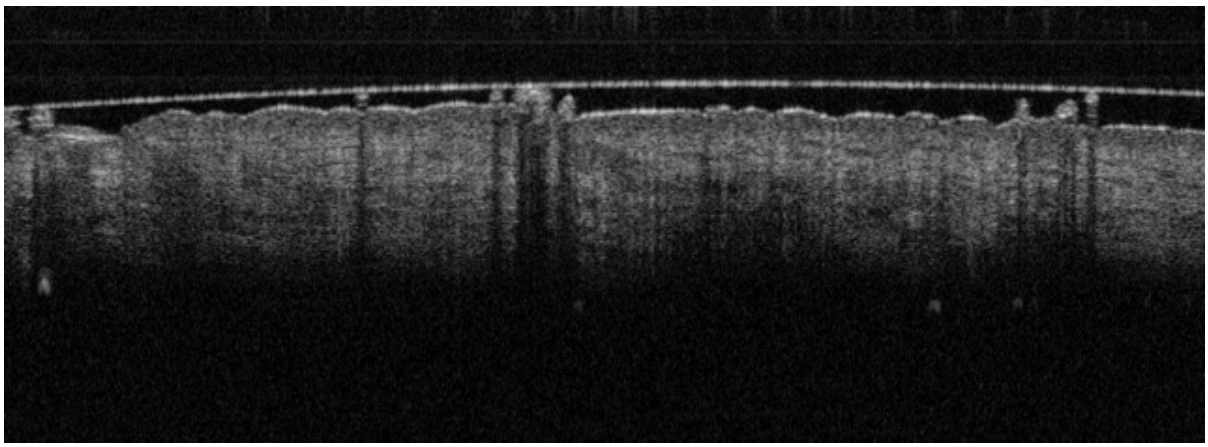

Figure (7.11) Dorsal forearm.

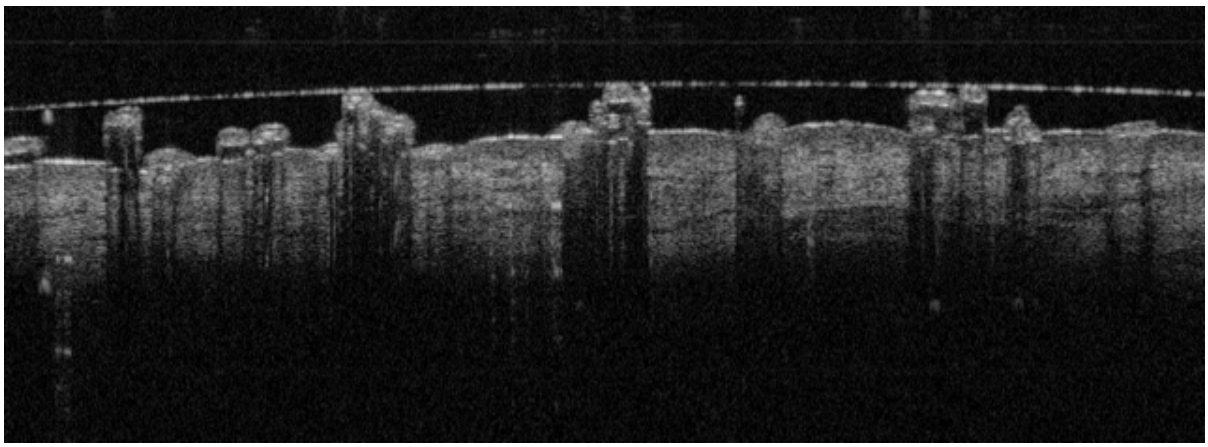

Figure (7.12) Chest.

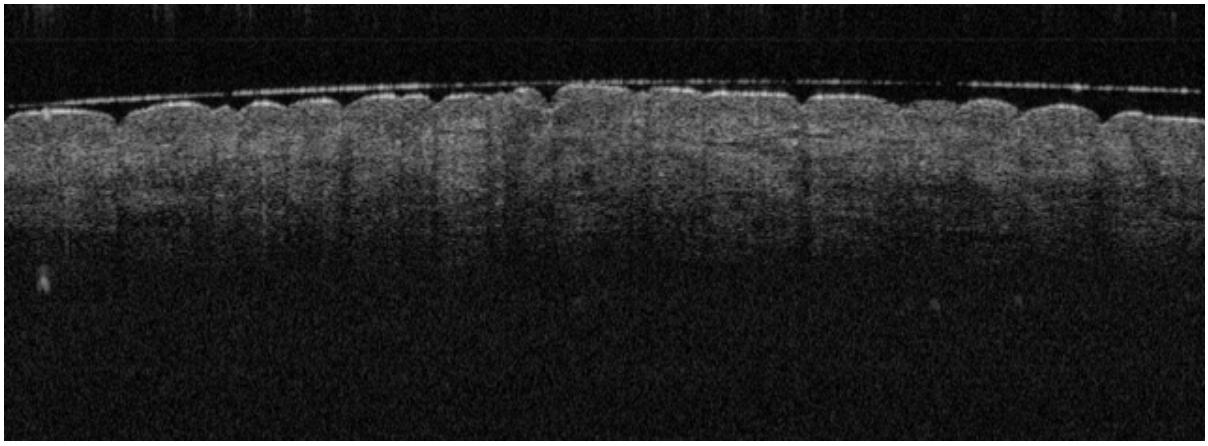

Figure (7.13) Calf.

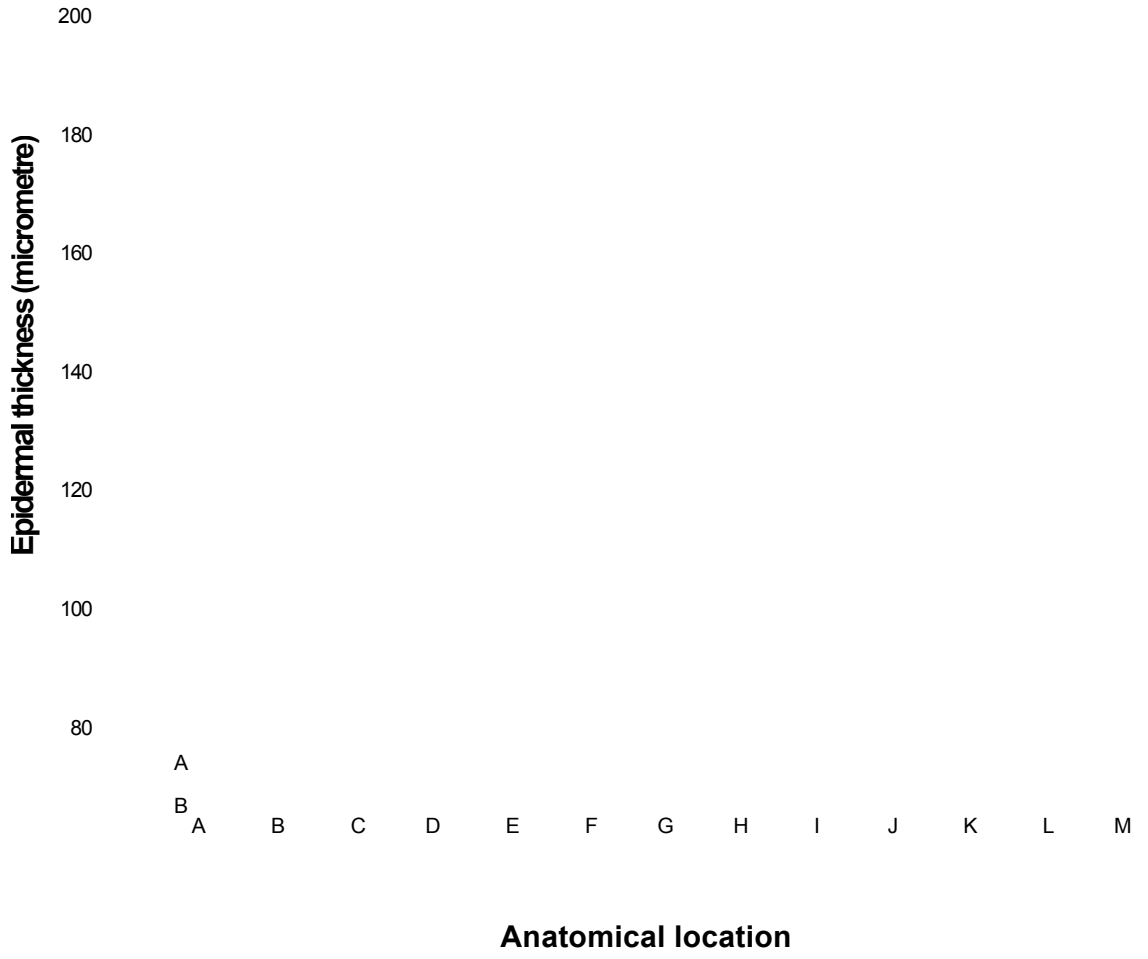

Figure (7.14) Box and whisker plot illustrates the mean of normal value of epidermal thickness in various anatomical body regions. (A) Forehead, (B) Nose, (C) Infra-orbital skin, (D) Cheek, (E) Chin, (F) Ear lobe, (G) Back of neck, (H) Palm of hand, (I) Back of hand, (J) Ventral forearm, (K) Dorsal forearm, (L) Chest, (M) Calf.

Section II: Epithelial layer thickness measurements of normal oral mucosa imaged by the OCT oral instrument in vivo

7.5 Background and objectives

With regard to the oral epithelial layer, thickness assessment at different anatomical locations in the oral cavity is fundamental for early recognition and diagnosis of precancerous and cancerous lesions. Up to the present time, little data and research exist vis-à-vis the thickness of epithelial layer of normal oral mucosa, especially utilising non-invasive techniques, such as confocal laser scanning microscopy (CLSM) or OCT in vivo. The purpose of this prospective clinical study was to provide a reference values for thickness of epithelium at different anatomical regions within the oral cavity using OCT oral system in vivo.

7.6 Materials & methods

7.6.1 Patients

Seventy healthy subjects were recruited for the current study. The study protocol approved by the NRES REC London-Dulwich (12/LO/0371), and informed consents were obtained from the volunteers. The cohort comprised of two ethnic groups: 38 Caucasian and 32 Black subjects. Inclusion criteria included patients above 18 years old, while exclusion criteria was any subject with history of any previous/current pathology (both benign and malignant) in the oral cavity.

7.6.2 Methods/ study design

The study protocol was explained to the recruited healthy volunteers before undergoing OCT imaging of their clinically normal oral mucosa. Images performed at 9 anatomical sites: buccal mucosa, floor of mouth, upper and lower lip (both vermilion and mucosal surfaces), lateral tongue, gingival tissue and hard palate. Soft palate, retromolar trigone, anterior palatine arch and palatine uvula measurements were not possible due to pharyngeal reflex that caused by relatively large size and geometry of the oral probe. For each location, one typical image was captured and we endeavoured to scan the exact site in all participants. All OCT images were scrutinised by a single investigator to measure the epithelial thickness using image J programme. The mean epithelial thickness on the OCT image was calculated from 7 measurements taken from the centre of the image and 3 lateral measures on each side at equal distances from the centre. These values were utilised in order to determine an overall mean for each site and their standard deviations.

7.7 Statistical analysis

For analysing the obtained data, we utilised SPSS statistical software (IBM Corp. Released 2013. IBM SPSS Statistics for Windows, Version 22.0. Armonk, NY: IBM Corp.) . Furthermore, two-way analysis of variance (ANOVA) was utilised to find out differences in epithelial thickness with regard to gender and ethnicity. For assessing the relationship between quantitative variables for epithelial thickness and age, a Pearson's Correlation method was used. P value < 0.05 was considered statistically significant.

7.8 Results

The mean age of patients was 35 years (range 19–63). A total of 70 healthy volunteers underwent OCT scanning of their oral mucosa at different anatomical regions. Females comprised 37 subjects, while males were 33.

The OCT images of different anatomical regions of oral mucous membrane divulged layered architecture of oral mucosa with a clear discrimination (represented by the basement membrane) between the darker, less reflective epithelial layer compared to the brighter, more backscattering lamina propria layer.

The epithelial layer demonstrated variable thickness across the anatomical locations scanned within the oral cavity. The thinnest epithelium measured was in the floor of mouth area (159.04μm), whereas the thickest epithelium (493.92μm) observed was in the buccal mucosa region (Table 7.2 & Fig. 7.24). We found no statistically significant differences in epithelial thickness for both sexes (P value = 0.114), as well as for both volunteer groups, i.e. Caucasian and black population (P value = 0.568). Moreover, Pearson's Correlation coefficient statistical method has shown no statistically significant correlation between epithelial thickness and age, except the floor of mouth where the epithelium was thinner in the older age group (older group from 40-63 years, young group from 19-39 years) compared to the young group {P value = 0.017 (correlation is significant at the 0.05 level (2-tailed)}.

In some of the OCT mages with subtle layering in particular hard palate, gingiva and vermillion border of lip, we identified epithelial thickness but with extreme difficulties. Figures (7.15-7.23) show OCT images of all the anatomical regions studied. Additionally, we encountered challenges in obtaining decent OCT images of hard palate, floor of mouth and gingiva among the anatomical locations examined.

OCT images of buccal mucosa, lower and upper lip mucosa, lateral tongue and floor of mouth showed dark (hypo-reflective) tube-like structures frequently appearing with tapering ends ranging from 1-3mm in length in sub-mucosa layer. No such structures have been observed in epithelial layer of all areas examined.

Table (7.2) Values of mean epithelial layer thickness of normal mucous membrane at different anatomical regions in the oral cavity. Measurements in μm.

Anatomical location	**Mean thickness ± SD (μm)**
Floor of mouth	159.04± 14.77
Hard palate	187.21± 4.82
Gingiva	221.28± 12.69
Lower lip vermilion	235.85± 11.48
Upper lip vermilion	243.83± 17.26
Lateral tongue	282.33± 16.01
Upper lip mucous	309.07± 20.56
Lower lip mucous	311.69± 18.04
Buccal mucosa	493.92± 25.10

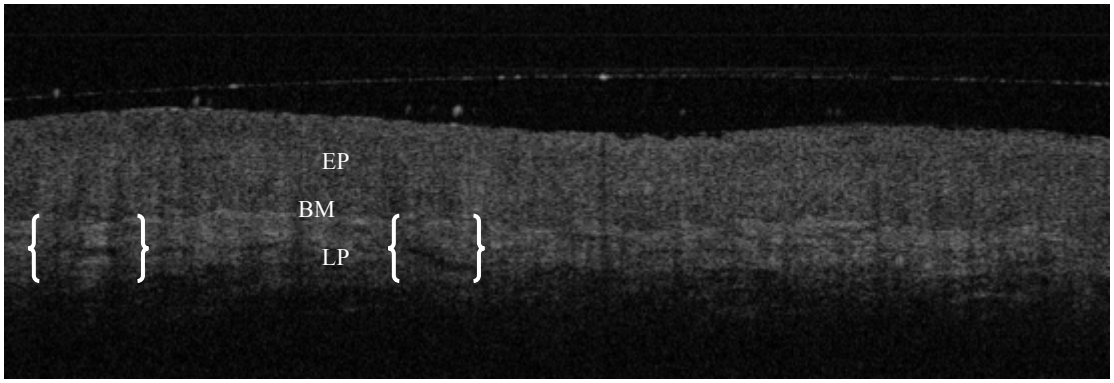

Figure (7.15) OCT image of buccal mucosa. EP= Epithelium, BM= basement membrane, LP= lamina propria. Blood and lymphatic vessels indicated by curly brackets appear as low-scattering tube-like structures in lamina propria layer.

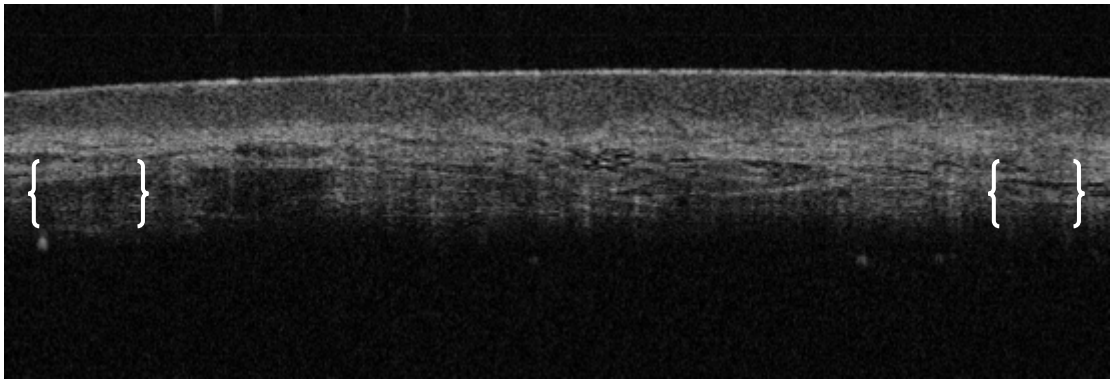

Figure (7.16) Lateral tongue. Blood/lymphatic vessels indicated by curly brackets.

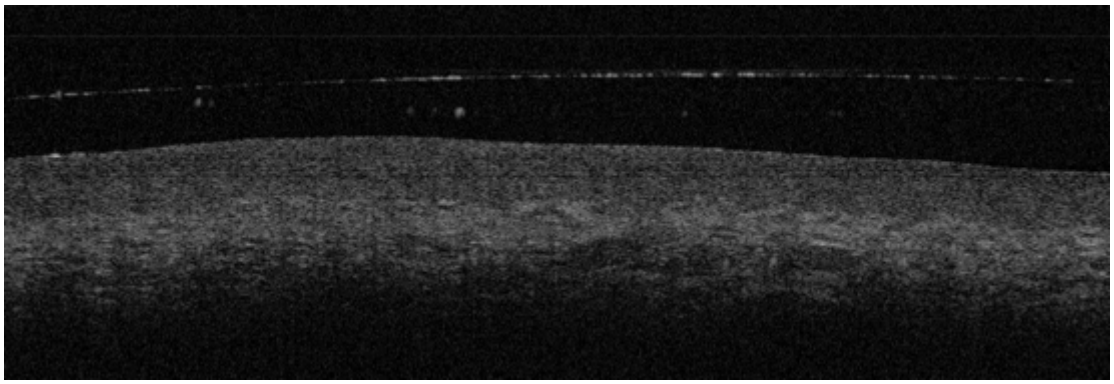

Figure (7.17) Lower lip mucosa.

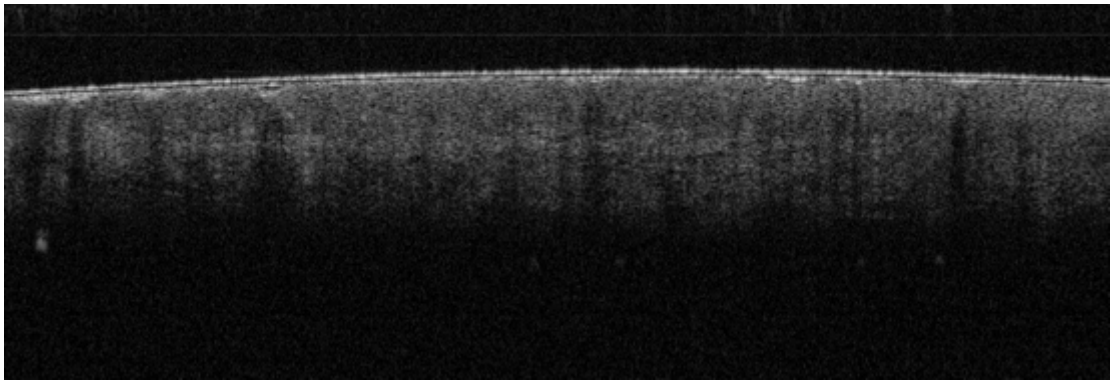

Figure (7.18) Lower lip vermillion.

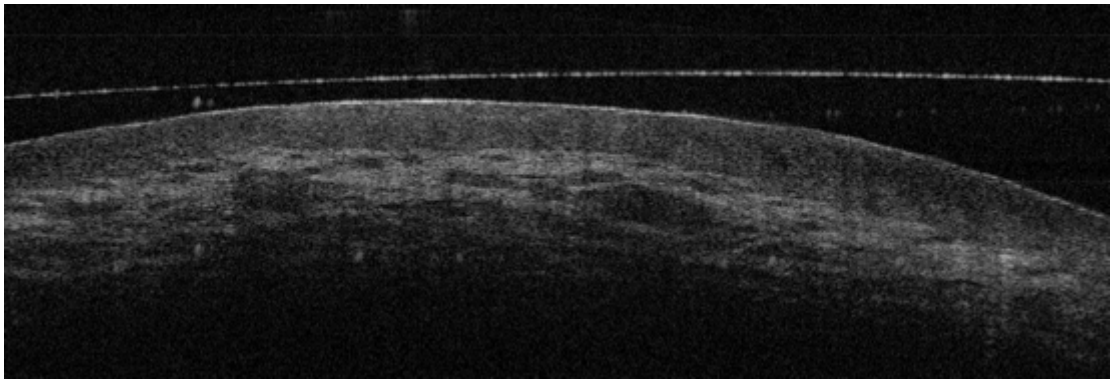

Figure (7.19) Upper lip mucosa.

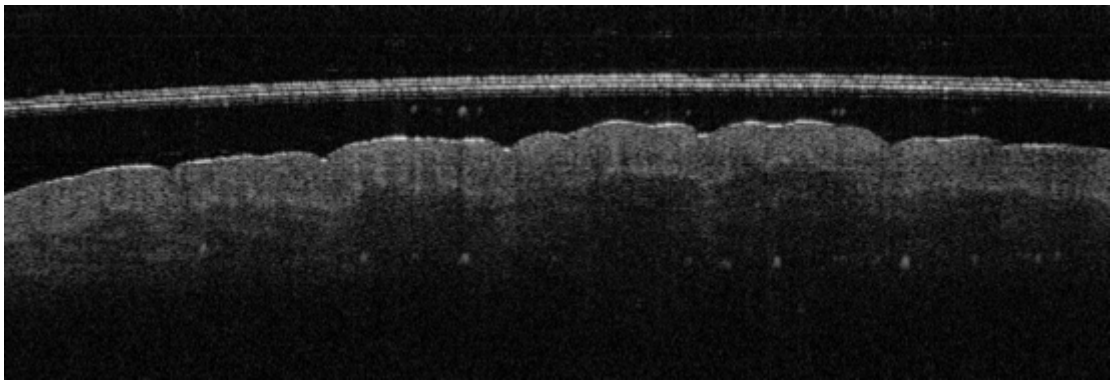

Figure (7.20) Upper lip vermillion.

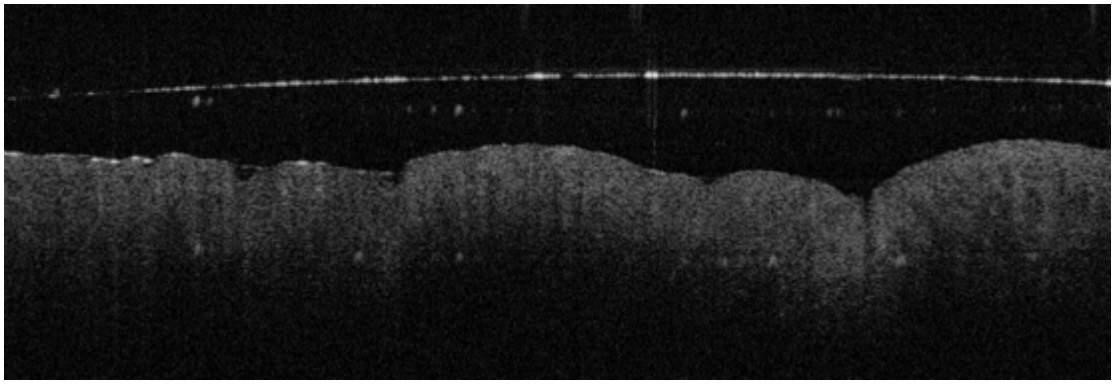

Figure (7.21) Hard palate.

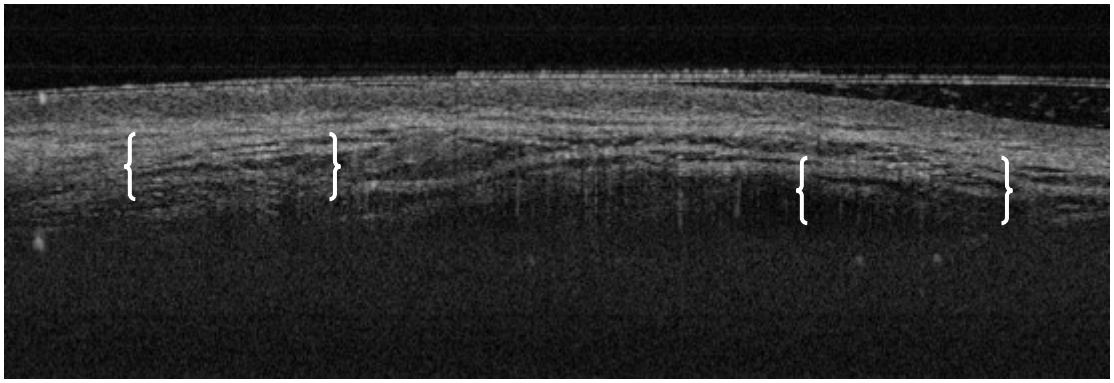

Figure (7.22) Floor of mouth. Blood and/ or lymphatic vessels in the lamina propria indicated by brackets.

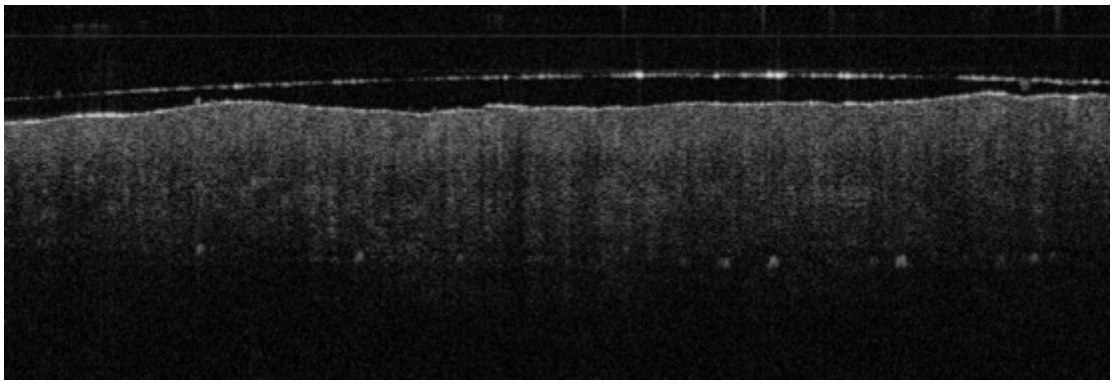

Figure (7.23) Gingival tissue.

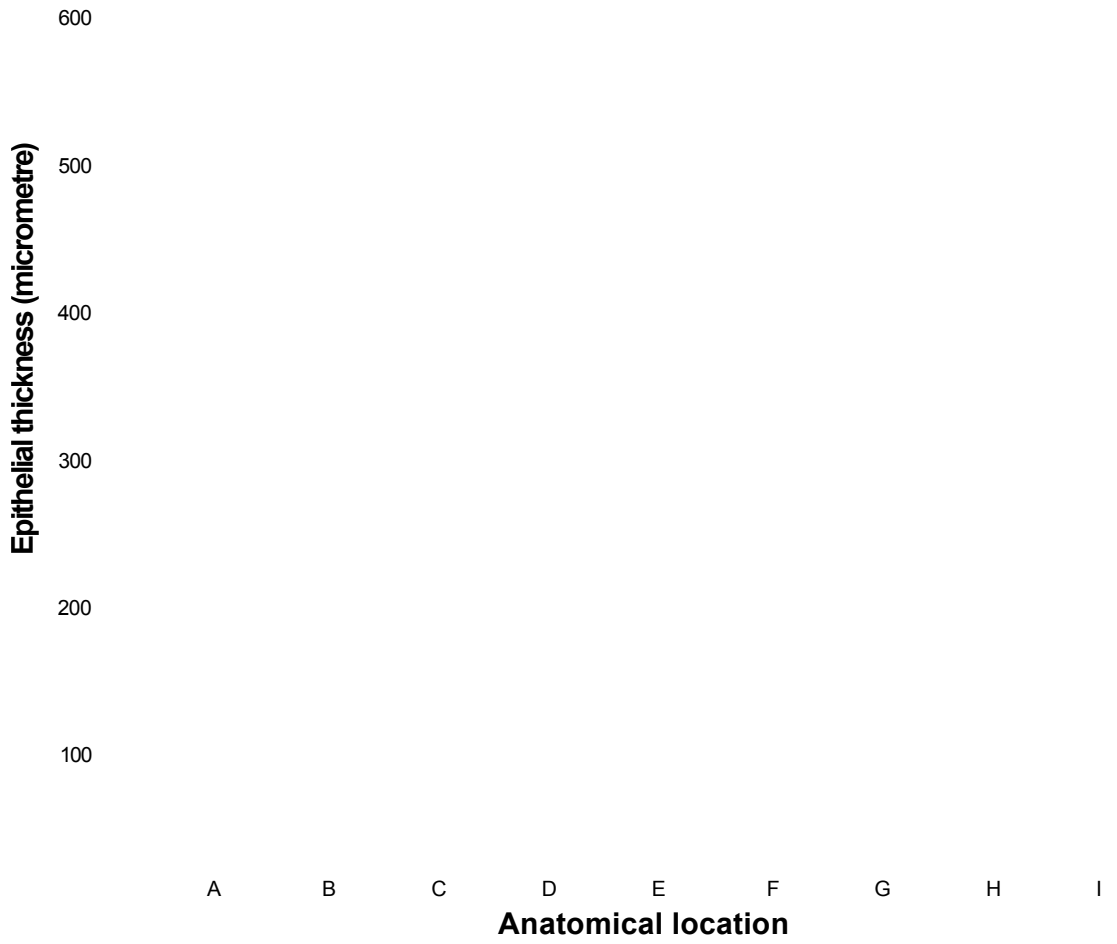

Figure (7.24) Box and whisker plot illustrates the mean of normal value of epithelial thickness in various anatomical regions within the oral cavity. (A) Buccal mucosa, (B) Lateral tongue, (C) Lower lip vermillion, (D) Lower lip mucosa, (E) Upper lip vermillion, (F) Upper lip mucosa, (G) Hard palate, (H) Floor of mouth, (I) Gingiva.

7.9 Discussion

In the present clinical investigation, we utilised OCT in vivo to obtain precise measurements of epidermal thickness in different anatomical regions of the body. The temperature of normal skin is approximately 37 °C and its water content is between 60-70%. In addition, it's well known that image quality would be negatively affected by the water content and temperature of the body tissue.

In excisional biopsies these constants are affected and could alter the optical properties of the skin (Troy & Thennadil, 2001). For this reason we conducted ET measurements in vivo to eschew the downsides of ex vivo measurements, of healthy skin around the surgical margins of excisional biopsies, including the known shrinkage of excised tissue (Kimura et al, 2003), which will adversely affect the accuracy of thickness measurements.

In this study, we noticed some regional dissimilarity on the OCT images of the examined anatomical locations. Glabrous skin (palm of the hand) for example, was the only location where stratum corneum and sweat gland ducts could be identified. Moreover, the dark (low-scattering) elongated structures that were observed in the reticular dermis layer of the posterior ear, which ranged from 1-4mm in length were in keeping with the hyaline cartilage of the ear. Mogensen et al (2008) reported similar findings in a clinical prospective study on 20 healthy volunteers, utilising both OCT and polarisation-sensitive OCT (PS-OCT) to scan skin tissue at different anatomical regions to measure ET and describe normal skin morphology.

The difficulties in recognising and measuring ET of forehead, cheek, chin and nose relative to other anatomical regions examined as well as the ill-defined skin layering in these regions may reflect the sizeable number of hair follicles and sebaceous glands residing in these anatomical regions.

In the present study, the means of ET (measured in vivo) were inconsistent with those measured by other researchers in two separate in vivo studies (Gambichler et al, 2006b; Mogensen et al, 2008). There was either over-estimation in ET measurements in our research or under-estimation by other researchers in the above-mentioned studies. For example, mean

ET of ear and back of hand measured by Mogensen et al were 85.11μm and 86.65μm, while our measurements were 103.14μm and 121.90μm, respectively. Nonetheless, there was parity in our and the above researchers' (Gambichler et al, 2006b; Mogensen et al, 2008) findings with regard to ET measurements between people of light skin (type I-III Fitzpatrick skin type scale) and those of darker skin (type IV-VI Fitzpatrick skin type scale). The only exception was the cheek, as we found that the epidermis in this region is thicker in darker skin volunteers when compared to lighter skin subjects (P value = 0.003). This is also in line with another study by Sandby-Moller et al (2003) who reported that ET does not correlate with type of skin.

Our study revealed that gender does not influenced epidermal thickness in the majority of the anatomical sites investigated. The clinical study by Mogensen et al (2008) also confirmed similar results. The only exceptions were the back of neck and forearm (dorsal antebrachium), where we found statistical significant difference, i.e. P value equal to 0.003 and 0.001 respectively. In females, the epidermis in these locations was thinner when compared to males. Similarly, in the clinical study of Gambichler et al (2006b), the authors reported that epidermis layer in the forehead region is significantly thinner in women compared to men.

Vis-à-vis the relation of ET and age, Mogensen et al (2008) study reported that the adult group had a thinner ET compared to children. These findings were not seen in our study as the protocol excluded volunteers below 18 years. Therefore, further studies including more volunteers of children, adult and old age groups of both genders, especially older groups from 60-90 years, are required to identify any relationship between ET and different age groups, gender, etc.

In the current prospective clinical study, we applied OCT in vivo to attain accurate measurements of epithelial thickness in different anatomical regions of the oral cavity.

So far, there are few optical imaging methods, for example CLSM and OCT that can be applied in vivo. These techniques possess high spatial resolution ranging from 1-15μm in order to accurately characterise pathological changes of oral mucous membrane as well as measuring their exact thickness. An ideal optical imaging method must have high-resolution

approaching 10μm (Ridgway et al, 2006) so that it can dependably distinguish abnormal changes of the mucosa. It is well known that thickness derived from excised tissue, i.e. gold standard histopathology, is subject to tissue shrinkage associated with fixation in formalin during histopathologic processing, which in the oral cavity ranges from 30-50% (Johnson et al, 1997). Additionally, the thickness obtained from ex vivo scanning of specimens using any optical imaging method is subject to shrinkage error. This is due to intrinsic contractile properties of the tissue itself immediately after excision, and not to fixation in formalin (Kerns et al, 2008; Ma et al, 2004; Golomb et al, 1991). Therefore, we aimed to obtain the measurements using in vivo method so as to generate reliable data that can serve as reference values of epithelial thickness in different anatomical oral regions.

Current imaging systems, for example ultrasonography, CT, MRI and positron emission tomography have spatial resolution as follow: 100-500μm, 500-1000μm, 500-1000μm and 1000-5000μm, respectively. These resolutions are inadequate for the recognition of pathological changes at the epithelial level (Ridgway et al, 2006). Other diagnostic imaging instruments, e.g. contact endoscopy, which is based on in vivo stains use, for example methylene blue, acetic acid or toluidine blue. Even though they achieve a high resolution of approximately 5μm, this modality allows examination of only the most superficial layers of the epithelium (Andrea et al, 1995). OCT imaging systems have a spatial resolution range from 5-20μm and a penetration depth from 1-2 mm, which depends upon the turbidity (optical absorption and scattering properties) of the scrutinised tissue. This allows non-invasive, in vivo imaging of macroscopic and microscopic characteristics of both epithelium and lamina propria structures, without application of chemical substances (Wilder-Smith et al, 2009b).

Identification of epithelial thickness was difficult on some of the OCT mages, especially those with very subtle change between epithelium and lamina propria layers. This is because we could barely detect the transition area from darker epithelium to brighter lamina propria (represented by the basement membrane), which could be possibly due to less collagen fibres content in the upper lamina propria layer compared to the brighter lower lamina propria layer. The hard palate was the most challenging location to recognise basement membrane, followed by gingiva then the vermillion border of lip. Moreover, because of the diametre and

geometry of the oral probe, we faced challenges in acquiring decent OCT images of hard palate, floor of mouth and gingiva among the anatomical locations examined. In our perspective, refinement of the OCT oral probe by reducing probe diametre and increasing its flexibility could assist and improve imaging of these anatomical locations in the oral cavity significantly as well as lessening the time spent on OCT scanning.

In this study, we noticed hypo-reflective tube-like structures in lamina propria but mainly in its lower layers, commonly appearing with tapering ends of varying length from 1-3mm or even longer. These structures are in keeping with blood and lymphatic vessels, which have been observed in the OCT images of buccal mucosa, upper and lower lips (mucosal surface), lateral tongue and floor of mouth. These structures have also been recognised by other researchers in their study to measure epithelial thickness within the oral cavity utilising OCT in vivo (Prestin et al, 2012).

The means of epithelial thickness measured in the current investigation were inconsistent with that measured by Prestin et al (2012), who used a commercial Niris OCT imaging system (Imalux, Cleveland, OH) in their in vivo clinical study. There were either over-estimation in epithelial thickness measurements in our study or under-estimation by Prestin and colleagues. For example, mean thickness of the floor of mouth and buccal mucosa measured by Prestin et al were 113μm and 350μm, while our measurements were 159μm and 493μm, respectively.

A number of researchers in two studies measuring thickness of healthy oral and oro-pharyngeal epithelium and underlying lamina propria, reported variation in epithelial thickness from 70-550μm, whereas sub-epithelial layer thickness reached 2000μm (Klein-Szanto & Schroeder, 1977; Paulsen & Thale, 1998). Arens and colleagues (2007), in a study including 161 patients underwent surgery to remove 206 benign and malignant lesions of the vocal folds, reported a progressive thickening of normal laryngeal epithelium from 147μm to 258μm in mild dysplasia, 301μm in moderate dysplasia, 445μm in severe dysplasia and 974 in early invasive carcinoma. In benign lesions, there were only slight epithelial thickenings of

about 100μm. Moderate dysplasia displayed a double increase and severe dysplasia showed a triple increase, while early invasive malignancy revealed even a sixfold increase of the mean epithelial thickness when compared to normal laryngeal mucous membrane.

Our study revealed that gender does not influenced epithelial thickness in all anatomical sites examined ($P = 0.114$). Furthermore, the present study revealed that all anatomic locations examined were influenced epithelial thickness insignificantly on an inter-individual level ($P = 0.757$), but on intra-individual level there were significant effects of anatomic sites on the epithelial thickness ($P < 0.003$). Vis-à-vis age and epithelial thickness relation, we found no effects of age in all anatomical regions examined. The exception was the floor of mouth epithelium, which was significantly thinner in the older age group between 40-63 years when compared to the younger group between 19-39 years. The reasons for this remain unclear.

Because our investigation included fewer occasional alcohol drinkers and tobacco product consumers, therefore it was not possible to rely on such a small group and perform statistical study on it, although during OCT image analyses to measure epithelial thickness, we noticed insignificant differences in their epithelial thickness when compared with the majority of our cohort study (non-smoker and non-drinker). The study of Prestin and associates (2012) reported that epithelium of anterior palatal arch and anterior floor of mouth was significantly thicker in men than women. In addition, smokers group have significantly thicker epithelium of anterior floor of mouth compared to non-smokers. Use of alcoholic beverages was not associated with any differences in thickness of epithelial layer. Regression analysis revealed a highly significant connection of age with thickness of palatine uvula epithelium and an inverse association of age with thickness of buccal mucosa epithelium. Accordingly, further studies including more volunteers of young and old age groups of both genders, especially older groups from 60-90 years, will be essential in order to find out any relations between epithelial thickness and different age groups, gender, smoker vs. non-smoker and alcohol drinker vs. teetotal.

7.10 Conclusion

Our findings indicate that the modified OCT oral instrument can be used in a simple way to evaluate and measure accurately both epidermal and epithelial thickness in vivo, thereby avoiding any discrepancies in thickness measurements generated by utilising other techniques, such as ex vivo scanning method or even the gold standard histopathology.

In our view, cutaneous and oral lesions can best be reliably assessed by excisional biopsy and histopathological investigation, which remains the gold standard. Nevertheless, OCT techniques are capable of distinguishing dysplasias and malignancies prior to surgery. Hence, small tumours can be removed completely by excisional biopsy procedure or in case of large tumours, the surgeon could perform a targeted incisional biopsy at the most suspicious location where premalignancy/ malignancy is strongly suspected. In this way, OCT may act as an adjunct that could considerably contribute to the early recognition of cutaneous and oral malignancy.

The results presented in this study indicate that both quantitative and qualitative evaluation of cutaneous and oral structures are feasible utilising the OCT instrument in vivo. Furthermore, the data presented here could serve as basic reference values for normal epidermal and epithelial thickness, which might be advantageous in various clinical and experimental matters.

Chapter 8

Comparison of Mohs micrographic surgery with OCT

Chapter 8

Comparison of Mohs micrographic surgery with OCT

8.1 Introduction

8.1.1 Mohs micrographic surgery

Mohs surgery, also known as chemosurgery or Mohs micrographic surgery (MMS), developed by Frederic E. Mohs in 1938, is a surgical procedure that is microscopically controlled used to treat common types of cutaneous malignancy. Mohs surgery allows complete margin control during skin cancer removal (CCPDMA – complete circumferential peripheral and deep margin assessment), using frozen section histology (National Comprehensive Cancer Network, 2006; Dhingra et al, 2007). CCPDMA or MMS permits for the elimination of a cutaneous cancer with high cure rate and a very narrow surgical margin (Bentkover et al, 2002; Minton, 2008).

The cure rate with MMS cited by most studies is from 97% to 99.8% (Mikhail & Mohs, 1991) for primary BCC. Two studies reported a lower cure rate for primary BCC, 95% and 96% (Smeets et al, 2004). Recurrent BCC has a lower cure rate with Mohs surgery, approximately 94% (Mikhail & Mohs, 1991). MMS has been used in melanoma-in-situ removal with a cure rate between 77% and 98%, and certain types of melanoma with a cure rate 52% (Mikhail & Mohs, 1991; Gross et al, 1999). Studies examining Mohs surgery for melanoma-in-situ reported a cure rate of 95% for frozen section Mohs, and from 98% to 99% for fixed tissue Mohs technique (Bene et al, 2008; Stevenson & Ahmed, 2005).

The treatment of choice for high-risk localised cutaneous SCCs and SCCs situated in cosmetically sensitive or critical areas is MMS. This is because of its capability to spare normal tissue as well as a high cure rate. Reported 5-year cure rates for primary SCCs are about 97%, while for recurrent SCCs are between 90-94%. Cure rates are consistently higher with Mohs surgery for all types of high risk SCCs than with other modalities (Rowe et al, 1992; Lawrence & Cottel, 1994).

Other indications for Mohs surgery include dermatofibrosarcoma protuberans, spindle cell tumours, sebaceous carcinomas, microcystic adnexal carcinoma, merkel cell carcinoma, Paget's disease of the breast, atypical fibroxanthoma, leiomyosarcoma, and angiosarcoma. Since the Mohs technique is controlled micrographically, it offers accurate removal of the malignant tissue, while healthy tissue is spared. It is also more cost effective compared to other surgical techniques when considering the cost of surgical removal and separate histology examination. Nonetheless, MMS should be reserved for the cutaneous malignancy treatment in anatomic areas where tissue preservation is of greatest importance, for instance in the facial region, hands, feet and genitals (Gross et al, 1999).

The MMS procedure is basically a pathology sectioning technique, which allows for the surgical margins to be completely examined under light microscopy. The Mohs technique is different from the standard 'bread loafing' method of sectioning (Fig. 8.1B), where examination of random samples of the surgical margin are performed (Connolly et al, 2012; National Comprehensive Cancer Network, 2011).

Four stages are involved in Mohs surgery:

1. Surgical removal of tissue (surgical oncology)
2. The piece of tissue is mapped, frozen and cut between 5-10μm in a cryostat, and stained with haematoxylin and eosin (H&E) and/ or other stains including toluidine blue
3. Interpretation of slides (histopathology)
4. Surgical defect reconstruction (reconstructive surgery)

Mohs technique is usually performed under local anaesthetic in an outpatient setting. Cutting around the visible tumour is performed using a small scalpel blade, positioned at an angle of 45 degrees. A very small surgical margin is utilised, usually about 1-1.5 mm of uninvolved skin or free margin. The amount of free margin removed is considerably less than the usual 4-6 mm, which is required for the standard excision of cutaneous malignancy (Maloney, 1999). Following each surgical removal of the cancerous tissue, the sample is processed, cut on the cryostat and placed on slides, stained with H&E and then read by the Mohs

surgeon/pathologist who examines the sections for tumour cells. The location of cancerous tissue is marked on the map (drawing of the tissue) if cancer is found, and the Mohs surgeon removes the indicated cancerous tissue from the patient in the second stage. This surgical procedure can be repeated in several stages until no further tumour is found (Fig. 8.1A). Then the Mohs surgeon/ plastic and reconstructive surgeon will perform the facial reconstructive surgery following removal of the skin cancer.

The technique is well described in current references (Maloney, 1999; Gross & Steinman, 2009). The mapping combined with the "smashing the pie pan" technique of processing is the essence of MMS surgery. If one imagines an aluminium pie pan as the blood covered surgical margin, and the topmost of the pie is the crust covered surface of the skin – the objective is to flatten the aluminium pie pan into one flat sheet, mark it, stain it, and examine it under light microscopy. Another author utilises the paradigm of peeling the skin off an orange (Mikhail & Mohs, 1991). Imagine an orange cut in half as the CCPDMA layer. The peel is considered to be the surgical margin. One can remove this peel and flatten it out on a glass slide in order to scrutinise the invasive cancer margins.

It is believed by some physicians that frozen section histology is the same as Mohs surgery, but it is not (Maloney, 1999). MMS is achieved by utilising fresh tissue samples, whereas frozen section histology might or might not be CCPDMA. Non-CCPDMA histology analysis normally uses a method of random tissue sampling, which is called "bread loafing". In "bread loafing", less than 5% of the entire surgical margin is examined (consider pulling 5 slices of bread out of a whole loaf of sliced bread and investigating simply those 5 slices in order to visualise the entire loaf). While in CCPDMA histology processing, the whole surgical margin is investigated (consider examining the whole outside crust of the same loaf of bread). In statistical terms, the false negative rate will become lower by examining more slices of bread (Gross et al, 1999). False negatives occur when a histopathologist reads cancer excision as free of residual cancer, albeit carcinoma may be present in the specimen and missed due to the random sampling method (Mikhail & Mohs, 1991) (Fig. 8.2).

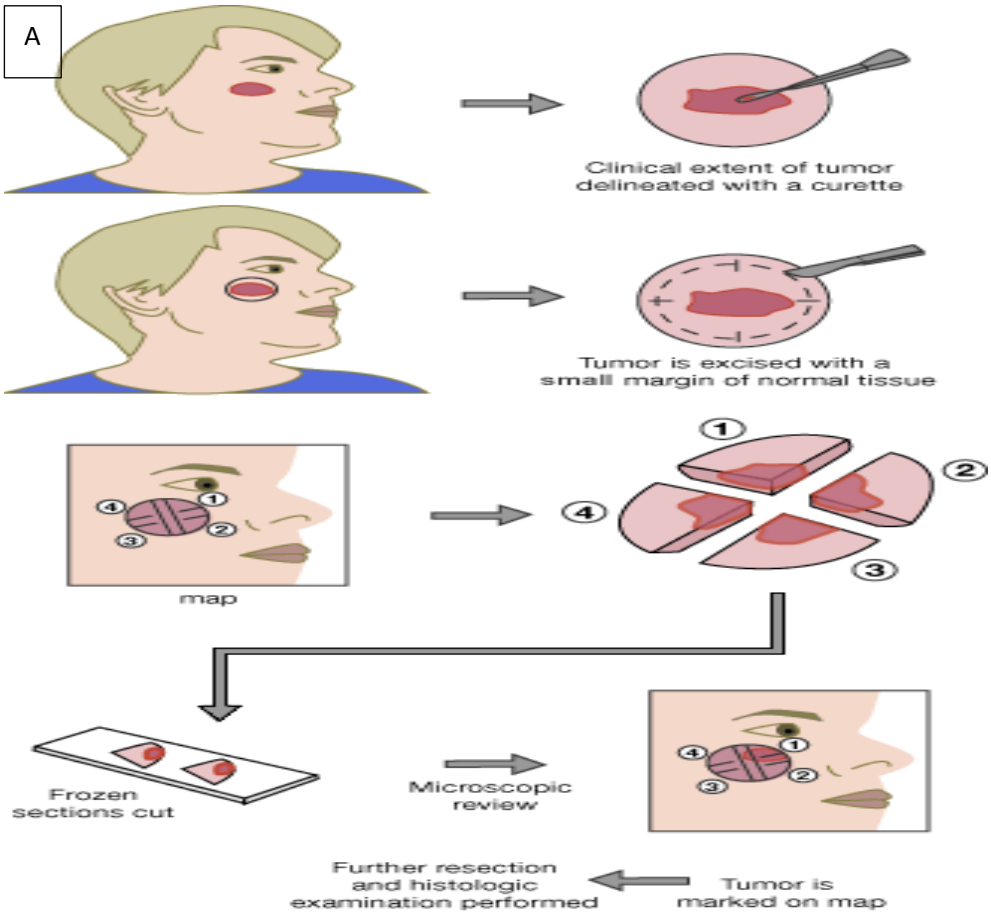

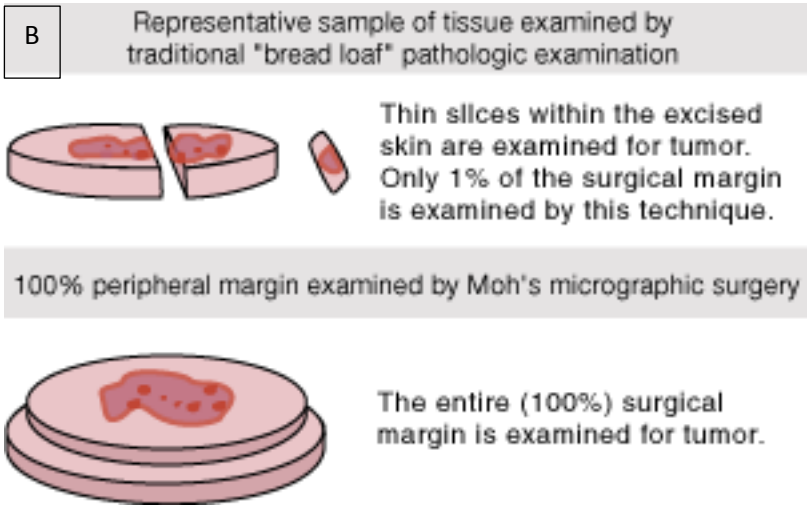

Figure (8.1) Schematic of MMS technique (A), diagram of histopathology examination of tissue margins (B).

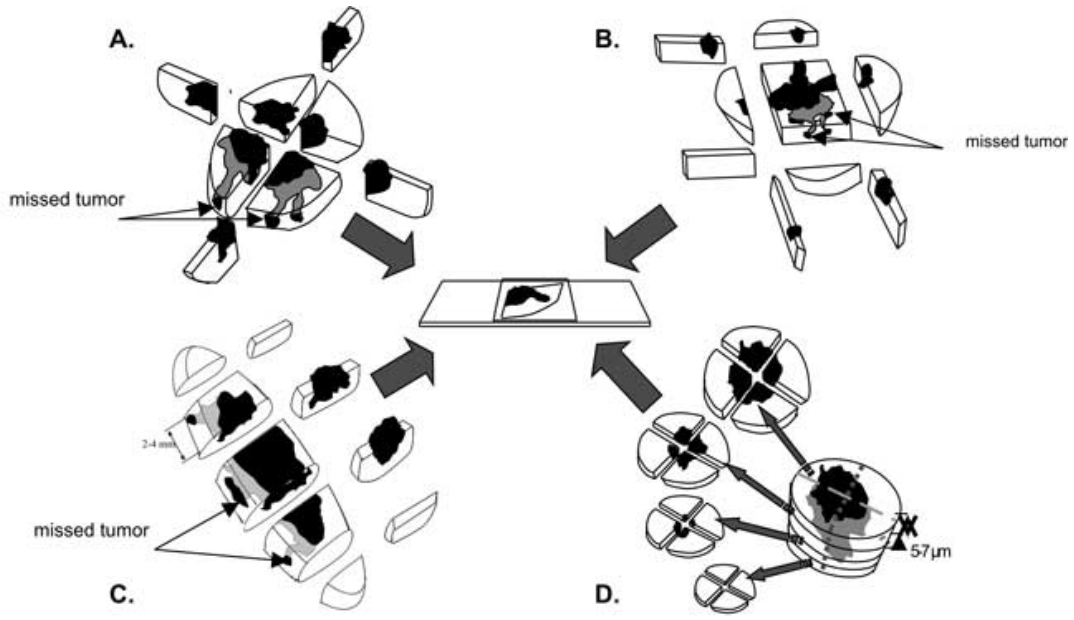

Figure (8.2) Schematic illustrates Mohs method compared with different methods of microscopic processing: cross sectioning (A), peripheral sectioning (B), bread loaf sectioning (C), Mohs method (D).

8.1.2 Aims

The purpose of this study was to:

1. Study the accuracy of a recently modified and validated OCT oral system in discerning normal facial skin cancer (BCC) margins by comparison with the frozen section histology of the specimens that undergo MMS.

2. Possibility of identifying the different BCC subtypes by comparing the OCT images with the corresponding histopathology slides.

8.2 Materials & methods

8.2.1 Patients

Seventy-three subjects with biopsy-proven BCC undergoing MMS at University College Hospital/ Dermatology Department were selected and recruited for the current study. Inclusion criteria included patients above 18 years old. Additional inclusion criteria were clinically apparent lesions that haven't undergone any previous treatment modality, for instance topical therapeutic agents such as imiquimod or 5-fluorouracil and PDT. The study protocol approved by the NRES REC London-Dulwich (12/LO/0371), and informed consents were obtained from all patients.

8.2.2 Methods/study designs

Subjects with biopsy proven BCCs on the facial region in whom a decision to undergo MMS, were prepared by mapping the boundary of the lesion with the naked eye using a surgical skin marker pen. Narrow clinically healthy margins of the skin surrounding the tumour were included in the excisional biopsy performed by the Mohs surgeon. Following the first and/or the second stages of MMS, the OCT oral instrument was used for immediate ex vivo scanning and capturing images of the margins of the specimen to verify its status. Four margins per biopsy tissue were studied (total number 292). The four locations scanned were at the 3, 6, 9 and 12 o'clock positions. Scanning was initiated from the periphery towards the centre for each location. As part of our routine practice in Dermatologic Surgery unit at UCLH, the biopsies were processed for horizontal frozen sections by a Mohs histotechnician after image acquisition of the specimen by OCT instrument. Then the acquired OCT images of the specimen margins were compared with the H&E sections.

Two investigators have independently examined and compared the OCT images with the H&E slides to find out whether or not the margins were clear or involved. The margin status of the histopathology was determined by a consultant histopathologist involved in this study. Assessment was conducted according to WHO guidelines. The criteria that have been considered to identify and rate a margin as negative (tumour-free) are the presence of an intact DEJ with the overlying normal epidermal layer and the underlying homogenous dermis layer (Fig. 8.3), whereas for identification of a BCC in the positive margin (tumour-laden margin), at least one of the following criteria was required; presence of honeycomb-like aggregates (lobules of small tumour), dark rounded areas (islands of tumour nests), or plug-like signal-intense structures (dense tumour clusters) with or without breached DEJ (Fig. 8.4). The two assessors re-examined all the OCT images after 5 weeks in order to determine intra-observer differences.

8.3 Statistical analysis

In order to assess the effectiveness; sensitivity, specificity and overall accuracy of OCT (not accounting for chance agreement) were calculated in Excel, Microsoft Office 2003 according to the data given by both investigators. Kappa statistics were calculated in '2015 GraphPad Prism Software' to assess the agreement between the readers and interpreted as poor if $\kappa <$

0.00, slight if $0.00 \leq \kappa \leq$ to 0.20, fair if $0.21 \leq \kappa \leq$ to 0.40, moderate if $0.41 \leq \kappa \leq$ to 0.60, substantial (or good) if $0.61 \leq \kappa \leq 0.80$, almost perfect (or excellent) if $\kappa > 0.80$ (Landis & Koch, 1977).

8.4 Results

The mean age of patients was 67.5 years (range 26–96). Men comprised 39 subjects, while women were 34. BCC lesions were mainly of mixed subtypes (two or more than two subtypes) in 27 cases, followed by nodular (20 cases), micronodular (11 cases), infiltrative (8 cases) and superficial subtype (7 cases) (Figures 8.7, 8.8 & 8.9). Cheek (17) and nose (17) were the main common locations for the BCC lesions, followed by forehead/temple (14), periorbital area (10) and scalp (10). Ears (3) and lips (2) were the least common locations in the head and neck areas for BCC lesions in this study (Table 8.1).

The histopathological analysis of 292 margins showed 232 tumour free margins and 48 tumour-involved margins. 12 margins were excluded because of distortion (severe artefact) during histopathologic processing as well as bad quality OCT images. Previously described honeycomb-like aggregates and plug-like signal-intense structures were not identified. Adnexal structures were also identified, but were often difficult to differentiate from tumour in some areas.

Sensitivity and specificity for the first observer for distinguishing the BCCs margins was 77% and 96.6%, respectively. The positive predictive value (PPV) was 82.2% and the negative predictive value (NPV) was 95.3%. Prevalence was 0.16, OCT accuracy was 93.2% and the kappa statistic was 0.75 (95% CI: From 0.65 to 0.86) (substantial agreement). There were 8 false positives and 11 false negatives, with positive likelihood ratio (LR+) of 22, suggesting that OCT is useful and provides evidence to support the diagnosis and negative likelihood ratio (LR-) of 0.24, which allows us to rule out the diagnosis (Table 8.2). The sensitivity and specificity for the second observer was 85.4% and 95.3%, respectively. The PPV was 78.8% and the NPV was 96.9%. Prevalence was 0.17, OCT accuracy was 93.5% and the kappa statistic was 0.78 (95% CI: From 0.68 to 0.87) (nearly excellent agreement). There were 11 false positives and 7 false negatives, with LR+ of 18 and LR- of 0.15 (Figures 8.5 & 8.6, Table 8.3).

The intra-observer agreement was substantial (Kappa statistic= 0.76). Furthermore, the degree of concordance between both readers (inter-observer agreement) was also good,

although the kappa statistic was a little lower (Kappa statistic= 0.63) according to Landis & Koch, 1977.

Table (8.1) Clinical data and BCC histopathology subtypes and location of the population studied (N = 73).

1. **Gender**	**No (%)**
Male	39 (53.5%)
Female	34 (46.5%)
2. **Age** (years), mean (range)	67.5 (26–96)
3. **Location of BCC**	
Cheek	17 (23.2%)
Nose	17 (23.2%)
Forehead/temple	14 (19.2%)
Scalp	10 (13.7%)
Periorbital	10 (13.7%)
Ear	3 (4.2%)
Lip	2 (2.8%)
4. **BCC subtypes**	
Mixed (two or more than two subtypes)	27 (37%)
Nodular	20 (27.4%)
Micronodular	11 (15%)
Infiltrative	8 (11%)
Superficial	7 (9.6%)

Table (8.2) BCC margins assessment by the **first investigator** (total 292 margins, 12 margins were excluded). Sensitivity 77%; specificity 96.5%; (PPV) 82.2%; (NPV) 95.3%; accuracy of OCT oral system 93.2%. TP: true positive, FP: false positive, TN: true negative, FN: false negative.

Histopathology				
OCT		Positive	Negative	Total
	Positive	37 (TP)	8 (FP)	45
	Negative	11 (FN)	224 (TN)	235
	Total	48	232	280

Table (8.3) BCC margins assessment by the **second investigator** (total 292 margins, 12 margins were excluded). Sensitivity 85.4%; specificity 96.9%; (PPV) 78.8%; (NPV) 96.9%; accuracy of OCT oral system 93.5%. TP: true positive, FP: false positive, TN: true negative, FN: false negative.

Histopathology				
OCT		Positive	Negative	Total
	Positive	41 (TP)	11 (FP)	52
	Negative	7 (FN)	221 (TN)	228
	Total	48	232	280

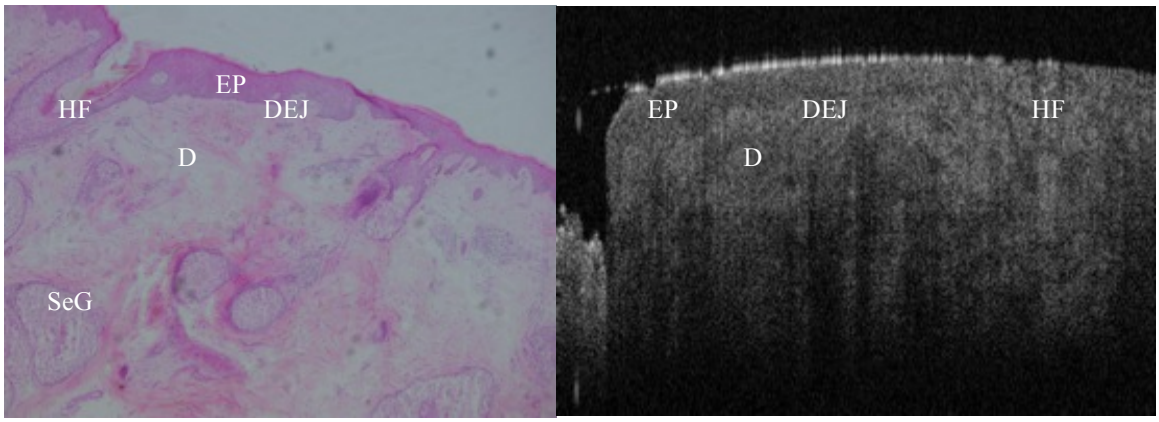

Figure (8.3) True negative margin from BCC lesion. Both OCT & histopathology images reveal no tumour cell nests, intact dermo-epidermal junction (DEJ) and homogenous dermis (D) within the 6 mm scan length. EP= epidermis; HF= hair follicle; SeG= sebaceous gland.

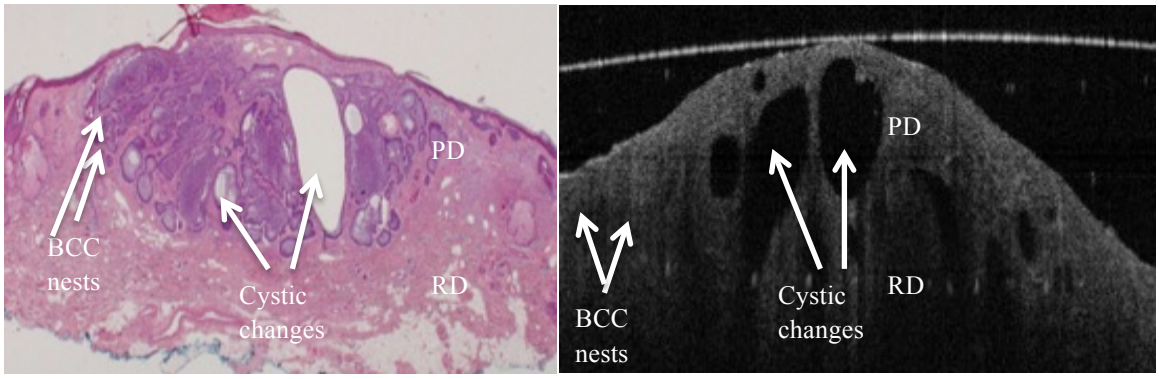

Figure (8.4) True positive margin from a tumour-laden resection margin of a nodulocystic (or nodular) BCC lesion. Both images show tumour nests and cystic changes in the papillary & reticular dermis layers (PD & RD), with breach in continuity of DEJ in some areas.

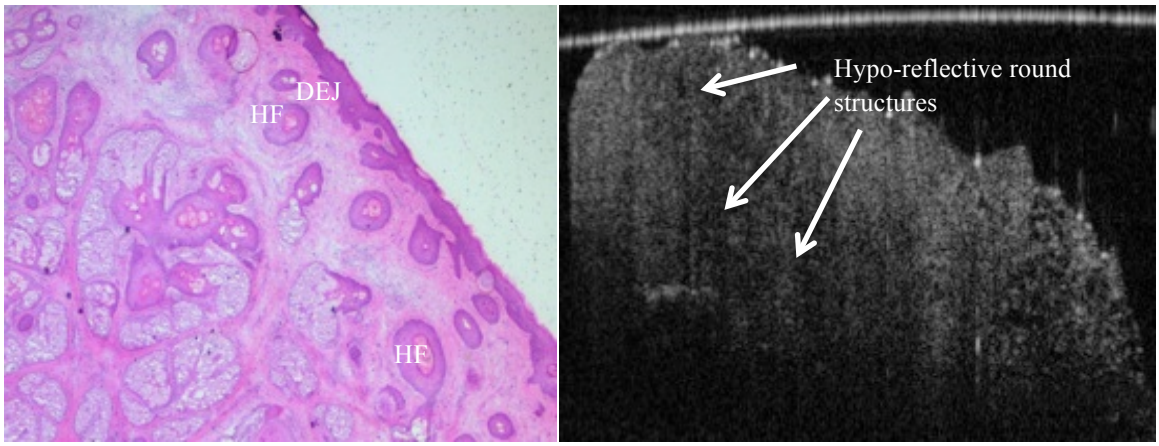

Figure (8.5) False positive margin of a BCC lesion. H&E image reveals intact DEJ with no tumour nests, whereas OCT image shows no clear distinction (DEJ) between epidermal and dermal layers, and the presence of numerous large hypo-reflective (low scattering) tumour-like round structures in both epidermal and dermal layers.

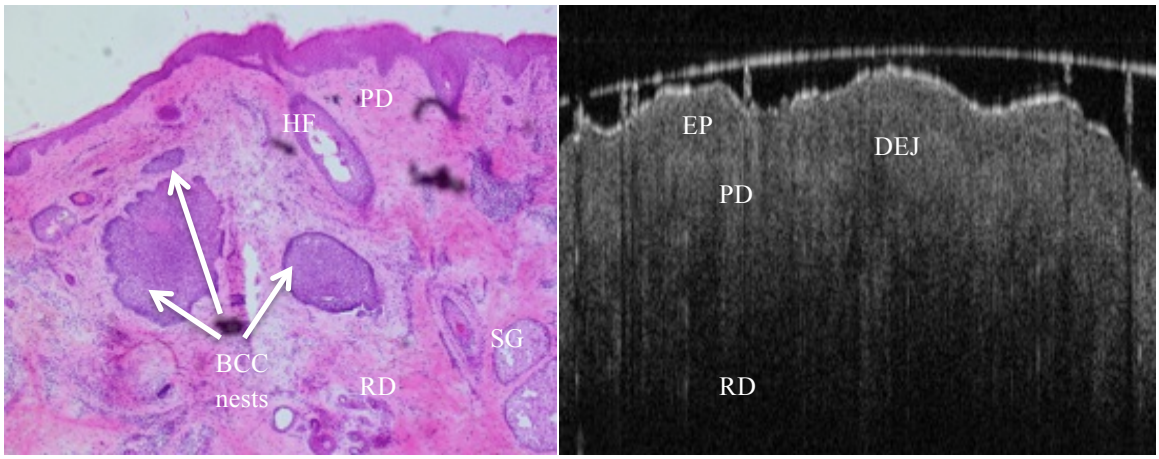

Figure (8.6) False negative margin of a BCC resection margin. H&E picture showing deep tumour nests of both nodular & micronodular subtypes in the reticular dermis, which is clearly beyond OCT penetration depth capability. OCT scan revealing distinct epidermis, intact DEJ and homogenous dermis.

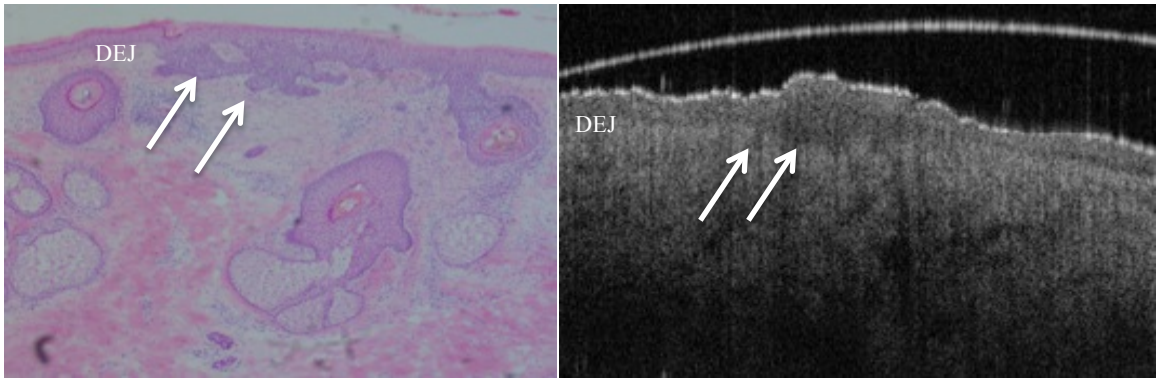

Figure (8.7) Superficial BCC shown in both histology slide & OCT image. Note the downward growth of basal cell layer of epidermis (arrows) without breach in the continuity of DEJ.

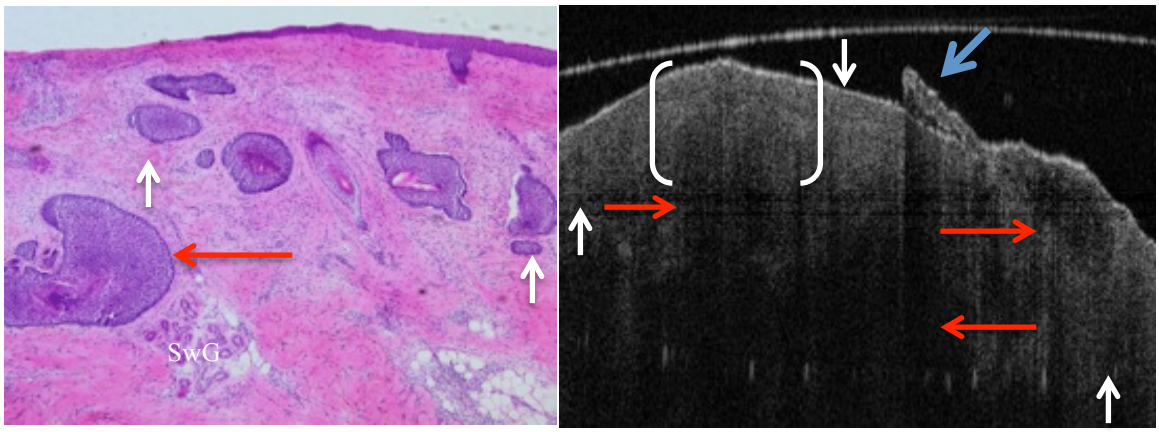

Figure (8.8) Mixed nodular & micronodular BCC subtypes shown in both histology slide & OCT image. Red arrows indicate nodular nests, whereas white arrows indicate micronodular basaloid nests. Palisading (halo-like region) is obvious around the ovoid basaloid nest (bracketed), which is due to the presence of either mucin secretion within a cleft or nuclear material that has been suggested to cause hypo-reflectivity (low scattering properties). SwG (sweat glands) can be seen in the pathology picture, which is beyond OCT penetration depth ability. Note that due to the high scattering nature of the crusting surface of epidermis on the right side of the OCT image (blue arrow), shadowing occurs that results in obscuring the layers and features in the region.

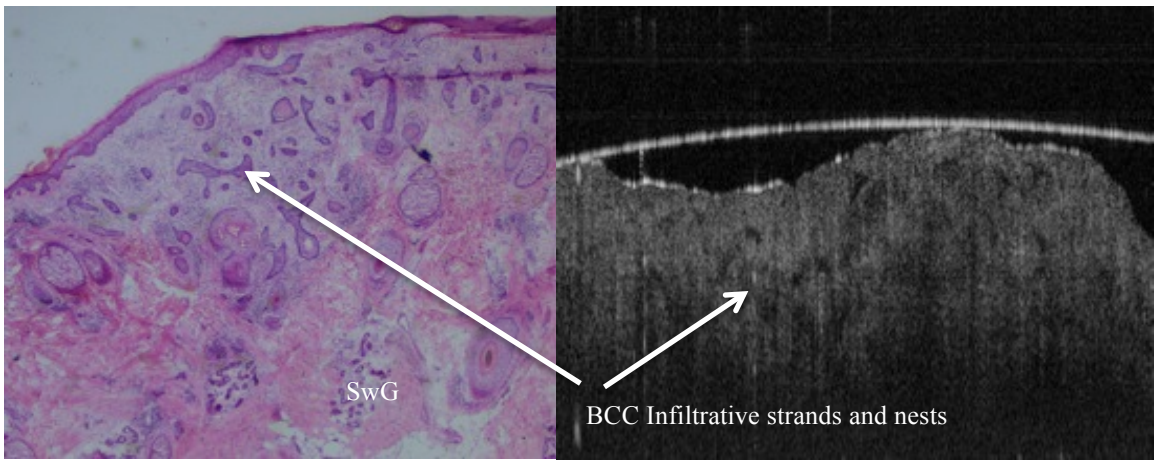

Figure (8.9) Infiltrative type BCC shown in both histopathology & OCT pictures. Note the dramatic alteration to the morphology of both epidermal and dermal layers in the region where the BCC nests resides in. Variability in shape & size of tumour cell nests is noticeable with jagged contours in comparison with other BCC subtypes. It is pretty much similar to a worm holes down into both epidermal & dermal layers.

8.5 Discussion

The results of the current investigation revealed that normal histopathological landmarks, for example epidermis, dermis (including both papillary and reticular layers) and DEJ could be clearly recognised using OCT instrument. This study shows that the normal skin characteristic layerings are lost in BCCs, and this is detectable on OCT images.

The OCT penetration depth in the current study is limited to a maximum of only 1.5-2mm, which is adequate to visualise both the epidermal and dermal layers where occurrence of most of the pathological changes can be observed. However, the BCC lesions and nests that penetrate deep (2mm onwards) in the lower reticular dermis or even subcutis (subcutaneous or hypodermis) layers are beyond OCT's scope owing to the relatively shallow penetration depth ability. The lateral and axial resolution of 10-15μm would not permit single cell detection. Nevertheless, One of the advantages of OCT over CLSM (or LSCM), which has achieved in near real time and noninvasively 1μm resolution with a 200-400μm field of view but with a very shallow depth of penetration up to 500μm (Rajadhyaksha et al, 1995; Rajadhyaksha et al, 1999a; Rajadhyaksha et al, 1999b; White et al, 1999; Collier et al, 2000; Collier et al, 2000), is the possibility of microanatomical structures analysis to a depth of 1500μm. This indicates the likelihood of diagnosing any abnormalities that extend from the papillary dermis to the upper reticular dermis. This involves regions where the epidermis has slight thickness, in which assessment of part of the reticular dermis can be achieved (Sauermann et al, 2000).

In the current investigation, BCC nodular and micronodular subtypes have shown a single important feature, i.e. circular or oval tumour aggregates formation in the epidermal and upper dermal layers, which was found to be distinctive feature in the lesions examined. While vis-à-vis infiltrative subtype, tumour nests are much smaller in width, which is about few cells width (the majority are two cell width), with jagged contours that gives the appearance of either straight or curved small spikes and strands of tissue. Furthermore, the superficial growth pattern BCC appear as atypical basaloid proliferation, which is parallel to the long axis of epidermal layer and showing little penetration into the dermal layer. This research showed that the OCT oral instrument diagnostic capability is ideal for BCC subtypes detection.

The OCT oral instrument features in BCC lesions were very distinctive. BCCs in this study showed diagnostically reliable features, albeit some difficulties were encountered by the investigators during assessment of some OCT images of the BCC lesions due to lack of sufficient contrast (image quality) and resolution. This had led to difficulties in easily defining the borders of the nests and strands of the BCC subtypes and differentiate them from the adnexal structures (particularly sebaceous glands), other anatomical features, and shadows and artefacts which had resulted owing to hyperreflectivity of the keratinised or ulcerated surface layers of the skin in the regions where the BCCs resides. This is in contradiction to a study carried out by Mogensen et al (2009) who assessed OCT imaging in the diagnosis of benign lesions and NMSC versus normal skin in 104 subjects. They concluded that the naked eye is superior to OCT for the diagnosis of NMSC.

Other research performed by Gambichler et al (2007a) on BCCs utilised in vivo OCT. The researchers have reported the capability of in vivo OCT in imaging the altered architecture of skin layers and histology correlates of BCC. The BCC tumour nests in its different shapes, i.e. lobules, islands, and infiltrating strands appeared similar in OCT images and histopathology pictures, regardless of the tumour subtype.

In comparison to the physical examination published rates at 92% by Berg and Atkins (2002) in a cutaneous cancer screening study, the accuracy of OCT for BCC diagnosis exceeds that of the physical examination at 93.2%. Moreover, OCT imaging has the capability to non-invasively, remotely and in real time confirms the diagnoses, while physical examination usually followed by a tissue biopsy. Utilising specified simple criteria, we have established that OCT scanning is sensitive and specific for BCC diagnosis, without huge difference amongst different subtypes of BCC.

In the current investigation, the practicability of OCT imaging in the identification of cutaneous tumour resection margins has been demonstrated. Utilising any optical non-invasive diagnostic method in order to improve the accuracy of excisions might advantage patients by preserving as much normal tissue as possible mainly in the head and neck region where functional and cosmetic reasons are of fundamental importance as well as lessening the number of repeat surgeries. However, the current OCT oral instrument technology needs

refining (by improving image resolution and penetration depth) in order to make it useful in the clinical setting.

The facial cutaneous malignancies tends to be widespread below the surface and in some cases have poor delineation, which means requiring several stages of Mohs in order to determine the margins of the tumour. Frozen or permanent histopathology preparation could take hours to days or is not possible with some tissues. This might have a significant effect on the prognosis of early stage disease. In a recent study by Cunha et al (2011) who investigated and compared a lab-based OCT microscope (EX1301; Michelson Diagnostics, Orpington, Kent, UK) with conventional frozen-section histopathology for visualising BCC during MMS by enrolling 38 patients, have reported that on the average the mean time to produce one OCT image was 7 minutes, whereas 20-40 minutes were required to produce H&E sections. However, in comparison to our hand-held oral probe OCT system that was used in the current investigation, the acquisition time was very fast, which was about 10 seconds. Hence, the time required to examine the margins of the excised tumours is at the most several seconds. Subsequently, this real-time intraoperative system is highly unlikely to considerably lengthen the time of the surgical procedure.

It is improbable that intraoperative OCT imaging will identify occult lesions at a distance of several millimetres from the primary tumour, as presently the greatest depth of penetration of OCT imaging is around 2mm. Therefore, in iceberg-shaped tumours for instance, resection margin analysis is becoming increasingly arduous. The majority of false negative readings in the current study were owing to this fact.

Notwithstanding that, the real-time morphological information attained by OCT scanning, vis-à-vis the epidermal and dermal layers in addition to the capability to demonstrate the junction between these two layers, makes it a promising mapping instrument. In diagnostic ability terms, these are the best performing parameters to distinguish tumour-laden margins.

Investigations of the surgical margins of BCCs have disclosed a gradual transition from more normal appearing images to frank tumours. Detection of features that could discriminate normal skin from cancer tissue is possible by scanning with OCT system**.** Therefore, a

research by Gossage and associates (2003) have suggested that statistical and spectral texture analysis together with OCT imaging would likely to provide automated methods of the diagnostic tissue differentiation.

8.6 Conclusion

This study shows the accuracy of the recently modified OCT oral instrument in identifying the margins status of BCCs located in the head and neck region, albeit with some false positive and negative margins of the excisional biopsies examined. By comparing to histopathology, a good correlation has been revealed by the OCT oral system.

Furthermore, the OCT oral system has shown good capability in discerning different BCC subtypes, for instance, imaging the various nests of BCCs (lobules, islands and infiltrating strands). Nevertheless, tumour identification could be more challenging in thick tumours that exceeds 2mm, which stretch beyond the OCT signal depth, especially with our modified OCT oral system- as we noticed a slight reduction in the penetration depth when compared with the standard OCT skin instrument. Eventually, intraoperative OCT imaging might guide BCC excision with MMS technique and the preservation of as much normal tissue as possible. In addition, it should be of value in the diagnosis and mapping of premalignant and malignant lesions in the head and neck region including the oral cavity.

Chapter 9

Assessment of premalignant/malignant lesions utilising OCT oral instrument: Immediate ex vivo study

Chapter 9

Assessment of premalignant/malignant lesions utilising OCT oral instrument: Immediate ex vivo study

9.1 Background and objectives

In oral cancer, local recurrence and high mortality rate is in part due to the incomplete removal of the primary tumour. In order to reduce the recurrence rate, one of the pivotal factors is to accomplish cancer-free surgical margins. In the previous chapter (MMS for BCC lesion removal), the modified OCT oral instrument proved successful in discerning tissue structures in healthy (tumour free margins) and pathological (tumour-laden) margins with good sensitivity, specificity and accuracy. The goal of this prospective clinical study was to assess the OCT oral instrument's abilities in examining oral premalignant and malignant lesion resection margins and to understand if this imaging technique could be used to guide surgical resection.

9.2 Materials & methods

9.2.1 Patients

Eighty-eight subjects who presented with suspicious intra-oral premalignant and malignant lesions to the UCLH/ Macmillan Cancer Centre- Head & Neck Department were selected and recruited for the current study. The protocol of this study was approved by the NRES REC London-Dulwich (12/LO/0371), and informed consent was obtained from all patients. Inclusion criteria included patients above 18 years of age and patients with T1 & T2 oral squamous cell carcinoma (OSCC) with thin resection margins that could be easily scanned with OCT imaging. Bulky tumours, i.e. T3 & T4 OSCC, are unsuitable for OCT scanning due to the irregular tumour margins. Other exclusion criteria were patients with a previous history of aero-digestive tract carcinoma who had received either radio- or chemotherapy.

9.2.2 Methods/study design

Subjects with white, red and/ or white and red patches (leukoplakia, erythroplakia and erythroleukoplakia) and unhealed ulcer lesions present for more than three weeks in the oral cavity were booked to undergo excisional biopsy surgical procedure under general anaesthetic after previous incisional biopsies confirming that these lesions were dysplastic and/ or malignant. Suspected lesions were mapped by the head and neck/maxillofacial

surgeon using surgical marker pen (including free surgical margins) before excision of the lesion using scalpel blade and/ or CO2 laser. Prior to surgical resection, photos of the lesions were taken utilising (Canon EOS 500D, Japan) camera so that the investigators would be able to envisage the clinical situation and to correlate them with images obtained from the OCT oral instrument after scanning the specimens. As well as digital images, diagrams and specimen orientation utilising sutures were included in the co-registration process (Fig. 9.1). These steps have enabled the histopathologist to recognise the scanned planes precisely and provide H&E sections co-localised to the OCT scan images. For each biopsy, the OCT oral instrument was used to acquire immediate ex vivo images (OCT system applied in the operating theatre) from several areas of interest including medial, lateral, anterior and posterior margins.

So as to ensure objectivity, one consultant oral and maxillofacial histopathologist, was involved in the study, examined all H&E slides and provided the histopathology diagnoses. Assessment was conducted according to WHO guidelines. Histopathological evaluation of each H&E section was scored using a scale of 0 (normal)-6 (SCC) according to the criteria established by MacDonald (1980) using the Smith & Pindborg (1969) technique for oral epithelial atypia scoring. The stained sections were graded on the scale of mild-moderate-severe dysplasia relying on the range and severity of individual features and the ratio of epithelial thickness affected.

For each H&E slide, the following numerical grading system was utilised:

- 0= healthy
- 1=hyperkeratosis
- 2=mild dysplasia
- 3=moderate dysplasia
- 4=severe dysplasia
- 5=CIS
- 6=SCC

The criteria for oral epithelial dysplasia were as follows: drop-shaped rete ridges, irregular epithelial stratification, individual cell keratinisation, basal cell hyperplasia, loss of intercellular adherence, loss of polarity, hyperchromatic nuclei, increased

nuclear/cytoplasmic ratio, anisocytosis, pleomorphic nuclei & cells, abnormal mitotic figures, and increased mitotic activity.

Two investigators, who were experienced in interpreting OCT images, examined all OCT images obtained from scanning the specimens' margins. Both investigators have good knowledge in interpreting OCT images as they had involved in many OCT-related research. A set of OCT images with their corresponding H&E slides for different grades of dysplasia and malignancy were used to consolidate the scorers' assessment dexterity and knowledge. Each scorer examined the images independently and classified and diagnosed them (blinded of the histopathological diagnosis) on a scale of 0 to 6 (where 0 is normal and 6 is SCC). This scale was devised to match the scale utilised for evaluating the H&E slides (MacDonald, 1980; Smith & Pindborg, 1969). After four weeks had elapsed, all OCT images were re-evaluated by the same scorers in order to work out the intra-observer agreement, whilst inter-observer agreement was assessed by comparing the scorers' findings. Scoring of OCT images were based on certain diagnostic features; changes in keratin layer, thickening of epithelium, epithelial proliferation and invasion, elongation of rete ridges, irregularity in epithelial stratification and basal cell hyperplasia. Epithelial invasion was described as loss of visible basement membrane.

The scoring for the OCT images were depending on the range and severity of individual features and the ratio of epithelial thickness affected. All OCT images were compared with their corresponding gold standard H&E pictures to expose whether or not the resection margins were positive or negative and to calculate sensitivity, specificity and accuracy of OCT oral system.

9.3 Statistical Analysis

In order to assess the effectiveness; sensitivity, specificity and overall accuracy of OCT (not accounting for chance agreement) were calculated in Excel, Microsoft Office 2003 according to the data given by both investigators. Cohen's Kappa statistics were calculated in '2015 GraphPad Prism Software' to assess the agreement between the readers and interpreted as poor if $\kappa < 0.00$, slight if $0.00 \leq \kappa \leq$ to 0.20, fair if $0.21 \leq \kappa \leq$ to 0.40, moderate if $0.41 \leq \kappa \leq$ to 0.60, substantial (or good) if $0.61 \leq \kappa \leq 0.80$, almost perfect (or excellent) if $\kappa > 0.80$ (Landis & Koch, 1977).

9.4 Results

52 (59.1%) males and 36 (40.9%) females participated in this research. The mean age of patients was 63 years (range 27-91 years). More than one third of the patients were current smokers (43%), while only 15% were non-smoker. Vis-à-vis drinking status, more than half of the cohort (56%) consumed alcoholic beverages on a regular basis, 18 subjects (20%) were teetotal and only 10 patients (11%) were paan chewers.

Ulcers were constituted 36% of the lesions presented, while the remainder (64%) showed as white, red and mixed white and red patches. 50% (n=44) of the lesions were leukoplakia, erythroplakia constituted 34%, while erythro-leukoplakia comprised the smallest group of the lesions at 16%. The distribution of the lesions anatomically revealed almost 30% in the ventro-lateral tongue (n=25), a quarter of the lesions in the floor of mouth (25%), 16 in retromolar trigone, 12 in the buccal mucosa, 5 on lower lip (Table 9.1).

The histopathology result of 352 margins (88 specimen, four images per specimen) revealed 275 (81.8%) tumour free margins, 36 (10.8%) margins involved with dysplasia of different grades (mild=4, moderate=13, and severe=19) and 25 (7.4%) SCC-involved margins (Figures 9.2-9.5). 16 margins were excluded owing to either distortion during histopathologic processing or bad quality OCT images. The H&E slides that have severe artefacts were excluded, while those bad quality OCT images, for instance blurred images, were also disregarded (Table 9.2).

The sensitivity and specificity for the first assessor was 83.6% and 94.5%, respectively. Whilst the positive predictive value (PPV) was 77.2% and the negative predictive value (NPV) was 96.2%. Prevalence was 0.18, OCT accuracy was 92.5% and the kappa statistic was 0.75 (95% CI: From 0.66 to 0.84) (substantial agreement).

There were 15 false positives and 10 false negatives, with positive likelihood ratio (LR+) of 15, suggesting that OCT is useful and provides evidence to support the diagnosis with a negative likelihood ratio (LR-) of 0.17, it allows us to rule out the malignant diagnosis with significant confidence (Tables 9.3 & 9.5).

The sensitivity and specificity for the second assessor was 82% and 93.8%, respectively. The PPV was 74.6% and the NPV was 95.9%. Prevalence was 0.18, OCT accuracy was 91.6% and the kappa statistic was 0.73 (95% CI: From 0.63 to 0.82) (substantial agreement). There were 17 false positives and 11 false negatives, with LR+ of 13 and LR- of 0.19 (Tables 9.4 & 9.5).

The intra-observer agreement was substantial (Kappa statistic= 0.74). Furthermore, the degree of concordance between both readers (inter-observer agreement) was also good, although the kappa statistic was a little lower (Kappa statistic= 0.69) according to Landis & Koch, 1977.

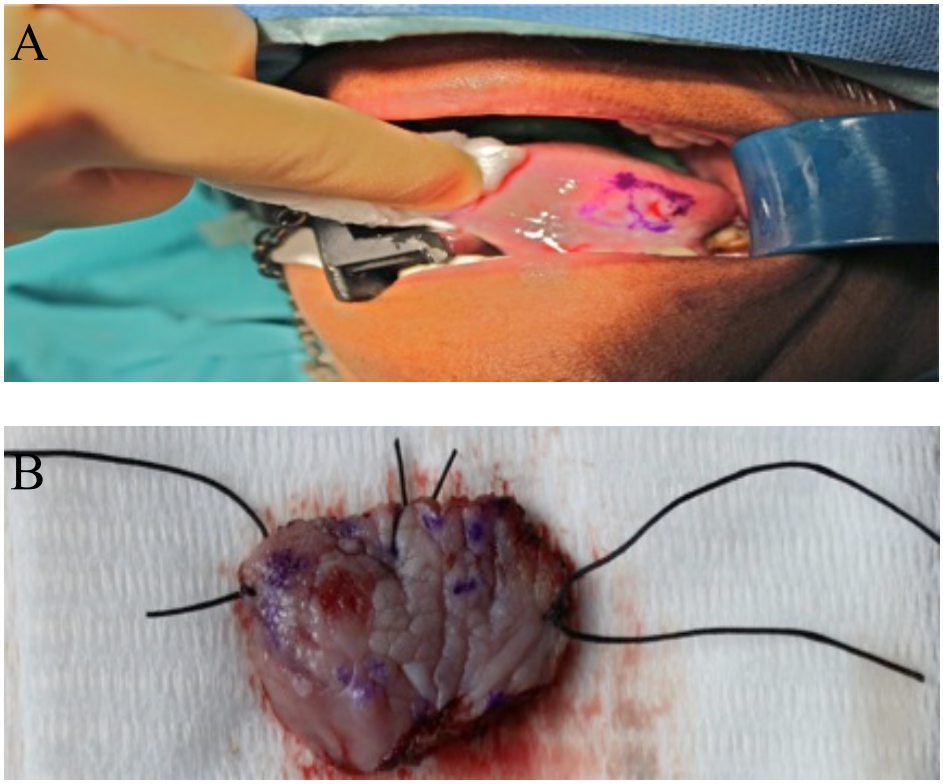

Figure (9.1) Assessment of tumour resection margin. **A**: Clinical photograph reveals marking of a dysplastic lesion on left lateral tongue preceding resection under general anaesthetic. **B**: shows specimen resected and orientated using sutures, then subjected to OCT scanning.

Table (9.1) Clinical data and location of the lesions of the population studied (N = 88).

1. **Gender**	**No (%)**
Male	52 (59%)
Female	36 (41%)
2. **Age** (years), mean (range)	63 (27–91)
3. **Location of lesion**	
Ventral-lateral tongue	25 (29%)
Floor of mouth	22 (26%)
Retromolar region	16 (18%)
Buccal mucosa	12 (14%)
Lower lip	5 (5%)
Upper lip	3 (3%)
Soft palate	3 (3%)
Dorsum of tongue	2 (2%)
4. **Colour of lesion**	
Leukoplakia	44 (50%)
Erythroplakia	30 (34%)
Erythroleukoplakia	14(16%)
5. **Clinical features**	
Patch	56(64%)
Ulcer	32(36%)
6. **Smoking status**	
Current smoker	38(43%)
Ex-smoker	37(42%)
Non-smoker	13(15%)
7. **Drinking status**	
Current drinker	49(56%)
Ex-drinker	21(24%)
Non-drinker	18(20%)
8. **Betel nut (Pan) chewing**	10(11%)

Table (9.2) Histopatholgical findings for the surgical margins of the examined biopsies.

Margins	**Numbers (%)**
Healthy	275 (81.8%)
Mild dysplasia	4 (1.2%)
Moderate dysplasia	13 (3.9%)
Severe dysplasia	19 (5.7%)
SCC	25 (7.4%)
Excluded margins	16
Total	**336** (16 margins not included)

Table (9.3) Oral lesions biopsy margins assessment by the **first assessor** (total 352 margins, 16 margins were excluded). Sensitivity 83.6%; specificity 94.5%; (PPV) 77.2%; (NPV) 96.2%; accuracy of OCT oral system 92.5%. TP: true positive, FP: false positive, TN: true negative, FN: false negative.

Histopathology				
OCT		**Positive**	**Negative**	**Total**
	Positive	51 (TP)	15 (FP)	66
	Negative	10 (FN)	260 (TN)	270
	Total	61	275	**336**

Table (9.4) Oral lesions biopsy margins assessment by the **second assessor** (total 352 margins, 16 margins were excluded). Sensitivity 82%; specificity 93.8%; (PPV) 74.6%; (NPV) 95.9%; accuracy of OCT oral system 91.6%. TP: true positive, FP: false positive, TN: true negative, FN: false negative.

Histopathology				
OCT		**Positive**	**Negative**	**Total**
	Positive	50 (TP)	17 (FP)	67
	Negative	11 (FN)	258 (TN)	269
	Total	61	275	**336**

Table (9.5) Assessors findings vs. parameters.

Parameters	**1st Assessor**	**2nd Assessor**
Sensitivity	83.6%	82%
Specificity	94.5%	93.8%
PPV	77.2%	74.6%
NPV	96.2%	95.9%
False positive	15	17
False negative	10	11
Prevalence	0.18	0.18
LR+	15	13
LR-	0.17	0.19
OCT accuracy	92.5%	91.6%
Kappa	0.75	0.73

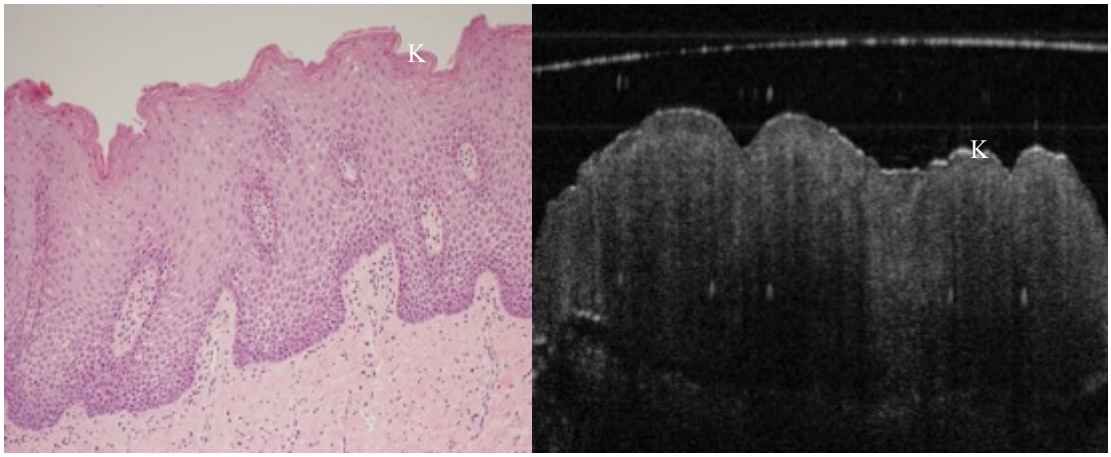

Figure (9.2) Both OCT & histopathology images reveal keratosis and mild epithelial dysplasia of a leukoplakic lesion on the buccal mucosa. K= keratosis.

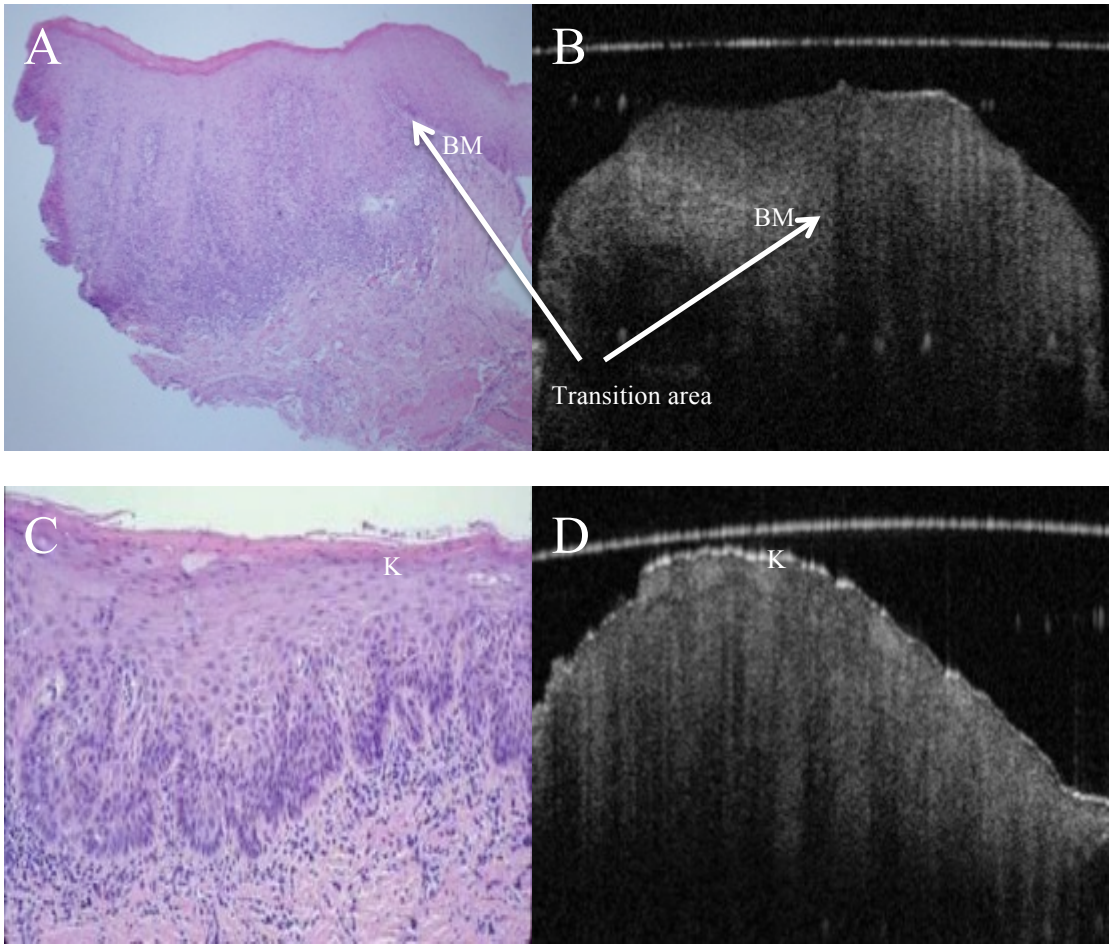

Figure (9.3) Both OCT & histopathology images (A&B) reveal transition between healthy margin and moderate epithelial dysplasia of a white patch lesion on the retromolar area, while the bottom set images (C&D) show hyperparakeratosis with moderate dysplasia of an involved margin of a leukoplakic lesion on lateral tongue. BM= basement membrane.

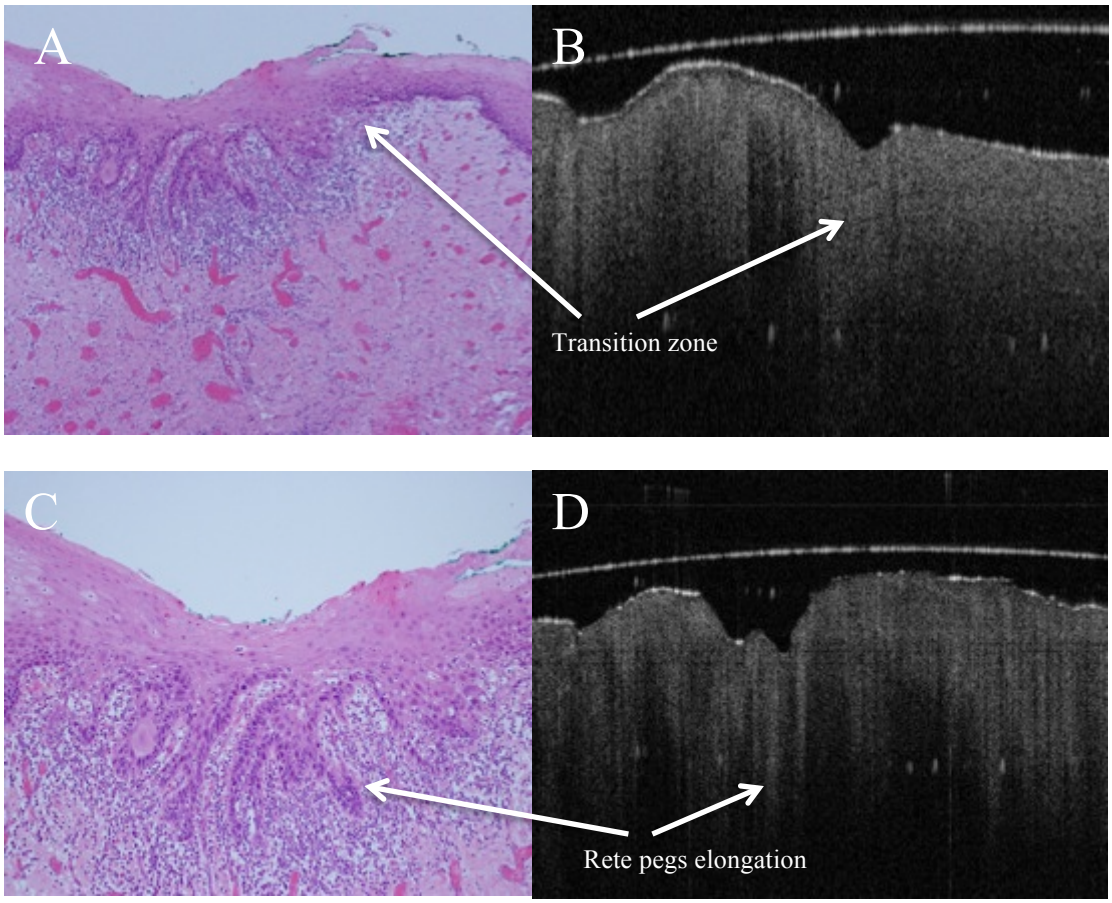

Figure (9.4) OCT & histopathology images (A&B) reveal healthy margin transition to severe epithelial dysplasia of an ulcer on floor of mouth, whereas the bottom set images (C&D) show severe epithelial dysplasia at the centre of the ulcer.

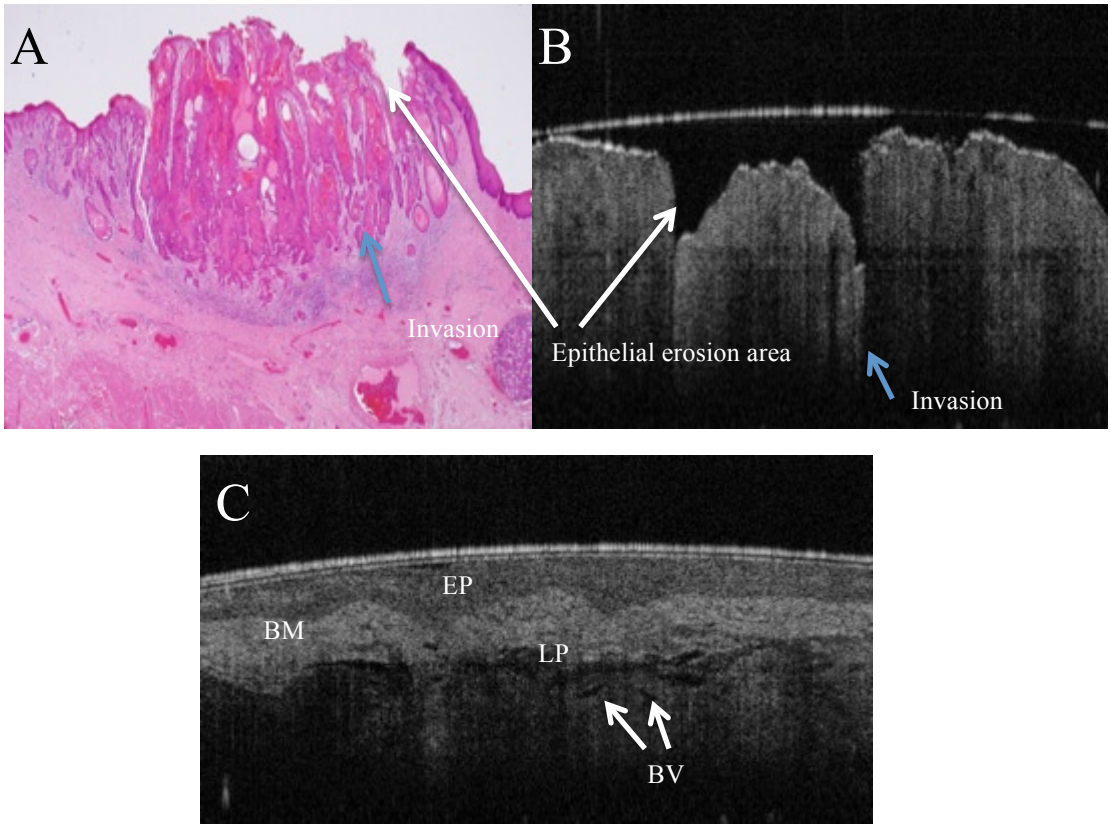

Figure (9.5) (A&B) OCT & histopathology images reveal invasive SCC in floor of mouth and lateral tongue. OCT image parallels histology status displaying high variability in epithelium thickness with areas of breakdown of the epithelium (erosion) (indicated by long white arrows) and the large epithelial down growth and invasion into the subepithelial layers (blue arrows). Furthermore, the basement membrane (disrupted and penetrated) is indiscernible through the entire OCT scan as a coherent prominent feature. (C) OCT image of the healthy tissue margin (corresponding to the margins shown in the H&E picture) that shows normal thickness epithelium, which is hyporeflective (dark) compared to the hyperreflective (bright) lamina propria that contains many hypoechoic tube-like structure that represent blood vessels. Intact basement membrane is also clearly visible. BM= basement membrane; EP= epithelium; LP= lamina propria; BV= blood vessel.

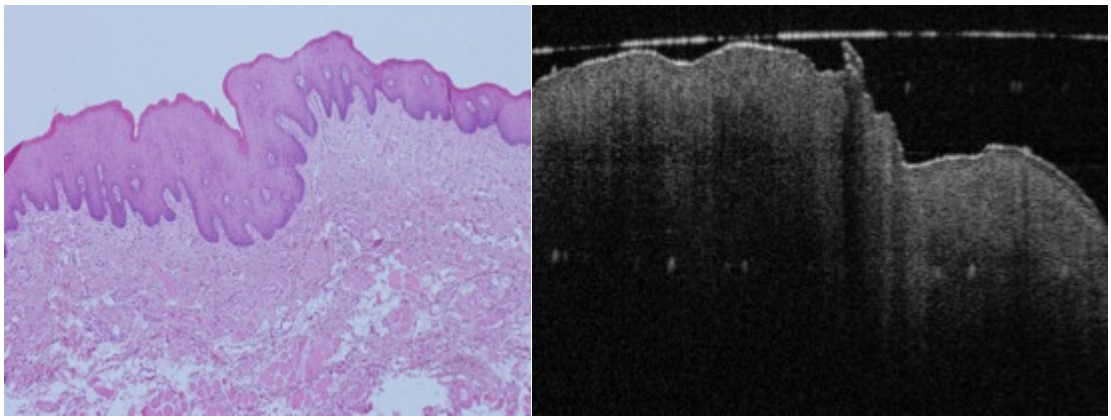

Figure (9.6) Histopathology picture of keratosis & epithelial hyperplasia (without dysplasia) of a white lesion on the lower lip with the corresponding OCT image that usually erroneously interpreted as mild or moderate dysplasia (false positive reading) owing to rete ridges elongation.

9.5 Discussion

Precise evaluation of tumour extension utilising conventional visual examination and palpation is critical. Some radiological modalities are currently used to evaluate tumour extent, such as MRI and CT, which possess insufficient image resolution and contrast to be able to correctly measure cancer dimensions with confidence. In a clinical study by Heissler et al (1994) on 46 patients with malignant carcinomas of the oral cavity and oropharynx to study the value of MRI in preoperative tumour (T) staging, reported confusion in delineating between the normal tissue and tumour, making recognition of most of the carcinoma within 5 mm margin very challenging that is unsuitable for most T1 and T2 malignancies of the oral cavity.

In another study utilising high-resolution ultrasound for interrogation of OSCC thickness and resection margin status, Songra and associates (2006) in a single blind prospective study on 14 patients with biopsy proven OSCC that had intraoral ultrasound imaging done preoperatively, reported that ultrasound detection of close surgical margins had sensitivity and specificity of 83% and 63% respectively. Compared to our results, the sensitivity was nearly similar, but specificity was inferior to ours (mean specificity =94.1%). Songra et al (2006) concluded that high-resolution ultrasound imaging, which applied intraorally, is a trustworthy modality in evaluating thickness of tumour and the clearance of surgical margins at the time of surgery.

A prospective clinical in vivo study carried out by Shintani and coworkers (1997) on 24 patients with tongue malignancy that underwent preoperative evaluation with intraoral ultrasonography to measure tumour thickness and the subsequent comparison with the measurements obtained from histological sections. They found out that tumour thickness were measurable within 1mm on the obtained high quality ultrasonic images, and that significant correlation was exist between ultrasonography images and H&E sections measurements. In their conclusion, they demonstrated that ultrasonography application in the oral cavity is an excellent approach to delineate extent of tumour and measurement of tumour thickness in malignancy of tongue.

In this prospective clinico-pathological ex vivo research, OCT oral system demonstrated efficacy and feasibility in detecting surgical free margins from tumour-laden margins of biopsies excised in different anatomical region in the oral cavity with very good sensitivity and specificity. Visibility of basement membrane was the major parameter (key landmark) in discerning healthy and dysplastic tissues from cancerous tissues. In malignancy, the invasive tumour penetrates through the basement membrane to the subepithelial layers, and become invisible in both OCT and H&E pictures.

Another important fact that assisted in detecting healthy from pathological margins was the obvious change in reflectivity between the epithelium and the underlying connective tissue layer (lamina propria), which is delineated by the basement membrane. Since the epithelial layer is mostly comprised of well-separated scatterers, for example cells (Kumar & Schmitt, 1996), multiple scattering in this layer is insignificant. Thus, scattering in the epithelial layer is chiefly in the forward direction that reflects the scattering property of a single cell. Furthermore, as epithelium acts as a strong absorber and not as a scatterer (Jacques, 1998; Igarashi et al, 2005), therefore the epithelium appears darker on OCT images when compared to the brighter lamina propria (Fig. 9.5C). In contrast, lamina propria's (which has similar composition and structure to the dermis layer of the skin) most common cell type is the fibroblast. In addition, collagen type I is the predominant fibre component of the extracellular matrix followed by both collagen type III and elastic fibers. All these components in lamina propria are highly backscattering, hence appear brighter compared to the surrounding structures including epithelium (Bashkatov et al, 2011). The homogeneity of this layer (lamina propria) becomes less consistent and uniform and loses its brightness as well in the presence of dysplasia/malignancy that invade through the basement membrane, thus aid in discriminating between healthy or surgical-free and tumour-involved margins.

The co-registration process that included digital images, diagrams of the specimens and orientation utilising sutures were extremely important so as to obtain as exactly as possible both OCT and histology images of the same area of interest. Sparing no effort were sought to correlate OCT scans with the histopathology sections by liaising directly with the consultant histopathologist who participated in the current investigation. However, no exact comparison between the OCT images and the corresponding H&E pictures were possible due to the well-

known fact of tissue shrinkage (up to 30%) after fixing the specimens in 10% buffered formalin and histological preparation (such as embedding and sectioning) during laboratory processing (Kimura et al, 2003), some degree of discrepancy between OCT and histopathology pictures was inevitable. This inconsistency can be clearly noticed in figure (9.5 A&B) for example, where OCT image displayed two dips (epithelial erosion), while corresponding H&E only showed one dip. This is probably has resulted in some of our false negatives and false positives investigators reading. Additionally, another reason behind the false positive readings was the presence of epithelial hyperplasia (without dysplasia), which has influenced on assessors' decision to consider it as mild or moderate dysplasia according to OCT images (Fig. 9.6).

The robust OCT and their correlative H&E training set pictures for dysplasia and malignancy had positive outcome on the assessors' ability to learn to read OCT images swiftly and precisely, as corroborated by the strong intra- and inter-rater reliability on OCT scores, in addition to the good agreement between OCT and H&E scores, albeit with some difficulties in precise grading of some of the dysplastic lesions on the OCT images due to insufficient resolution to view subcellular features. This is apparent in figure (9.3 C&D) where basement membrane can be easily recognised on the H&E slide, whereas it can be hardly detected on the OCT image. The resolution of the OCT oral system that we utilised in our research only provides an idea of structural architectural changes but not cellular changes.

In a recent clinical study, Jerjes et al (2010) examined 34 biopsies of suspicious intraoral lesions from 27 subjects utilising ex vivo OCT imaging to assess the feasibility of this modality in identifying malignant tissue. Four variables in this pilot research were scrutinised: changes in keratin; epithelium; sub-epithelial layers; and identification of the basement membrane. From this they calculated whether or not there were architectural changes and the data were then compared with H&E diagnoses. The authors concluded that OCT technique might recognise diseased areas but could not provide a diagnosis or differentiate between lesions and that their pilot work approves the feasibility of utilising OCT to distinguish architectural changes in malignant tissues.

Similar to our findings in the previous chapter (MMS versus ex vivo OCT), some false negative readings on the OCT images were perhaps because of iceberg-shaped tumours, which penetrate deep in the submucosa and that cannot be detected at the margins of the specimens with a shallow penetration depth of about 2mm maximum. Moreover, to make matters worse, some tumours develop finger-like projections beneath the subepithelial layers. These types of submucosal tumour extensions penetrate deep in a way that surpasses the OCT detection capability.

In the present investigation, the most challenging aspect in discriminating and diagnosing the dysplastic margins on OCT images was the lack of insufficient contrast and resolution (magnification) in order to be able to accurately score and grade them as we encountered insurmountable difficulties in visualising the cellular features (for example, anisocytosis, nuclear/cytoplasmic ratio and so forth) that suggest and help in grading the lesion as mild, moderate and severe dysplasia. Single cell detection would not be achievable with OCT lateral and axial resolution of 10-15μm. Subtle changes in the epithelial cells/shapes and aggregations (for e.g., basal cell hyperplasia) might affect the histological diagnosis from moderate to severe dysplasia or even from the latter to invasive carcinoma in the presence of epithelial invasion and budding, which will ultimately influence clinicians' decision-making in the treatment options of the dysplastic/ malignant lesion. Low-resolution OCT images compared to high-resolution H&E pictures has influenced on the discrepancy between the two diagnostic methods in the current study.

9.6 Conclusion

The present prospective ex vivo OCT work, for interrogating precancerous and cancerous lesion margins, demonstrated a capability of the new OCT instrument systems in recognising healthy from dysplastic and malignant margins with reasonable degree of sensitivity, specificity as well as accuracy, albeit with difficulties in grading the dysplastic lesions. Since the resolution abilities of OCT technique are briskly rising, their capability in differentiating between dysplasia's different stages is also likely to advance. Hence, this modality may aid in declining the delay in diagnosis of malignancy in addition to notably increasing the clinicians' capability in recognising and diagnosing pre-cancer/cancer of the oral cavity correctly.

Furthermore, it can also be concluded that epithelial thickness change and status of the basement membrane were key points in the detection and diagnosis of invasive carcinoma whatsoever the optical modality used. Our study revealed that these two parameters played key roles in interpreting OCT images.

Finally the current work will pave the way in applying the OCT oral instrument in vivo to interrogate intraoral pathological (benign and malignant) conditions to study it's accuracy, sensitivity and specificity and aid the clinicians in reaching the diagnosis more expeditiously plus in treatment decision-making in future.

Chapter 10

In vivo OCT oral system for interrogating and diagnosing different suspicious oral lesions and premalignancy/malignancy

Chapter 10

In vivo OCT oral system for interrogating and diagnosing different suspicious oral lesions and premalignancy/malignancy

10.1 Background and objectives

In the previous chapter, we demonstrated the ex vivo OCT oral instrument ability in identifying healthy margin from margins involved with dysplasia and/ or malignancy, with good sensitivity, specificity and with good kappa score inter-observer reliability. To the best of our knowledge, there is little in the literature, utilising OCT in vivo to detect suspicious lesions, especially in the oral cavity. This is due to rigidity and limited length of most of the OCT skin probes that act as a major hindrance in applying this high-resolution imaging modality in hard and soft tissues of the oral cavity. There are very few systems that possess an oral probe such as the commercial Niris OCT imaging system [Imalux, Cleveland, OH]. The goal of this clinical study was to investigate in real-time and non-invasively, the capability of the recently modified Michelson OCT oral instrument in identifying and aid diagnosis of lesions in the head and neck region including the oral cavity.

10.2 Materials and Methods

10.2.1 Patients

130 subjects who presented with undiagnosed lesions in the head and neck region including the oral cavity to the UCLH/ Macmillan Cancer Centre- Head & Neck/Maxillofacial Department were selected and recruited for the current study. The protocol of this study was approved by the NRES REC London-Dulwich (12/LO/0371), and informed consent was obtained from all patients. Inclusion criteria were patients over 18 years of age who presented with suspicious intraoral lesions.

Patients were undergone detailed clinical examination in order to evaluate the size and site of their suspicious lesions as well as the clinical characteristic of the lesion. Smoking and drinking status were also recorded (Table 10.1).

10.2.2 Methods/study design

After examination of the lesions and digital photos taken (using Canon EOS 500D camera, Japan), the lesions in doubt were subjected to in vivo OCT scanning. OCT images acquired from several areas of interest including margins and centres of the lesions prior to injection of local anaesthesia as the solution will lead to blurred images as confirmed by other researchers (Mogensen et al, 2009). The lesions then underwent either excisional or incisional biopsy (as clinically appropriate) under local/general anaesthetic. 130 biopsies were obtained at the end of the study (1 biopsy per patient). After the lesions were biopsied using scalpel blade and/ or CO2 laser, they routinely sent off to the histopathology department to obtain H&E pictures so as to be compared with the in vivo OCT images. In order to ensure objectivity, one consultant oral and maxillofacial histopathologist, who is involved in the current investigation, examined all H&E slides and provided the histopathology diagnoses. Assessment was conducted according to WHO guidelines. Regarding the dysplasia H&E slides, similar histopathologic evaluation has been followed for scoring mild, moderate and severe dysplasia as in the ex vivo study in the previous chapter according to the criteria established by MacDonald (1980) using the Smith & Pindborg (1969) technique for oral epithelial atypia scoring.

Two assessors, who experienced in interpreting OCT images, scrutinised all OCT images acquired from scanning the lesions' margins and centres. They were provided with a brief clinical history of the dubious lesions, and were asked to write their comments on each OCT image on a premade pro forma. Each assessor examined the OCT images independently and was blinded to the histological diagnosis.

Each observer was asked to provide a diagnosis for the patients' lesions so as to be compared with the actual histopathology reports later. After four weeks had elapsed, all OCT images were re-evaluated by the same scorers in order to work out the intra-observer agreement. The inter-observer agreement was obtained by comparing the individual scorers' findings. Based upon 4 criteria, the investigators scored the OCT images:

- Keratin layer thickness (increased, decreased or no change)
- Epithelial layer (increased, decreased or no change)
- Status of the basement membrane (intact, breached or difficult to assess)
- Changes in the lamina propria (homogeneous or non-homogeneous) (Table 10.2)

Afterwards, all OCT images were compared with their corresponding H&E pictures to expose the concordance (kappa agreement) of OCT technique with the gold standard histopathology and to calculate OCT accuracy.

10.3 Statistical Analysis

In order to assess the effectiveness; sensitivity, specificity and overall accuracy of OCT (not accounting for chance agreement) were calculated in Excel, Microsoft Office 2003 according to the data given by both investigators. Cohen's Kappa statistics (κ) were calculated in '2015 GraphPad Prism Software' to assess the agreement between the readers and interpreted as poor if $\kappa < 0.00$, slight if $0.00 \leq \kappa \leq$ to 0.20, fair if $0.21 \leq \kappa \leq$ to 0.40, moderate if $0.41 \leq \kappa \leq$ to 0.60, substantial (or good) if $0.61 \leq \kappa \leq 0.80$, almost perfect (or excellent) if $\kappa > 0.80$ (Landis & Koch, 1977).

10.4 Results

The majority of the patients were males [n=72 (55.4%)], while the number of females who took part in this clinical study were 58 (44.6%). The mean age of patients was 60 years (range 22-94 years). More than a third of the patients were current smokers (37%), while only 21% were non-smoker. Regarding drinking status, 79 subjects (61%) consumed alcoholic beverages on a regular basis, 23 subjects (17.5%) were teetotal and only 14 patients (10.5%) were paan chewers (Table 10.1).

Nearly half of the lesions clinically appeared as patches (46%), followed by ulcer (27.5%), then plaque lesions constitute 12%, whereas bulla constituted the least lesion group in the cohort studied (1.5%). There was variability in lesion colours: 45.5% (n=59) of the lesions were leukoplakic, erythroplakic lesion constituted 28%, while erythro-leukoplakic lesion comprised 21.5%, and only 6 lesions were bluish. The anatomical distribution of the lesions shown quarter (25%) of them (most prevalent site) located in the ventral-lateral tongue (n=33), followed by 19 lesions on floor of mouth, 17 on retromolar trigone, 16 on dorsum of tongue, 15 on buccal mucosa (Table 10.1).

The histopathological diagnosis of the population studied (n=130) divulged that more than half of the lesions (n=78) were premalignant and malignant and were as follows: 42 dysplasia of different grades followed by 36 OSCC (Figures 10.10-10.13). While benign intraoral lesions were less common and included the following: 9 Keratosis, 8 non-specific ulcers, 7 chronic hyperplastic candidiasis and 18 cases distributed equally between fibro-epithelial hyperplasia, papilloma and mucocoele. Fibro-epithelial polyp constituted 5 lesions, whereas pemphigus vulgaris (3) and lipoma (2) were the least common lesions in this study (Table 10.1 & Figures 10.1-10.9).

The results of assessing the four diagnostic parameters by both investigators were detailed in table 2. A total of 650 OCT images were obtained (130 lesions, 5 images per lesion) and compared with their corresponding H&E. The histopathology results of the biopsied lesions' margins disclosed 518 pathology-free margins and 87 pathology-involved margins (pathology here means both benign and malignant). 45 OCT and H&E pictures were excluded and disregarded due to either blurry images or severe artefact slides, respectively.

The sensitivity and specificity for the first investigator was 78.2% and 93.8%, respectively. Whilst the positive predictive value (PPV) was 68% and the negative predictive value (NPV) was 96.2%. Prevalence was 0.14, OCT accuracy was 91.5% and the kappa statistic was 0.67 (95% CI: From 0.59 to 0.76) (substantial agreement). There were 32 false positives and 19 false negatives, with positive likelihood ratio (LR+) of 13, suggesting that OCT is useful and provides evidence to support the diagnosis and negative likelihood ratio (LR-) of 0.23, which allows us to rule out the diagnosis (Tables 10.3 & 10.5). The sensitivity and specificity for the second investigator was 81.6% and 93.4%, respectively. The PPV was 67.6% and the NPV was 96.8%. Prevalence was 0.14, OCT accuracy was 91.7% and the kappa statistic was 0.69 (95% CI: From 0.61 to 0.77) (substantial agreement). There were 34 false positives and 16 false negatives, with LR+ of 12 and LR- of 0.20 (Tables 10.4 & 10.5).

The intra-observer agreement was substantial (Kappa statistic= 0.71). Furthermore, the degree of concordance between both readers (inter-observer agreement) was also good (Kappa statistic= 0.70) according to Landis & Koch, 1977.

With regard to the agreement between the assessors in assessing the four diagnostic parameters on the 605 OCT images, the results were as follow: there was excellent weighted kappa (0.87) vis-à-vis keratin layer thickness, almost perfect agreement (weighted kappa= 0.92) regarding epithelial layer thickness, excellent agreement (weighted kappa= 0.95) for basement membrane status and almost perfect agreement concerning changes in lamina propria (weighted kappa= 0.96).

Table (10.1) Clinical data and location of the lesions of the population studied (N = 130).

1. **Gender**	**No (%)**
Male	72 (55.4%)
Female	58 (44.6%)
2. **Age** (years), mean (range)	60 (22–94)
3. **Types of lesion (Histopathology diagnosis)**	
Dysplasia (all grades)	42 (32.3%)
SCC	36 (27.6%)
Keratosis	9 (6.9%)
Non-specific ulcers	8 (6.1%)
Chronic hyperplastic candidiasis	7 (5.3%)
Fibro-epithelial hyperplasia	6 (4.7%)
Papilloma	6 (4.7%)
Mucocoele	6 (4.7%)
Fibro-epithelial polyp	5 (3.9%)
Pemphigus vulgaris	3 (2.3%)
Lipoma	2 (1.5%)
3. **Location of lesion**	
Ventral-lateral tongue	33 (25%)
Floor of mouth	19 (15.5%)
Retromolar region	17 (13%)
Dorsum of tongue	16 (12%)
Buccal mucosa	15 (11.5%)

Lower lip	12 (10%)
Upper lip	6 (5%)
Soft palate	6 (5%)
Hard palate	3 (2.5%)
Gingiva	3 (2.5%)
4. **Colour of lesion**	
Leukoplakia	59 (45.5%)
Erythroplakia	37 (28%)
Erythroleukoplakia	28 (21.5%)
Bluish	6 (5%)
5. **Clinical features**	
Patch	60 (46%)
Ulcer	36 (27.5%)
Plaque	16 (12%)
Papule	11 (8.5%)
Macule	5 (4.5%)
Bulla	2 (1.5%)
6. **Smoking status**	
Current smoking	48 (37%)
Ex-smoker	55 (42%)
Non-smoker	27 (21%)
7. **Drinking status**	
Current drinker	79 (61%)
Ex-drinker	28 (21.5%)
Non-drinker	23 (17.5%)
8. **Betel nut (Pan) chewing**	14 (10.5%)

Table (10.2) Assessment of four diagnostic parameters (tissue structures) on the OCT images by both assessors (total 650 images, 45 were excluded). KL= keratin layer, EL= epithelial layer, BM= basement membrane, LP= lamina propria. Increase= ⇑, no change= ⇔, decrease= ⇓.

Parameters	**First assessor**			**Second assessor**		
KL	⇑	⇔	⇓	⇑	⇔	⇓
	202	168	235	240	181	184
EL	⇑	⇔	⇓	⇑	⇔	⇓
	404	189	12	423	172	10
BM	Intact	Breached	Difficult to assess	Intact	Breached	Difficult to assess
	450	140	15	443	137	25
LP	Homogenous	Non-homogenous		Homogenous	Non-homogenous	
	377	228		369	236	

Table (10.3) Margins assessment by the **first investigator** (total 605 margins, 45 margins were excluded). Sensitivity 78.2%; specificity 93.8%; (PPV) 68%; (NPV) 96.2%; accuracy of OCT oral system 91.5%. TP= true positive, FP= false positive, TN= true negative, FN= false negative.

Histopathology				
OCT		**Positive**	**Negative**	**Total**
	Positive	68 (TP)	32 (FP)	100
	Negative	19 (FN)	486 (TN)	505
	Total	87	518	**605**

Table (10.4) Margins assessment by the **second investigator** (total 605 margins, 45 margins were excluded). Sensitivity 81.6%; specificity 93.4%; (PPV) 67.6%; (NPV) 96.8%; accuracy of OCT oral system 91.7%. TP= true positive, FP= false positive, TN= true negative, FN= false negative.

Histopathology				
OCT		**Positive**	**Negative**	**Total**
	Positive	71 (TP)	34 (FP)	105
	Negative	16 (FN)	484 (TN)	500
	Total	87	518	**605**

Table (10.5) Assessors findings vs. parameters.

Parameters	**1st Investigator**	**2nd Investigator**
Sensitivity	78.2%	81.6%
Specificity	93.8%	93.4%
PPV	68%	67.6%
NPV	96.2%	96.8%
False positive	32	34
False negative	19	16
Prevalence	0.14	0.14
LR+	13	12
LR-	0.23	0.20
OCT accuracy	91.5%	91.7%
Kappa	0.67	0.69

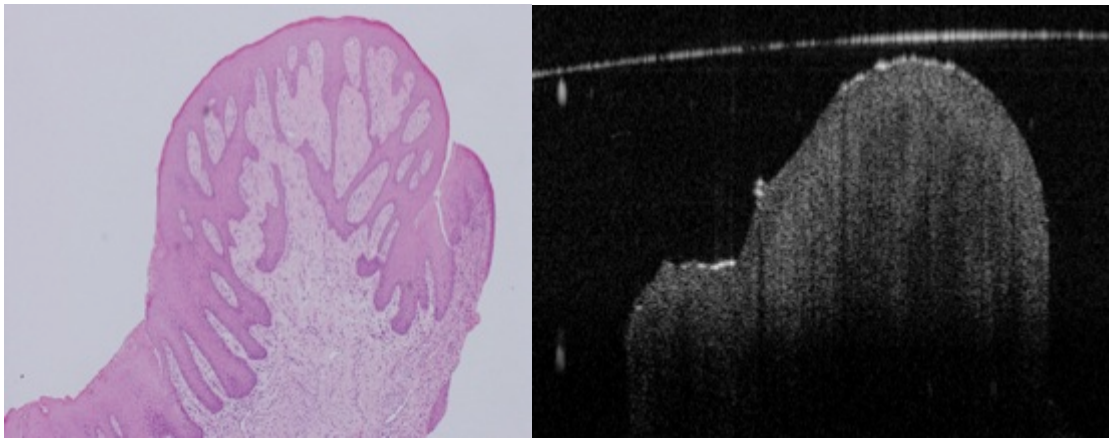

Figure (10.1) OCT & histopathology images reveal fibroepithelial polyp on lateral tongue.

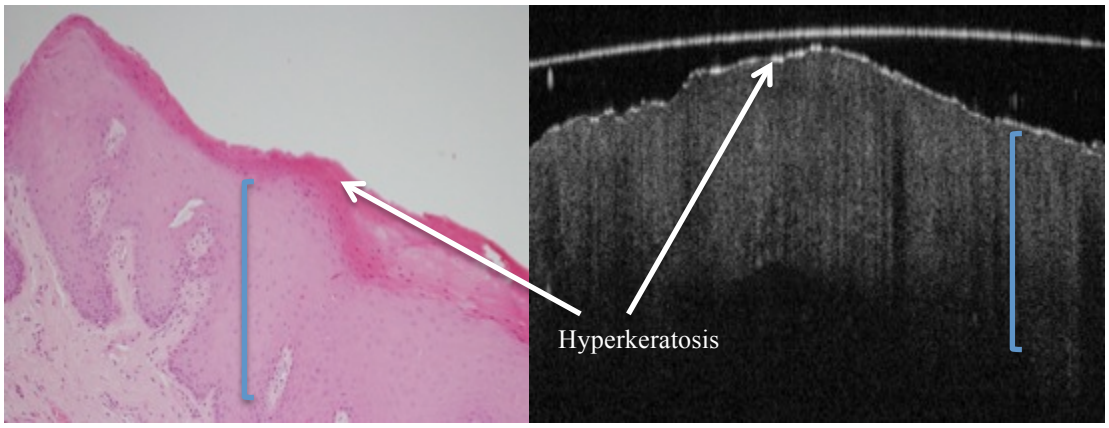

Figure (10.2) OCT & histology images disclose keratosis of a white lesion on buccal mucosa. One can also note epithelial hyperplasia (square bracket).

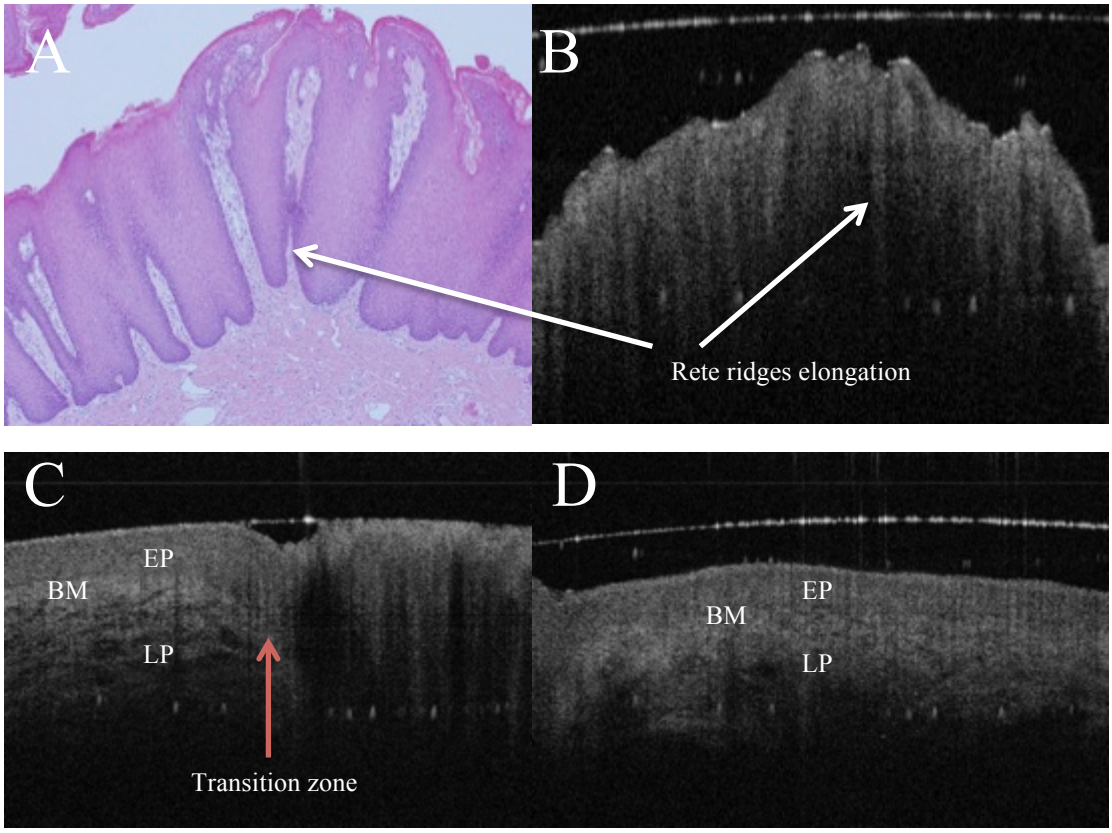

Figure (10.3) Histopathology of an elevated white lesion on left side lower lip revealed chronic hyperplastic candidiasis (**A**) with the characteristic finger-like projections of the epithelial layer, with the corresponding OCT image (**B**). Red arrow on OCT image shows transition zone from normal thickness epithelium toward the hyperplastic candidiasis (**C**), while image (**D**) is the contralateral normal side imaged to notice the disparity between normal and pathological side. BM= basement membrane; EP= epithelium; LP= lamina propria.

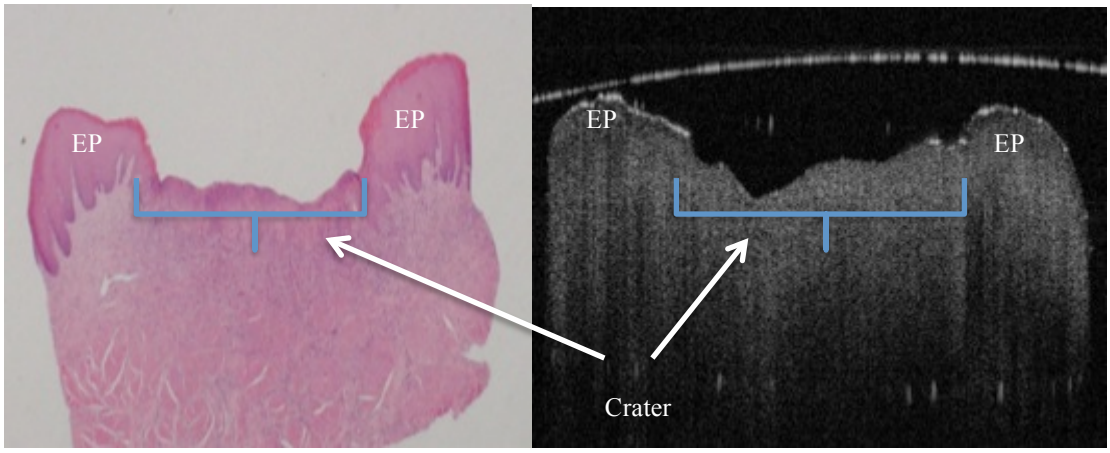

Figure (10.4) Histopathology diagnosis of an ulcer on lateral tongue revealed non-specific ulcer. Epithelial surface tissue disintegration can also be observed on the OCT image, which appears as depressed floor (crater) surrounded by edges that are sharply defined.

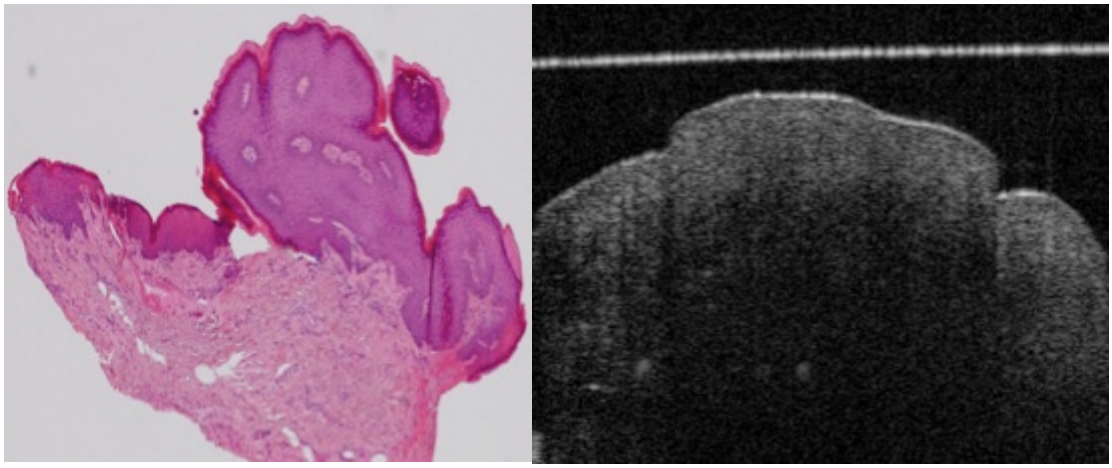

Figure (10.5) Histopathology and OCT images of a squamous papilloma on upper lip. Both images depict the papillary exophytic mass as a result of stratified squamous epithelium proliferation.

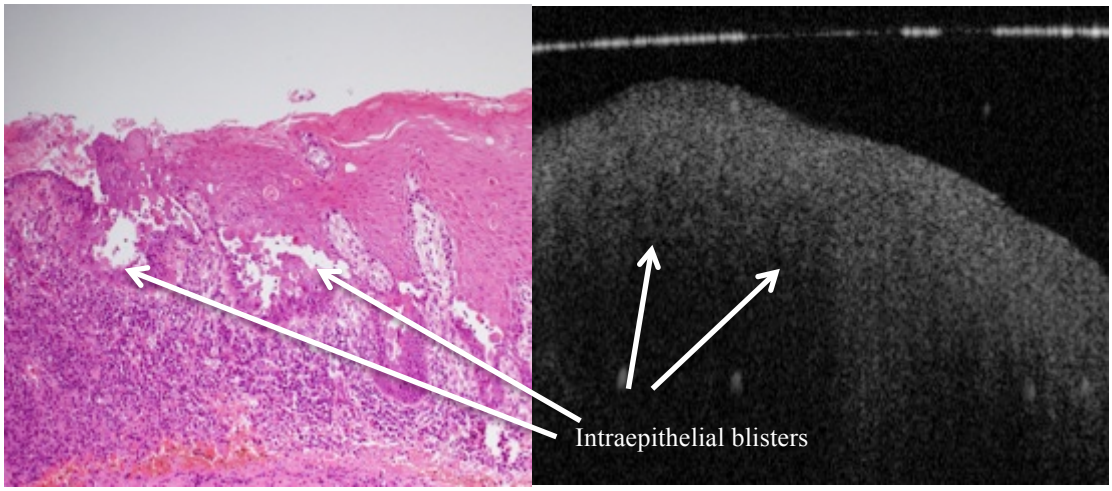

Figure (10.6) Histopathology and in vivo OCT images of a pemphigus vulgaris lesion on soft palate. Intraepithelial blisters (suprabasal split) that are filled with transudative fluid appear as dark (hyporeflective) structures in the OCT image.

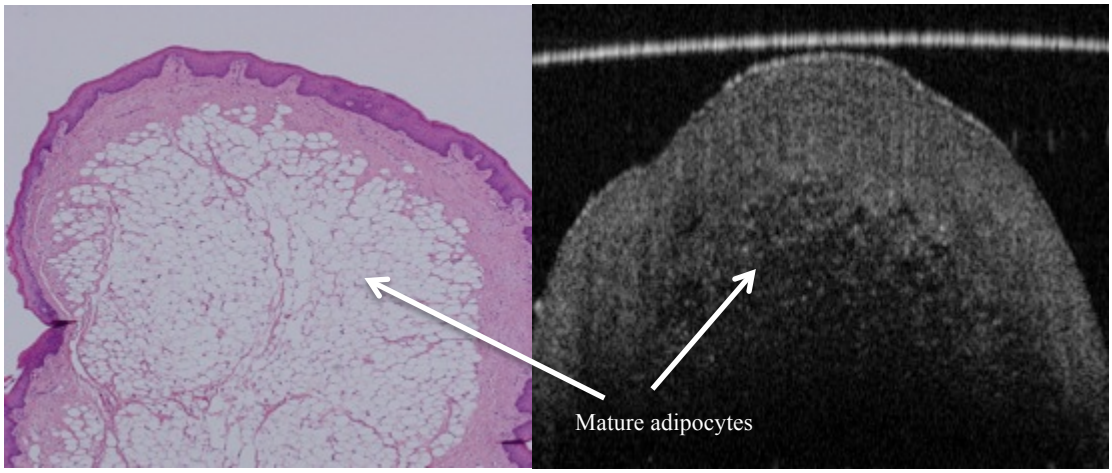

Figure (10.7) Histology and in vivo OCT images of a lipoma in floor of mouth. OCT image shows its diagnostic ability in detecting the adipocytes that appear as round/polygonal in shape and hyporeflective compared to the surrounding structures.

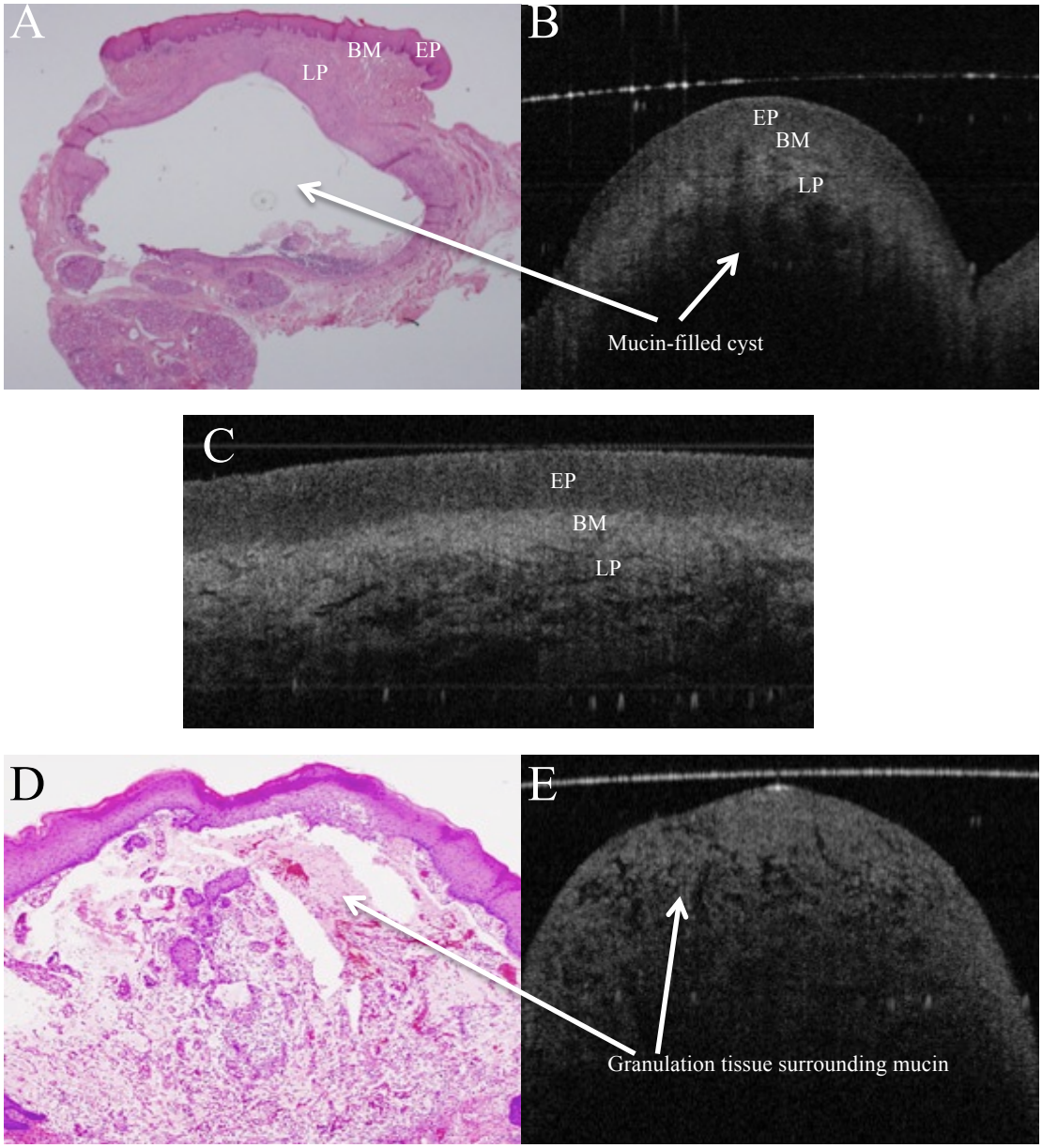

Figure (10.8) Histopathology slide and in vivo OCT image of a mucocoele (mucous retention cyst) on the lower lip (**A&B**). The non-scattering properties of mucin fluid rendered the cyst completely dark (hyporeflective). (**D&E**) Histology & in vivo OCT image of a mucous extravasation cyst that appears as mucin surrounded by granulation tissue. Image (**C**) represents the contralateral side (normal lower lip mucosa). In image (**E**), BM is imperceptible and the LP is non-homogeneous compared with the mucous retention cyst (this does not necessarily mean dysplasia or invasive carcinoma). BM= basement membrane; EP= epithelium; LP= lamina propria.

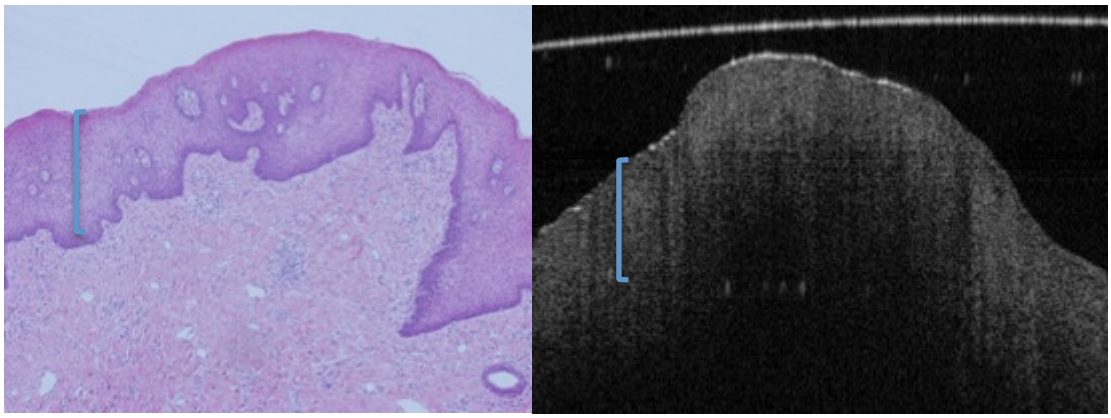

Figure (10.9) Histology picture and in vivo OCT image of a fibroepithelial hyperplasia on posterior dorsum tongue (with no dysplasia). The hyperplastic epithelium on OCT image (square bracket) might be misdiagnosed as mild/moderate dysplasia due to insufficient resolution of the image, when compared to gold standard histopathology, to visualise cellular atypia.

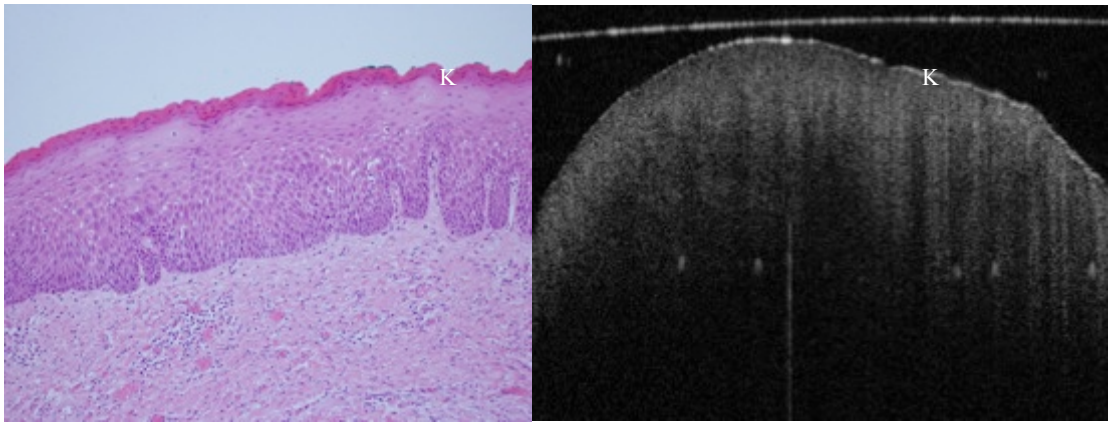

Figure (10.10) In vivo OCT image & histopathology picture of a white patch on posterior lateral tongue reveals keratosis & mild to moderate epithelial dysplasia. K= keratosis.

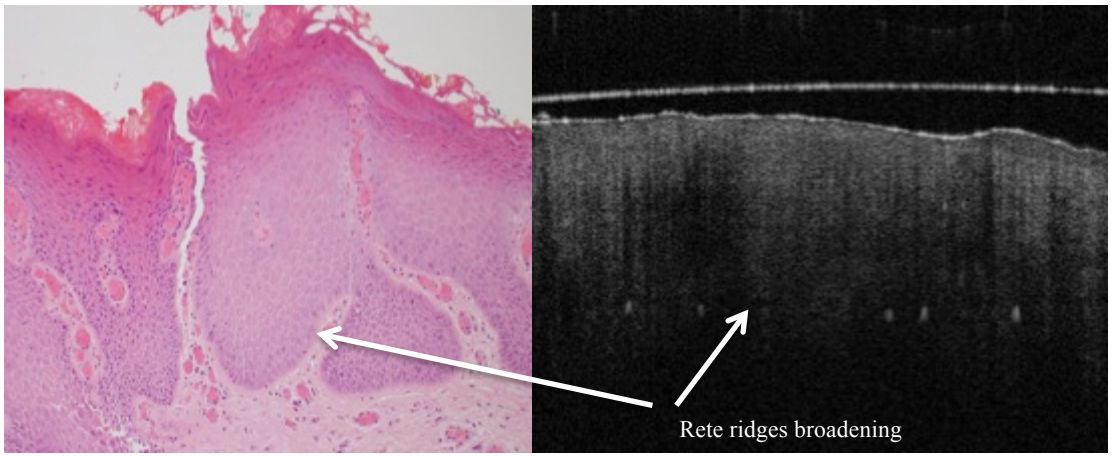

Figure (10.11) In vivo OCT image & histopathology slide divulge keratosis and moderate epithelial dysplasia of an erythroplakic lesion on anterior lateral tongue.

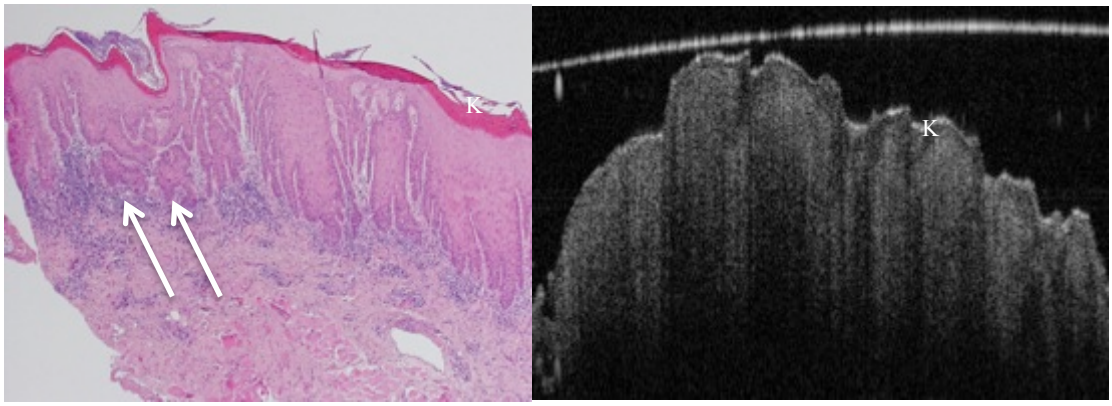

Figure (10.12) OCT (in vivo) & histopathology images reveal hyperkeratosis & severe epithelial dysplasia of a speckled leukoplakia on floor of mouth. Early invasive carcinoma (arrows) shown on histology cannot be visualised on the corresponding OCT image due to lack of sufficient depth of penetration as well as inferior image resolution compared to H&E slide.

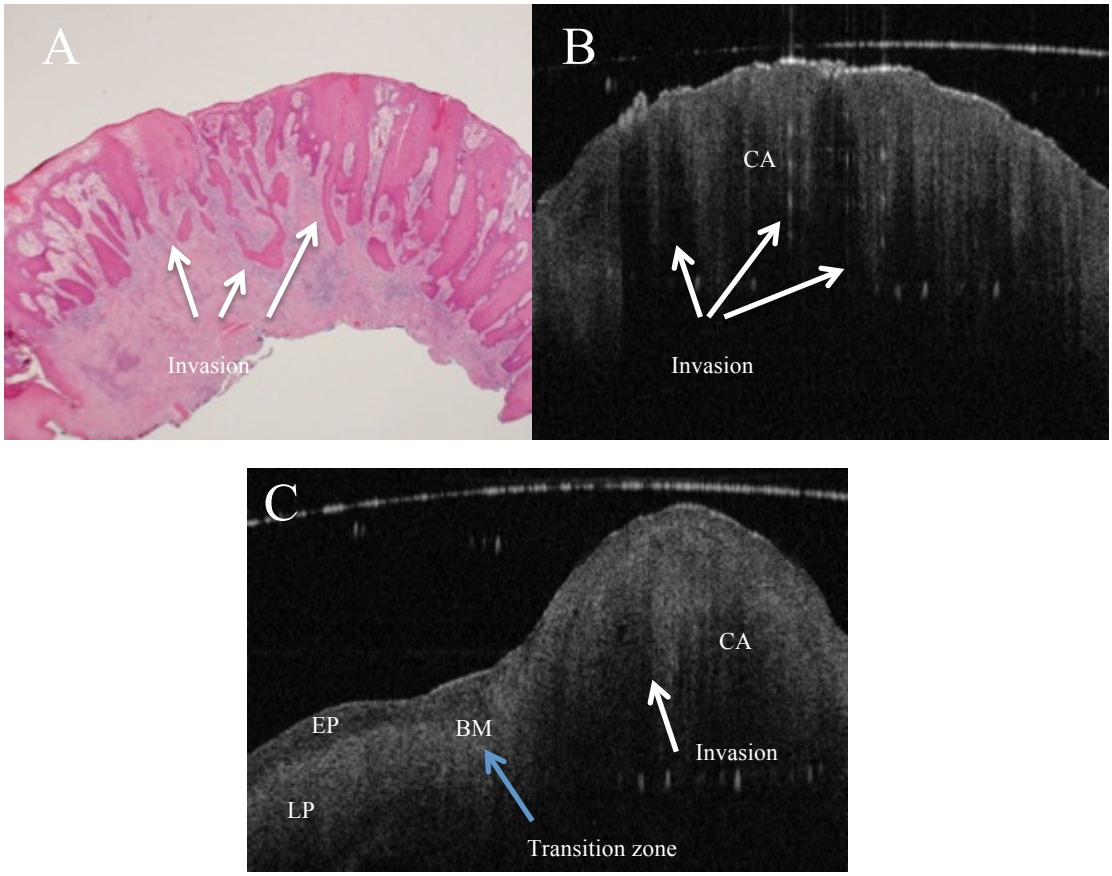

Figure (10.13) In vivo OCT & histopathology images (**A&B**) of an erythro-leukoplakic lesion on soft palate revealing multifocal carcinoma (CA). OCT image matches histopathology in displaying multifocal epithelial down growth and invasion into the subepithelial layers (white arrows). Furthermore, the basement membrane is indiscernible through the entire OCT scan as a coherent prominent landmark. The bottom image (**C**) is an in vivo OCT image of a transition zone (blue arrow) between healthy tissue & invasive carcinoma (CA) invading through the basement membrane. It also shows normal thickness stratified squamous epithelium, which is darker compared to the homogeneous lamina propria, while crossing the transition zone, epithelial downgrowth and invasion can be clearly recognised, and lamina propria become non-homogeneous. BM= basement membrane; EP= epithelium; LP= lamina propria; CA= invasive carcinoma.

10.5 Discussion

Existing techniques for diagnosis of premalignancy and malignancy of the oral cavity demand to be improved and amplified by better early recognition, monitoring and screening methods. A new non-invasive optical diagnostic method is required that would provides in situ and in real-time accurate and reliable diagnosis of cancers in the head and neck region including the oral cavity.

The results of the current prospective study revealed that in vivo OCT oral instrument imaging technique can produce cross-sectional, high-resolution in vivo images of epithelial and subepithelial layer architectural changes, recognising increase or decrease in both keratin cell layer and epithelial layer, changes in epithelial stratification and structure, detecting the status of basement membrane and the homogeneousness of lamina propria as well. The results of our prospective clinical work have demonstrated very good capability and applicability of in vivo OCT imaging to recognise and diagnose different suspicious benign and malignant lesions in different anatomical locations in the oral cavity with good intra- and inter-rater reliability.

OCT imaging procedure of the subjects recruited in the present study was uncomplicated, fast and well tolerated by all patients. Moreover, OCT imaging protocol resulted in addition of an extra 5-10 minutes to the duration of the patients visit. Accordingly, it will be well received identically by both clinicians and patients for introducing this non-invasive and in real-time OCT imaging modality to routine patient visits. Nonetheless, we encountered difficulties in scanning those lesions situated far posterior in the oral cavity, for instance posterior tongue, soft palate and so on due to pharyngeal (gag) reflex in some cases, which act as hindrance in capturing decent images. While in other cases, inaccessibility due to diametre and geometry of the newly introduced oral probe was the second obstacle in obtaining OCT images. We envisage that refinements in the oral probe such as reduced diametre and increased flexibility would significantly improve imaging in inaccessible anatomical locations and reduce the time spent on OCT scanning.

The good agreement between gold standard histopathology and OCT diagnosis for benign intraoral lesions, oral dysplastic and malignant lesions established in the present human prospective clinical in vivo OCT study matched data from previous animal and human OCT imaging researches (Matheny et al, 2003; Matheny et al, 2004; Wilder-Smith et al, 2004; Wilder-Smith et al, 2009b), where, Kappa value (inter-observer agreement) varied from 0.62-0.78, average sensitivity and specificity of OCT versus histology for both observers ranged from 79.9–93.6%. Many authors in numerous studies have investigated other existing non-invasive diagnostic procedures, mainly vital staining and oral brush cytology. They concluded that even though staining agents sensitivity, for example Toluidine blue, Tolonium chloride and Lugol iodine for oral cancer detection in the hands of experts usually approaches 90%, however, specificity of these agents is poor, falling quickly when non-experts, for instance screeners in field units, use this method (Silverman et al, 1984; Epstein et al, 1992; Onofre et al, 2001; Epstein et al, 2002; Epstein et al, 2003; Patton, 2003). In order to perform these examinations satisfactorily, sizeable clinical experience is essential to achieve that. Vis-à-vis Utilising oral brush biopsy samples as a non-invasive modality for diagnosis of oral cancer and precancer, a great deal of researchers have studies this method and reported moderate sensitivity levels between 70% to 90% for detecting intraoral epithelial dysplasia or invasive carcinoma, but with poor specificity ranged between 3–44%. The authors concluded that oral brush cytology approach is of inadequate diagnostic usefulness without reinforcement by biopsy procedure (Poate et al, 2004; Acha et al, 2005; Ogden et al, 1991; Sciubba, 1999; Nicholas et al, 1991; Rick & Slater, 2003; Rosin et al, 1997; Huang et al, 1999).

In a prospective, double-blinded study conducted by Isenberg et al (2005) to evaluate the accuracy of endoscopic OCT (EOCT) in the detection of dysplasia in 33 patients with Barrett's esophagus reported that their EOCT system accuracy was 78% in detecting the presence or absence of dysplasia with sensitivity of 68% and specificity of 82%. PPV was 53% and NPV was 89%. The diagnostic accuracy in the current investigation was much higher (91.6%) compared to Isenberg and associates' work, although dysplasia is different in the oesophagus compared with the oral cavity. The authors also recommended that additional modifications, including improved resolution and identifying more would-be OCT characteristics of dysplasia, are necessary before clinical application of EOCT.

In a more recent study performed by Wilder-Smith and colleagues (2009b), to investigate the clinical capability of non-invasive in vivo OCT for detecting intraoral precancerous/ cancerous lesions by recruiting 50 subjects with oral lesions, reported 93.1% for both sensitivity and specificity for detecting CIS or SCC versus non-cancer, while for detecting SCC versus all other pathologies, the sensitivity was 93.1% and specificity was 97.3%. The researchers concluded the excellent ability of in vivo OCT imaging technique in recognising and diagnosing intraoral premalignancy and malignancy in human subjects. The results in our study, which is very similar to the above study, indicates that our modified OCT system is as specific as Wilder-Smith et al's system, but the sensitivity was inferior.

Another recent immediate ex vivo prospective clinical research conducted by Hamdoon et al (2013), who analysed 125 patients with suspicious intraoral lesions including both benign and malignant lesions, to assess the OCT imaging technique on biopsy material in identifying potentially malignant and malignant lesions of the oral cavity. The results of their study showed that sensitivity was 85%, while specificity was 78% in assessing oral precancerous and cancerous lesions. The PPV and NPV were 86.5% and 77.5%, respectively and the accuracy of OCT was 82%. In comparison to our results, the OCT sensitivity, specificity and accuracy of their work were slightly inferior. We postulate that this could be due to the difference in the study design, where they scanned the suspicious tissues ex vivo, while we applied OCT in vivo to interrogate the dubious lesions. In addition, one of the most essential facts during in vivo OCT scanning of the lesions is that it will give clinicians the opportunity to utilise and scan the contralateral anatomical side to refer to it as a reference point, especially in the presence of slight or subtle change in the pathological side. Intraoperative (or in clinical setting) OCT visualisation of normal tissue when scanning doubtful lesions has a great significance in reaching the diagnosis more swiftly and also save time in both clinics or in operation theatre.

Finally, a group of researchers in a prospective clinical study analysed in vivo OCT to image 56 pathologic lesions (including leukoplakia, lichen planus and OSCC) in 43 patients with intraoral precancer and cancer lesions. The authors concluded excellent diagnostic accuracy of OCT in detecting benign and malignant neoplasm of the oral cavity with very good sensitivity (83%), specificity (98%), accuracy (81%) and substantial inter-rater reliability

(Kappa value= 0.76) (Fomina et al, 2004). The intraoral and oropharyngeal mucosae were studied using OCT system by Ridgway et al (2006) in 41 subjects during operative endoscopy, and captures OCT images was combined with endoscopic photography for gross and histologic image correlation. The authors found out that OCT images of the oral cavity and oropharynx have provided micro-anatomical information of epithelium, basement membrane, and lamina propria and displayed distinct zones of normal, altered, and ablated tissue microstructures for each pathologic process examined. Our current investigation also revealed similar findings observed by Fomina et al & Ridgway et al.

10.6 Conclusion

The robust agreement between diagnoses based on the OCT oral instrument and the gold standard histopathology shown in the present clinical study supports the notion that OCT is a practical technique for the early recognition, diagnosis and monitoring of intraoral lesions. Since the introduction of the technique into a wider clinical setting and as it experiences additional testing and optimisation, the OCT's primary usage might be to signal the need for biopsy. As the OCT technology is continuously evolving and undergoing refinements in terms of image contrast, resolution and improving depth of penetration, this imaging method could assists in gradual reduction of the need for biopsy, surgical margin delineation and offer evaluation/monitoring of the efficacy of malignancy treatments through regular follow-up visits.

Chapter 11

Suggestions

Chapter 11

Suggestions

Suggested further studies

1. Recruitment of a larger cohort age group population including older population (60-90 years) to measure the mean epidermal and epithelial thickness of skin and mucosa and to compare the differences in thickness between young and older age groups.

2. In vivo combined investigation of OCT with another biomedical optical imaging modality, such as high-frequency ultrasound (HFUS) in early recognition and detection of cutaneous/oral pre-malignancy/ malignancy and possible mapping of the lesions. Then consequent comparison of the accuracy of the above imaging modalities with the gold standard histology.

3. OCT oral instrument application in Mohs surgery prior to biopsy, i.e. in vivo scanning/ delineation of BCC lesion to study the practicability of OCT technique in clinical setting.

4. OCT guided PDT treatment of SCC in the facial region. Pre-PDT OCT scanning of the lesions undergoing treatment, re-scanning of the lesions post-PDT at 1, 3 and 6 month to monitor the effectiveness of the treatment.

5. In vivo OCT scanning of oral premalignant and malignant lesion margins before excisional biopsy under GA, followed by immediate ex vivo scanning of the biopsied tissue margins. After that, analyses of both in vivo and ex vivo OCT images of the lesion to compare any differences in terms of image quality and contrast, and consequently comparing the images with the gold standard histopathology.

References

References

Aalders, M.C., Triesscheijn, M., Ruevekamp, M., de Bruin, M., Baas, P., Faber, D.J., Stewart, F.A. (2006): Doppler optical coherence tomography to monitor the effect of photodynamic therapy on tissue morphology and perfusion. *J Biomed Opt* **11**(4): 044011.

Abnet, C.C., Kamangar, F., Islami, F., Nasrollahzadeh, D., Brennan, P., Aghcheli, K., et al. (2008) Tooth loss and lack of regular oral hygiene are associated with higher risk of esophageal squamous cell carcinoma. *Cancer Epidemiol Biomarkers Prev*, **17**(11): 3062–8.

Abramowitz, M., Spring, K.R., Keller, H.E., Davidson, M.W. (2002) Basic principles of microscope objectives. *Biotechniques*, **33**(4): 772-4, 776-8, 780-1.

Acha, A., Ruesga, M.T., Rodriguez, M.J., Martinez, de., Pancorbo, M.A., Aguirre, J.M. (2005): Applications of the oral scraped (exfoliative) cytology in oral cancer and precancer. *Oral Med Oral Pathol Oral Cir Bucal*, **10**(2): 95–102.

Adelstein, D.J., Lavertu, P., Saxton, J.P., et al (2000): Mature results of a phase III randomized trial comparing concurrent chemoradiotherapy with radiation therapy alone in patients with stage III and IV squamous cell carcinoma of the head and neck. *Cancer*, **88**: 876–883.

Alex, A., Považay, B., Hofer, B., Popov, S., Glittenberg, C., Binder, S., Drexler, W. (2010): Multispectral in vivo three-dimensional optical coherence tomography of human skin. *J Biomed Opt*, **15** (2):026025.

Almadori, G., Palidetti, G., Cerullo, M., Ottaviani, F., D'Alatri, L. (1990) Marijuana smoking as a possible cause of tongue carcinoma in young patients. *J Laryngol Otol*, **104**(11): 896-9.

Al-Rawi, N.H. & Talabani, N.G. (2008) Squamous cell carcinoma of the oral cavity: a case series analysis of clinical presentation and histological grading of 1,425 cases from Iraq. *Clin Oral Investig*, **12**(1): 15–8.

Altieri, A., et al. (2004) Wine, beer and spirits and risk of oral and pharyngeal cancer: a case-control study from Italy and Switzerland. *Oral Oncol*, **40**(9): 904-9.

Altintas, M.A., Altintas, A.A., Guggenheim, M., Niederbichler, A.D., Knobloch, K., Vogt, P.M. (2009): In vivo evaluation of histo-morphological alterations in first-degree burn injuries by means of confocal-laser-scanning microscopy more than ‘‘virtual histology?’’. *J Burn Care Res*, **30**(2): 315–320.

Ambrosch, P., Freudenberg, L., Kron, M., Steiner, W. (1996): Selective neck dissection in the management of squamous cell carcinoma of the upper digestive tract. *Eur Arch Otorhinolaryngol*, **253**:329–335.

American joint committee on cancer (AJCC)- cancer staging manual. 7th ed. Springer; 2010.
American Cancer Society (ACS). Cancer Facts and Figures. American Cancer Society Report, 1–4 (2008).

Andre, K., Schraub, S., Mercier, M., et al. (1995) Role of alcohol and tobacco in the aetiology of head and neck cancer: A case-control study in the Doubs region of France. *Oral Oncol Eur J Cancer*, **31**:301-309.

Andrea, M., Dias, O., Santos, A. (1995): Contact endoscopy during microlaryngeal surgery: a new technique for endoscopic examination of the larynx. *Ann Otol Rhinol Laryngol*, **104**: 333-339.

Annertz, K., et al. (2002): Incidence and survival of squamous cell carcinoma of the tongue in Scandinavia, with special reference to young adults. *Int J Cancer*, **101**(1): 95-9.

Arbustini, E., Grasso, M., Diegoli, M., et al. (1991): Coronary atherosclerotic plaques with and without thrombus in ischemic heart syndromes: A morphologic, immunohistochemical, and biochemical study. *Am J Cardiol*, 68: 36–50.

Arens, C., Glanz, H., Wönckhaus, J., Hersemeyer, K., Kraft, M. (2007): Histologic assessment of epithelial thickness in early laryngeal cancer or precursor lesions and its impact on endoscopic imaging. *Eur Arch Otorhinolaryngol*, 2007, **264**(6): 645-9.

Argiris, A. (2005): Induction chemotherapy for head and neck cancer: will history repeat itself? *J Natl Compr Canc Netw*, **3**(3): 393-403.

Arvidson-Bufano, U.B., Blank, L.W., Yellowitz, J.A. (1996): Nurses' oral health assessments of nursing home residents pre- and post-training: A pilot study. *Spec Care Dentist*, **16**:58-64.

Atlas of cancer in India. Available from: http://www.canceratlasindia.org/map.htm.

Axéll, T. & Rundquist, L. (1987) Oral lichen planus--a demographic study. *Community Dent Oral Epidemiol,* **15**(1): 52-6.

Axéll, T., Pindborg, J.J., Smith, C.J., et al. (1996) Oral white lesions with special reference to precancerous and tobacco-related lesions: Conclusions of an international symposium held in Uppsala, Sweden, May 18-21 1994. International Collaborative Group on Oral White Lesions. *J Oral Pathol Med*, **25**:49-54.

Aziz, S.R. (Spring 1997). "Oral submucous fibrosis: an unusual disease". *J N J Dent Assoc*, **68** (2): 17–9.

Aziz, S.R. (2010): Coming to America: betel nut and oral submucous fibrosis. *J Am Dent Assoc*, **141**(4): 423-8.

Bagan, J., Sarrion, G. & Jimenez, Y. (2010) Oral cancer: clinical features. *Oral Oncol*, **46**(6): 414-7.

Bagnardi, V., et al. (2001): A meta-analysis of alcohol drinking and cancer risk. *Br J Cancer*, **85**(11): 1700-5.

Balaram, P., Sridhar, H., Rajkumar, T., Vaccarella, S., Herrero, R., Nandakumar, A., Ravichandran, K., Ramdas, K., Sankaranarayanan, R., Gajalakshmi, V., Muñoz, N., Franceschi, S. (2002) Oral cancer in southern India: the influence of smoking, drinking, paan-chewing and oral hygiene. *Int J Cancer*. **98**(3):440-5.

Bánóczy, J. (1977) Follow-up studies in oral leukoplakia. *J Maxillofac Surg*, **5**:69-75.

Banoczy, J. & Squier, C. (2004): Smoking and disease. *Eur J Dent Educ*, 8(Suppl 4): 7–10.

Barbero, A.M. & Frasch, H.F. (2009) Pig and guinea pig skin as surrogates for human in vitro penetration studies: a quantitative review. *Toxicol In Vitro*, **23**(1): 1-13.

Barnes, L., Everson, J.W., Reichart, P., Sidransky, D., editors. (2005) Pathology and genetics of head and neck tumours. Lyon, France: IARC Press.

Basal Cell and Squamous Cell Skin Cancers. National Comprehensive Cancer Network, 2006. pp. BCC–2, BCC–3.

Bashkatov, N. A., Genina, E. A., Tuchin, V. V. (2011): Optical properties of skin, subcutaneous, and muscle tissues: A review. *Journal of Innovative Optical health Sciences,* **4** (1): 9-38.

Baumann, B., Götzinger, E., Pircher, M., Sattmann, H., Schütze, C., Schlanitz, F., Ahlers, C., Schmidt-Erfurth, U., Hitzenberger, C.K. (2010): Segmentation and quantification of retinal lesions in age-related macular degeneration using polarization- sensitive optical coherence tomography. *J Biomed Opt*, **15** (6): 061704.

Bedi, R. (1996): Betel quid and tobacco chewing among the United Kingdom's Bangladeshi community. In: The proceedings of the CRC/DoH symposium on cancer and minority ethnic groups. *Br J Cancer*, **74**(Suppl): 73–7.

Bechara, F.G., Gambichler, T., Stucker, M., Orlikov, A., Rotterdam, S., Altmeyer, P., Hoffmann, K. (2004): Histomorphologic correlation with routine histology and optical coherence tomography. *Skin Res Technol*, **10**(3): 169–173.

Bene, N.I., Healy, C., Coldiron, B.M. (2008): "Mohs micrographic surgery is accurate 95.1% of the time for melanoma in situ: a prospective study of 167 cases". *Dermatologic Surgery*, **34** (5): 660–4.

Bentkover, S.H., Grande, D.M., Soto, H., Kozlicak, B.A., Guillaume, D., Girouard, S. (2002): "Excision of head and neck basal cell carcinoma with a rapid, cross-sectional, frozen-section technique". *Archives of Facial Plastic Surgery*, **4** (2): 114–9.

Bernard, N.A., Scully, C., Everson, J.W., Cunnigham, S., Porter, S.R. (1993) Oral cancer development in patients with oral lichen planus. *J Oral Path Med*, **22**: 421-4.

Bernier, J. (2005): Alteration of radiotherapy fractionation and current chemotherapy: a new frontier in head and neck oncology? *Nat Clin Pract Oncol*, **2**: 305-14.

Berta, G.N., Mognetti, B., Spadaro, M., Trione, E., Amici, A., Forni, G., Carlo, F.D. and Cavallo, F. (2005) Anti-HER-2 DNA vaccine protects Syrian hamsters against squamous cell carcinomas. *British Journal of Cancer*, **93:**1250 –1256.

Black, R.J., Bray, F., Ferley, J., Parkin, D.M. (1997): Cancer incidence and mortality in the European Union: cancer registry data and estimates of national incidence for 1990. *Eur J Cancer*, **33**:1075–107.

Bland, J.M. & Altman, D.G. (1986) Statistical methods for assessing agreement between two methods of clinical measurement. *Lancet*, **1**(8476): 307-10.

Blank, L.W., Arvidson-Bufano, U.B., Yellowitz, J.A. (1996): The effect of nurses' background on performance of nursing home resident oral health assessments pre- and post-training. *Spec Care Dentist*, **16**: 65-70.

Bloching, M., Reich, W., Schubert, J., Grummt, T., Sandner, A. (2007): The influence of oral hygiene on salivary quality in the Ames test, as a marker for genotoxic effects. *Oral Oncol*, **43**(9): 933–9.

Blot, W.J., McLaughlin, J.K., Winn, D.M., et al. (1988): Smoking and drinking in relation to oral and pharyngeal cancer. *Cancer Res*, **48**:3282-3287.

Blot, W. (1992): Alcohol and cancer. *Cancer Research*, **1**; 52(7 Suppl): 2119-2123.

Blot, W. (1994) Oral and Pharyngeal cancers in Doll R (ed). Trends in Cancer Incidence and Mortality. Vol. 19/20, 23-42.Cancer Surveys.

Boccia, S., Cadoni, G., Sayed-Tabatabaei, F.A., et al. (2008) CYP1A1, CYP2E, GSTM1, GSTT1, EPHX1, exons 3 and 4, and NAT2 polymorphisms, smoking, consumption of alcohol and fruit and vegetables and risk of head and neck cancer. *J Cancer Res Clin Oncol*, **134**(1): 93-100.

Boffetta, P., Hecht, S., Gray, N. et al (2008): Smokeless tobacco and cancer. *Lancet Oncol***, 9**: 667-675.

Bolz, M., Ritter, M., Schneider, M., Simader, C., Scholda, C., Schmidt- Erfurth, U. (2009): A systematic correlation of angiography and high-resolution optical coherence tomography in diabetic macular oedema. *Ophthalmology*, **116** (1): 66–72.

Boonstra, H., Oosterhius, J.W., Oosterhuis, A.M., Fleuren, G.J. (1983): Cervical tissue shrinkage by formaldehyde fixation, paraffin wax embedding, section cutting and mounting. *Virchows Arch A Pathol Anat Hitospathol*, **402**:195-201.

Bouquot, J.E. & Gorlin, R.J. (1986): Leukoplakia, lichen planus, and other oral keratoses in 23,616 white Americans over the age of 35 years. *Oral Surg Oral Med Oral Pathol*, **61**:373-381.

Bouquot, J.E. & Meckstroth, R.L. (1998): Oral cancer in a tobacco-chewing U.S. population – no apparent increased incidence or mortality. *Oral Surg Oral Med Oral Pathol Oral Radiol Endod*, **86**:697-706.

Bouquot, J.E. & Whitaker, S.B. (1994) Oral leukoplakia— Rationale for diagnosis and prognosis of its clinical subtypes or "phases." *Quintessence Int*, **25**:133-140.

Bouma, B.E., Tearney, G.J., Yabushita, H., Shishkov, M., Kauffman, C.R., De Joseph Gauthier, D., MacNeill, B.D., Houser, S.L., Aretz, H.T., Halpern, E.F., Jang, I.K. (2003): Evaluation of intracoronary stenting by intravascular optical coherence tomography. *Heart*, **89** (3): 317– 320.

Bouma, B.E., Yun, S.H., Vakoc, B.J., Suter, M.J., Tearney, G.J. (2009): Fourier-domain optical coherence tomography: recent advances toward clinical utility. *Curr Opin Biotech*, **20** (1): 111–118.

Boyle, P., Macfarlane, G.J. and T.Z.et al. (1992): Recent advances in epidemiology of head and neck cancer. *Curr Opin Oncol*, **4**: 471-477.

Boyle, P. & Ferlay, J. (2005): Cancer incidence and mortality in Europe, 2004. *Ann Oncol*, **16**:481–8.

Bogdanov-Berezovsky, A., Rosenberg, L., Cagniano, E. & Silberstein, E. (2008): The role of frozen section histological analysis in the treatment of head and neck skin basal and squamous cell carcinomas. *Isr Med Assoc J*, **10**(5): 344-5.

Bonner, J.A., Harari, P.M., Giralt, J., Azarnia, N., Shin, D.M., Cohen, R.B., Jones, C.U., Sur, R., Raben, D., Jassem, J., Ove, R., Kies, M.S., Baselga, J., Youssoufian, H., Amellal, N., Rowinsky, E.K., Ang, K.K. (2006): Radiotherapy plus cetuximab for squamous-cell carcinoma of the head and neck. *N Engl J Med*, **354**: 567–578.

Bosetti, C., et al. (2008): Tobacco Smoking, Smoking Cessation, and Cumulative Risk of Upper Aerodigestive Tract Cancers. *Am J Epidemiol*, **167**(4): 468-73.

Bourhis, J., Calais, G., Eschwege, F. (1998): Chemoradiotherapy of carcinomas of the upper aerodigestive tract. *Cancer Radiother*, **2**: 679–688.

Branchet, M.C., Boisnic, S., Frances, C., Robert, A.M. (1990): Skin thickness changes in normal aging skin. *Gerontology*, **36**:28-35.

Brandizzi, D., Gandolfo, M., Velazco, M.L., Cabrini, R.L., Lanfranchi, H.E. (2008) Clinical features and evolution of oral cancer: a study of 274 cases in Buenos Aires, Argentina. *Med Oral Pathol Oral Cir Bucal,***13**: 544–8.

Bray, F., Sankila, R., Ferlay, J., Parkin, D.M. (2002): Estimates of cancer incidence and mortality in Europe in 1995. *Eur J Cancer*, **38**(1):99–166.

Brazil: Ministry of Health. Estimate 2008, Brazilian cancer incidence. Rio de Janeiro: National Cancer Institute (INCA); 2007.

Brezinski, M.E., Tearney, G.J., Bouma, B.E., Izatt, J.A., Hee, M.R., Swanson, E.A., Southern, J.F., Fujimoto, J.G. (1996a): Optical coherence tomography for optical biopsy: properties and demonstration of vascular pathology. *Circulation*, **93** (6): 1206–1213.

Brezinski, M.E., Tearney, G.J., Bouma, B.E., et al. (1996b): Imaging of coronary artery microstructure (in vitro) with optical coherence tomography. *Am J Cardiol*, **77**:92–93.

Brezinski, M.E., Tearney, G.J., Weissman, N.J., Boppart, S.A., Bouma, B.E., Hee, M.R., Weyman, A.E., Swanson, E.A., Southern, J.F., and Fujimoto, J.G. (1997): Assessing atherosclerotic plaque morphology: Comparison of optical coherence tomography and high frequency intravascular ultrasound. *Br Heart J*,**77**: 397- 404.

Brezinski, M.E., Saunders, K., Jesser, C., Li, X., Fujimoto, J.G. (2001): Index matching to improve optical coherence tomography imaging through blood. *Circulation*, **103**(15): 1999–2003.

Brezinski, M. (2002): Characterizing arterial plaque with optical coherence tomography. *Curr Opin Cardiol*, **17**: 648–655.

Brezinski, M.E. (2007): Applications of optical coherence tomography to cardiac and musculoskeletal diseases: bench to bedside? *J Biomed Opt*, **12** (5): 051705.

British Dental Association. BDA occasional paper No. 6. Opportunistic oral cancer screening; April 2000.

Brizel, D.M., Albers, M.E., Fisher, S.R., et al (1998): Hyperfractionated irradiation with or without concurrent chemotherapy for locally advanced head and neck cancer. *N Engl J Med*, **338**:1798–1804.

Brown, R.L., Suh, J.M., Scarborough, J.E., et al. (1965): Snuff dippers' intraoral cancer: Clinical characteristics and response to therapy. *Cancer*, **18**: 2-13.

Brown, D.M. & Regillo, C.D. (2007): Anti-VEGF agents in the treatment of neovascular age-related macular degeneration: applying clinical trial results to the treatment of everyday patients. *Am J Ophthalmol*, **144**(4): 627–637.

Brown, J.S., Blackburn, T.K., Woolgar, J.A., Lowe, D., Errington, R.D., Vaughan, E.D., Rogers, S.N. (2007): A comparison of outcomes for patients with oral squamous cell carcinoma at intermediate risk of recurrence treated by surgery alone or with post-operative radiotherapy. *Oral Oncol*, **43**: 764–773.

Burke, A.P., Farb, A., Malcom, G.T., et al. (1997): Coronary risk factors and plaque morphology in men with coronary disease who died suddenly. *N Engl J Med*, **336**: 1276–1282.

Cahill, R.A. & Mortensen, N.J. (2010): Intraoperative augmented reality for laparoscopic colorectal surgery by intraoperative near-infrared fluorescence imaging and optical coherence tomography. *Minerva Chir*, **65**(4): 451–462.

Calais, G., Alfonsi, M., Bardet, E., et al (1999): Randomised trial of radiation therapy versus concomitant chemotherapy and radiation therapy for advanced-stage oropharynx carcinoma. *J Natl Cancer Inst*, **91**: 2081-86.

Cancer in Wales 1995-2009: A comprehensive report. 2012.

Cancer Research Campaign (CRC)-Oral Cancer 2000.

Cancer Research Campaign. CancerStats. Oral cancer – UK. UK: CRC; April 2005.

Carpenter, J.M., Syms, M.J. & Sniezek, J.C. (2005) Oral carcinoma associated with betel nut chewing in the Pacific: an impending crisis? *Pac Health Dialog*, **12**(1):158-62.

Castellsague, X., et al. (2004): The role of type of tobacco and type of alcoholic beverage in oral carcinogenesis. *Int J Cancer*, **108**(5): 741-749.

Chang, T.S., Bressler, N.M., Fine, J.T., Dolan, C.W., Ward, J., Klesert, T.R., Marina, Study Group (2007): Improved vision-related function after ranibizumab treatment of neovascular age-related macular degeneration—results of a randomized clinical trial. Arch Ophthalmol, **125**(11): 1460–1469.

Chang, P.M., Teng, H.W., Chen, P.M., Chang, S.Y., Chu, P.Y., Tsai, T.L., et al. (2008): Methotrexate and leucovorin double-modulated 5-fluorouracil combined with cisplatin (MPFL) in metastatic/recurrent head and neck cancer. *J Chin Med Assoc*, **71**:336-41.

Chao, K.S., Majhail, N., Huang, C.J., et al. (2001):Intensity-modulated radiation therapy reduces late salivary toxicity without compromising tumor control in patients with oropharyngeal carcinoma: a comparison with conventional techniques. *Radiother Oncol*, **61**:275–280.

Chaturvedi, A.K., Engels, E.A., Anderson, W.F., Gillison, M.L. (2008): Incidence trends for human papillomavirus-related and -unrelated oral squamous cell carcinomas in the United States. *J Clin Oncol*, **26**:612-619.

Chen, J., Katz, R.V., & Krutchkoff, D.J. (1990): Intraoral squamous cell carcinoma. Epidemiologic patterns in Connecticut from 1935 to 1985. *Cancer*, **66**: 1288-96.

Chen, Z., Milner, T.E., Srinivas, S., Wang, X., Malekafzali, A., van Gemert, M.J., Nelson, J.S. (1997): Noninvasive imaging of in vivo blood flow velocity using optical Doppler tomography. *Opt Lett*, **22**(14): 1119–1121.

Chen, T.C., Cense, B., Park, B.H., Pierce, M.C., de Boer, J.F. (2004): Polarization sensitive optical coherence tomography measurement of thickness and birefringence of healthy retinal nerve fibre layer tissue. *Invest Ophth Vis Sci*, **45** (Suppl 2):U114.

Chen, C.H., Hsu, M.Y., Jiang, R.S., Wu, S.H., Chen, F.J., Liu, S.A. (2012): Shrinkage of head and neck cancer specimens after formalin fixation. *J Chin Med Assoc*., **75**(3): 109-13.

Chiu, C.J., Chang, M.L., Chiang, C.P., Hahn, L.J., Hsieh, L.L., Chen, C.J. (2002): Interaction of collagen-related genes and susceptibility to betel quid- induced oral submucous fibrosis. *Cancer Epidemiol Biomarkers Prev*, **11**(7): 646-653.

Choma, M., Sarunic, M., Yang, C., Izatt, J. (2003): Sensitivity advantage of swept source and Fourier domain optical coherence tomography. *Opt Express*, **11**(18): 2183–2189.

Chu, C.R., Izzo, N.J., Irrgang, J.J., Ferretti, M., Studer, R.K. (2007): Clinical diagnosis of potentially treatable early articular cartilage degeneration using optical coherence tomography. *J Bio- med Opt*, **12** (5):051703.

Cnattingius, S., Galanti, R., Grafstrom, R., Hergens, M.P., Nyren, O., Pershagen, G., editors. Karolinska institute. (2005): Health risks from Swedish snuff, 1–95.

Cogliano, V., et al. (2004) Smokeless tobacco and tobacco-related nitrosamines. *Lancet Oncol*, **5**(12): 708.

Cogliano, V.J., Baan, R., Straif, K., et al. (2011) Preventable exposures associated with human cancers. *J Natl Cancer Inst*, **103**(24): 1827-39

Cohen, E.E., Lingen, M.W. & Vokes, E.E. (2004): The expanding role of systemic therapy in head and neck cancer. *J Clin Oncol*, **22**: 1743-52.

Cole, D., Patel, P. & Matar, J. (1994): Floor of mouth cancer. *Arch Otolaryngol Head Neck Surg*, **120**:260–263.

Collier, T., Lacy, A., Richards-Kortum, R., Malpica, A., Follen, M. (2002): Near real-time confocal microscopy of amelanotic tissue: detection of dysplasia in *ex vivo* cervical tissue. *Academic Radiol.*, **9***:* 504-512.

Collier, T., Shen, P., de Pradier, B., Richards-Kortum, R. (2000): Near real time confocal microscopy of amelanotic tissue: dynamics of aceto-whitening enable nuclear segmentation. *Optics Express*, **6***:* 40-48.

Connolly, S.M., Baker, D.R., Coldiron, B.M., *et al.*(2012): "AAD/ACMS/ASDSA/ASMS 2012 appropriate use criteria for Mohs micrographic surgery: a report of the American Academy of Dermatology, American College of Mohs Surgery, American Society for Dermatologic Surgery Association, and the American Society for Mohs Surgery". *Journal of the American Academy of Dermatology*, **67** (4): 531–50.

Conway, D., Macpherson, L.M.D., Warnakulasuriya, K.A.A.S., Ogden, G., Stockton, D.L.(2006): Incidence of oral and oropharyngeal cancer in the United Kingdom (1990– 1999) – current status, recent trends and intercountry comparisons. *Oral Oncol*, **42**:586–92.

Cooper, J.S., Pajak, T.F., Forastiere, A.A., Jacobs, J., Campbell, B.H., Saxman, S.B., Kish, J.A., Kim, H.E., Cmelak, A.J., Rotman, M., Machtay, M., Ensley, J.F., Chao, K.S., Schultz, C.J., Lee, N., Fu, K.K. (2004): Postoperative concurrent radiotherapy and chemotherapy for high-risk squamous-cell carcinoma of the head and neck. *N Engl J Med*, **350**(19): 1937-44.

Cooper, J.S., Pajak, T.F., Forastiere, A.A., Jacob, J., Campbell, B.H., Saxman, SB, Kish, JA, Kim, HE, Cmelak, AJ, Rotman, M., Machtay, M., Ensley, J.F., Chao, KS, Schultz CJ, LEE, N, Fu, KK. (2006): Long-term survival results of a phase III intergroup trial (RTOG 95-01) of surgery followed by radiotherapy vs. radiotherapy for resectable high risk squamous cell carcinoma of the head and neck. Annual Meeting of the American Society for Therapeutic Radiology and Oncology (ASTRO); Philadelphia, USA; Nov 5-6.

Cooper, J.S., Porter, K., Mallin, K., et al. (2009) National Cancer Database report on cancer of the head and neck: 10-year update. *Head Neck*, **31**:748–758.

Corcuff, P., Bertrand, C., Leveque, J.L. (1993): Morphometry of human epidermis in vivo by real-time confocal microscopy. *Arch Dermatol Res*, **285**:475-81.

Cox, S.C. & Walker, D.M. (1996): "Oral submucous fibrosis a review". *Aust Dent J. London*, **41** (5): 294–9.

Cruz, G.D., Le Geros, R.Z., Ostroff, J.S., Hay, J.L., Kenigsberg, H., Franklin, D.M. (2002): Oral cancer knowledge, risk factors and characteristics of subjects in a large oral cancer screening program. *J Am Dent Assoc*, **133**:1064-71.

Danaei, G,, Vander Hoorn, S., Lopez, A.D., Murray, C., Ezzati, M. (2005): Comparative Risk Assessment collaborating group (Cancers). Causes of cancer in the world: comparative risk assessment of nine behavioural and environmental risk factors. *Lancet*, **366**:1784-1793.

Davidson, B.J., Kulkarny, V., Delacure, M.D. & Shah, J.P. (1993): Posterior triangle metastases of squamous cell carcinoma of the upper aerodigestive tract. *Am J Surg*, **166**: 395–398.

Dauendorffer, J.N., Bastuji-Garin, S., Gue´ro, S., Brousse, N., Fraitag, S. (2009): Shrinkage of skin excision specimens: formalin fixation is not the culprit. *Br J Dermatol*, **160**:810-4.

Davies, M.J., Richardson, P.D., Woolf, N., et al. (1993): Risk of thrombosis in human atherosclerotic plaques: Role of extracellular lipid, macrophage, and smooth muscle cell content. *Br Heart J*, **69**:377–381.

Day, T.A., Davis, B.K., Gillespie, M.B., Joe, J.K., Kibbey, M., Martin-Harris, B., Neville, B., Richardson, M.S., Rosenzweig, S., Sharma, A.K., Smith, M.M., Stewart, S., Stuart, R.K. (2003): Oral cancer treatment. *Curr Treat Options Oncol*, **4**(1):27-41.

de Boer, J.F., Cense, B., Park, B.H., Pierce, M.C., Tearney, G.J., Bouma, B.E. (2003): Improved signal-to-noise ratio in spectral-domain compared with time-domain optical coherence tomography. *Opt Lett*, **28**(21): 2067–2069.

DeCoro, M., Wilder-Smith, P. (2010): Potential of optical coherence tomography for early diagnosis of oral malignancies. *Expert Rev Anticancer Ther*, **10**(3): 321-9.

DeLancey, J.O., Thun, M.J., Jemal, A., Ward,E.M. (2008): Recent trends in Black-White dispar- ities in cancer mortality. *Cancer Epidemiol Biomarkers Prev*, **17**:2908-2912.

Denoix, P.F. (1946): Enquete permanent dans les centre santi cancereaux. *Bull Inst Nat Hyg*, **1**:70–5.

de Veld, D.C., Skurichina, M., Witjes, M.J., Duin, R.P., Sterenborg, H.J., Roodenburg, J.L. (2005a): Autofluorescence and diffuse reflectance spectroscopy for oral oncology. *Lasers Surg Med*, **36**:356-364.

de Veld, D.C., Bakker Schut, T.C., Skurichina, M., Witjes, M.J., Van der Wal, J.E., Roodenburg, J.L., Sterenborg, H.J. (2005b): Autofluorescence and Raman microspectroscopy of tissue sections of oral lesions. *Lasers Med Sci*, **19**:203-209.

de Veld, D.C., Witjes, M.J., Sterenborg, H.J., Roodenburg, J.L. (2005c): The status of *in vivo* autofluorescence spectroscopy and imaging for oral oncology. *Oral Oncol*, 2005c; **41**:117-131.

de Visscher, J.G., Bouwes Bavinck, J.N., van der Waal, I. (1997) Squamous cell carcinoma of the lower lip in renal-transplant recipients. Report of six cases. *Int J Oral Maxillofac Surg*, **26**:120-123.

Dhingra, N., Gajdasty, A., Neal, J.W., Mukherjee, A.N., Lane, C.M. (2007): "Confident complete excision of lid-margin BCCs using a marginal strip: an alternative to Mohs' surgery". *The British Journal of Ophthalmology*, **91** (6): 794–6.

Diaz-Sandoval, L.J., Bouma, B.E., Tearney, G.J., Jang, I.K. (2005): Optical coherence tomography as a tool for percutaneous coronary interventions. *Catheter Cardiovasc Interv*, **65**(4): 492–496.

Di Lullo, G.A., Sweeney, S.M., Korkko, J., Ala-Kokko, L., San Antonio, J.D. (2002) Mapping the ligand-binding sites and disease-associated mutations on the most abundant protein in the human, type I collagen. *J Biol Chem*, **277**(6): 4223-31.

Donald, P.J. (1986) Marijuana smoking-possible cause of head and neck carcinoma in young patients. *Otolaryngol Head Neck Surg*, **94**: 517-521.

Donnelly, D.W., Gavin, A.T. and Comber, H. (2009): Report. Northern Ireland Cancer Registry/National Cancer Registry, Ireland.

Doors, M., Berendschot, T.T.J.M., de Brabander, J., Webers, C.A.B., Nuijts, R.M.M.A. (2010): Value of optical coherence tomography for anterior segment surgery. *J Cataract Refr Surg*, **36** (7): 1213–1229.

Drexler, W. et al (1999): In vivo ultrahigh-resolution optical coherence tomography. *Optics Lett*, **24**, 1221–1223.

Drexler, W., Morgner, U., Ghanta, R.K., Kärtner, F.X., Schuman. J.S., Fujimoto, J.G. (2001): Ultrahigh-resolution ophthalmic optical coherence tomography. *Nat Med*, **7**(4): 502–507.

Drexler, W. (2004): Ultrahigh-resolution optical coherence tomography. *J Biomed Opt*, **9**(1): 47–74.

Drexler, W., Andersen, P.E. (2009): Optical coherence tomography in biophotonics. *J Biophotonics*, **2**(6–7): 339–341.

D'Souza, G., Kremier, A.R., Viscidi, R., Pawlita, M., Fakhry, C., Koch, W.M., et al. (2007): Case control study of human papillomavirus and oropharyngeal cancer. *New Eng J Med*, **356**:1944–56.

D'Souza, G., Agrawal, Y., Halpern, J., Bodison, S., Gillison,M.L. (2009): Oral sexual behaviors associated with prevalent oral human papillomavirus infection. *J Infect Dis*, **199**: 1263-1269.

Dye, B.A., Wang, R., Lashley, R., Wei, W., Abnet, C.C., Wang, G., et al. (2007) Using NHANES oral health examination protocols as part of an esophageal cancer screening study conducted in a high-risk region of China. *BMC Oral Health*, **17**:7–10. 11.

Edge, S.B., Byrd, D.R., Compton, C.C., Fritz, A.G., Greene, F.L., Trotti, A., editors. (2009): AJCC cancer staging manual. 7th ed. Chicago, IL: Springer.

Edwards, D.M., Jones, J. (1999): Incidence of and survival from upper aerodigestive tract cancers in the UK: the influence of deprivation. *Eur J Cancer*, **35**:968–72.

Einhorn, J. & Wersäll, J. (1967) Incidence of oral carcinoma in patients with leukoplakia of the oral mucosa. *Cancer*, **20**:2189-2193.

Eisen, D. (2002) The clinical features, malignant potential and systemic associations of oral lichen planus: a study of 723 patients. *J Am Acad Dermatol*, **46**: 207-214.

Epstein, J., Scully, C., Spinelli, U. (1992): Toluidine blue and Lugol's iodine solution for the assessment of oral malignant disease and lesions at risk of malignancy. *J Oral Pathol Med*, **21**:160–163.

Epstein, J.B., Zhang, L., Rosin, M. (2002): Advances in the diagnosis of oral premalignant and malignant lesions. *J Can Dent Assoc*, **68**(10): 617–621.

Epstein, J.B., Feldman, R., Dolor, R.J., Porter, S.R. (2003): The utility of tolonium chloride rinse in the diagnosis of recurrent or second primary cancers in patients with prior upper aerodigestive tract cancer. *Head Neck*, **25**: 911-921.

Epstein, J.B., Gorsky, M., Lonky, S., Silverman, S. Jr., Epstein, J.D., Bride, M. (2006): The efficacy of oral lumenoscopy (ViziLite) in visualizing oral mucosal lesions. *Spec Care Dentist* 2006, **26**:171-174.

Epstein, J.B., Sciubba, J., Silverman, S., Sroussi, H.Y. (2007): Utility of toluidine blue in oral premalignant lesion and squamous cell carcinoma: continuing research and implications for clinical practice. *Head Neck*, **29**:948–58.

Epstein, J.B., Silverman, S. Jr., Epstein, J.D., Lonky, S.A., Bride, M.A. (2008): Analysis of oral lesion biopsies identified and evaluated by visual examination, chemiluminescence and toluidine blue. *Oral Oncol*, **44**:538-544.

Fan, C., Wang, Y., Wang, R.K. (2007): Spectral domain polarization sensitive optical coherence tomography achieved by single camera detection. *Opt Express*, **15**(13): 7950–7961.

Farah, C.S. & McCullough, M.J. (2007): A pilot case control study on the efficacy of acetic acid wash and chemiluminescent illumination (ViziLite trade mark) in the visualisation of oral mucosal white lesions. *Oral Oncol,* **43**:820-824.

Farb, A., Burke, A.P., Tang, A.L., et al. (1996): Coronary plaque erosion without rupture into a lipid core. A frequent cause of coronary thrombosis in sudden coronary death. *Circulation*, **93**:1354–1363.

Farrell, T.J., Patterson, M.S., Wilson, B. (1992): A diffusion theory model of spatially resolved, steady-state diffuse reflectance for the non-invasive determination of tissue optical properties in vivo. *Med. Phys*, **19**(4): 879–888.

Fedele, S. (2009): Diagnostic aids in the screening of oral cancer. *Head Neck Oncol*, **1**:5.

Feller, L., Altini, M., Slabbert, H. (1991) Pre-malignant lesions of the oral mucosa in a South African sample: A clinicopathologic study. *J Dent Assoc South Africa*, **46**:261-265.

Fercher, A.F., Roth, E. (1986): Ophthalmic laser interferometry. In: Proceedings of the SPIE—The International Society for Optical Engineering, **658**, 48–51.

Fercher, A.F., Mengedoht, K., Werner, W. (1988): Eye-length measurement by interferometry with partially coherent light. *Opt Lett*, **13**(3): 186–8.

Fercher, A.F., Hitzenberger, C.K., Drexler, W., Kamp, G., Sattmann, H. (1993): In vivo optical coherence tomography. *Am J Ophthalmol*, **116**(1): 113–114.

Fercher, A.F. (1996): Optical coherence tomography. *J. Biomed. Opt*, **1**: 157–173.

Ferlay, J., Pisani, P., Parkin, D.M. (2004): GLOBOCAN 2002. Cancer incidence, mortality and prevalence worldwide. IARC Cancer Base (2002 estimates). Lyon: IARC Press.

Fettig, A., Pogrel, M.A., Silverman, S. Jr., et al. (2000) Proliferative verrucous leukoplakia of the gingiva. *Oral Surg Oral Med Oral Pathol Oral Radiol Endod*, **90**:723-730.

Flaitz, C.M., Nichols, C.M., Adler-Storthz, K., et al. (1995) Intraoral squamous cell carcinoma in human immunodeficiency syndrome virus infection. A clinicopathologic study. *Oral Surg Oral Med Oral Pathol Oral Radiol Endod*, **80**: 55-62.

Flaitz, C.M. & Silverman, S. Jr. (1998) Human Immunodeficiency Virus (HIV)-Associated Malignancies. In Silverman S Jr (ed). Oral Cancer, 4th ed. Hamilton, Ontario, Canada: BC Decker, Inc;165-170.

Flaitz, C.M., Nichols, C.M., Walling, D.M., Hicks, M.J. (2002): Plasmoblastic lymphoma: an HIV-associated entity with primary oral manifestation. *Oral Oncol*, **38**(1) 96-102.

Fomina, Iu.V., Gladkova, N.D., Leont'ev, V.K., Urutina, M.N., Gazhva, S.I., Snopova, L.B., Gelikonov, V.M., Kamenskiĭ,V.A. (2004): Optical coherence tomography in the evaluation of the oral cavity mucosa. Part II. Benign and malignant diseases. *Stomatologiia (Mosk)*, **83**(4): 25-32.

Forastiere, A.A. (1992): Chemotherapy of head and neck cancer. *Ann Oncol*, **3**(Suppl 3): 11–14.

Forsea, A.M., Carstea, E.M., Ghervase, L., Giurcaneanu, C., Pavelescu, G. (2010): Clinical application of optical coherence tomography for the imaging of non-melanocytic cutaneous tumours: a pilot multi-modal study. *J Med Life*, **3**(4): 381–389.

Fox, M. (2002): *Optical Properties of Solids*. Oxford University Press, USA. ISBN 0-19-850612-0.

Franceschi, S., Favero, A., Conti, E., Talamini, R., Negri, E. (1991) Food groups, oils and butter, and cancer of the oral cavity and pharynx. *British Journal of Cancer*, **80**(3): 614-620.

Franceschi, S., Levi, F., La Vecchia, C., Conti, E., Dal Maso, L., Barzan, L., et al. (1999) Comparison of the effect of smoking and alcohol drinking between oral and pharyngeal cancer. *Int J Cancer*, **83**: 1-4.

Freedman, N.D, et al. (2008): Fruit and vegetable intake and head and neck cancer risk in a large United States prospective cohort study. *Int J Cancer*, **122**(10): 2330-6.

Frisch, M. and Biggar, R.J. (1999) Aetiological parallel between tonsillar and anogenital squamous cell carcinomas. *Lancet*, **354**(9188): 1442-3.

Fujimoto, J.G., Boppart, S.A., Tearney, G.J., Bouma, B.E., Pitris, C., Brezinski, M.E. (1999): High resolution in vivo intra-arterial imaging with optical coherence tomography. *Heart*, **82**(2): 128–133.

Fujimoto, J.G., Pitris, C., Boppart, S.A., Brezinski, M.E. (2000): Optical coherence tomography: an emerging technology for biomedical imaging and optical biopsy. *Neoplasia*, **2**(1-2): 9-25.

Fujimoto, J.G. (2003): Optical coherence tomography for ultrahigh resolution in vivo imaging. *Nat Biotechnol*, **21**(11): 1361–1367.

Gambichler, T., Huyn, J., Tomi, N.S., Moussa, G., Moll, C., Sommer, A., Altmeyer, P., Hoffmann, K. (2006a): A comparative pilot study on ultraviolet-induced skin changes assessed by non-invasive imaging techniques in vivo. *Photochem Photobiol*, **82** (4): 1103–1107.

Gambichler, T., Matip, R., Moussa, G., et al. (2006b): In vivo data of epidermal thickness evaluated by optical coherence tomography: effects of age, gender, skin type, and anatomic site. *J Dermatol Sci*, **44**: 145–152.

Gambichler, T., Moussa, G., Bahrenberg, K., Vogt, M., Ermert, H., Weyhe, D., Altmeyer, P., Hoffmann, K. (2007a): Preoperative ultrasonic assessment of thin melanocytic skin lesions using a 100-MHz ultrasound transducer: a comparative study. *Dermatol Surg*, **33**(7): 818–824.

Gambichler, T., Moussa, G., Regeniter, P., Kasseck, C., Hofmann, M.R., Bechara, F.G., Sand, M., Altmeyer, P., Hoffmann, K. (2007b): Validation of optical coherence tomography in vivo using cryostat histology. *Phys Med Biol*, **52**(5): N75–N85.

Gambichler, T., Regeniter, P., Bechara, F.G., Orlikov, A., Vasa, R., Moussa, G., Stücker, M., Altmeyer, P., Hoffmann, K. (2007c): Characterization of benign and malignant melanocytic skin lesions using optical coherence tomography in vivo. *J Am Acad Dermatol*, **57**(4): 629–637.

Gambichler, T., Orlikov, A., Vasa, R., Moussa, G., Hoffmann, K., Stücker, M., Altmeyer, P., Bechara, F.G. (2007d): In vivo optical coherence tomography of basal cell carcinoma. *J Dermatol Sci*, **45**(3): 167–173.

Gambichler, T., Jaedicke, V., Terras, S. (2011): Optical coherence tomography in dermatology: technical and clinical aspects. *Arch Dermatol Res*, **303**(7): 457-73.

Gandolfo, S., Pentenero, M., Broccoletti, R., Pagano, M., Carrozzo, M., Scully, C. (2006): Toluidine blue uptake in potentially malignant oral lesions in vivo: clinical and histological assessment. *Oral Oncol*, **42**:89-95.

Garavello, W., Giordano, L., Bosetti, C., Talamini, R., Negri, E., Tavani, A., Maisonneuve, P., Franceschi, S., La Vecchia, C1. (2008) Diet diversity and the risk of oral and pharyngeal cancer. *Eur J Nutr*, **47**(5): 280-284.

Garavello, W., Bertuccio, P., Levi, F., et al. (2010): The oral cancer epidemic in central and eastern Europe. *Int J Cancer*, **127**: 160-171.

Gardner, E.S., Sumner, W.T., Cook, J.L. (2001): Predictable tissue shrinkage during frozen section histopathologic processing for Mohs micrographic surgery. *Dermatol Surg*, **27**: 813.

Garrote, L.F., Herrero, R., Reyes, R.M.O., et al. (2001): Risk factors for cancer of the oral cavity and oro-pharynx in Cuba. *Br J Cancer*, 2001; **85**:46–54.

Gaucher, D., Sebah, C., Erginay, A., Haouchine, B., Tadayoni, R., Gaudric, A., Massin, P. (2008): Optical coherence tomography features during the evolution of serous retinal detachment in patients with diabetic macular oedema. *Am J Ophthalmol*, **145** (2): 289–296.

Giattina, S.D., Courtney, B.K., Herz, P.R., Harman, M., Shortkroff, S., Stamper, D.L., Liu, B., Fujimoto, J.G., Brezinski, M.E. (2006): Assessment of coronary plaque collagen with polarization sensitive optical coherence tomography (PS-OCT). *Int J Cardiol*, **107**(3): 400–409.

Gilgen, H.H., Novak, R.P., Salathe, R.P., Hodel, W. & Beaud, P. (1989): Submillimetre optical reflectometry. *IEEE J Lightwave Technol*, **7**:1225–1233.

Gillenwater, A., Jacob, R., Ganeshappa, R., Kemp, B., El-Naggar, A.K., Palmer, J.L., Clayman, G., Mitchell, M.F., Richards-Kortum, R. (1998a): Non-invasive diagnosis of oral neoplasia based on fluorescence spectroscopy and native tissue autofluorescence. *Arch Otolaryngol Head Neck Surg*, **124**:1251-1258.

Gillenwater, A., Jacob, R., Richards-Kortum, R. (1998b): Fluorescence spectroscopy: A technique with potential to improve the early detection of aerodigestive tract neoplasia. *Head Neck*, **20**:556-562.

Gillison, M.L. (2004) Human papillomavirus-associated head and neck cancer is a distinct epidemiologic, clinical, and molecular entity. *Semin Oncol*, 2004. **31**(6): 744-54.

Gillison, M.L. & Shah, K.V. (2011) Human papillomavirus-associated head and neck squamous cell carcinoma: Mounting evidence for an etiologic role for human papillomavirus in a subset of head and neck cancers. *Curr Opin Oncol*, **13**:183-188.

Gladkova, N.D., Petrova, G.A., Nikulin, N.K., Radenska-Lopovok, S.G., Snopova, L.B., Chumakov, Y.P., Nasonova, V.A., Gelikonov, V.M., Gelikonov, G.V., Kuranov, R.V., Sergeev, A.M., Feldchtein, F.I. (2000): In vivo optical coherence tomography imaging of human skin: norm and pathology. *Skin Res Technol*, **6**(1): 6–16.

Globocan 2008 v1.2, Cancer Incidence and Mortality Worldwide: IARC Cancer Base No.10 [Internet]. Lyon, France: International Agency for Research on Cancer, 2010. Available from http://globocan.iarc.fr

Glogau, R.G. (2000): The risk of progression to invasive disease. *J Am Acad Dermatol*, **42**(1): 23–24.

Godin, B. & Touitou, E. (2007) Transdermal skin delivery: predictions for humans from in vivo, ex vivo and animal models. *Adv Drug Deliv Rev*, **59**(11):1152-61.

Goldberg, H.I., Lockwood, S.A.,Wyatt, S.W., et al. (1994): Trends and differentials in mortality from cancers of the oral cavity and pharynx in the United States, 1973-1987. *Cancer*, **74**:565-572.

Goldstein, N.S., Soman, A., Sacksner, J. (1999): Disparate surgical margin lengths of colorectal resection specimens between in vivo and in vitro measurements. The effects of surgical resection and formalin fixation on organ shrinkage. *Am J Clin Pathol*, **111**: 349.

Golomb, F.M., Doyle, J.P., Grin, C.M., Kopf, A.W., Silverman, M.K., Levenstein, M.J. (1991): Determination of preexcision surgical margins of melanomas from fixed tissue specimens. *Plast Reconstr Surg*, **88**: 804.

Gonzalo, N., Serruys, P.W., Okamura, T., Shen, Z.J., Onuma, Y., Garcia- Garcia, H.M., Sarno, G., Schultz, C., van Geuns, R.J., Ligthart, J., Regar, E. (2009): Optical coherence tomography assessment of the acute effects of stent implantation on the vessel wall: a systematic quantitative approach. *Heart*, **95**(23): 1913–1919.

Gorsky, M., Epstein, J.B., Oakley, C., Le, N.D., Hay, J., Stevenson-Moore, P. (2004) Carcinoma of the tongue: a case series analysis of clinical presentation, risk factors, staging, and outcome. *Oral Surg Oral Med Oral Pathol Oral Radiol Endod*, **98**(5): 546–52.

Gossage, K.W., Tkaczyk, T.S., Rodriguez, J.J., Barton, J.K. (2003): Texture analysis of optical coherence tomography images: feasibility for tissue classification. *J Biomed Opt*, **8**(3): 570–575.

Gotzinger, E., Pircher, M., Geitzenauer, W., Ahlers, C., Baumann, B., Michels, S., Schmidt-Erfurth, U., Hitzenberger, C.K. (2008): Retinal pigment epithelium segmentation by polarization sensitive optical coherence tomography. *Opt Express*, **16**(21): 16410– 16422.

Gross, K.G., Steinman, H.K., Rapini, R.P. (1999): *Mohs Surgery: Fundamentals and Techniques*. Saint Louis: Mosby. pp. 49-66, 193-203, 211–220.

Grulich, A. E., et al. (2007) Incidence of cancers in people with HIV/AIDS compared with immunosuppressed transplant recipients: a meta-analysis. *Lancet*, **370**(9581): 59-67.

Guagliumi, G. & Sirbu, V. (2008): Optical coherence tomography: high resolution intravascular imaging to evaluate vascular healing after coronary stenting. *Catheter Cardiovasc Interv*, **72** (2): 237.

Guha, N., Boffetta, P., Wünsch Filho, V., Eluf Neto, J., Shangina, O., Zaridze, D., et al. (2007) Oral health and risk of squamous cell carcinoma of the head and neck and oesophagus: results of two multicentric case-control studies. *Am J Epidemiol*, **166**(10): 1159–73.

Guo, Z., Yamaguchi, K., Sanchez-Cespedes, M., Westra, W.H., Koch, W.M., Sidransky, D. (2001): Allelic losses in OraTest-directed biopsies of patients with prior upper aerodigestive tract malignancy. *Clin Cancer Res*,**7**:1963-1968.

Gupta, P.C., Mehta, F.S., and Pindborg, J.J. (1984) Mortality among reverse chutta smokers in south India. *Br Med J (Clin Res Ed),* **289**(6449): 865-6.

Gupta, P.C., Murti, P.R., Bhonsle, R.B. (1996): Epidemiology of cancer by tobacco products and the significance of TSNA. *Crit Rev Toxicol*, **26**(2): 183-98.

Gupta, P.C. & Warnakulasuriya, S. (2002): Global epidemiology of areca nut usage. *Addict Biol*, **7**(1): 77-83.

Gyatsho, J., Kaushik, S., Gupta, A., Pandav, S., Ram, J. (2008): Retinal nerve fibre layer thickness in normal, ocular hypertensive, and glaucomatous Indian eyes: an optical coherence tomography study. *J Glaucoma*, **17**(2): 122–127.

Halloppeau, H. (1910) Sur un cas de lichen de Wilson gingival avec neoplasie voisine dans la region maxillaire. *Bull Soc Fr Dennatol Syphgr*, **17**: 32.

Hamdoon, Z. Jerjes, W., Mckenzie, G., Jay, A., Hopper, C. (2010): Assessment of tumour resection margins using optical coherence tomography. *Head & Neck Oncology,* **2**(Suppl 1): O7.

Hamdoon, Z., Jerjes, W., Upile, T., Hopper, C. (2011): Optical coherence tomography-guided photodynamic therapy for skin cancer: case study. *Photodiagnosis Photodyn Ther*, **8**(1): 49–52.

Hamdoon, Z., Jerjes, W., Upile, T., McKenzie, G., Jay, A., Hopper, C. (2013): Optical coherence tomography in the assessment of suspicious oral lesions: an immediate ex vivo study. *Photodiagnosis Photodyn Ther*, 10(1): 17-27.

Hammarstedt, L., Lindquist, D., Dahlstrand, H., et al. (2006): Human papillomavirus as a risk factor for the increase in incidence of tonsillar cancer. *Int J Cancer*, 2006; **119**: 2620-2623.

Hammer, D.X., Mujat, M., Iftimia, N.V., Lue, N., Ferguson, R.D. (2010): Multimodal adaptive optics for depth-enhanced high-resolution ophthalmic imaging. *Proc SPIE*, **7550**(1): 755011–755012.

Hansen, L.S., Olson, J.A., Silverman, S. Jr. (1985) Proliferative verrucous leukoplakia. A long-term study of thirty patients. *Oral Surg Oral Med Oral Pathol*, **60**:285-298.

.

Hashibe, M., Straif, K., Tashkin, D.P., et al. (2005) Epidemiologic review of marijuana use and cancer risk. *Alcohol*, **35**: 265-275.

Hashibe, M., Brennan, P., Chuang, S.C., et al. (2009): Interaction between tobacco and alcohol use and the risk of head and neck cancer: pooled analysis in the International Head and Neck Cancer Epidemiology Consortium. *Cancer Epidemiol Biomarkers Prev*, **18**:541-550.

Haya-Fernández, M.C., Bagán, J.V., Murillo-Cortés, J., Poveda-Roda, R., Calabuig, C. (2004) The prevalence of oral leukoplakia in 138 patients with oral squamous cell carcinoma. *Oral Dis*, **10**(6):346–8.

Heck, J.E., et al. (2009) Sexual behaviours and the risk of head and neck cancers: a pooled analysis in the International Head and Neck Cancer Epidemiology (INHANCE) consortium. *Int J Epidemiol*.

Heintzelman, D.L., Utzinger, U., Fuchs, H., Zuluaga, A., Gossage, K., Gillenwater, A.M., Jacob, R., Kemp, B., Richards-Kortum, R.R. (2000): Optimal excitation wavelengths for *in vivo* detection of oral neoplasia using fluorescence spectroscopy. *Photochem Photobiol*,**72**:103-113.

Heissler, E., Steinkamp, H.J., Heim, T., Zwicker, C., Felix, R., Bier, J. (1994: Value of magnetic resonance imaging in staging carcinomas of the oral cavity and oropharynx. *Int J Oral Maxillofac Surg*, **23**: 22–27.

Henk, J.M. (1992): Treatment of oral cancer by interstitial irradiation using iridium-192. *Br J Oral Maxillofac Surg*, **30**: 355–359.

Hermann, B., Fernandez, E.J., Unterhuber, A., Sattmann, H., Fercher, A.F., Drexler, W., Prieto, P.M., Artal, P. (2004): Adaptive-optics ultrahigh-resolution optical coherence tomography. *Opt Lett*, **29** (18): 2142–2144.

Herrero, R., Castellsague, X., Pawlita, M., et al. (2003): Human papillomavirus and oral cancer: the International Agency for Research on Cancer multicenter study. *J Natl Cancer Inst*, **95**:1772–83.

Hillman, T.R., Adie, S.G., Seemann, V., Armstrong, J.J., Jacques, S.L., Sampson, D.D. (2006): Correlation of static speckle with sample properties in optical coherence tomography. *Opt Lett*, **31**(2): 190–192.

Hindle, I., Downer, M.C., & Speight, P.M. (1996) The epidemiology of oral cancer. *Brit J Oral Max Fac Surg*, **34**: 471-476.

Hirata, R.M., Jaques, D.A., Chambers, R.G., Tuttle, J.R., Mahoney, W.D. (1975) Carcinoma of the oral cavity. An analysis of 478 cases. *Ann Surg*, **182**(2):98–103.

Hoang, K.C., Edris, A., Su, J., Mukai, D.S., Mahon, S., Petrov, A.D., Kern, M., Ashan, C., Chen, Z., Tromberg, B.J., Narula, J., Brenner, M. (2009): Use of an oxygen-carrying blood substitute to improve intravascular optical coherence tomography imaging. *J Biomed Opt*, **14**(3):034028.

Ho, C.M., Lam, K.H., Wei, W.I., et al. (1992) Occult lymph node metastasis in small oral tongue cancers. *Head Neck*, **14**:359-363.

Ho, P.S., Ko, Y.C., Yang, Y.H., Shieh, T.Y., Tsai, C.C. (2002): The incidence of oropharyngeal cancer in Taiwan: an endemic betel quid chewing area. *J Oral Pathol Med*, **31**:213-219.

Holmes, Jr. L., Desvignes-Kendrick, M., Slomka, J., Mahabir, S., Beeravolu, S., Emani, S.R. (2008) Is dental care utilization associated with oral cavity cancer in a large sample of community-based United States residents? *Commun Dent Oral Epidemiol*.

Holmstrup, P., Thorn, J.J., Rindum, J., Pindborg, J.J. (1988) Malignant development of lichen planus-affected oral mucosa. *J Oral Path*, **17**: 219-25.

Horowitz, A.M. & Nourjah, P.A. (1996): Factors associated with having oral cancer examinations among US adults 40 years of age and older. *J Public Health Dent*, **56**:331-5.

Horowitz, A.M., Drury, T.F., Goodman, H.S., et al. (2000): Oral pharyngeal cancer prevention and early detection. Dentists' opinions and practices. *J Am Dent Assoc*, **131**:453-462.

Horowitz, A.M., Siriphant, P., Sheikh, A., et al. (2001): Perspectives of Maryland dentists on oral cancer. *J Am Dent Assoc*, **131**:65-72.

Hougaard, J.L., Heijl, A., Bengtsson, B. (2007): Glaucoma detection using different stratus optical coherence tomography protocols. *Acta Ophthalmol Scan*, **85**(3): 251–256.

Hsu, P.K., Huang, H.C., Hsieh, C.C., Hsu, H.S., Wu, Y.C., Huang, M.H., et al. (2007): Effect of formalin fixation on tumour size determination in stage I non-small cell lung cancer. *Ann Thorac Surg*,**84**:1825.

Huang, D., Swanson, E.A., Lin, C.P., Schuman, J.S., Stinson, W.G., Chang, W., Hee, M.R., Flotte, T., Gregory, K., Puliafito, C.A., Fujimoto, J.G. et al (1991): Optical coherence tomography. *Science*, **254**(5035): 1178–1181.

Huang, M.F., Chang, Y.C., Liao, P.S., Huang, T.H., Tsay, C.H., Chou, M.Y. (1999): Loss of heterozygosity of p53 gene of oral cancer detected by exfoliative cytology. *Oral Oncol*, **35**: 296–301.

Hudson-Peacock, M.J., Matthews, J.N.S., Lawrence, C.M. (1995): Relation between size of skin, excision, wound and specimen. *J Am Acad Dermatol*, **32**: 1010.

Hughes, C.J., Gallo, O., Spiro, R.H., Shah, J.P. (1993): Management of occult neck metastases in oral cavity squamous carcinoma. Am J Surg, **166**:380–383.

Hui, Y.H., Chandan, R.C., Shimoni, E., Clark, S., et al. (2007) Handbook of Food Products Manufacturing: Health, Meat, Milk, poultry, seafood, and vegetables. John Whiley & sons, Inc., Hoboken, New Jersey, USA. 368-369.

Huzaira, M., Rius, F., Rajadhyaksha, M., Anderson, R., Gonzalez, S. (2001): Topographic variations in normal skin, as viewed by in vivo reflectance confocal microscopy. *J Invest Dermatol*, **116**:846-52.

Idris, A.M., Ahmed, H.M., Mukthar, B.I., Gander, A.F., El-Beshir, E.I. (1995) Descriptive epidemiolology of oral neoplasms in Sudan 1970–1985 and the role of toombak. *Int J Cancer*, **61**:155–8.

Igarashi, T., Nishino, K., & Nayar, S. K. (2005): The appearance of human skin. Technical report: CUCS-024-05. Department of Computer Science, Columbia University, New York, NY 10027, USA.

Inaguma, M. & Hashimoto, K. (1999): Porphyrin-like fluorescence in oral cancer: *In vivo* fluorescence spectral characterization of lesions by use of a near ultraviolet excited autofluorescence diagnosis system and separation of fluorescent extracts by capillary electrophoresis. *Cance*, **86**:2201-2211.

Ingrams, D.R., Dhingra, J.K., Roy, K., Perrault, D.F. Jr., Bottrill, I.D., Kabani, S., Rebeiz, E.E., Pankratov, M.M., Shapshay, S.M., Manoharan, R., Itzkan, I., Feld, M.S. (1997): Autofluorescence characteristics of oral mucosa. *Head Neck*, **19:27**-32.

International Agency for Research on Cancer (IARC), 1986.

International Agency for Research on Cancer. IARC monographs on the evaluation of carcinogenic risks to humans. Betel-quid and areca-nut chewing and some areca-nut related nitrosamines, vol. 85. IARC; 2004.

International Agency for Research on Cancer. Smokeless Tobacco and Some Tobacco-Specific N-Nitrosamines. IARC Monographs on the Evaluation of Carcinogenic Risks to Humans. Vol 89. Lyon, France: IARC; 2007.

ISD Scotland, September 2011.

ISD Scotland Cancer Statistics. Head Accessed March 2012.

Isenberg, G., Sivak, M.V. Jr., Chak, A., Wong, R.C., Willis, J.E., Wolf, B., Rowland, D.Y., Das, A., Rollins, A. (2005): Accuracy of endoscopic optical coherence tomography in the detection of dysplasia in Barrett's esophagus: a prospective, double-blinded study. *Gastrointest Endosc*, **62**(6): 825-31.

Izatt, J.A., Hee, M.R., Huang, D., Fujimoto, J.G., Swanson, E.A., Lin, C.P., Shuman, J.S., Puliafito, C.A. (1993): Ophthalmic diagnostics using optical coherence tomography. *Proc SPIE*, **1877**:136–144

Izatt, J.A., Hee, M.R., Swanson, E.A. et al. (1994a): Micrometre-scale resolution imaging of the anterior eye with optical coherence tomography. *Arch. Ophthamol*, **112**: 1584–1589.

Izatt, J.A., Hee, M.R., Owen, G.M., Swanson, E.A. & Fujimoto, J.G. (1994b): Optical coherence microscopy in scattering media. *Optics Lett*, **19**: 590–592.

Izatt, J.A., Kulkarni, M.D., Yazdanfar, S., Barton, J.K., Welch, A.J. (1997): In vivo bidirectional colour Doppler flow imaging of picoliter blood volumes using optical coherence tomography. *Opt Lett*, **22**(18): 1439–1441.

Jacques, S. L. (1998): Skin optics. Oregon Medical Laser Center monthly news and articles on Biomedical Optics and Medical Lasers, http://omlc.ogi.edu/news/jan98/skinoptics.html.

Jacob, B.J., Straif, K., Thomas, K., et al. (2004) Betel quid without tobacco as a risk factor for oral precancers. *Oral Oncol*, **40**: 697-704.

Jainkittivong, A., Swasdison, S., Thangpisityotin, M., Langlais, R.P. (2009) Oral squamous cell carcinoma: a clinicopathological study of 342 Thai cases. *J Contemp Dent Pract*, **10**(5): 33–40.

Jang, I.K., Bouma, B.E., Kang, D.H., Park, S.J., Park, S.W., Seung, K.B., Choi, K.B., Shishkov, M., Schlendorf, K., Pomerantsev, E., Houser, S.L., Aretz, H.T., Tearney, G.J. (2002): Visualization of coronary atherosclerotic plaques in patients using optical coherence tomography: comparison with intravascular ultra- sound. *J Am Coll Cardiol*, **39**(4): 604–609.

Jang, I.K., Tearney, G.J., Mac-Neill, B., Takano, M., Moselewski, F., Iftima, N., Shishkov, M., Houser, S., Thomas Aretz H., Halpern, E.F., Bouma, B.E. (2005): In vivo characterization of coronary atherosclerotic plaque by use of optical coherence tomography. *Circulation*, **111**(12): 1551–1555.

Jayalekshmi, P.A., Gangadharan, P., Akiba, S., Nair, R.R., Tsuji, M., Rajan, B. (2009): Tobacco chewing and female oral cavity cancer risk in Karunagappally cohort, India. *Br J Cancer*, **100**:848-852.

Jemal, A., Siegel, R., Ward, E., Murray, T., Xu, J., Smigal, C., Thun, M.J. (2006). Cancer statistics, 2006, **56**(2): 106-30.

Jemal, A., Siegel, R., Ward, E., Murray, T., Xu, J., Thun, J. (2007) *CA Cancer J. Clin*, **57**: 43–66.

Jemal, A., Siegel, R., Ward, E. et al. (2008) Cancer statistics. *CA Cancer J. Clin*, **58**(2), 71–96.

Jemal, A., Bray, F., Center, M.M., Ferlay, J., Ward, E., & Forman, D. (2011): Global Cancer Statistics. *CA Cancer J Clin*, **61**:69–90.

Jeppesen, P., Knudsen, S.T., Poulsen, P.L., Mogensen, C.E., Schmitz, O., Bek. T. (2007): Response of retinal arteriole diameter to increased blood pressure during acute hyperglycaemia. *Acta Ophthalmol Scan*, **85**(3): 280–286.

Jerjes, W., Upile, T., Conn, B., et al. (2009): In vitro examination of suspicious oral lesions using optical coherence tomography. *Br J Oral Maxillofac Surg*, **48**: 1–78.

Jerjes, W., Upile, T., Conn, B., Hamdoon, Z., Betz, C.S., McKenzie, G., Radhi, H., Vourvachis, M., El Maaytah, M., Sandison, A., Jay, A., Hopper, C. (2010): In vitro examination of suspicious oral lesions using optical coherence tomography. *Br J Oral Maxillofac Surg*, **48**(1): 18-25.

Johnson, N.W. (1991): Orofacial neoplasm: global epidemiology, risk factors and recommendations for research. *International Dental Journal*, **41**: 365-375.

Johnson NW, Warnakulasuriya S, Tavassoli M (1996) Hereditary and environmental risk factors: clinical and laboratory risk markers for head and neck, especially oral cancer and precancer. *European Journal of Cancer Prevention,* **5**: 5-17.

Johnson, R.E., Sigman, J.D., Funk, G.F., Robinson, R.A., Hoffman, H.T. (1997): Quantification of surgical margin shrinkage in the oral cavity. *Head Neck*, **19**:281-286.

Johnson, N.W. (2001): Tobacco use and oral cancer: A global perspective. *J Dent Educ*, **65**:328- 339.

Jonmarker, S., Valdman, A., Lindberg, A., Hellstro¨m, M., Egevad, L. (2006): Tissue shrinkage after fixation with formalin injection of prostatectomy specimens. *Virchows Arch*, **449**:297e301.

Jørgensen, T.M., Thomadsen, J., Christensen, U., Soliman, W., Sander, B. (2007): Enhancing the signal-to-noise ratio in ophthalmic optical coherence tomography by image registration—method and clinical examples. *J Biomed Opt*, 12(4):041208.

Jorgensen, T.M., Tycho, A., Mogensen, M., Bjerring, P., Jemec, G.B. (2008): Machine-learning classification of non-melanoma skin cancers from image features obtained by optical coherence tomography. *Skin Res Technol*, **14**(3): 364–369.

Jovanovic, A., Schulten, E.A., Kostense, P.J., et al. (1993) Tobacco and alcohol related to the anatomical site of oral squamous cell carcinoma. *J Oral Pathol Med*, **22**:459-462.

Kahn, M.A., Dockter, M.E., Hermann-Petrin, J.M. (1994) Proliferative verrucous leukoplakia. Four cases with flow cytometric analysis. *Oral Surg Oral Med Oral Pathol*, **78**:469-475.

Kaiser, P.K., Blodi, B.A., Shapiro, H., Acharya, N.R. (2007): Angio-graphic and optical coherence tomographic results of the marina study of ranibizumab in neovascular age-related macular degeneration. *Ophthalmology*, **114**(10): 1868–1875.

Kalev-Landoy, M., Day, A.C., Cordeiro, M.F., Migdal, C. (2007): Optical coherence tomography in anterior segment imaging. *Acta Ophthalmol Scan*, **85**(4): 427–430.

Kaplan, B.R. (1991) Oral lichen planus and squamous carcinoma: case report and update of the literature. *Rhode Island Dent J*, **24**: 405-414.

Karamouzis, M.V., Grandis, J.R., Argiris, A. (2007): Therapies directed against epidermal growth factor receptor in aerodigestive carcinomas. *JAMA*, **298**(1): 70-82.

Khandwala, M., Penmetsa, B.R., Dey, S., Schofield, J.B., Jones, C.A., Podoleanu, A. (2010): Imaging of periocular basal cell carcinoma using en face optical coherence tomography: a pilot study. *Brit J Ophthalmol*, **94**(10): 1332–1336.

Kerns, M.J., Darst, M.A., Olsen, T.G., Fenster, M., Hall, P., Grevey, S. (2008): Shrinkage of cutaneous specimens: formalin or other factors involved? *J Cutan Pathol*, **35**:1093-6.

Kerr, A.R., Sirois, D.A., Epstein, J.B. (2006): Clinical evaluation of chemiluminescent lighting: an adjunct for oral mucosal examinations. *J Clin Dent*, **17**:59-63.

Kimura, M., Tayama, N., Chan, R.W. (2003): Geometrical deformation of vocal fold tissues induced by formalin fixation. *Laryngoscope*, **113**(4): 607-13.

King, G.N. & Thornhill, M.H. (1996) Dental attendance patterns in renal transplant recipients. *Oral Dis*, **2**(2): 145-7.

Klein–Szanto, A.J. & Schroeder, H.E. (1977): Architecture and density of the connective tissue papillae of the human oral mucosa. *J Anat*, **123**: 93–109.

Kolodgie, F.D., Virmani, R., Burke, A.P., et al. (2004): Pathologic assessment of the vulnerable human coronary plaque. *Heart*, 2004; **90**:1385–1391.

Korde, V.R., Bonnema, G.T., Xu, W., Krishnamurthy, C., Ranger-Moore, J., Saboda, K., Slayton, L.D., Salasche, S.J., Warneke, J.A., Alberts, D.S., Barton, J.K. (2007): Using optical coherence tomography to evaluate skin sun damage and precancer. *Lasers Surg Med*, **39**(9): 687–695.

Kovacs, I., Ferencz, M., Nemes, J., Somfai, G., Salacz, G., Recsan, Z. (2007): Intraocular lens power calculation for combined cataract surgery, vitrectomy and peeling of epiretinal membranes for macular oedema. *Acta Ophthalmol Scan*, **85**(1): 88–91.

Kowalski, L.P., Bagietto, R., Lara, J.R., et al (2000): Prognostic significance of the distribution of neck node metastasis from oral carcinoma. *Head Neck*, **22**:207–214.

Kowalski, L.P. (2002): Results of salvage treatment of the neck in patients with oral cancer. *Arch Otolaryngol Head Neck Surg*, **128**:58–62.

Kramer, I.R., Lucas, R.B., Pindborg, J.J., et al. (1978) WHO Collaborating Centre for Oral Precancerous Lesions. Definition of leukoplakia and related lesions: An aid to studies on oral pre- cancer. *Oral Surg Oral Med Oral Pathol*, **46**:518-539.

Kreimer, A.R., et al. (2005) Human papillomavirus types in head and neck squamous cell carcinomas worldwide: a systematic review. *Cancer Epidemiol Biomarkers Prev*, 2005. **14**(2): 467-75.

Kreimer, A.R., et al. (2006): Diet and body mass, and oral and oropharyngeal squamous cell carcinomas: Analysis from the IARC multinational case-control study. *Int J Cancer*, **118**(9): 2293-7.

Kulapaditharom, B. & Boonkitticharoen, V. (2001): Performance characteristics of fluorescence endoscope in detection of head and neck cancers. *Ann Otol Rhinol Laryngol*, **110**:45-52.

Kulkarni, M.D., Thomas, C.W., Izatt, J.A. (1997): Image enhancement in optical coherence tomography using deconvolution. *Electron Lett*, **33**(16): 1365–1367.

Kumar, G. & J.M. Schmitt, J.M. (1996): Micro-optical properties of tissue. In Proceedings of SPIE: Advances in Laser and Light Spectroscopy to Diagnosis Cancer and Other Diseases 3: Optical Biopsy, volume 2679, pages 106–116.

Kume, T., Akasaka, T., Kawamoto, T., Okura, H., Watanabe, N., Toyota, E., Neishi, Y., Sukmawan, R., Sadahira, Y., Yoshida, K. (2006): Measurement of the thickness of the fibrous cap by optical coherence tomography. *Am Heart J*, **152**(4): 755.e1–4.

Ladekarl, M. (1994): The influence of tissue processing on quantitative histopathology in breast cancer. *J Microsc*, **174** (Pt 2): 93.

Lamirel, C., Newman, N., Biousse, V. (2009): The use of optical coherence tomography in neurology. *Rev Neurol Dis*, **6**(4): 105–120.

Lamont, E.B. & Vokes, E.E. (2001): Chemotherapy in the management of squamous-cell carcinoma of the head and neck. *Lancet Oncol*, **2**:261–269.

Landis, J.R. & Koch, G.G. (1977): The measurement of observer agreement for categorical data. *Biometrics,* **33**, 159-174.

Larsson, J., Holm, K., Lövestam-Adrian, M. (2006): The presence of an operculum verified by optical coherence tomography and other prognostic factors in macular hole surgery. *Acta Ophthalmol Scan*, **84**(3): 301–304.

La Vecchia, C., Tavani, A., Franceschi, S., Levi, F., Corrao, G., Negri, E. (1997): Epidemiology and prevention of oral cancer. *Oral Oncol*, **33**:302–12.

La Vecchia, C., Franceschi, S., Favero, A., Talamini, R., Negri, E. (1999) Alcohol intake and cancer of the upper digestive tract. Pattern of risk in Italy is different from that in Denmark. *BMJ*, **318**(7193): 1289-90.

La Vecchia, C., Lucchini, F., Negri, E., Levi, F. (2004): Trends in oral cancer mortality in Europe. *Oral Oncol*, **40**(4): 433–9.

Lawrence, N. & Cottel, W.I. (1994): Squamous cell carcinoma of skin with perineural invasion. *J Am Acad Dermatol*. **31**(1): 30-3.

Lee, K., Kunjappu, J., Jockusch, S., Turro, N. J., Widerschpan,T., et al. (2005) Amplification of the Index of Refraction of Aqueous Immersion Fluids by Ionic Surfactants. Proc. of SPIE Vol. 5753, 537-553.

Lee, Y.C., et al. (2009): Active and involuntary tobacco smoking and upper aerodigestive tract cancer risks in a multicenter case-control study. *Cancer Epidemiol Biomarkers Prev*, **18**(12): 3353-61.

Lefebvre, J.L., Chevalier, D., Luboinski, B., et al. (1996): Larynx preservation in pyriform sinus cancer: preliminary results of a European Organization for Research and Treatment of Cancer phase III trial. EORTC Head and Neck Cancer Cooperative Group. *J Natl Cancer Inst*, **88**:890–899.

Leitgeb, R., Hitzenberger, C., Fercher, A. (2003a): Performance of Fourier domain vs time domain optical coherence tomography. *Opt Express*, **11**(8): 889–894.

Leitgeb, R., Schmetterer, L., Drexler, W., Fercher, A., Zawadzki, R., Bajraszewski, T. (2003b): Real-time assessment of retinal blood flow with ultrafast acquisition by colour Doppler Fourier domain optical coherence tomography. *Opt Express*, **11**(23): 3116–3121.

Leitgeb, R.A., Schmoll, T., Kolbitsch, C. (2009): Dynamic retinal optical coherence microscopy without adaptive optics. *Proc SPIE*, 7372:737208

Levi, F., Pasche, C., La Vecchia, C., Lucchini, F., Franceschi, S., and Monnier, P. (1998) Food groups and risk of oral and pharyngeal cancer. *International journal of cancer*, **77**: 705-709.

Levitz, D., Thrane, L., Frosz, M., Andersen, P., Andersen, C., Andersson-Engels, S., Valanciunaite, J., Swartling, J., Hansen, P. (2004): Determination of optical scattering properties of highly scattering media in optical coherence tomography images. *Opt Express*, **12**(2): 249–259.

Lewin, F., Norell, S.E., Johansson, H., et al. (1998): Smoking tobacco, oral snuff, and alcohol in the aetiology of squamous cell carcinoma of the head and neck. A population-based case-referent study in Sweden. *Cancer*, **82**:1367-1375.

Li, Q.X., Fu, Q.Q., Shi, S.W., Wang, Y.F., Xie, J.J., Yu, X., Cheng, X., Liao, Y.H. (2010): Relationship between plasma inflammatory markers and plaque fibrous cap thickness determined by intravascular optical coherence tomography. *Heart*, **96**(3): 196–201.

Lind, P.O. (1987) Malignant transformation in oral leukoplakia. *Scand J Dent Res*, **95**: 449-455.

Lindel, K., Beer, K.T., Laissue, J., et al. (2001) Human papillomavirus positive squamous cell carcinoma of the oropharynx: A radiosensitive subgroup of head and neck carcinoma. *Cancer*,**92**:805- 813.

Lingen, M.W., Kalmar, J.R., Karrison, T., Speight, P.M. (2008): Critical evaluation of diagnostic aids for the detection of oral cancer. *Oral Oncol*, **44**:10–22.

Llewellyn, C.D., Johnson, N.W. & Warnakulasuriya, K.A. (2001): Risk factors for squamous cell carcinoma of the oral cavity in young people – a comprehensive literature review. *Oral Oncol*, **37**:401–18.

Llewellyn, C.D., Linklater, K., Bell, J., Johnson, N.W., Warnakulasuriya, S. (2004a): An analysis of risk factors for oral cancer in young people: a case-control study. *Oral Oncol*, **40**:304–13. 29.

Llewellyn, C.D., Johnson, N.W., Warnakulasuriya, K.A.A.S. (2004b): Risk factors for oral cancer in newly diagnosed patients aged 45 years and younger: a case-control study in Southern England. *J Oral Pathol Med*, **33**:525–32.

Llewellyn, C.D., Johnson, N.W., Warnakulasuriya, S. (2004c): Factors associated with delay in presentation among younger patients with oral cancer. *Oral Surg Oral Med Oral Pathol Oral Radiol Endod*,**97**(6):707-13.

Low, A.F., Tearney, G.J., Bouma, B.E., Jang, I.K. (2006): Technology insight: optical coherence tomography: current status and future development. *Nat Clin Pract Card*, **3**:154–162.

Lucas, R., McMichael. T., Smith, W. & Armstrong, B.K. (2006): Solar ultraviolet radiation: global burden of disease from solar ultraviolet radiation. J Oral Geneva (Switzerland): World Health Organization.

Lucenteforte, E., Garavello, W., Bosetti, C., et al. (2008) Dietary factors and oral and pharyngeal cancer risk. *Oral Oncol*, Nov 4.

Lum, H. & Mitzner, W. (1985): Effects of 10% formalin fixation on fixed lung volume and lung tissue shrinkage. A comparison of eleven laboratory species. *Am Rev Respir Dis*, **132**: 1078.

Ma, G.W., Rong, T.H., Long, H., et al. (2004): Shrinkage of resected specimens of esophageal carcinoma. *Ai Zheng*, **23**: 193.

Macfarlene, G.J., Boyle, P., Evstifeeva, T.V., Robertson, C., Scully, C. (1994a) Rising trends of oral cancer mortality among males worldwide: the return of an old public health problem. *Cancer Causes and Control*, **5**(3): 259-65.

Macfarlene, G.J., Evstifeeva, T.V., Robertson, C., Boyle, P., Scully, C. (1994b) Trends of oral cancer mortality among females worldwide. *Cancer Causes and Control*, **5**: 255-258.

Macfarlane, G.J., Zheng, T., Marshall, J.R., Boffetta, P., Niu, S., Brasure, J., Merletti, F., Boyle, P. (1995) Alcohol, tobacco, diet and the risk of oral cancer: a pooled analysis of three case-control studies. *Eur J Cancer B Oral Oncol*, **31**(3):181-7.

MacNeill, B.D., Lowe, H.C., Takano, M., et al. (2003): Intravascular modalities for detection of vulnerable plaque: Current status. *Arterioscler Thromb Vasc Biol*, **23**:1333–1342.

Makita, S., Hong, Y., Yamanari, M., Yatagai, T., Yasuno, Y. (2006): Optical coherence angiography. *Opt Express*, **14**(17): 7821–7840.

Maloney, M.E. (1999): *Surgical dermatopathology*. Malden, Mass: Blackwell Science. pp. 112–3, 1111-7.

Mao, L. & Oh, Y. (1998) Does marijuana or crack cocaine cause cancer? *J Natl Cancer Inst*,**90**(16):1182-4.

Marshall, J.R. and Boyle, P. (1996) Nutrition and oral cancer. *Cancer Causes Control*, **7**(1): 101-11.

Mikhail, G.R. & Mohs, F.E. (1991): *Mohs micrographic surgery*. Philadelphia: W.B. Saunders. pp. 3–4, 7, 13-5.

Minton, T.J. (2008): "Contemporary Mohs surgery applications". *Current Opinion in Otolaryngology & Head and Neck Surgery*, **16** (4): 376–80.

Marschall, S., Sander, B., Mogensen, M., Jørgensen, T.M., Andersen, P.E. (2011): Optical coherence tomography-current technology and applications in clinical and biomedical research. *Anal Bioanal Chem*, **400**(9): 2699-2720.

Martin, I.C., Kerawala, C.J., Reed, M. (1998): The application of toluidine blue as a diagnostic adjunct in the detection of epithelial dysplasia. *Oral Surg Oral Med Oral Pathol Oral Radiol Endod*, **85**:444-446.

Marugame, T., Matsuda, T., Kamo, K., Katanoda, K., Ajiki, W., Sobue, T. (2007) Japan cancer surveillance research group. Cancer incidence and incidence rates in Japan in 2001 based on the data from 10 population-based cancer registries. *Japanese J Clin Oncol*, **37**:884–91.

Marur, S., D'Souza, G., Westra, W.H., Forastiere, A.A. (2010): HPV-associated head and neck cancer: a virus-related cancer epidemic. *Lancet Oncol*, **11**:781-789.

Mashberg, A., & Meyers, H. (1976) Anatomical site and size of 222 early asymptomatic oral squamous cell carcinoma: a continuing prospective study of oral cancer. II. *Cancer*, **37**(5): 2149-57.

Mashberg, A. (1983): Final evaluation of tolonium chloride rinse for screening of high-risk patients with asymptomatic squamous carcinoma. *J Am Dent Assoc*, **106**:319-323.

Mashberg, A., Merletti, F., Boffetta, P., Gandolfo, S., Ozzello, F., Fracchia, F.,et al. (1989) Appearance, site of occurrence, and physical and clinical characteristics of oral carcinoma in Torino, Italy. *Cancer*, **63**(12):2522–7.

Mashberg, A., Boffetta, P., Winkelman, R.,et al. (1993) Tobacco smoking, alcohol drinking, and cancer of the oral cavity and oropharynx among U.S. veterans. *Cancer*,**72**:1369-1375.

Mashberg, A. & Samit, A. (1995) Early diagnosis of asymptomatic oral and oropharyngeal squamous cancers. *CA Cancer J Clin*, **45**:328-351.

Matheny, E.S., Hanna, N., Mina-Araghi, R., Jung, W.G., Chen, Z., Wilder-Smith, P., Brenner, M. (2003): Optical coherence tomography of malignant Hamster Cheek Pouches. *J Invest Med*, **51**(1): S78.

Matheny, E.S., Hanna, N.M., Jung, W.G., et al. (2004) Optical coherence tomography of malignancy in hamster cheek pouches. *J Biomed Opt*, **9**:978–981.

Mayne, S.T., Morse, D., Winn, D. (2006): Cancers of the oral cavity and pharynx. In: Schottenfeld, D., Fraumeni, J.F. Jr., eds. Cancer Epidemiology and Prevention. 3rd ed. Oxford: Oxford University Press: 674-696.

Mayor, S. (2002) Introduce the single European diet. *Health and Ageing*, 58-9.

Mazeron, J.J., Grimard, L., Raynal, M., et al. (1990): Iridium-192 curietherapy for T1 and T2 epidermoid carcinomas of the floor of mouth. *Int J Radiat Oncol Biol Phys*, **18**:1299–1306.

McIntosh, L., McCullough, M.J., Farah, C.S. (2009): The assessment of diffused light illumination and acetic acid rinse (Microlux/DL) in the visualisation of oral mucosal lesions. Oral Oncol, **45**:227–31.

Meyer, W., Schwarz, R. & Neurand, K. (1978) The skin of domestic mammals as a model for the human skin, with special reference to the domestic pig. *Curr Probl Dermatol*, **7**:39-52.

Meyer, M.S., Joshipura, K., Giovannucci, E., Michaud, D.S. (2008) A review of the relationship between tooth loss, periodontal disease, and cancer. *Cancer Causes Control*, **19**(9):895–907.

Michalski, M.C., Briard, V., Michel, F. (2001) Optical parameters of milk fat globules for laser light scattering measurements. *Lait*, **81**: 787-796.

Michaud, D.S., Liu, Y., Meyer, M., Giovannucci, E., Joshipura, K. (2008) Periodontal disease, tooth loss, and cancer risk in male health professionals: a prospective cohort study. *Lancet Oncol*, **9**(6): 550–8.

Michels, S., Pircher, M., Geitzenauer, W., Simader, C., Götzinger, E., Findl, O., Schmidt-Erfurth, U., Hitzenberger, C.K. (2008): Value of polarisation-sensitive optical coherence tomography in diseases affecting the retinal pigment epithelium. *Brit J Ophthalmol*, **92** (2): 204–209.

Mignogna, MD., Lo muzio, L., Lo Russo, L., Fedele, S., Ruoppo, E., Bucci, E. (2001) Clinical guidelines in early detection of oral squamous cell carcinoma arising in oral lichen planus: a 5-year experience. *Oral Oncol*, **37**: 262-267.

Milian, A., Bagan. J.V., Vera, F. (1993) Squamous cell carcinoma of the oral cavity: a follow up study of 85 cases and analysis of prognostic variables. *Bull Group Int Rech Sci Stomatol Odontol*, **36**(1–2): 29–35.

Miller, C.S. &White, D.K. (1996) Human papillomavirus expression in oral mucosa, premalignant conditions, and squamous cell carcinoma. A retrospective review of the literature. *Oral Surg Oral Med Oral Pathol Oral Radiol Endod*, **82**:57-68.

Mogensen, M., Morsy, H.A., Thrane, L., Jemec, G.B.E. (2008): Morphology and epidermal thickness of normal skin imaged by optical coherence tomography. *Dermatology*, **217**(1): 14–20.

Mogensen, M., Jemec, G.B.E., Thrane, L., Jørgensen, T.M., Andersen, P.E. (2009a): OCT imaging of skin cancer and other dermatological diseases. *J Biophotonics*, **2**(6–7): 442–451.

Mogensen, M., Nürnberg, B.M., Forman, J.L., Thomsen, J.B., Thrane, L., Jemec, G.B.E. (2009b): In vivo thickness measurement of basal cell carcinoma and actinic keratosis with optical coherence tomography and 20-MHz ultrasound. *Br J Dermatol*, **160**(5): 1026–1033.

Mogensen, M., Jørgensen, T.M., Nürnberg, B.M., Morsy, H.A., Thomsen, J.B., Thrane, L., Jemec, G.B.E. (2009c): Assessment of optical coherence tomography imaging in the diagnosis of non- melanoma skin cancer and benign lesions versus normal skin: observer-blinded evaluation by dermatologists and pathologists. *Dermatol Surg*, **35**(6): 965–972.

Mollaoglu, N. (2000) Oral lichen planus: a review. *Br J Oral Maxillofac Surg*, **38**(4):370-7.

Moller, H. (1989) Changing incidence of cancer of the tongue, oral cavity, and pharynx in Denmark. *J Oral Pathol Med*, **18**(4): 224-9.

Monteiro-Riviere, N. & Riviere, J. E. (1996) Advances in Swine in Biomedical Research. *Plenum Press*, New York, 425–458.

Mork, J., Lie, A.K., Glattre, E., et al. (2001) Human papillomavirus infection as a risk factor for squamous cell carcinoma of the head and neck. *N Engl J Med*, **344**:1125-1131.

Morsy, H., Kamp, S., Thrane, L., Behrendt, N., Saunder, B., Zayan, H., Elmagid, E.A., Jemec, G.B. (2010): Optical coherence tomography imaging of psoriasis vulgaris: correlation with histology and disease severity. *Arch Dermatol Res*, **302**(2): 105–111.

Mulder, H. & Walstra, P. (1974): The milk fat globule. Emulsion science as applied to milk products and comparable foods, Commonwealth Agricultural Bureaux, Farnham Royal, Bucks, UK.

Muller, M.G., Valdez, T. A., Georgakoudi, I., Backman, V., Fuentes, C., Kabani, S., Laver, N., Wang, Z., Boone, C.W., Dasari, R.R., Shapshay, S.M., Feld, M.S. (2003): Spectroscopic detection and evaluation of morphologic and biochemical changes in early human oral carcinoma. *Cancer*, **97**:1681-1692.

Murata, A., Wallace-Bradley, D., Tellez, A., Alviar, C., Aboodi, M., Sheehy, A., Coleman, L., Perkins, L., Nakazawa, G., Mintz, G., Kaluza, G.L., Virmani, R., Granada, J.F. (2010): Accuracy of optical coherence tomography in the evaluation of neointimal coverage after stent implantation. *J Am Coll Cardiol Img*, **3**(1): 76–84.

Murti, P.R., Bhonsle, R.B., Pindborg, J.J., et al. (1985): Malignant transformation rate in oral submucous fibrosis over a 17-year period. *Community Dent Oral Epidemiol*, **13**:340-341.

Murti, P.R., Daftary, D.K., Bhonsle, R.B., Gupta, P.C., Mehta, F.S., Pindborg, J.J. (1986): Malignant potential of oral lichen planus: observation in 722 patients from India. *J Oral Pathol*, **15**: 71-77.

Murti, P.R., Bhonsle, R.B., Gupta, P.C., et al. (1995): Etiology of oral submucous fibrosis with special reference to the role of areca nut chewing. *J Oral Pathol Med*, **24**:145-152.

Nadkarni, S.K., Pierce, M.C., Park, B.H., de Boer, J.F., Whittaker, P., Bouma, B.E., Bressner, J.E., Halpern, E., Houser, S.L., Tearney, G.J. (2007): Measurement of collagen and smooth muscle cell content in atherosclerotic plaques using polarization-sensitive optical coherence tomography. *J Am Coll Cardiol*, **49** (13): 1474–1481.

Nagao, T., Ikeda, N., Warnakulasuriya, S., Fukano, H., Yuasa, H., Yano, M., et al. (2000): Serum antioxidant micronutrients and the risk of oral leukoplakia among Japanese. *Oral Oncology*, **36**:466–70.

National Cancer Control Programme, Sri Lanka, 2005

National Cancer Institute, Brazil, 2007.

National Cancer Intelligence Network (NCIN) Cancer Incidence by Deprivation England, 1995-2004. 2008a.

National Cancer Intelligence Network (NCIN) One, five and ten-year cancer prevalence by cancer network 2008b.

National Comprehensive Cancer Network (2011): *National Comprehensive Cancer Network clinical practice guidelines in oncology (NCCN Guidelines): Basal cell and squamous cell skin cancers*, Fort Washington, Pennsylvania.

National Institute of Dental and Craniofacial Research, 2001.

Nelson, J.S., Kelly, K.M., Zhao, Y., Chen, Z. (2001): Imaging blood flow in human port-wine stain in situ and in real time using optical Doppler tomography. *Arch Dermatol*, **137**(6): 741–744.

Neerken, S., Lucassen, G.W., Bisschop, M.A., et al. (2004): Characterization of age-related effects in human skin: a comparative study that applies confocal laser scanningmicroscopy and optical coherence tomography. *J Biomed Opt*, **9**:274-81.

Neville, B.W., Damm, D.D., Allen, C.M., et al. (2002) Oral & maxillofacial pathology. 2nd ed. Phila., PA: Saunders, 337-369.

Neville, B.W., & Day, T.A. (2002): Oral cancer and precancerous lesions. *CA Cancer J Clin*, **52**: 195-215.

Nichols, M.L., Quinn, F.B. Jr., Schnadig, V.J., Zaharopoulos, P., Hokanson, J.A., Des Jardins, L., et al. (1991): Interobserver variability in the interpretation of brush cytologic studies from head and neck lesions. *Arch Otolaryngol Head Neck Surg*, **117**:1350–1355.

Nieuwenhuis, E.J., Pijpers, R., Castelijns, J.A. & Snow, G.B. (2003): Lymphoscintigraphic details of sentinel lymph node detection in 82 patients with squamous cell carcinoma of the oral cavity and oropharynx. *Nucl Med Commun*, **24**: 651–656.

Northern Ireland Cancer Registry, September 2011.

Nunes, F.D., Loducca, S.V., de Olivera, E.M., de Araujo, V.C. (2002): Well-differentiated liposarcoma of the tongue. *Oral Oncol*, **38**(1): 117-9.

Nutting, C.M., Morden, J.P., Harrington, K.J., Urbano, T.G., Bhide, S.A., Clark, C., Miles, E.A., Miah, A.B., Newbold, K., Tanay, M., Adab, F., Jefferies, S.J., Scrase, C., Yap, B.K., A'Hern, R.P., Sydenham, M.A., Emson, M., Hall, E. (2011): PARSPORT Trial Management Group. Parotid-sparing intensity modulated versus conventional radiotherapy in head and neck cancer (PARSPORT): a phase 3 multicentre randomised controlled trial. *Lancet Oncol*, **12**: 127–136.

O'Brien, C.J., Lahr, C.J., Soong, S.J., et al. (1986): Surgical treatment of early-stage carcinoma of the oral tongue–would adjuvant treatment be beneficial? Head Neck Surg, **8**:401–408.

O'Brien, C.J., Lauer, C.S., Fredricks, S., Clifford, A.R., McNeil, E.B., Bagia, J.S. & Koulmandas, C. (2003): Tumor thickness influences prognosis of T1 and T2 oral cavity cancer – but what thickness? *Head Neck*, **25**: 937–945.

Office for National Statistics. General Lifestyle Survey 2009 smoking and drinking among adults. 2010.

Office for National Statistics, October 2011.

Ogden, G.R., Cowpe, J.G., Green, M.W. (1991): Detection of field change in oral cancer using oral exfoliative cytologic study. *Cancer*, **68**:1611–1615.

Oh, E.S., Laskin, D.M. (2007): Efficacy of the ViziLite system in the identification of oral lesions. *J Oral Maxillofac*, **65**:424-426.

Oliver, A.J., Helfrick, J.F., Gard, D. (1996): Primary oral squamous cell carcinoma: a review of 92 cases. *J Oral Maxillofac Surg*, **54**(8): 949–54.

Olmedo, J.M., Warschaw, K.E., Schmitt, J.M., Swanson, D.L. (2006): Optical coherence tomography for the characterization of basal cell carcinoma in vivo: a pilot study. *J Am Acad Dermatol*, **55** (3): 408–412.

Onizawa, K., Saginoya, H., Furuya, Y., Yoshida, H. (1996): Fluorescence photography as a diagnostic method for oral cancer. *Cancer Lett*, **108**:61-66.

Onizawa, K., Saginoya, H., Furuya, Y., Yoshida, H., Fukuda, H. (1999): Usefulness of fluorescence photography for diagnosis of oral cancer. *Int J Oral Maxillofac Surg*, **28**:206-210.

Onofre, M.A., Sposto, M.R., Navarro, C.M. (2001): Reliability of toluidine blue application in the detection of oral epithelial dysplasia and in situ and invasive squamous cell carcinomas. *Oral Surg Oral Med Oral Pathol Oral Radiol Endod*, **91**:535-540.

O'Shaughnessy, J.A., Kelloff, G.K., Gordon, G.B., Dannenberg, A.J., Hong, W.K., Fabin, C.J., et al. (2002): Treatment and prevention of intraepithelial neoplasia: an important target for accelerated new agent development. *Clin Cancer Res*, **8**:314– 46.

Oxford Cancer Intelligence Unit, United Kingdom Head and Neck E-Atlas, Accessed March 2012.

Ozaki, Y., Okumura, M., Ismail, T.F., Naruse, H., Hattori, K., Kan, S., Ishikawa, M., Kawai, T., Takagi, Y., Ishii, J., Prati, F., Serruys, P.W. (2010): The fate of incomplete stent apposition with drug-eluting stents: an optical coherence tomography-based natural history study. *Eur Heart J*, **31**(12): 1470–1476.

Ozawa, N., Sumi, Y., Chong, C., Kurabayashi, T. (2009): Evaluation of oral vascular anomalies using optical coherence tomography. *Br J Oral Maxillofac Surg*, **47**: 622–626.

Parkin, D.M., Pisani, P. & Ferlay, J. (1999): Estimates of the worldwide incidence of 25 major cancers in 1990. *Int J Cancer*, **80**(6): 827-41.

Parkin, D.M., Whelan, S.L., Fearlay, J., et al, editors. (2002): Cancer incidence in five continents,vol VIII. IARC Scientific Publications No. 155. Lyon: IARC Press.

Parkin, D.M. (2011a) Tobacco-attributable cancer burden in the UK in 2010. *Br J Cancer*, **105** (2): 6-13.

Parkin, D.M. (2011b) Cancers attributable to consumption of alcohol in the UK in 2010. *Br J Cancer*, **105** (2): 14-18.

Parkin, D.M. (2011c) Cancers attributable to infection in the UK in 2010. *Br J Cancer*,**105** (2):49-56.

Parkin, D.M., Boyd, L., Walker, L.C. (2011): The fraction of cancer attributable to lifestyle and environmental factors in the UK in 2010. Summary and conclusions. *Br J Cancer*, **105** (2): 77-81.

Parkin, D.M. & Boyd, L. (2011): Cancers attributable to dietary factors in the UK in 2010. I Low consumption of fruit and vegetables. Br J Cancer,**105** (2): 19-23.

Parrish, J.A. (1981): New concepts in therapeutic photomedicine; photochemistry, optical targeting and the therapeutic window. *J Invest Dermatol*, **77**(1): 45–50.

Patton, L.L. (2003): The effectiveness of community-based visual screening and utility of adjunctive diagnostic aids in the early detection of oral cancer. *Oral Oncol*, **39**(7): 708–723.

Patton, L.L., Epstein, J.B., Kerr, A.R. (2008): Adjunctive techniques for oral cancer examination and lesion diagnosis: a systematic review of the literature. *J Am Dent Assoc*, **139**:896-905.

Patwari, P., Weissman, N.J., Boppart, S.A., et al. (2000): Assessment of coronary plaque with optical coherence tomography and high- frequency ultrasound. *Am J Cardiol*, **85**:641–644.

Paulsen, F. & Thale, A. (1998): Epithelial-connective tissue boundary in the oral part of the human soft palate. *J Anat*, **193: 457**–467.

Pavia, M., et al. (2006): Association between fruit and vegetable consumption and oral cancer: a meta-analysis of observational studies. Am J Clin Nutr, **83**(5): 1126-34.

Pelucchi, C., Talamini, R., Negri, E., Levi, F., Conti, E., Franceschi, S., La Vecchia, C. (2003) Folate intake and risk of oral and pharyngeal cancer. *Ann Oncol*, **14**(11): 1677-81.

Perea-milla Lopez, E., et al. (2003) Lifestyles, environmental and phenotypic factors associated with lip cancer: a case-control study in southern Spain. *Br J Cancer*, **88**(11): 1702-7.

Peters, L.J., Goepfert, H., Ang, K.K., et al (1993): Evaluation of the dose for postoperative radiation therapy of head and neck cancer: first report of a prospective randomized trial. *Int J Radiat Oncol Biol Phys*, **26**: 3-11.

Petersen, P.E. (2005) Strengthening the prevention of oral cancer: the WHO perspective. *Community Dent Oral Epidemiol*, **33**: 397–399.

Petridou, E., Zavras, A.I., Lefatzis, D. (2002): The role of diet and specific micronutrients in the aetiology of oral carcinoma. *Cancer*, **94**:2981–8.

Petti, S. (2003) Pooled estimate of world leukoplakia prevalence: a systematic review. *Oral Oncol,* **39**: 770-80.

Petti, S. (2009) Lifestyle risk factors for oral cancer. *Oral Oncol*, **45**(4-5): 340-50.

Pierce, M.C., Strasswimmer, J., Hyle Park, B., Cense, B., De Boer, J.F. (2004): Birefringence measurements in human skin using polarization-sensitive optical coherence tomography. *J Biomed Opt*, **9**(2): 287–291.

Pindborg, J.J., Renstrup, G., Poulsen, H.E., et al. (1963) Studies in oral leukoplakia.V. Clinical and histologic signs of malignancy. *Acta Odont Scand*, **21**:407-414.

Pindborg, J.J. & Sirsat, S.M. (1966): Oral submucous fibrosis. *Oral Surg Oral Med Oral Pathol*, **22**(6): 764-779.

Pindborg, J.J. (1977): Epidemiological studies in oral cancer. *Int Dent J*, **27**: 2: 172-8.

Pindborg, J.J., Murti, P.R., Bhonsle, R.B., Gupta, P.C., Daftary, D.K., Mehta, F.S. (1984): Oral submucous fibrosis as a precancerous condition. *Scand J Dent Res*, **92**(3): 224-229.

Pinto, T.L. & Waksman, R. (2006): Clinical applications of optical coherence tomography. *J Interv Cardiol*, **19**(6): 566-73.

Pircher, M., Götzinger, E., Leitgeb, R., Fercher, A.F., Hitzenberger, C.K. (2003): Speckle reduction in optical coherence tomography by frequency compounding. *J Biomed Opt,* **8**(3): 565–569.

Pircher, M., Götzinger, E., Leitgeb, R., Sattmann, H., Findl, O., Hitzenberger, C. (2004): Imaging of polarization properties of human retina in vivo with phase resolved transversal PS-OCT. *Opt Express*, **12**(24): 5940–5951.

Pitiphat, W., Diehl, S.R., Laskaris, G., Cartsos, V., Douglass, C.W., Zavras, A.I. (2002): Factors associated with delay in the diagnosis of oral cancer. *J Dent Res*, **81**:192-7.

Poate, T.W., Buchanan, J.A., Hodgson, T.A. et al. (2004): An audit of the efficacy of the oral brush biopsy technique in a specialist oral medicine unit. *Oral Oncol*, **40**(8): 829–834.

Podd, T.J., Carton, A.T., Barrie, R., Dawes, P.K., Roberts, J.T., Stassen, L.F., Henderson, R., Macleod, R.L., Piggot, T.A. (1994): Treatment of oral cancers using iridium-192 interstitial irradiation. *Br J Oral Maxillofac Surg*, **32**: 207–213.

Podoleanu, A.G., et al. (1998): Transversal and longitudinal images from the retina of the living eye using low coherence reflectometry. *J Biomed Optics*, **3**:12–20 (1998).

Podoleanu, A.G., Rogers, J.A., Jackson, D.A. & Dunne, S. (2000): Three-dimensional OCT images from retina and skin. *Optics Express*,7.

Poh, C.F., Zhang, L., Anderson, D.W. et al. (2006): Fluorescence visualization detection of field alterations in tumor margins of oral cancer patients. *Clin Cancer Res*, **12**(22): 6716–6722.

Poh, C.F., Ng, S.P., Williams, P.M. et al. (2007): Direct fluorescence visualization of clinically occult high-risk oral premalignant disease using a simple hand-held device. *Head Neck*, **29**: 71–76.

Považay, B., Bizheva, K., Hermann, B., Unterhuber, A., Sattmann, H., Fercher, A.F., Drexler, W., Schubert, C., Ahnelt, P.K., Mei, M., Holzwarth, R., Wadsworth, W.J., Knight, J.C., Russel, P.S.J. (2003): Enhanced visualization of choroidal vessels using ultrahigh resolution ophthalmic OCT at 1050 nm. *Opt Express*, **11** (17): 1980–1986.

Prati, F., Cera, M., Ramazzotti, V., Imola, F., Giudice, R., Albertucci, M. (2007): Safety and feasibility of a new non-occlusive technique for facilitated intracoronary optical coherence tomography (OCT) acquisition in various clinical and anatomical scenarios. *Euro Intervention*, **3**: 365–370.

Prestin, S., Rothschild, S.I., Betz, C.S., Kraft, m. (2012) Measurement of epithelial thickness within the oral cavity using optical coherence tomography. *Head Neck*, Feb, 9.

Pritt, B., Tessitore, J.J., Weaver, D.L., Blaszyk, H. (2005): The effect of tissue fixation and processing on breast cancer size. *Hum Pathol*, **36**: 756-60.

Pukkala, E., Söderholm, A.L. & Lindqvist, C. (1994): Cancers of the lip and oropharynx in different social and occupational groups in Finland. *Eur J Cancer B Oral Oncol*, **30B**(3): 209-15.

Puliafito, C.A., Hee, M.R., Schuman, J.S., Fujimoto, J.G. (1996) Optical coherence tomography of ocular diseases. 2nd ed. Thorofare, NJ: Slack Inc.

Quester, R. & Schroder, R. (1997): The shrinkage of the human brain stem during formalin fixation and embedding in paraffin. *J Neurosci Methods*, **75**: 81.

Queyrat, L. (1911) Erythroplasie de gland. *Bull Soc Franc Derm Syph*, **22**:378-382.

Quinn, M.W.H., Cooper, N., Rowan, S. (2005): Cancer Atlas of the United Kingdom and Ireland 1991-2000.Office for National Statistics.

Raffel, O.C., Merchant, F.M., Tearney, G.J., Chia S., DeJoseph Gauthier, D., Pomerantsev, E., Mizuno, K., Bouma, B.E., Jang, I.K. (2008): In vivo association between positive coronary artery remodelling and coronary plaque characteristics assessed by intravascular optical coherence tomography. *Eur Heart J*, **29** (14): 1721–1728.

Rahman, M., Sakamoto, J., and Fukui, T. (2003) Bidi smoking and oral cancer: a meta-analysis. *Int J Cancer*, **106**(4): 600-4.

Rajadhyaksha, M., Grossman, M., Esterowitz, D., Webb, R. H., Anderson, R. R. (1995): *In vivo* confocal scanning laser microscopy of human skin: melanin provides strong contrast. *J. Investig. Dermatol.*, **104***:* 946-952.

Rajadhyaksha, M., Gonzalez, S., Zavislan, J. M., Anderson, R. R., Webb, R. H. (1999a): *In vivo* confocal scanning laser microscopy of human skin. II. Advances in instrumentation and comparison with histology. *J. Investig. Dermatol.*, **113***:* 293-303.

Rajadhyaksha, M., Anderson, R. R., Webb, R.H. (1999b): Video-rate confocal scanning laser microscope for imaging human tissues *in vivo*. *Appl. Optics*, **38***:* 2105-2115.

Rajendran, R. (1995) Oral submucous fibrosis: aetiology, pathogenesis, and future research. *Bull World Health Organ*; **72** (6): 985-96.

Rajentheran, R., McLean, N.R., Kelly, C.G., Reed, M.F., Nolan, A. (1999) Malignant transformation of oral lichen planus. *Eur J Surg Oncol*, **72**(6): 985-96.

Ram, S. & Siar, C.H. (2005): Chemiluminescence as a diagnostic aid in the detection of oral cancer and potentially malignant epithelial lesions. *Int J Oral Maxillofac Surg*, **34**:521-527.
Regar, E., Schaar, J.A., Mont, E., et al. (2003): Optical coherence tomography. *Cardiovasc Radiat Med*, **4**: 198-204.

Regezi, J.A. & Sciubba, J. (1993) Oral Pathology. WB Saunders Co, NY, USA 77–90.

Reibel, J. (2003) Prognosis of oral pre-malignant lesions: significance of clinical, histopathological, and molecular biological characteristics. *Crit Rev Oral Biol Med*, **14**:47–62.

Reichart, P.A. & Philipsen, H.P. (2005) Oral erythroplakia- a review. *Oral Oncol*, **41**(6): 551-61.

Reichart, P.A. & Nguyen, X.H. (2008) Betel quid chewing, oral cancer and other oral mucosal diseases in Vietnam: a review. *J Oral Pathol Med*, **37**(9): 511-4.

Remontet, L., Buemi, M., Velten, M., Jougla, E., Esteve, J. (2002) Évolution de l'incidence et de la mortalité par cancer en France de 1978 à 2000. Collective expert evaluation report. Lyon: INSERM.

Rick, G.M., Slater, L. (2003): Oral brush biopsy: The problem of false positives. *Oral Surg Oral Med Oral Pathol Oral Radiol Endod,* **96**:252.

Richie, J.P. Jr., Kleinman, W., Marina, P., et al. (2008) Blood ion, glutathione, and micronutrient levels and the risk of oral cancer. *Nutr Cancer*, **60**: 474-482.

Ridgway, J.M., Armstrong, W.B., Guo, S., et al. (2006): In vivo optical coherence tomography of the human oral cavity and oropharynx. *Arch Otolaryngol Head Neck Surg*,**132**: 1074–1081.

Robinson, K.L. & Macfarlane, G.J. (2003): Oropharyngeal cancer incidence and mortality in Scotland: are rates still increasing? *Oral Oncol*, **39**:31-36.

Roblyer, D., Kurachi, C., Stepanek, V. et al. (2009): Objective detection and delineation of oral neoplasia using autofluorescence imaging. *Cancer Prev Res*, **2**(5): 423–431.

Rodriguez, T., et al. (2004) Risk factors for oral and pharyngeal cancer in young adults. *Oral Oncol*, **40**(2): 207-13.

Roed-Petersen, B. (1971) Cancer development in oral leukoplakia: Follow-up of 331 patients. *J Dent Res*, **50**:711.

Rogowska, J., Brezinski, M.E. (2000): Evaluation of the adaptive speckle suppression filter for coronary optical coherence tomography imaging. *IEEE T Med Imaging*, **19**(12): 1261–1266.

Rosenberg, D. & Cretin, S. (1989): Use of meta analysis to evaluate tolonium chloride in oral cancer screening. *Oral Surg Oral Med Oral Pathol*, **67**:621-627.

Rosin, M.P., Epstein, J.B., Berean, K., Durham, S., Hay, J., Cheng, X., et al. (1997): The use of exfoliative cell samples to map clonal genetic alterations in the oral epithelium of high-risk patients. *Cancer Res*, **57**:5258–5260.

Rosin, M.P., Poh, C.F., Guillard, M., Williams, P.M., Zhang, L., MacaUlay, C. (2007): Visualization and other emerging technologies as change makers for oral cancer prevention. *Ann NY Acad Sci,* **1098**:167–183.

Ross, G., Shoaib, T., Soutar, D.S., Camilleri, I.G., Gray, H.W., Bessent, R.G., Robertson, A.G. & MacDonald, D.G. (2002): The use of sentinel node biopsy to upstage the clinically N0 neck in head and neck cancer. *Arch Otolaryngol Head Neck Surg*, **128**: 1287–1291.

Rowe, D.E., Carroll, R.J., Day, C.L. Jr. (1992): Prognostic factors for local recurrence, metastasis, and survival rates in squamous cell carcinoma of the skin, ear, and lip. Implications for treatment modality selection. *J Am Acad Dermatol*. **26**(6): 976-90.

Rubin, P.H. (1993): Clinical oncology. A multidisciplinary approach to physicians and students. 7th ed. Philadelphia: Saunders.

Sakai, S., Nakagawa, N., Yamanari, M., Miyazawa, A., Yasuno, Y., Matsumoto, M. (2009): Relationship between dermal birefringence and the skin surface roughness of photoaged human skin. *J Biomed Opt*, **14**(4):044032.

Sandby-Møller, J., Poulsen, T., Wulf, H.C. (2003): Epidermal thickness at different body sites: relationship to age, gender, pigmentation, blood content, skin type and smoking habits. *Acta Derm Venereol*, **83**(6): 410-3.

Sander, B., Larsen, M., Thrane, L., Hougaard, J.L., Jørgensen, T.M. (2005): Enhanced optical coherence tomography imaging by multiple scan averaging. *Brit J Ophthalmol*, **89**(2): 207–212.

Sapkota, A., Hsu, C.C., Zaridze, D., Shangina, O., Szeszenia-Dabrowska, N., Mates, D., Fabiánová, E., Rudnai, P., Janout, V., Holcatova, I., Brennan, P., Boffetta, P., Hashibe, M. (2008) Dietary risk factors for squamous cell carcinoma of the upper aerodigestive tract in central and eastern Europe. *Cancer Causes Control*, **19**(10): 1161-70.

Sauermann, K., Clemann, S., Jaspers, S., et al. (2002): Age-related changes of human skin investigated with histometric measurements by confocal laser scanning microscopy. *Skin Res Technol*, **8**: 52-6.

Saxer, C.E., de Boer, J.F., Park, B.H., Zhao, Y., Chen, Z., Nelson, J.S. (2000): High-speed fiber based polarization-sensitive optical coherence tomography of in vivo human skin. *Opt Lett*, **25**(18): 1355–1357.

Schantz, S.P., Kolli, V., Savage, H.E., Yu, G., Shah, J.P., Harris, D.E., Katz, A., Alfano, R.R., Huvos, A.G. (1998): In vivo native cellular fluorescence and histological characteristics of head and neck cancer. *Clin Cancer Res*, **4**:1177-1182.

Schantz, S.P. &Yu, G.P. (2002) Head and neck cancer incidence trends in young Americans, 1973-1997, with a special analysis for tongue cancer. *Arch Otolaryngol Head Neck Surg*, **128**:268- 274.

Schmitt, J.M. (1997): Array detection for speckle reduction in optical coherence microscopy. *Phys Med Biol*, **42**(7): 1427–1439.

Schmitt, J.M. (1998): Restoration of optical coherence images of living tissue using the CLEAN algorithm. *J Biomed Opt*, **3** (1): 66–75.

Schmitt, J.M. (1999): Optical coherence tomography (OCT): a review. *IEEE J Sel Top Quantum Electr*, **5**(4): 1205–1215.

Schmitt, J.M., Xiang, S.H., Yung, K.M. (1999): Speckle in optical coherence tomography. *J Biomed Opt*, **4**(1): 95–105.

Schmitt, J.M. (2001): Optical coherence tomography (OCT): a review. *IEEE J Sel Topics Quantum Electron*, **7**(2): 931–935.

Schned, A.R., Wheeler, K.J., Hodorowski, C.A., et al. (1996): Tissue shrinkage correction factor in the calculation of prostate cancer volume. *Am J Surg Pathol*, **20**: 1501.

Schnetler, J.F.C. (1992): Oral cancer diagnosis and delays in referral. Br J Oral & Maxillofac Surg, **30**:210-3.

Schoop, R.A., Noteborn, M.H., Baatenburg, D.E. and Jong, R.J. (2009) A mouse model for oral squamous cell carcinoma. *J Mol Histol*, **40:**177-181.

Schwartz, J.L. and Shklar, G. (1997) Verification in syngeneic hamsters of in vitro transformation of hamster oral mucosa by 7,12-dimethylbenz(a)anthracene. *Oral Oncol*, **33**: 431-438.

Schwimmer, E. (1877) Die idiopathischen Schleim- hautplaques der Mundhöhle (Leukoplakia buccalis). *Arch Dermat Syph*, **9**:570-611.

Scientific Committees on Emerging and Newly Identified Health Risk (SCENIHR). European Commission; February 2008. Available from: http:// ec.europa.eu/health/ph_risk/committees/04_scenihr/docs/scenihr_o_013.pdf.

Sciubba, J.J. (1999): Improving detection of precancerosu and cancerous oral lesions: Computer-assisted analysis of the oral brush biopsy. *J Am Dent Assoc*, **130**:1445–1457.

Scully, C. & El-Kom, M. (1985) Lichen planus: a review and update on pathogenesis. *J Oral Path*, **14**: 431-458.

Scully C. (2002) Oral squamous cell carcinoma; from a hypothesis about a virus, to concern about possible sexual transmission. *Oral Oncol*, **38**(3): 227-34.

Scully, C. (2005) Oral cancer; the evidence for sexual transmission. *Br Dent J*, **199**: 203-207.

Scully, C. & Bagan, J. (2009). Oral squamous cell carcinoma overview. *Oral Oncol*, **45**: 301-308.

Scully, C. & Moles, D.R. (2008): Oral cancer. In: Heggenhougen K, Quah S, editors. International Encyclopaedia of Public Health, vol. 4. San Diego: Academic Press; 668–77.

Scully, C., Bagan, J.V., Hopper, C., Epstein, J.B. (2008): Oral cancer: current and future diagnostic techniques. *Am J Dent*, **21**(4): 199-209.

Shafer, W.B. & Waldron, C.A. (1961) A clinical and histopathologic study of oral leukoplakia. *Surg Gynecol Obstet*, **112**: 411-420.

Shafer, W.G. & Waldron, C.A. (1975) Erythroplakia of the oral cavity. *Cancer*, **36**:1021-1028.

Shah, J.P., Candela, F.C., Poddar, A.K. (1990) The patterns of cervical lymph node metastasis from squamous carcinoma of the oral cavity. *Cancer*, **66**:109-113.

Sharma, U., Chang, E.W., Yun, S.H. (2008): Long-wavelength optical coherence tomography at 1.7 μm for enhanced imaging depth. *Opt Express*, **16**(24): 19712–19723.

Shaw, R.J., Pace-Balzan, A. & Butterworth, C. (2011): Contemporary clinical management of oral squamous cell carcinoma. *Periodontol 2000*, **57**(1): 89-101.

Shiboski, C.H., Schmidt, B.L., Jordan, R.C. (2005): Tongue and tonsil carcinoma: increasing trends in the U.S. population ages 20-44 years. *Cancer*, **103**:1843-1849.

Shintani, S., Nakayama, B., Matsuura, H., Hasegawa, Y. (1997): Intraoral ultrasonography is useful to evaluate tumor thickness in tongue carcinoma. *Am J Surg*, **173**(4): 345-7.

Silverman, S. Jr. (1968) Observations on the clinical characteristics and natural history of oral leukoplakia. *J Am Dent Assoc*, **76**:772-777.

Silverman, S. Jr & Griffith, M. (1972) Smoking characteristics of patients with oral carcinoma and the risk for second oral primary carcinoma. *J Am Dent Assoc*, **85**:637-640.

Silverman, S. Jr., Gorsky, M., Lozada, F. (1984a) Oral leukoplakia and malignant transformation: A follow-up study of 257 patients. *Cancer*, **53**:563-568.

Silverman, S. Jr., Migliorati, C., Barbosa, J. (1984b): Toluidine blue staining in the detection of oral precancerous and malignant lesions. *Oral Surg Oral Med Oral Pathol*, **57**: 379-382.

Silverman, S., Gorsky, M., & Lozada-Nur, F. (1985): A prospective follow-up study of 570 patients with oral lichen planus: persistence, remission and malignant association. *Oral Surg Oral Med Oral Path*, **60**: 30-4.

Silverman, M.K., Golomb, F.M., Kopf, A.W., et al. (1992): Verification of a formula for determination of preexcision surgical margins from fixed tissue melanoma specimens. *J Am Acad Dermatol*, **27**: 214.

Silverman, S. Jr., & Gorsky, M. (1997) Proliferative verrucous leukoplakia. A follow-up study of 54 cases. *Oral Surg Oral Med Oral Pathol Oral Radiol Endod*, **84**:154-157.

Silverman, S. Jr & Shillitoe, E.F. (1998) Etiology and Predisposing Factors. In: Silverman S Jr ed. Oral Cancer, 4th ed. Hamilton, Ontario, Canada: BC Decker Inc, 7-24.

Silverman, S. Jr. (1998) Epidemiology. In: Silverman S Jr ed. Oral Cancer. 4th ed. Hamilton, Ontario, Canada: BC Decker Inc, 1-6.

Silverman, S. Jr., Dillon, W.P., Fischbein, N.J. (1998) Diagnosis In: Silverman S Jr ed. Oral Cancer. 4th ed. Hamilton, Ontario, Canada: BC Decker Inc; 41-66.

Silverman, S. Jr. (2001): Demographics and occurrence of oral and pharyngeal cancers. The outcomes, the trends, the challenge. *J Am Dent Assoc*, **132**:7-11.

Siu, K.F., Cheung, H.C., Wong, J. (1986): Shrinkage of the esophagus after resection for carcinoma. *Ann Surg*, **203**:173.

Smeets, N.W., Krekels, G.A., Ostertag, J.U., et al. (2004): "Surgical excision vs Mohs' micrographic surgery for basal-cell carcinoma of the face: randomised controlled trial". *Lancet* **364** (9447): 1766–72.

Smith, R.G. (1972): "Optical power handling capacity of low loss optical fibers as determined by stimulated Raman and Brillouin scattering". *Appl. Opt.* **11** (11): 2489–94.

Smith, R.A., Cokkinides, V., von Eschenbach, A.C., et al. (2002): American Cancer Society guidelines for the early detection of cancer. *CA Cancer J Clin*, **52**:8-22.

Smith, E.M., et al. (2004) Human papillomavirus in oral exfoliated cells and risk of head and neck cancer. *J Natl Cancer Inst*, **96**(6): 449-55.

Soliman, W., Sander, B., Soliman, K.A.E.N., Yehya, S., Rahamn, M.S.A., Larsen, M. (2008): The predictive value of optical coherence tomography after grid laser photocoagulation for diffuse diabetic macular oedema. *Acta Ophthalmol*, **86**(3): 284–291.

Songra, A.K., Ng, S.Y., Farthing, P., Hutchison, I.L., Bradley, P.F. (2006): Observation of tumour thickness and resection margin at surgical excision of primary oral squamous cell carcinoma—assessment by ultrasound. *Int. J. Oral Maxillofac. Surg*, **35**(4): 324-31.

Spiro, R.H. & Strong, E.W. (1971): Epidermoid carcinoma of the mobile tongue: treatment by partial glossectomy alone. *Am J Surg*, **122**:707–710.

Spiro, J.D., Spiro, R.H., Shah, J.P., et al. (1988): Critical assessment of supraomohyoid neck dissection. *Am J Surg*, **156**:286–289.

Spitz, M.R., et al. (1992) Association between malignancies of the upper aerodigestive tract and uterine cervix. *Head Neck*, **14**(5): 347-51.

Sri Lanka National Cancer Control Programme, 2005.

Stamper, D., Weissman, N.J., Brezinski, M. (2006): Plaque characterization with optical coherence tomography. *J Am Coll Cardiol*, **47**:C69–C79.

Steiner, R., Kunzi-Rapp, K., Scharffetter-Kochanek, K. (2003): Optical coherence tomography: clinical applications in dermatology. *Med Laser Appl*, **18**(3): 249–259.

Stevenson, O., Ahmed, I. (2005): "Lentigo maligna: prognosis and treatment options". *American Journal of Clinical Dermatology*, **6** (3): 151–64.

Strasswimmer, J., Pierce, M.C., Park, B.H., Neel, V., de Boer, J.F. (2004): Polarization-sensitive optical coherence tomography of invasive basal cell carcinoma. *J Biomed Opt*, **9**(2): 292–298.

Sugerman, P.B. & Shillitoe, E.J. (1997): The high risk human papillomaviruses and oral cancer: Evidence for and against a causal relationship. *Oral Dis*, **3**:130-147.

Sugerman, P.B., & Savage, N.W. (2002): Oral cancer in Australia: 1983–1996. *Aust Dent J*, **47**:45–56.

Surveillance epidemiology and end results (SEER). Cancer Statistics Review, 1975-2004. National Cancer Institute. Available from http://seer.cancer.gov/statfacts/html/oralcav.

Surveillance Epidemiology and End Results (SEER), 2009.

Suzuki, T., Wakai, K., Matsuo, K., et al. (2006) Effect of dietary antioxidants and risk of oral, pharyngeal and laryngeal squamous cell carcinoma according to smoking and drinking habits. *Cancer Sci*, **97**: 760-767.

Svistun, E., Alizadeh-Naderi, R., El-Naggar, A., Jacob, R., Gillenwater, A., Richards-Kortum, R. (2004): Vision enhancement system for detection of oral cavity neoplasia based on autofluorescence. *Head Neck*, **26**:205-215.

Swango, P.A. (1996): Cancers of the oral cavity and pharynx in the United States: An epidemiologic overview. *J Public Health Dent*, **56**:309-318.

Swanson, E.A. et al. (1992): High-speed optical coherence domain reflectometry. *Optics Lett*, **17**: 151–153.

Swanson, E.A., Izatt, J.A., Hee, M.R., Huang, D., Lin, C.P., Schuman, J.S., Puliafito, C.A., and Fujimoto, J.G. (1993): In vivo retinal imaging by optical coherence tomography. *Opt Lett*,**18**:1864 -1866.

Swerdlow, A.J., Marmot, M.G., Grulich, A.E., Head J. (1995): Cancer mortality in Indian and British ethnic immigrants from the Indian subcontinent to England and Wales.*Br J Cancer*, **72**:1312–9.

Takada, K., Yokohama, I., Chida, K. & Noda, J. (1987): New measurement system for fault location in optical waveguide devices based on an interferometric technique. *Appl.Optics*, **26**: 1603–1608.

Talamini, R., et al. (2000): Oral hygiene, dentition, sexual habits and risk of oral cancer. *Br J Cancer*, **83**(9): 1238-42.

Talamini, R., Bosetti, C., La Vecchia, C., Dal Maso, L., Levi, F., Bidoli, E., Negri, E., Pasche, C., Vaccarella, S., Barzan, L., Franceschi, S. (2002) Combined effect of tobacco and alcohol on laryngeal cancer risk: a case-control study. *Cancer Causes Control*.**13**(10):957-64.

Tan, O., Li, G., Ake, Tzu-Hui, L., Varma, R., Huang, D. (2008): Mapping of macular substructures with optical coherence tomography for glaucoma diagnosis. *Ophthalmology*, **115**(6): 949–956.

Tanno, N. & Kishi, S. (1999): Optical coherence tomographic imaging and clinical diagnosis. *Med Imaging Technol*, **17**(1): 3–10.

Tearney, G.J., Brezinski, M.E., Bouma, B.E., Boppart, S.A., Pitris, C., Southern, J.F., Fujimoto, J.G. (1997): In vivo endoscopic optical biopsy with optical coherence tomography. *Science*, **276**(5321): 2037–2039.

Tearney, G.J., Yabushita, H., Houser, S.L., Thomas Aretz, H., Jang, I.K., Schlendorf, K.H., Kauffman, C.R., Shishkov, M., Halpern, E.F., Bouma, B.E. (2003): Quantification of macrophage content in atherosclerotic plaques by optical coherence tomography. *Circulation*, **107**(1): 113–119.

Tearney, J.G., Jang, I.K., Bouma, B.E. (2006): Optical coherence tomography for imaging the vulnerable plaque. *J Biomed Opt*, **11** (2):021002.

Thames Cancer Registry, 2007.

Thomas, S. & Kearsley, J. (1993) Betel nut and oral cancer: a review. *Eur J Cancer Oral Oncol*, **29**: 251-5.

Titford, M.E. & Horenstein, M.G. (2005): Histomorphologic assessment of formalin substitute fixatives for diagnostic surgical pathology. *Arch Pathol Lab Med*, **129**:502.

Treu, C.M., Lupi, O., Bottino, D.A., Bouskela, E. (2011): Side stream dark field imaging: the evolution of real-time visualization of cutaneous microcirculation and its potential application in dermatology. *Arch Dermatol Res*, **303**:69–78.

Troy, T.L. & Thennadil, S.N. (2001): Optical properties of human skin in the NIR wavelength range of 1000-2200 nm. *J. Biomedical Opt*, **6**:167-76.

Trullenque-Eriksson, A., Muñoz-Corcuera M, Campo-Trapero J et al. (2009): Analysis of new diagnostic methods in suspicious lesions of the oral mucosa. *Med. Oral Pathol. Oral Cir. Bucal.,* **14**(5), 210–216.

Tsai, M.T., Lee, H.C., Lee, C.K. et al. (2008a): Effective indicators for diagnosis of oral cancer using optical coherence tomography. *Opt Express*, **16**: 15847–15862.

Tsai, M.T., Lee, H.C., Lu, C.W. et al (2008b): Delineation of an oral cancer lesion with swept-source optical coherence tomography. *J Biomed Opt*, **13**: 044012.

Tsai, M.T., Lee, C.K., Lee, H.C. et al. (2009): Differentiating oral lesions in different carcinogenesis stages with optical coherence tomography. *J Biomed Opt*, **14**: 044028.

Unterhuber, A., Povazay, B., Bizheva, K., Hermann, B., Sattmann, H,. Stingl, A., Le, T., Seefeld, M., Menzel, R., Preusser, M., Budka, H., Schubert, C., Reitsamer, H., Ahnelt, P.K., Morgan, J.E., Cowey, A., Drexler, W. (2004): Advances in broad bandwidth light sources for ultrahigh resolution optical coherence tomography. *Phys Med Biol*, **49**(7): 1235–1246.

US Department of Health & Human Services, 1986.

US Department of Health and Human Services. A Surgeon General's report on the Health Consequences of Smoking. Atlanta, GA: US Department of Health and Human Services, Centres for Disease Control and Prevention, Office of Smoking and Health; 2004.

Vakoc, B., Yun, S., de Boer, J., Tearney, G., Bouma, B. (2005): Phase- resolved optical frequency domain imaging. *Opt Express*, **13**(14): 5483–5493.

van der Meer, F.J., Faber, D.J., Sassoon, D.M.B., Aalders, M.C., Pasterkamp, G., van Leeuwen, T.G. (2005): Localized measurement of optical attenuation coefficients of atherosclerotic plaque constituents by quantitative optical coherence tomography. *IEEE T Med Imaging*, **24**(10): 1369–1376.

van Soest, G., Goderie, T., Regar, E., Koljenovic, S., van Leenders, G.L.J.H., Gonzalo, N., van Noorden, S., Okamura, T., Bouma, B.E., Tearney, G.J., Oosterhuis, J.W., Serruys, P.W., van der Steen, A.F.W. (2010): Atherosclerotic tissue characterization in vivo by optical coherence tomography attenuation imaging. *J Biomed Opt*, **15** (1):011105.

Van Wyk, C.W., Stander, I., Padayachee, A., Grobler-Rabie, A.F. (1993) The areca nut chewing habit and oral squamous cell carcinoma in South African Indiana. *S Afr Med J*, **31**: 517-21.

van Zuuren, E.J., de Visscher, J.G., Bouwes Bavinck, J.N. (1988) Carcinoma of the lip in kidney transplant recipients. *J Amer Acad Dermatol*, **38**: 497-499.

Vermorken, J.B. (2005): Medical treatment in head and neck cancer. *Ann Oncol*, **2**: 258–264.
Vermorken, J.B., Remenar, E., van Herpen, C., Gorlia, T., Mesia, R., Degardin, M., Stewart, J.S., Jelic, S., Betka, J., Preiss, J.H., van den Weyngaert, D., Awada, A., Cupissol, D., Kienzer, H.R., Rey, A., Desaunois, I., Bernier, J., Lefebvre, J.L. (2007): EORTC 24971 / TAX 323 Study Group. Cisplatin, fluorouracil, and docetaxel in un- resectable head and neck cancer. *N Engl J Med*, **357**: 1695–1704.

Villard, J.W., Feldman, M.D., Kim, J., Milner, T.E., Freeman, G.L. (2002): Use of a blood substitute to determine instantaneous murine right ventricular thickening with optical coherence tomography. *Circulation*, **105**(15): 1843–1849.

Virmani, R., Kolodgie, F.D., Burke, A.P., Farb, A., Schwartz, S.M. (2000): Lessons from sudden coronary death: a comprehensive morphological classification scheme for atherosclerotic lesions. *Arterioscl Throm Vas*, **20**(5): 1262–1275.

Virmani, R., Burke, A.P., Farb, A., et al. (2002): Pathology of the unstable plaque. *Prog Cardiovasc Dis*, **44**:349–356.

Vo-Dinh, T. (2002): *Biomedical Photonics Handbook*. Taylor & Francis, Inc. ISBN 0-8493-1116-0.

Vokes,E.E., Kies,M.S., Haraf, D.J., et al. (2000) :Concomitant chemoradiotherapy as primary therapy for locoregionally advanced head and neck cancer. *J Clin Oncol*, **18**:1652–1661.

Waldron, C.A. & Shafer, W.G. (1975) Leukoplakia revisited: A clinicopathologic study of 3256 oral leukoplakias. *Cancer*, **36**: 1386-1392.

Wang, Y., Nelson, J.S., Chen, Z., Reiser, B.J., Chuck, R.S., Windeler, R.S. (2003a): Optimal wavelength for ultrahigh-resolution optical coherence tomography. *Opt Express*, **11**(12): 1411–1417.

Wang, Y., Zhao, Y., Nelson, J.S., Chen, Z., Windeler, R.S. (2003b): Ultrahigh-resolution optical coherence tomography by broad- band continuum generation from a photonic crystal fiber. *Opt Lett*, **28**(3): 182–184.

Wang, L., Wang, Y., Guo, S, Zhang, J., Bachman, M. (2004): Frequency domain phase-resolved optical Doppler and Doppler variance tomography. *Optics communications*, **242**(4–6): 345–350.

Wang, R.K. (2005): Reduction of speckle noise for optical coherence tomography by the use of nonlinear anisotropic diffusion. *Proc SPIE*, **5690**(1): 380–385.

Wang, L.V. & Wu, H.I. (2007): *Biomedical Optics*. Wiley. ISBN 978-0-471-74304-0.

Warnakulasuriya, S. (1995) Analytical studies of the evaluation of the role of betel-quid in carcinogenesis. In: Betel-quid and tobacco smoking. Usage and health issues, chapter 6 London: *Transcultural health*; 61-70.

Warnakulasuriya, K.A. & Johnson, N.W. (1996): Sensitivity and specificity of OraScan (R) toluidine blue mouth rinse in the detection of oral cancer and precancer. *J Oral Pathol Med*, **25**:97-103.

Warnakulasuriya, K.A., Johnson, N.W., Linklater, K.M., Bell, J. (1999a): Cancer of mouth, pharynx and nasopharynx in Asian and Chinese immigrants resident in Thames regions. *Oral Oncol*, **35**:471–5.

Warnakulasuriya, K.A., Harris, C.K., Scarrott, D.M., Watt, R., Gelbier, S., Peters, T.J., et al. (1999b): An alarming lack of public awareness towards oral cancer. *Br Dent J*, **187**:319-22.

Warnakulasuriya, S. (2002) Effectiveness of tobacco counselling in the dental office. *J Dent Educ*, **66**(9): 1079-87.

Warnakulasuriya, S., Mak, V., Moller, H. (2007a): Oral cancer survival in young people in South East England. *Oral Oncol*, **43**:982–6.

Warnakulasuriya, S., Johnson, N.W., van der Wall, I. (2007b): Nomenclature and classification of potentially malignant disorders of the oral mucosa. *J Oral Pathol Med*, **36**:575–80.

Warnakulasuriya, S., & Ralhan R. (2007): Clinical, pathological, cellular and molecular lesions caused by oral smokeless tobacco- a review. *J Oral Pathol Med*, **36**: 63-77.

Warnakulasuriya, S. (2009): Global epidemiology of oral and oropharyngeal cancer. *Oral Oncol*, **45**:309–16.

Warnakulasuriya, S. (2010): Living with oral cancer: Epidemiology with particular reference to prevalence and life-style changes that influence survival. *Oral Oncol*, **46**: 407-410.

Welsh Cancer Intelligence and Surveillance Unit, September 2011.

Welzel, J., Lankenau, E., Birngruber, R., Engelhardt, R. (1997): Optical coherence tomography of the human skin. *J Am Acad Dermatol*, **37**(6): 958–963.

Welzel, J. (2001): Optical coherence tomography in dermatology: a review. *Skin Res Technol*, **7**:1-9.

Welzel, J., Noack, J., Lankenau, E., Engelhardt, R. (2002): Optical coherence tomography in dermatology. Handbook of optical coherence tomography. Marcel Dekker, Inc., New York.

Wen, C.P., Tsai, M.K., Chung, W.S., et al. (2010): Cancer risks from betel quid chewing beyond oral cancer: a multiple-site carcinogen when acting with smoking. *Cancer Causes Control*, **21**:1427-1435.

Wendt, C.D., Peters, L.J., Delclos, L., et al (1990): Primary radiotherapy in the treatment of stage I and II oral tongue cancers: importance of the proportion of therapy delivered with interstitial therapy. *Int J Radiat Oncol Biol Phys*, **18**:1287–1292.

Werner, M., Chott, A., Fabiano, A., Battifora, H. (2000): Effect of formalin tissue fixation and processing on immunohistochemistry. Am J Surg Pathol, **24**:1016.

White, W. M., Rajadhyaksha, M., Gonzalez, S., Fabian, R. L., Anderson, R. R. (1999): Noninvasive imaging of human oral mucosa *in vivo* by confocal reflectance microscopy. *Laryngoscope*, **109***:* 1709-1717.

Whitton, J.T. & Everall, J.D. (1973): The thickness of the epidermis. *Br J Dermatol*, **89**(5): 467-76.

Wilder-Smith, P., Jung, W.G., Brenner, M., Osann, K., Beydoun, H., Messadi, D., Chen, Z. (2004): Optical coherence tomography for the diagnosis of oral malignancy. *Lasers Surg Med*, **35**:269–275.

Wilder-Smith, P., Krasieva, T., Jung, W.G., Zhang, J., Chen, Z., Osann, K., Tromberg, B. (2005) Non-invasive imaging of oral premalignancy and malignancy. *J Biomed Opt*, **10**(5): 051601.

Wilder-Smith, C., Wilder-Smith, P., Kawakami-Wong, H., Voronets, J., Osann, K., Lussi, A. (2009a): Quantification of dental erosions in patients with GERD using optical coherence tomography before and after double-blind, randomized treatment with esomeprazole or placebo. *Am J Gastroenterol*, **104**: 2788–2795.

Wilder-Smith, P., Lee, K., Guo, S., Zhang, J., Osann, K., Chen, Z., et al. (2009b): In vivo diagnosis of oral dysplasia and malignancy using optical coherence tomography: preliminary studies in 50 patients. *Lasers Surg Med*, **41**:353–7.

Wilder-Smith, P., Holtzman, J., Epstein J., Le, A. (2010): Optical diagnostics in the oral cavity: an overview. *Oral Diseases*, **16**: 717-728.

Winn, D.M., Blot, W.J., Shy, C.M., et al. (1981): Snuff dip- ping and oral cancer among women in the southern United States. *N Engl J Med*, **304**:745- 749.

Winn, D.M., Ziegler, R.G., Pickle, L.W., et al. (1984) Diet in the etiology of oral and pharyngeal cancer among women from the southern United States. *Cancer Res*, **44**:1216-1222.

Winn, D.M., et al. (1991): Mouthwash use and oral conditions in the risk of oral and pharyngeal cancer. *Cancer Res*, **51**(11): 3044-7.

Winn, D.M. (1995): Diet and nutrition in the etiology of oral cancer. *Am J Clin Nutr*, **61**:437-445.

Winn, D.M., et al. (2001): Mouthwash in the etiology of oral cancer in Puerto Rico.*Cancer Causes Control*, **12**(5): 419-29.

Woolgar, J.A. (1999): Histological distribution of cervical lymph node metastases from intraoral/oropharyngeal squamous cell carcinomas. *Br J Oral Maxillofac Surg*, **37**:175–180.

World Health Organization (2010) Fact sheet no. 317: cardio- vascular diseases. WHO, Geneva. http://www.who.int/ mediacentre/factsheets/fs317/en/., accessed 19 Nov 2010

Wunsch-Fiho, V. & de Camargo, A. (2001): The burden of mouth cancer in Latin America and the Caribbean: epidemiologic issues. *Seminars Oncol*, **28**:158–68.

Www.michelsondiagnostics.com.

Www.iftbu.org/milk.htm.

Www.physicsclassroom.com/class/refrn/u14l1d.cfm.

Wynder, E.L. & Bross, I.J. (1957): etiological factors in mouth cancer; an approach to its prevention. *Br Med J*, 18; **1**(5028): 1137-43.

Wynder, E.L., Hultberg, S. and Jaconsson, F. (1957) Environmental factors in cancer of the upper alimentary tract: a Swedish study with specific reference to Plummer Vinson syndrome. *Cancer*, **10**: 470-482.

Xiang, S.H., Zhou, L., Schmitt, J.M. (1998): Speckle noise reduction for optical coherence tomography. *Proc SPIE*, **3196** (1): 79–88.

Yabushita, H., Bouma, B.E., Houser, S.L., Thomas Aretz, H., Jang, I.K., Schlendorf, K.H., Kauffman, C.R., Shishkov, M., Kang, D.H., Halpern, E.F., Tearney, G.J. (2002): Characterization of human atherosclerosis by optical coherence tomography. *Circulation*, **106**(13): 1640–1645.

Yamada, R., Okura, H., Kume, T., Saito, K., Miyamoto, Y., Imai, K., Tsuchiya, T., Maehama, T., Okahashi, N., Obase, K., Hayashida, A., Neishi, Y., Kawamoto, T., Yoshida, K. (2010): Relationship between arterial and fibrous cap remodelling. *Circ Cardiovasc Interv*, **3** (5): 484–490.

Yamaguchi, T., Terashima, M., Akasaka, T., Hayashi, T., Mizuno, K., Muramatsu, T., Nakamura, M., Nakamura, S., Saito, S., Takano, M., Takayama, T., Yoshikawa, J., Suzuki, T. (2008): Safety and feasibility of an intravascular optical coherence tomography image wire system in the clinical setting. *Am J Cardiol*, **101** (5): 562–567.

Yang, P., Sun, Z., Chan, D., Cartwright, C.A., Vijjeswarapu, M., Ding, J., Chen, X. and Newman, R.A. (2008) Zyflamend reduces LTB4 formation and prevents oral carcinogenesis in a 7,12- dimethylbenz[a]anthracene (DMBA)-induced hamster cheek pouch model. *Carcinogenesis*, **29:** 2182–2189.

Yasuno, Y., Hong, Y., Makita, S., Yamanari, M., Akiba, M., Miura, M., Yatagai, T. (2007): In vivo high-contrast imaging of deep posterior eye by 1-μm swept source optical coherence tomography and scattering optical coherence angiography. *Opt Express*, **15** (10): 6121–6139.

Yazdanfar, S., Rollins, A.M., Izatt, J.A. (2000): Imaging and velocimetry of the human retinal circulation with colour Doppler optical coherence tomography. *Opt Lett*, **25**(19): 1448–1450.

Yeap, B.H., Muniandy, S., Lee, S.K., Sabaratnam, S., Singh, M. (2007): Specimen shrinkage and its influence on margin assessment in breast cancer. *Asian J Surg*, **30**:183-7.

Yellowitz, J.A. & Goodman, H.S. (1995): Assessing physicians' and dentists' oral cancer knowledge, opinions and practices. *J Am Dent Assoc*, **126**:53-59.

Yellowitz, J., Horowitz, A.M., Goodman, H.S., et al. (1998): Knowledge, opinions and practices of general dentists regarding oral cancer: A pilot survey. *J Am Dent Assoc*, **129**:579-583.

Yellowitz, J.A., Horowitz, A.M., Drury, T.F., et al. (2000) Survey of U.S. dentists' knowledge and opinions about oral pharyngeal cancer. *J Am Dent Assoc*, **131**:653-661.

Youngquist, R., Carr, S. & Davies, D. (1987): Optical coherence-domain reflectometry: a new optical evaluation technique. *Optics Lett*, **12**:158–160.

Yu, B. (2009): Evaluation of statin-induced lipid-rich plaque progression by optical coherence tomography (OCT) combined with intravascular ultrasound (IVUS). http://clinicaltrials.gov/ct2/ show/NCT01023607, accessed 22 Mar 2011.

Yun, S.H., Tearney, G.J., de Boer, J.F., Bouma, E.B. (2004): Motion artifacts in optical coherence tomography with frequency-domain ranging. *Opt Express*, **12**(13): 2977–2998.

Yusuf, H. & Yong, S.L. (2002) Oral submucous fibrosis in a 12-year-old Bangladeshi boy: a case report and review of literature. *Int J Paediatric Dent*. **12**(4): 271-6.

Zain, R.B., Ikeda, N., Razak, I.A., et al. (1997) A national epidemiological survey of oral mucosal lesions in Malaysia. *Community Dent Oral Epidemiol*, **25**(5): 377-83.

Zain, R.B., Ikeda, N., Gupta, P.C., Warnakulasuriya, S., van Wyk, C.W., Shrestha, P., Axéll, T. (1999) Oral mucosal lesions associated with betel quid, areca nut and tobacco chewing habits: consensus from a workshop held in Kuala Lumpur, Malaysia, November 25-27, 1996. *J Oral Pathol Med*, **28**(1): 1-4.

Zakrzewska, J.M., Lopes, V., Speight, P., et al. (1996) Proliferative verrucous leukoplakia: A report of ten cases. *Oral Surg Oral Med Oral Pathol Oral Radiol Endod*, **82**:396-401.

Zawadzki, R., Jones, S., Olivier, S., Zhao, M., Bower, B., Izatt, J., Choi, S., Laut, S., Werner, J. (2005): Adaptive-optics optical coherence tomography for high-resolution and high-speed 3D retinal in vivo imaging. *Opt Express*, **13**(21): 8532–8546.

Zelefsky, M.J., Harrison, L.B., Fass, D.E., et al. (1990): Postoperative radiotherapy for oral cavity cancers: impact of anatomic subsite on treatment outcome. *Head Neck*, **12**:470–475.

Zhang, Z.F., Morgenstern, H., Spitz, M.R., et al. (1999) Marijuana use and increased risk of squamous cell carcinoma of the head and neck. *Cancer Epidemiol Biomarkers Prev*, **8**:1071-1078.

Zhang, L., Williams, M., Poh, C.F., Laronde, D., Epstein, J., Durham, S., Nakamura, H., Berean, K., Hovan, A., Le, N.D., Hislop, G., Priddy, R., Hay, J., Lam, W.L., Rosin, M.P. (2005): Toluidine blue staining identifies high-risk primary oral premalignant lesions with poor outcome. *Cancer Re*, **65**:8017-8021.

Zhang, J. & Chen, Z. (2005): In vivo blood flow imaging by a swept laser source based Fourier domain optical Doppler tomography. *Opt Express*, **13**(19): 7449–7457.

Zhao, Y., Chen, Z., Saxer, C., Xiang, S., de Boer, J.F., Nelson, J.S. (2000): Phase-resolved optical coherence tomography and optical Doppler tomography for imaging blood flow in human skin with fast scanning speed and high velocity sensitivity. *Opt Lett*, **25**(2): 114–116.

Zheng, TZ, Boyle, P, Hu, HF, Duan, J, Jian, PJ, Ma, DQ, et al. (1990) Dentition, oral hygiene, and risk of oral cancer: a case-control study in Beijing, People's republic of China. *Cancer Causes Control*, **1**(3): 235-41.

Znaor, A., et al. (2003) Independent and combined effects of tobacco smoking, chewing and alcohol drinking on the risk of oral, pharyngeal and esophageal cancers in Indian men. *Int J Cancer*, **105**(5): 681-6.

Conference presentations and awards

1. Rashed D, Fedele S, Perrett CM, Hopper C, & Cook RJ. Validation of OCT oral instrument by comparing with the commercially available OCT dermatology probe using laboratory engineering standards and porcine tissues. European Conferences on Biomedical Optics (ECBO) meeting, Munich, Germany, May 2013. (Oral Presentation)

2. Rashed D, Fedele S, Perrett CM, Hopper C, & Cook RJ. Validation of OCT oral instrument by comparing with the commercially available OCT dermatology probe using laboratory engineering standards and porcine tissues. Laser Europe Conference, Manchester, UK, May 2013. (Oral Presentation)

3. Rashed D, Fedele S, Perrett CM, Hopper C, & Cook RJ. Validation of a new real-time in-situ optical coherence tomography with modified oral probe by comparing with the certified CE marking optical coherence tomography dermatology probe. BiOS SPIE Photonic West, San Francisco, CA, USA, Feb 2014. (Poster Presentation)

4. Rashed D, Fedele S, Perrett CM, Hopper C, & Cook RJ. Shrinkage of porcine cutaneous specimen after formalin fixation and histopathology preparation: utilising OCT for dimensional change measurements. Laser Europe Conference, Amsterdam, the Netherlands, May 2014. (Oral Presentation)

5. Rashed D, Shah D, Freeman A, Hopper C, & Perrett CM. Comparison of Mohs micrographic surgery with OCT. Laser Europe Conference, Brighton, UK, April 2015. (Oral Presentation)

Conference awards

The Springer award for outstanding talk on “Mohs micrographic surgery and optical coherence tomography”.

Appendices

Appendix 1 (Raw data of OCT skin & oral instrument)

1. Raw data of OCT skin instrument

Slope angle 4.62° in water + surfactant. R= reading

Amount	1st R of θ D	2nd R of θ D	3rd R of θ D	4th R of θ D	5th R of θ D	6th R of θ D	Mean of θ D
1ml surfactant	4.95°	5.00°	5.05°	5.08°	5.05°	4.95°	**5.01°**
2ml surfactant	5.10°	5.20°	5.25°	5.27°	5.15°	5.15°	**5.18°**
3ml surfactant	5.30°	5.35°	5.40°	5.45°	5.45°	5.30°	**5.37°**
4ml surfactant	5.45°	5.50°	5.60°	5.63°	5.48°	5.50°	**5.52°**
5ml surfactant	5.65°	5.70°	5.80°	5.85°	5.75°	5.75°	**5.75°**
6ml surfactant	5.90°	6.00°	6.05°	6.05°	5.90°	6.05°	**5.99°**

Slope angle 7.61° in water + surfactant

Amount	1st R of θ D	2nd R of θ D	3rd R of θ D	4th R of θ D	5th R of θ D	6th R of θ D	Mean of θ D
1ml surfactant	5.45°	5.60°	5.55°	5.56°	5.45°	5.60°	**5.53°**
2ml surfactant	5.60°	5.60°	5.78°	5.70°	5.70°	5.74°	**5.68°**
3ml surfactant	5.80°	6.00°	6.00°	5.85°	5.85°	5.92°	**5.90°**
4ml surfactant	6.00°	6.20°	6.19°	6.10°	6.05°	6.05°	**6.09°**
5ml surfactant	6.20°	6.40°	6.25°	6.38°	6.20°	6.32°	**6.29°**
6ml surfactant	6.40°	6.60°	6.50°	6.56°	6.40°	6.40°	**6.47°**

Slope angle 8.95° in water + surfactant

Amount	1st R of θ D	2nd R of θ D	3rd R of θ D	4th R of θ D	5th R of θ D	6th R of θ D	Mean of θ D
1ml surfactant	6.00°	6.15°	6.10°	6.06°	6.06°	6.00°	**6.06°**
2ml surfactant	6.15°	6.35°	6.15°	6.30°	6.32°	6.27°	**6.25°**
3ml surfactant	6.35°	6.40°	6.50°	6.50°	6.58°	6.52°	**6.47°**
4ml surfactant	6.60°	6.85°	6.80°	6.60°	6.78°	6.78°	**6.73°**
5ml surfactant	6.85°	6.85°	6.92°	6.95°	7.00°	7.00°	**6.92°**
6ml surfactant	7.00°	7.20°	7.20°	7.05°	7.17°	7.09°	**7.11°**

Slope angle 11.44° in water + surfactant

Amount	1st R of θ D	2nd R of θ D	3rd R of θ D	4th R of θ D	5th R of θ D	6th R of θ D	Mean of θ D
1ml surfactant	6.60°	6.80°	6.69°	6.60°	6.64°	6.76°	**6.68°**
2ml surfactant	6.80°	6.80°	7.00°	7.00°	6.95°	6.91°	**6.91°**
3ml surfactant	7.00°	7.00°	7.20°	7.10°	7.06°	7.19°	**7.09°**
4ml surfactant	7.20°	7.45°	7.38°	7.24°	7.24°	7.41°	**7.32°**
5ml surfactant	7.45°	7.70°	7.49°	7.50°	7.38°	7.33°	**7.47°**
6ml surfactant	7.70°	7.70°	7.74°	7.95°	7.95°	7.86°	**7.81°**

Slope angle 4.62° in water + milk

Amount	1st R of θ D	2nd R of θ D	3rd R of θ D	4th R of θ D	5th R of θ D	6th R of θ D	Mean of θ D
1ml milk	3.60°	3.70°	3.75°	3.66°	3.73°	3.60°	**3.67°**
2ml milk	3.75°	3.75°	3.94°	3.85°	3.80°	3.80°	**3.81°**
3ml milk	3.95°	4.00°	3.98°	4.20°	4.14°	4.06°	**4.05°**
4ml milk	4.20°	4.35°	4.35°	4.20°	4.28°	4.32°	**4.28°**
5ml milk	4.35°	4.55°	4.45°	4.39°	4.35°	4.35°	**4.40°**
6ml milk	4.55°	4.55°	4.80°	4.71°	4.64°	4.64°	**4.64°**

Slope angle 7.61° in water + milk

Amount	1st R of θ D	2nd R of θ D	3rd R of θ D	4th R of θ D	5th R of θ D	6th R of θ D	Mean of θ D
1ml milk	4.20°	4.30°	4.34°	4.26°	4.45°	4.45°	**4.33°**
2ml milk	4.50°	4.70°	4.60°	4.56°	4.50°	4.67°	**4.58°**
3ml milk	4.70°	4.90°	4.84°	4.75°	4.79°	4.70°	**4.78°**
4ml milk	4.90°	4.90°	5.15°	5.07°	5.05°	5.00°	**5.01°**
5ml milk	5.15°	5.40°	5.22°	5.33°	5.15°	5.30°	**5.25°**
6ml milk	5.40°	5.60°	5.60°	5.56°	5.45°	5.55°	**5.52°**

Slope angle 8.95° in water + milk

Amount	1st R of θ D	2nd R of θ D	3rd R of θ D	4th R of θ D	5th R of θ D	6th R of θ D	Mean of θ D
1ml milk	4.90°	5.20°	5.08°	5.02°	4.97°	4.90°	**5.01°**
2ml milk	5.20°	5.40°	5.40°	5.20°	5.35°	5.29°	**5.30°**
3ml milk	5.40°	5.65°	5.50°	5.40°	5.57°	5.51°	**5.50°**
4ml milk	5.65°	5.80°	5.80°	5.65°	5.77°	5.78°	**5.74°**
5ml milk	5.80°	6.00°	6.00°	5.91°	5.82°	5.80°	**5.88°**
6ml milk	6.00°	6.00°	6.20°	6.07°	6.03°	6.15°	**6.07°**

Slope angle 11.44° in water + milk

Amount	1st R of θ D	2nd R of θ D	3rd R of θ D	4th R of θ D	5th R of θ D	6th R of θ D	Mean of θ D
1ml milk	5.65°	5.90°	5.84°	5.70°	5.75°	5.75°	**5.76°**
2ml milk	5.90°	5.90°	6.10°	6.03°	5.93°	6.00°	**5.96°**
3ml milk	6.10°	6.35°	6.22°	6.17°	6.10°	6.31°	**6.20°**
4ml milk	6.35°	6.55°	6.39°	6.51°	6.43°	6.40°	**6.43°**
5ml milk	6.55°	6.80°	6.75°	6.68°	6.56°	6.56°	**6.65°**
6ml milk	6.80°	7.00°	7.00°	6.90°	6.95°	6.95°	**6.93°**

2. Raw data of OCT oral instrument

Slope angle 4.62° in water + surfactant

Amount	1st R of θ D	2nd R of θ D	3rd R of θ D	4th R of θ D	5th R of θ D	6th R of θ D	Mean of θ D
1ml surfactant	3.85°	3.97°	3.89°	4.00°	4.05°	4.05°	**3.96°**
2ml surfactant	4.05°	4.19°	4.39°	4.14°	4.28°	4.10°	**4.19°**
3ml surfactant	4.40°	4.49°	4.55°	4.60°	4.40°	4.58°	**4.50°**
4ml surfactant	4.60°	4.85°	4.74°	4.65°	4.65°	4.78°	**4.71°**
5ml surfactant	4.85°	5.00°	5.00°	4.85°	4.93°	4.90°	**4.92°**
6ml surfactant	5.00°	5.20°	5.11°	5.06°	5.00°	5.02°	**5.06°**

Slope angle 7.61° in water + surfactant

Amount	1st R of θ D	2nd R of θ D	3rd R of θ D	4th R of θ D	5th R of θ D	6th R of θ D	Mean of θ D
1ml surfactant	4.60°	4.80°	4.80°	4.60°	4.67°	4.75°	**4.70°**
2ml surfactant	4.80°	5.00°	4.90°	4.97°	5.05°	5.05°	**4.96°**
3ml surfactant	5.05°	5.40°	5.34°	5.23°	5.11°	5.05°	**5.19°**
4ml surfactant	5.40°	5.55°	5.45°	5.45°	5.43°	5.44°	**5.45°**
5ml surfactant	5.55°	5.90°	5.86°	5.76°	5.69°	5.60°	**5.72°**
6ml surfactant	5.90°	6.00°	6.10°	6.04°	6.06°	5.93°	**6.00°**

Slope angle 8.95° in water + surfactant

Amount	1st R of θ D	2nd R of θ D	3rd R of θ D	4th R of θ D	5th R of θ D	6th R of θ D	Mean of θ D
1ml surfactant	5.40°	5.45°	5.65°	5.56°	5.46°	5.40°	**5.48°**
2ml surfactant	5.65°	5.85°	5.78°	5.66°	5.66°	5.85°	**5.74°**
3ml surfactant	5.85°	6.00°	6.00°	5.88°	5.85°	5.90°	**5.91°**
4ml surfactant	6.00°	6.00°	6.25°	6.25°	6.15°	6.08°	**6.12°**
5ml surfactant	6.25°	6.50°	6.36°	6.36°	6.46°	6.46°	**6.39°**
6ml surfactant	6.50°	6.70°	6.50°	6.58°	6.69°	6.69°	**6.61°**

Slope angle 11.44° in water + surfactant

Amount	1st R of θ D	2nd R of θ D	3rd R of θ D	4th R of θ D	5th R of θ D	6th R of θ D	Mean of θ D
1ml surfactant	6.00°	6.00°	6.30°	6.15°	6.04°	6.09°	**6.09°**
2ml surfactant	6.30°	6.55°	6.48°	6.36°	6.40°	6.40°	**6.41°**
3ml surfactant	6.55°	6.80°	6.80°	6.58°	6.67°	6.75°	**6.69°**
4ml surfactant	6.80°	7.00°	6.90°	6.86°	6.93°	6.96°	**6.90°**
5ml surfactant	7.00°	7.00°	7.20°	7.07°	7.14°	7.08°	**7.08°**
6ml surfactant	7.20°	7.50°	7.44°	7.31°	7.31°	7.22°	**7.33°**

Slope angle 4.62° in water + milk

Amount	1st R of θ D	2nd R of θ D	3rd R of θ D	4th R of θ D	5th R of θ D	6th R of θ D	Mean of θ D
1ml milk	2.90°	2.93°	3.10°	3.04°	3.02°	3.00°	**2.99°**
2ml milk	3.10°	3.35°	3.25°	3.16°	3.10°	3.35°	**3.21°**
3ml milk	3.35°	3.55°	3.45°	3.38°	3.35°	3.51°	**3.43°**
4ml milk	3.55°	3.80°	3.68°	3.56°	3.60°	3.75°	**3.65°**
5ml milk	3.80°	4.00°	4.00°	3.85°	3.94°	3.94°	**3.92°**
6ml milk	4.00°	4.20°	4.11°	4.01°	4.15°	4.00°	**4.07°**

Slope angle 7.61° in water + milk

Amount	1st R of θ D	2nd R of θ D	3rd R of θ D	4th R of θ D	5th R of θ D	6th R of θ D	Mean of θ D
1ml milk	3.55°	3.85°	3.78°	3.60°	3.68°	3.68°	**3.69°**
2ml milk	3.85°	4.10°	4.03°	4.10°	3.85°	3.93°	**3.97°**
3ml milk	4.10°	4.35°	4.20°	4.25°	4.35°	4.17°	**4.23°**
4ml milk	4.35°	4.50°	4.48°	4.41°	4.39°	4.36°	**4.41°**
5ml milk	4.50°	4.75°	4.60°	4.69°	4.74°	4.75°	**4.67°**
6ml milk	4.75°	4.98°	4.82°	4.92°	4.92°	4.80°	**4.86°**

Slope angle 8.95° in water + milk

Amount	1st R of θ D	2nd R of θ D	3rd R of θ D	4th R of θ D	5th R of θ D	6th R of θ D	Mean of θ D
1ml milk	4.35°	4.55°	4.48°	4.38°	4.38°	4.47°	**4.43°**
2ml milk	4.55°	4.80°	4.80°	4.66°	4.70°	4.64°	**4.69°**
3ml milk	4.80°	5.00°	4.86°	4.94°	4.90°	5.00°	**4.91°**
4ml milk	5.00°	5.00°	5.25°	5.17°	5.10°	5.04°	**5.09°**
5ml milk	5.25°	5.45°	5.40°	5.30°	5.28°	5.42°	**5.35°**
6ml milk	5.45°	5.64°	5.47°	5.58°	5.65°	5.61°	**5.56°**

Slope angle 11.44° in water + milk

Amount	1st R of θ D	2nd R of θ D	3rd R of θ D	4th R of θ D	5th R of θ D	6th R of θ D	Mean of θ D
1ml milk	5.00°	5.30°	5.14°	5.04°	5.23°	5.05°	**5.12°**
2ml milk	5.30°	5.45°	5.39°	5.34°	5.37°	5.39°	**5.37°**
3ml milk	5.45°	5.65°	5.56°	5.48°	5.45°	5.61°	**5.53°**
4ml milk	5.65°	5.90°	5.80°	5.67°	5.78°	5.65°	**5.74°**
5ml milk	5.90°	6.00°	6.06°	6.20°	6.14°	6.17°	**6.07°**
6ml milk	6.20°	6.50°	6.43°	6.25°	6.35°	6.40°	**6.35°**

Appendix 2

(Table 1) OCT skin instrument (fresh porcine tissue). R= reading

Type of tissue	1st R	2nd R	3rd R	4th R	5th R	6th R	7th R	8th R	9th R	10thR	Mean ±SD of θD
Skin	19.89	19.76	19.64	19.49	19.28	19.17	19.31	19.86	19.76	19.72	**19.53±0.25**
Fat	15.79	15.82	15.62	15.57	15.42	15.26	15.19	15.40	15.67	15.53	**15.52±0.21**
Muscle	11.57	11.51	11.32	11.73	11.87	11.20	11.15	11.59	11.53	11.70	**11.51±0.23**

(Table 2) OCT oral instrument (fresh porcine tissue). R= reading

Type of tissue	1st R	2nd R	3rd R	4th R	5th R	6th R	7th R	8th R	9th R	10thR	Mean ±SD
Skin	19.06	19.19	19.28	19.89	19.80	19.73	19.55	19.43	19.82	19.61	**19.53±0.28**
Fat	15.82	15.73	15.61	15.56	15.50	15.12	15.27	15.77	15.33	15.70	**15.54±0.23**
Muscle	11.54	11.50	11.34	11.78	11.86	11.16	11.19	11.59	11.60	11.67	**11.52±0.23**

(Table 3) OCT skin instrument (porcine tissue in PBS). R= reading

Type of tissue	1st R	2nd R	3rd R	4th R	5th R	6th R	7th R	8th R	9th R	10thR	Mean ±SD
Skin	21.09	21.04	20.03	20.81	20.66	20.38	20.23	20.70	21.00	20.57	**20.65±0.35**
Fat	16.60	16.87	16.91	16.16	16.10	16.31	16.44	16.32	17.00	16.99	**16.57±0.21**
Muscle	13.00	12.95	12.83	12.76	12.49	12.48	12.21	12.10	12.12	12.88	**12.58±0.34**

(Table 4) OCT oral instrument (porcine tissue in PBS). R= reading

Type of tissue	1st R	2nd R	3rd R	4th R	5th R	6th R	7th R	8th R	9th R	10thR	Mean ±SD
Skin	21.02	20.96	20.83	20.61	20.34	20.27	20.62	20.49	20.91	20.56	**20.66±0.26**
Fat	17.00	17.00	16.93	16.11	16.07	16.30	16.49	16.38	16.84	16.81	**16.59±0.36**
Muscle	12.99	12.91	12.86	12.71	12.44	12.41	12.26	12.07	12.10	12.75	**12.55±0.33**

(Table 5) OCT skin instrument (porcine tissue after freezing). R= reading

Type of tissue	1st R	2nd R	3rd R	4th R	5th R	6th R	7th R	8th R	9th R	10thR	Mean ±SD
Skin	19.01	19.10	19.19	19.16	19.45	19.58	19.69	19.82	19.86	19.86	**19.47±0.33**
Fat	15.01	15.09	15.20	15.49	15.55	15.55	15.23	15.31	15.60	15.06	**15.30±0.22**
Muscle	11.05	11.05	11.14	11.41	11.38	11.36	11.26	11.19	11.12	11.21	**11.21±0.13**

(Table 6) OCT oral instrument (porcine tissue after freezing). R= reading

Type of tissue	1st R	2nd R	3rd R	4th R	5th R	6th R	7th R	8th R	9th R	10thR	Mean ±SD
Skin	19.03	19.07	19.16	19.19	19.49	19.66	19.54	19.89	19.21	19.12	**19.33±0.28**
Fat	15.58	15.03	15.34	15.29	15.23	15.02	15.10	15.17	15.51	15.44	**15.27±0.19**
Muscle	11.01	11.29	11.08	11.17	11.11	11.19	11.30	11.42	11.23	11.23	**11.20±0.11**

Appendix 3

(Table 1) Fresh porcine skin **second** parallel holes measurements by both OCT skin & oral instruments. Letters from A-J stands for the different measurements in X & Z planes in millimetre using image J programme.

OCT	**A**	**B**	**C**	**D**	**E**	**F**	**G**	**H**	**I**	**J**
Skin	0.82	0.37	0.40	0.38	0.76	1.10	0.64	0.37	0.41	0.47
Oral	0.83	0.38	0.39	0.39	0.76	1.10	0.65	0.37	0.41	0.48

(Table 2) Fresh porcine skin **third** parallel holes measurements by both OCT skin & oral instruments. Letters from A-J stands for the different measurements in X & Z planes in millimetre using image J programme.

OCT	**A**	**B**	**C**	**D**	**E**	**F**	**G**	**H**	**I**	**J**
Skin	0.92	0.55	0.38	0.44	0.56	1.02	0.75	0.40	0.51	0.55
Oral	0.92	0.55	0.37	0.43	0.56	1.02	0.75	0.39	0.52	0.54

(Table 3) Fresh porcine skin **fourth** parallel holes measurements by both OCT skin & oral instruments. Letters from A-J stands for the different measurements in X & Z planes in millimetre using image J programme.

OCT	**A**	**B**	**C**	**D**	**E**	**F**	**G**	**H**	**I**	**J**
Skin	0.97	0.52	0.32	0.30	0.41	0.76	0.80	0.52	0.39	0.43
Oral	0.97	0.52	0.33	0.31	0.42	0.77	0.80	0.50	0.39	0.44

(Table 4) Fresh porcine skin **fifth** parallel holes measurements by both OCT skin & oral instruments. Letters from A-J stands for the different measurements in X & Z planes in millimetre using image J programme.

OCT	**A**	**B**	**C**	**D**	**E**	**F**	**G**	**H**	**I**	**J**
Skin	0.89	0.56	0.42	0.44	0.42	0.76	0.90	0.50	0.50	0.47
Oral	0.89	0.56	0.41	0.44	0.43	0.76	0.90	0.51	0.50	0.47

(Table 5) Fresh porcine skin **sixth** parallel holes measurements by both OCT skin & oral instruments. Letters from A-J stands for the different measurements in X & Z planes in millimetre using image J programme.

OCT	A	B	C	D	E	F	G	H	I	J
Skin	0.75	0.48	0.40	0.42	0.44	0.80	0.76	0.48	0.33	0.32
Oral	0.76	0.48	0.40	0.42	0.44	0.80	0.76	0.48	0.33	0.32

(Table 6) Porcine skin (formalin-fixed) **second** parallel holes measurements by both OCT skin & oral instruments. Letters from A-J stands for the different measurements in X & Z planes in millimetre using image J programme.

OCT	A	B	C	D	E	F	G	H	I	J
Skin	0.88	0.35	0.35	0.37	0.70	1.12	0.75	0.35	0.39	0.45
Oral	0.88	0.34	0.35	0.37	0.70	1.12	0.75	0.35	0.38	0.45

(Table 7) Porcine skin (formalin-fixed) **third** parallel holes measurements by both OCT skin & oral instruments. Letters from A-J stands for the different measurements in X & Z planes in millimetre using image J programme.

OCT	A	B	C	D	E	F	G	H	I	J
Skin	0.96	0.52	0.37	0.42	0.53	1.06	0.77	0.36	0.46	0.50
Oral	0.95	0.51	0.37	0.42	0.54	1.07	0.77	0.36	0.47	0.49

(Table 8) Porcine skin (formalin-fixed) **fourth** parallel holes measurements by both OCT skin & oral instruments. Letters from A-J stands for the different measurements in X & Z planes in millimetre using image J programme.

OCT	A	B	C	D	E	F	G	H	I	J
Skin	1.03	0.50	0.25	0.24	0.38	0.83	0.91	0.39	0.38	0.42
Oral	1.03	0.50	0.25	0.24	0.37	0.83	0.92	0.40	0.38	0.42

(Table 9) Porcine skin (formalin-fixed) **fifth** parallel holes measurements by both OCT skin & oral instruments. Letters from A-J stands for the different measurements in X & Z planes in millimetre using image J programme.

OCT	A	B	C	D	E	F	G	H	I	J
Skin	0.93	0.54	0.38	0.42	0.39	0.80	0.92	0.48	0.48	0.45
Oral	0.93	0.54	0.38	0.41	0.39	0.80	0.93	0.48	0.48	0.45

(Table 10) Porcine skin (formalin-fixed) **sixth** parallel holes measurements by both OCT skin & oral instruments. Letters from A-J stands for the different measurements in X & Z planes in millimetre using image J programme.

OCT	A	B	C	D	E	F	G	H	I	J
Skin	0.82	0.46	0.38	0.40	0.39	0.83	0.77	0.46	0.31	0.30
Oral	0.82	0.46	0.38	0.40	0.39	0.83	0.77	0.46	0.31	0.30

Appendix 4

(Table 1) Porcine skin parallel holes measurements (histopathology). Letters from A-J stands for the different measurements in X & Z planes in millimetre using "Nanozoomer Digital Pathology" programme with an integrated scale.

Holes	A	B	C	D	E	F	G	H	I	J
1	0.92	0.41	0.50	0.42	0.87	1.23	0.91	0.37	0.39	0.39
2	0.91	0.32	0.33	0.35	0.67	1.15	0.77	0.33	0.37	0.43
3	0.89	0.50	0.33	0.39	0.51	1.08	0.79	0.35	0.45	0.48
4	1.08	0.48	0.23	0.22	0.36	0.85	0.94	0.37	0.36	0.38
5	0.98	0.52	0.35	0.41	0.37	0.84	0.97	0.45	0.46	0.43
6	0.85	0.44	0.36	0.38	0.37	0.85	0.80	0.44	0.29	0.28

Appendix 5

Table (1) Illustrate mean % change of X plane dimensions (fresh-formalin fixed tissue). Highlighted figures were expansion, while the rest were contraction.

OCT	A	B	E	F	G	H	Mean	SD
Skin	7.44%	5.15%	8.47%	4.27%	8.35%	9.64%	**7.22**%	**2.08**%
Oral	7.02%	5.98%	9.15%	4.20%	8.63%	9.41%	**7.40**%	**2.05**%

Table (2) Illustrate mean % of formalin fixed tissue shrinkage in Z-plane (fresh-formalin fixed).

OCT	C	D	I	J	Mean (%)	SD
Skin	10.31%	8.04%	4.94%	9.64%	**7.01%**	**2.66%**
Oral	9.81%	9.17%	5.32%	5.48%	**7.44%**	**2.37%**

Table (3) Illustrate mean % change of X plane dimensions (fresh-histopathology). Highlighted figures were expansion, while the rest were contraction.

OCT	A	B	E	F	G	H	Mean	SD
Skin	11.96%	9.75%	12.58%	7.21%	12.39%	14.07%	**11.33**%	**2.45**%
Oral	11.48%	9.81%	13.13%	6.97%	11.83%	14.15%	**11.23**%	**2.55**%

Table (4) Illustrate mean % of histopathology tissue shrinkage in Z-plane (fresh- histopathology).

OCT	C	D	I	J	Mean (%)	SD
Skin	16.54%	13.31%	9.41%	10.52%	**12.45%**	**3.18%**
Oral	16.98%	14.02%	9.69%	10.59%	**12.82%**	**3.34%**